Enclosure 1

Three-Dimensional Structural Analysis Results – Base Case

Report No.: 0006004.403
Revision No.: 0
Project No.: 0006004
January 2009

Structural Evaluation of the Oyster Creek Drywell
Summary Report

Prepared for:

Exelon Nuclear
Contract # 01002562, Release # 0016
Chicago, Illinois

Prepared by:

Structural Integrity Associates, Inc.
San Jose, California

Prepared by: _____ Date: 01/09/09
Soo Bee Kok

Reviewed by: _____ Date: 01/09/09
Stan Tang, P.E.

Approved by: _____ Date: 01/09/09
Marcos Legaspi Herrera, P.E.

REVISION CONTROL SHEET

Document Number: 0006004.403

Title: Structural Evaluation of the Oyster Creek Drywell Summary Report

Client: Exelon Nuclear

SI Project Number: **0006004.00** Quality Program: ☒ Nuclear ☐ Commercial

Section	Pages	Revision	Date	Comments
	i – xiii	0	01/09/09	Initial Issue
1.0	1-1 – 1-3			
2.0	2-1 – 2-6			
3.0	3-1 – 3-11			
4.0	4-1 – 4-34			
5.0	5-1 – 5-38			
6.0	6-1 – 6-59			
7.0	7-1 – 7-24			
8.0	8-1 – 8-60			
9.0	9-1 – 9-12			
10.0	10-1 – 10-2			
11.0	11-1 – 11-4			

Table of Contents

List of Tables

List of Figures

EXECUTIVE SUMMARY

This summary report presents the results of the finite element structural analysis of the primary containment drywell shell at the Oyster Creek Nuclear Generating Station (Oyster Creek). This structural analysis uses modern updated methods, which provide the following benefits compared to the previous evaluation:

- Detailed full three dimension (3-D) representation of the finite element model, which comprises approximately 406,000 elements and 400,000 nodes.
- Eliminates conservative assumptions made in earlier evaluations to better represent the actual structure configuration and loading.
- Advanced computer machine capable of solving large analyses quickly.
- Advanced computer software capable of performing complex analyses.

This analysis captures the current condition of the drywell shell, both inside and outside the sandbed region, as defined by the ultrasonic (UT) thickness measurements taken during the 2006 refueling outage (which were confirmed during the 2008 refueling outage), along with conservative thickness estimates for areas between UT thickness measurement locations. This analysis, therefore, models the drywell thicknesses realistically, but maintains some conservatism.

The evaluation presented in this report uses assumptions that introduce some conservatisms (and thus additional margin) into the analysis and results. These include conservatisms in geometry, wall thickness, loads, load combinations and allowable stresses. These conservatisms are discussed throughout this report.

The analysis concludes that the buckling safety factors for all regions of the drywell shell meet the ASME Code requirements by an adequate margin.

In summary, the minimum sandbed region buckling safety factors (SF) are:

- Refueling: SF = 3.54, which exceeds Level A/B required SF of 2.00.
- Flooding: SF = 2.02, which exceeds Level C required SF of 1.67 (and the Level D required SF of 1.34).

1.0 INTRODUCTION

This summary report presents the results of the three-dimensional (3-D) finite element structural analysis of the primary containment drywell shell at the Oyster Creek Nuclear Generating Station (Oyster Creek). This structural analysis uses modern updated methods and drywell shell thickness data collected during the 2006 refueling outage to better quantify the margin that exists above the ASME Boiler and Pressure Vessel Code (ASME Code) required minimum for buckling. This report presents the base case analysis. Separate companion reports present sensitivity studies that determine the degree to which uncertainties in the size of thinned areas affect ASME Code margins.

Oyster Creek began operation in 1969. The Chicago Bridge and Iron Company designed the Oyster Creek drywell shell [1]. In the 1980s, the licensee identified that the presence of water from the reactor cavity, along with sand (acting to keep the water in direct contact with an uncoated drywell shell) and improper sandbed drainage had caused corrosion of the exterior of the drywell shell in an area known as the sandbed region. The sandbed region sits between approximately elevations 8'11" and 12'3" (Figure 1-1). This portion of the shell was designed with a sandbed on the exterior to provide structural support as the shell transitions from being embedded in concrete on both sides below an approximate elevation of 8'11" to being embedded only on the interior above that elevation.

The corrosion was not evenly distributed either among or within the ten sections of bays that make up the sandbed region. In general, corrosion was greatest in the vicinity of the torus vent headers. This is an area of generally lower stress because these vent headers and their reinforcing plates stiffen the shell and reduce the stresses in their influence zone. In addition, there was an air-water interface located near the top of the sandbed region between approximately elevations 11' and 12', above which there was virtually no corrosion. For reference, the as-designed thickness of the drywell shell in the sandbed region is 1.154". The uneven distribution of corrosion resulted in maximum general average metal loss of about 0.35" in part of Bay 19. Some bays exhibited almost no observable corrosion.

The licensee took multiple mitigating actions in the 1980s and early 1990s to address the corrosion problem, including removal of the sand and application of an epoxy coating system on the exterior surface of the drywell shell in the sand bed region. Ultrasonic (UT) thickness measurements collected since 1992, coupled with visual inspections of the epoxy coating system, demonstrate that corrosion of the exterior of the drywell shell in the sandbed region has been arrested.

In the early 1990s, General Electric (GE) was retained to analyze the structural integrity of the drywell shell [2]. The GE analyses were based on a 36° slice of the drywell shell. The NRC-approved minimum thickness acceptance criteria for the sandbed region of the drywell shell are based on the analyses performed by GE. This 3-D finite element structural analysis does not alter those criteria, but merely uses modern updated methods to better quantify the margin that exists above ASME Code required minimum for buckling.

The base case analysis presented in this report is designed to model the current condition of the drywell shell. In the sandbed region, the current condition is defined by the UT thickness measurements taken during the 2006 refueling outage (Measurements were also taken during the 2008 refueling outage. The results of these measurements confirm the measurements used in this analysis.), along with conservative thickness estimates for areas between UT thickness measurement locations. The base case therefore models drywell thickness realistically, but maintains some conservatism.

In this analysis, the remainder of the drywell shell, outside the sandbed region, is also modeled in a detailed fashion. This detail includes: head connection detail (including bolts), vent lines, penetrations, access hatch, detailed knuckle representation, weld pads/supports and other support structures. This detailed model shows the drywell to be a non-symmetric structure that is more realistically analyzed with a three-dimensional model such as the model presented in this report. The evaluation presented in this report uses several assumptions that introduce conservatism and thus margin into the analysis and results. These include conservatisms in geometry, wall thickness, loads, load combinations and allowable stresses. These conservatisms are discussed throughout this report.

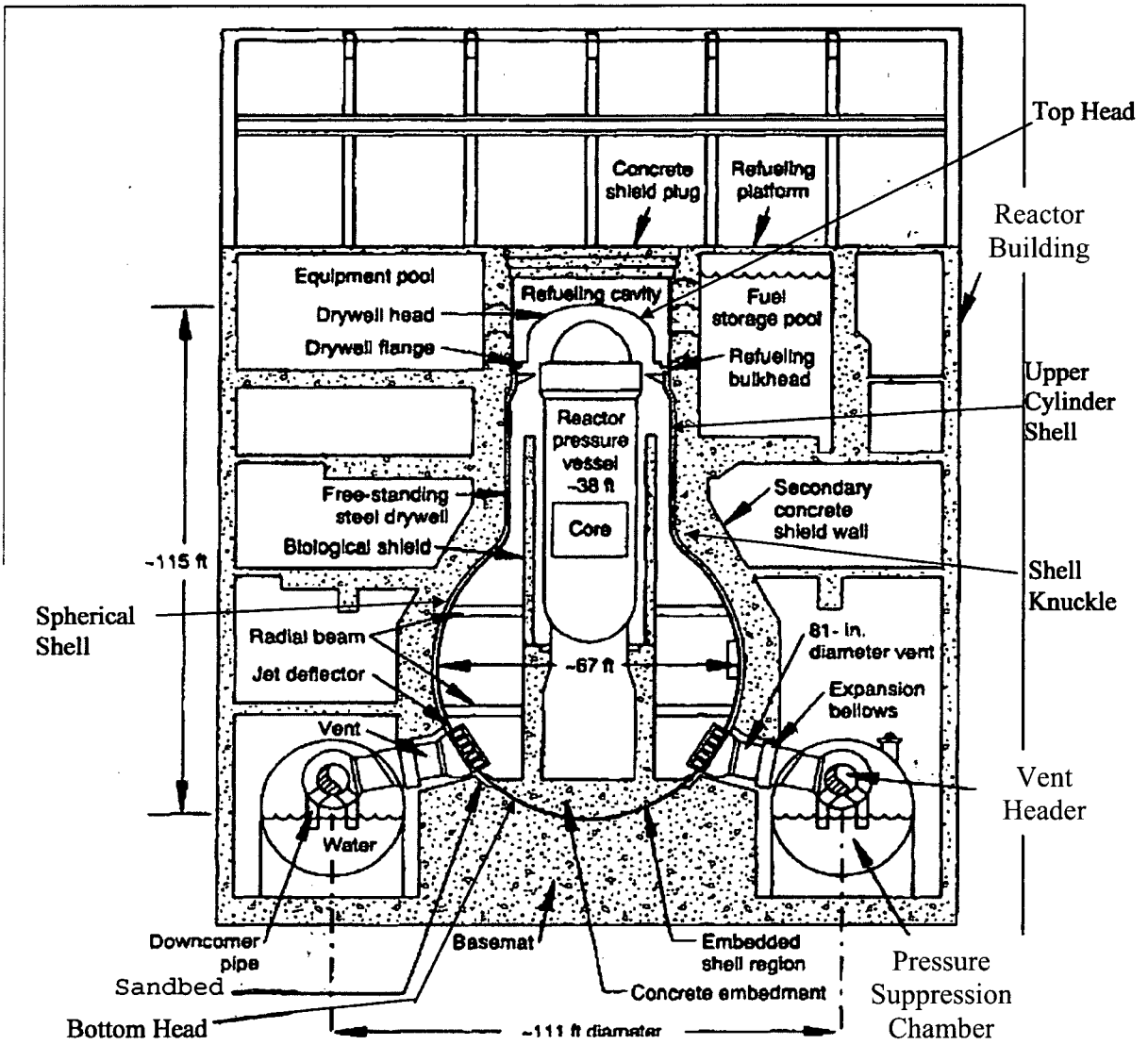

Figure 1-1: Oyster Creek Containment Schematic

2.0 DRYWELL DESCRIPTION

Oyster Creek is a GE boiling water reactor (BWR) with a Mark I containment design as shown in Figure 1-1. The overall drywell general plan is obtained from Reference 3. The drywell is an inverted light bulb shaped containment vessel housing the primary nuclear vessel, the reactor coolant recirculation system, control rod drives and other primary systems. The drywell is connected to the suppression pool (torus) via 10 vent headers. Under accident conditions the primary objective of the drywell is to contain and channel reactor coolant flow to the torus, through the vent headers. The torus contains a suppression pool and gas space for the reduction of pressure by condensation and for containment of the reactor system coolant.

The major components in the drywell are the elliptical top head, cylindrical shell, spherical shell, vent lines with vent headers and downcomers and a suppression chamber (torus). There are 208 penetrations, including the vent lines, in the drywell shell.

The following sections provide a general description of the significant components and dimensions in the drywell. All of these components listed below have been included in the finite element model. All dimensions are obtained from Reference 3.

2.1 Top Head

The top head consists of a 2:1 elliptical head with a cylindrical section. The inside radius of the head is 16'-5 15/16". The height of the head is 8'-2 15/16". The thickness of the head is 1 3/16".

The cylindrical portion of the top head is comprised of two sections, one portion above the bolt flange assembly, and the other is below the bolt flange assembly. The height of the cylindrical shell that is above the bolt flange assembly is 4'- 9". The cylindrical shell joining the elliptical head and the bolt flange assembly has a nominal wall thickness of 1 ½".

The bottom portion of the cylindrical portion of the top head is the bolt-flange assembly. At the bottom of the cylindrical shell top head is the upper flange assembly with a diameter of 397 ¼".

The upper flange stiffeners are on the inside diameter, with a thickness of 2 ¼" and 5 ½" wide. The upper flange bolting ring assembly is on the outside diameter with a thickness of 2 ¼" and 5 ½". The bolt ring assembly has 96 eyebolts with a diameter of 2 ½", 3'-9" in length, evenly distributed around the circumference. The radius to the bolt hole centerline is 16'-10 ½" (measured from the drywell centerline). Vertical stiffeners, ¾" thick are located next to the bolt holes.

2.2 Upper Cylindrical Shell

The upper cylindrical shell extends from an elevation of approximately 71'-2" to 94'-9". It has an inside diameter for 33'-0" and a nominal wall thickness of 0.64".

At the top of the upper cylindrical shell is the lower flange bolting ring assembly and the lower flange stiffeners assembly. The cylindrical shell thickness next to the lower flange is 1 ¼", extended to a length 2'-6" below the top face of the lower flange.

The lower flange is 2 ¼" thick and 4 ½" wide. On the inside of the cylindrical shell is a stiffener 3/4" thick and 1' wide. Under the stiffener are vertical gusset plates, 3/8" thick, distributed in a pattern of 10°, 12 ½°, 15°, 15°, 12 ½°, and 10° along the circumference of the drywell, and repeated at 15° beyond this pattern.

At elevation 88'-8 1/2", there is a stiffener, ½" thick and 6" wide on the inside of the cylindrical shell. On top of the stiffener are gussets 3/8" thick. The spacing of these stiffeners is the same as those at the upper stiffeners.

Stiffeners on the outside of the cylindrical shell are the stiffeners for the eyebolt assembly. The eyebolt assembly shows how the bolts are connected to the stiffeners. The bottom end of the bolt has an eye to insert a cotter pin through the hole in the stiffeners. The stiffeners are 2 ¾" thick

and 7" wide. Between the lower flange and the stiffeners are the gussets. These gussets have a thickness of 1". On the outside of the stiffeners is a smaller stiffener. This smaller stiffener is 7 3/8" wide and 1" thick. There are three guided bolts evenly distribution along the bolting assembly. Next to the guided bolts, the stiffener thickness increases to 1 ¾".

At elevation 82' 9", there are 8 stabilizer insert plates, 2 ¼" thick, evenly distributed around the circumference. The stabilizer insert plates have a 5' 3" outside diameter, with a taper at the outside edge from the nominal thickness to 11/16" over a distance of 4 1/8". On the outside, two plates forming a male lug are welded onto the stabilizer insert plates at the elevation of 82'-2". The inner plate is 12 ½"x2 1/8" x 1' 6". The lug plate is 4 ¾" x 3" x 1' 6".

2.3 Knuckle

The knuckle is the stiffened transition between the upper cylinder and spherical portions of the drywell shell. The knuckle plate nominal thickness is 2 5/8". The top and bottom of the knuckle plate is at an elevation of 71'-10 25/32", and 65'- 2 7/16", respectively.

There is a row of weld pads at an elevation of 66' 3 5/32" in the knuckle component. It has 15 pads circular in shape with a diameter of 8", evenly located around the circumference of the knuckle component.

2.4 Spherical Shell

The spherical shell begins at an elevation of 2'-3" and ends at an elevation of 65'-2 7/16". The spherical shell has an inside radius of 35'. The center of the spherical shell is at an elevation of 37'-3". The bottom portion of spherical shell from elevation 2'-3" to 6'-10 5/16" is described further in Section 2.5. The remainder of the spherical shell has three different nominal wall thicknesses. From elevation 6'-10 5/16" to 23'-6 7/8", the nominal spherical shell thickness is 1.154". From elevation 23'-6 7/8" to 50'-11 1/8", the nominal wall thickness is 0.77". From elevation 50'-11 1/8" to 65'-2 7/16", the nominal wall thickness is 0.722".

There are 10 vent line penetrations at elevation 15'-7 ¼", evenly distributed around the spherical circumference starting at 0° azimuth. The penetration diameter is 7'-10". The insert plate has an outside radius of 5'-7 23/32" and an inside radius of 4'-1 25/32". The thickness of the insert plate is 2 7/8". The reinforcing penetration cylinder has a length of 1'-5" with a thickness of 2 ½".

The personnel lock and equipment hatch is at an elevation of 27'-6", and azimuth angle of 342°. The insert plate has a chord diameter of 14'-8 13/32". The reinforcing penetration cylinder has an inside diameter of 10'-0" with a wall thickness of 2 3/8" and extends out to 35'-9 1/8" from the centerline of the drywell. The wall thickness is then reduced to ½" and extends out to 40'-2" from the centerline of the reactor pressure vessel. In addition, the drywell shell adjacent to the equipment hatch has a wall thickness of 1.0625" while the drywell shell below the equipment hatch has a wall thickness of 1.154".

There are two rows of welding pads in the spherical shell. These are at elevation 61'-1 31/32" and 54'-9". There are 20 pads at elevation 61'-1 31/32" and 24 pads at the lower elevation. They are all distributed evenly around the circumference. The size of each weld pad is 8" diameter and ½" thick.

An upper beam support is located at an elevation 49'-3". It consists of a T-stiffener around the spherical circumference with vertical gussets at different azimuths. The stiffener is 12" x 5/8" and 8" x 2". The gussets are channel like with a height of 5'-0 1/16" and 1" thick separated by a distance of 12 ¼" with a bottom plate 8 3/16"x15 ¼"x1". There are 20 beam support gussets distributed at differential azimuths.

The lower beam seats are located at an elevation with a meridional radius 31'-3". There are 20 seats distributed at different azimuth angle around the circumference. The seat pad is 22" in diameter and 1" thick. A channel like structure is welded onto the seat pad.

2.5 Bottom Head

The bottom head of the drywell is from the bottom of the spherical shell to an elevation at 6'-10 5/16". The nominal wall thickness is 0.676. The entire bottom head is embedded in concrete on both the inside and outside surfaces.

2.6 Vent Lines, Headers and Downcomers

The main portion of the vent line is at an angle of 38°-12'-28" with horizontal elevation. This main portion has three sections: a conical section with a wall thickness of 7/16" and a length of 1'-11 13/16", a middle section with a wall thickness of ¼" and a length of 14'-3/4", and an end section with a wall thickness of 5/16" and a length of 4'-2 5/16". The cross component in the vent line is at an angle of 17° with the elevation. It has three components, a pipe section, cross section and an elliptical head. The pipe section has a thickness of 5/16" with a length of 2'-5 3/16". The cross section has a ¼" wall thickness and a length of 8'-2" with a 4'-7" diameter branch opening. The elliptical head has a wall thickness of 5/16".

The centerline of the headers is at a radius of 50'-6" from the vertical axis of the drywell. It has an inside diameter of 4'-7" with a wall thickness of ¼". The center length of the header is 15'-11 15/16" with the end length of 3'-8 23/32".

The downcomers extend from the headers at 45° and turns vertical downward in three sections. The downcomers have an outside diameter of 2'. The 45° section has a wall thickness of ½". The other two sections have a wall thickness of ¼". The vertical downcomers are 7' on center from one side of the downcomers to the other side. The downcomers are extended to 110.16" vertically from the center of the headers.

The vent line penetrations at the drywell are shielded by a vent jet deflector. The deflector is a perforated circular plate with 5'-0" radius and 2 ½" thick. It is supported by 20 gussets evenly distributed around the outside edge of the plate. The gussets are 1'-10 ½" high and 7/8" thick.

2.7 Material Specifications

The general material specifications are provided in Reference 3. These are summarized below:

- Plates – A212 Grade B FBX to A300, minimum longitudinal Charpy V notch impact test values of 20 ft-lbs at 0° F on full size specimens.
- Forgings – A350 Grade LF1, Charpy V-notch impact test values of 13 ft-lbs at 0 °F.
- Pipe – A333 Grade "O" seamless, Charpy V-notch impact test values of full size specimens of 13 ft-lbs at 0 °F.
- Miscellaneous Plate & Structural Steel – A36.

Specifications as identified in Reference 3;

1. Burns & Roe Specification S-2299-4.
2. ASME Code, Section VIII, Latest Edition and Addenda with nuclear code case interpretations 1272N-5, 1272N-5 and all other applicable case interpretations.
3. AISC specification for structural steel latest edition.

2.8 Penetrations

There are 208 penetrations in the drywell, as shown in Table 5-3. The sizes vary from 36" to 1" except the vent openings (X-49) and equipment hatch (X-1). The penetration details are from Reference 3.

3.0 DRYWELL THICKNESS DESCRIPTION

In November of 1986, thinning of the Oyster Creek drywell shell was observed. At that time, GPUN implemented a program to monitor the drywell shell wall thickness. Since then, the licensee monitors the Oyster Creek drywell wall thickness using ultrasonic techniques. Measurements are taken from both the interior and exterior of the drywell shell depending on the elevation.

For this analysis (Base Case), representative thicknesses in the sandbed region were defined based on the actual ultrasonic measurements taken from inside the drywell during the 2006 refueling outage. The UT measurements taken from outside the drywell are less representative since these measurements purposely concentrated on local thin areas (less than 2 ½" in diameter) and due to the surface preparations needed to obtain accurate external UT reading. However, the external readings were used to define locally thinned areas within certain bays.

For regions outside the sandbed areas, a representative value was chosen based on the thinnest average grid values from the monitoring program and associated calculations that have been provided to the regulator in various presentations and submittals. Although this remains conservative (selecting the thinnest average value), the variability in the data is not significant and the values used are consistent with those previously provided to regulatory organizations.

For the sandbed region, because of the concern regarding the margin in that region, representative general thickness values are determined based on the following:

a) As noted earlier, internal grid measurements were used as the basis for the representative thickness. These measurements were considered to be the most accurate since the coating on the inside surface of the drywell was removed for the measurements and a protective grease coating was applied after measurements were taken (to eliminate the possibility of internal surface corrosion). The average internal grid measurements were used as the primary indicator of the representative general thickness of each bay. However, other data sources were used to verify or augment the applicable values for each of the bays. These other sources of data were the

external data, pictures of the external surfaces of the sandbed, and the trench data in Bays 5 and 17.

b) The external individual UT readings were deliberate attempts to identify the thinnest local areas less than 2 ½" inches in diameter in each bay. Therefore, using these values (only) to define representative general thicknesses is not appropriate. However, the external data was used to define locally thin areas that are thinner than 0.736" (see item c below) and that are included in the analysis model.

c) The measurement data makes it evident that the wall loss experienced while the sand was present (in the sandbed) did not encompass the entire sandbed region from elevation 8'11" to 12' 3" since the regions were either not completely filled with sand or not completely filled with water. Pictures taken in 1992 of the external shell surface (after sand removal) confirmed the presence of a "transition" line at approximate elevation 11'. Above this "transition" line the thickness of the vessel is close to nominal wall thickness in most bays and below the line are areas that exhibit wall loss due to the corrosion. Therefore, the general wall thickness of each sandbed bay has been divided into two areas; above and below elevation 11' 0". This will reduce the conservatism that would be introduced by assuming the entire bay thickness is equivalent to an average of the external readings or the average of the internal grids readings.

d) Where the internal grid measurements were clearly not representative of the corrosion on the shell in that bay, representative measurements from adjacent bays were utilized to provide a representative general thickness.

e) Where the trenches were cut out of the drywell floor (elevation 10' 3") allowing UT measurements from the inside the Drywell in large areas, these measurements were used to determine the general thickness of these bays (Bays 5 and 17). The trench UT data consists of hundreds of individual UT readings over a large area, rather than only 49 readings or less over smaller regions. Therefore, the results of these inspections are concluded to be representative of the general thickness of these two bays.

f) Where the internal data indicates a "transition" line through the grid, the average of the lower readings were used to define that particular bay general thickness below elevation 11'.

g) In one case (Bay 15) there were no internal grid or external individual data available below elevation 11'. Therefore, an average of the two adjacent bays was used. The basis for this approach is the assumption that there is a general wall thickness gradient between the two adjacent bays that would adequately represent the general thickness of the bay between them.

h) For Bays 9, 15, and 17 (above elevation 11') there are multiple internal grids. Therefore in these bays, the weighted average of the multiple grids were calculated by summing the total number of valid thickness readings and dividing by the total number of valid readings.

In several bays of the sandbed region there are locally thinned areas that are thinner than 0.736" and are confined to an area no larger than 36" by 36". These areas were modeled in the finite element model as defined locally thinned circular areas rather than square areas (to facilitate computer modeling). The circular areas completely capture the documented square areas. This introduces some additional conservatism since the area of the circles exceeds the area of the squares.

Tables 3-1 and 3-2 provide representative thicknesses of the Drywell Vessel based on 2006 inspection and other past inspections. These values were used as general thickness values for the associated region. Table 3-3 summarizes the wall thickness used in the analysis. The modeling of the locally thinned areas is summarized in Table 3-4.

In addition since there are several locally thinned areas in the sandbed, specific thin areas will be modeled per Figure 3-1 through Figure 3-5. All thinning wall thickness information is contained in Reference 4.

Table 3-1: Regions other than the Sandbed [4]

Region	Elevations	Value in mils	References
Cylindrical Region	71' 6" to 93'	604	1) Oyster Creek License Renewal ACRS 1/18/07 Presentations Slide 14 2) 1994 average grid value for grid 9-20 Calculation C-1302-187-5320-037 Revision 3 appendix 7 page A7-20 of 29
Knuckle Region	65' 2 7/8" to 71' 6"	2530	1) Oyster Creek License Renewal ACRS 1/18/07 Presentations Slide 14 2) 2006 average grid value for bay 9 Calculation C-1302-187-5320-037 Revision 3 page 11 of 48
Upper Spherical Region	50' 11/18" to 65' 2 7/8"	676	1) Oyster Creek License Renewal ACRS 1/18/07 Presentations Slide 14 2) 1994 average grid value for grid 13 –32 - Calculation C-1302-187-5320-037 Revision 3 appendix 5 page A5-23 of 38
Middle Spherical Region	37' 3" to 50' 11/18"	678	1) Oyster Creek License Renewal ACRS 1/18/07 Presentations Slide 14 2) 2006 average grid value for grid 13–31 - Calculation C-1302-187-5320-037 Revision 3 appendix 3 page A3-24 of 36
Lower Spherical Region	To 23' 6 7/8" to 37' 3"	1160	1) Oyster Creek License Renewal ACRS 1/18/07 Presentations Slide 14 2) 2006 average grid value for bay 19- Calculation C-1302-187-5320-037 Revision 3 page 11 of 48
Embedded Region (1.154" Nominal Thickness)	6' 7" below 8' 11"	1113	1) Oyster Creek License Renewal ACRS 1/18/07 Presentations Slide 124 2) Tech Eval 00546049-07, Attachment 7 page 1 of 2 "Water Found in Drywell Bay 5 – UT Data Evaluation
Embedded Region (0.676 Nominal Thickness)	Below 6' 7"	636	1) Tech Eval 00546049-07, page 8 of 10 "Water Found in Drywell Bay 5 – UT Data Evaluation

Table 3-2: Sandbed Region General Area Thicknesses [4]

BAY	Above Elevation 11'-0" (mils)	Basis	Below Elevation 11'-0" (mils)	Basis
1	826	Same value as used for Bay 19 (adjacent bay)	826	Same value as used for Bay 19 (adjacent bay)
3	1180	Internal grid average (single grid)	950	Numerical average thickness between Bays 1 & 5
5	1185	Internal grid average (single grid)	1074	Average of internal trench data points (six 49 point grids).
7	1133	Internal grid average (single grid)	1034	Numerical average thickness between Bays 5 & 9
9	1074	Weighted average of two internal grids (49 point and 7 point)	993	Smaller of the two internal grid averages (49 point grid)
11	860	Average of two internal grids (both 49 point)	860	Average of two internal grids (both 49 point)
13	907	Average of two internal grids (both 49 point; 7 point grid data not used)	907	Average of three internal grids (both 49 point; 7 point grid data not used)
15	1062	Weighted average of two internal grids (49 point and 7 point)	935	Numerical average thickness between Bays 13 & 17
17	863	Weighted average of the bottom of internal grid 17A (28 points) and internal grid 17D (49 points) Data for grid 17/19 not used.	963	Average of internal trench data points (six 49 point grids).
19	826	Average of three internal grids (all 49 points)	826	Average of three internal grids (all 49 points)

Table 3-3: Summary of Oyster Creek Drywell Thicknesses For Use In Analysis

LOCATION		THICKNESS (mils)
Cylindrical Region		604
Knuckle Region		2530
Upper Spherical Region		676
Middle Spherical Region		678
Lower Spherical Region (Note 1)		1160
Embedded Region (1154 Nominal Thickness)		1113
Embedded Region (676 Nominal Thickness)		636
SANDBED REGION		
BAY	Above Elevation 11'-0" (mils)	Below Elevation 11'-0" (mils)
1	826	826
3	1180	950
5	1185	1074
7	1133	1034
9	1074	993
11	860	860
13	907	907
15	1062	935
17	863	963
19	826	826

Table 3-4: Local Thinned Area Modeling

Sandbed Region	Diameter (inches)		Thickness (mils)	
Bay 1	51		696	
Bay 13	18		658	
Bay 15	18		711	
Bay 17	18 (1)	51 (2)	663 (1)	850 (2)
Bay 19	51		720	

Notes: (1) Inner circle of locally thinned area.
(2) Outer ring of locally thinned area.

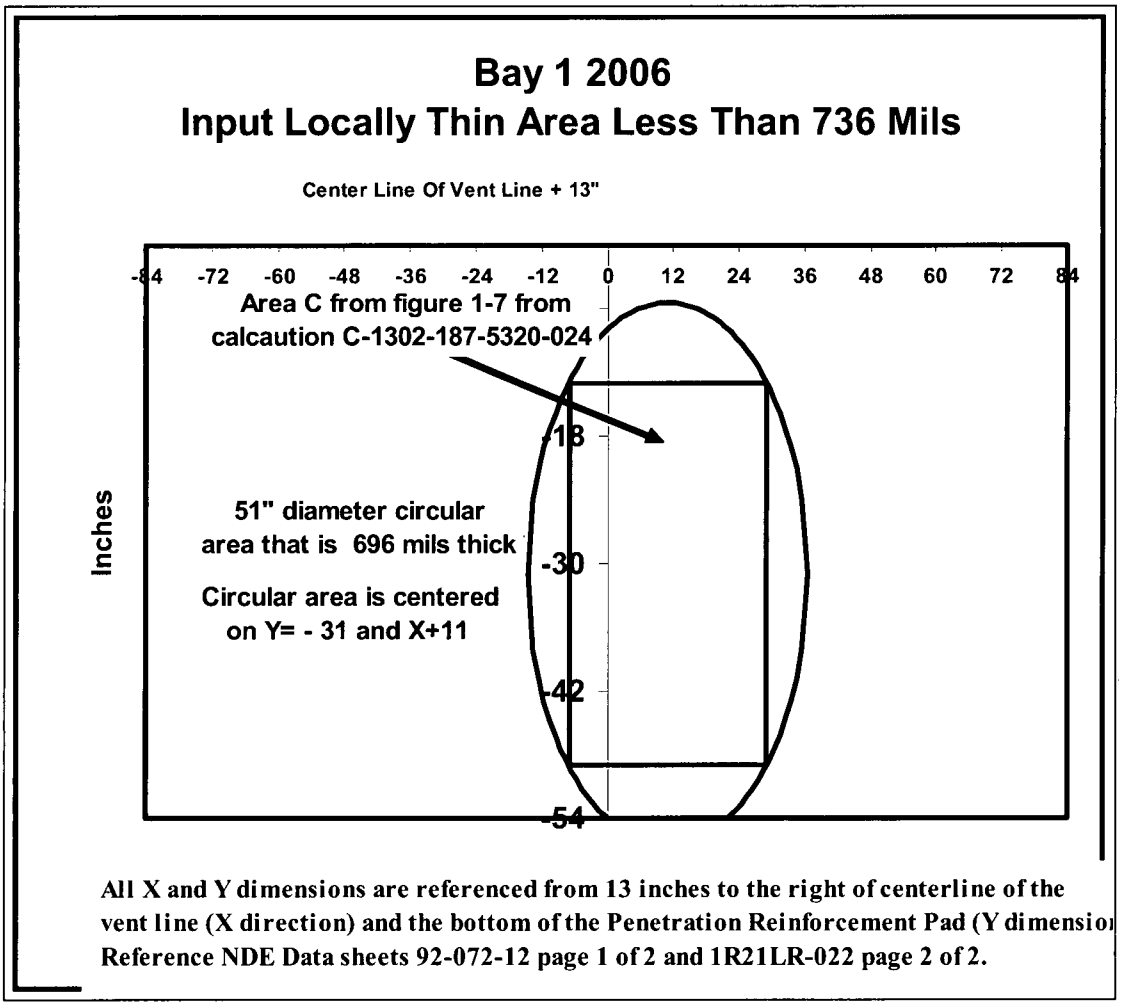

Figure 3-1: Bay 1 2006 [4]

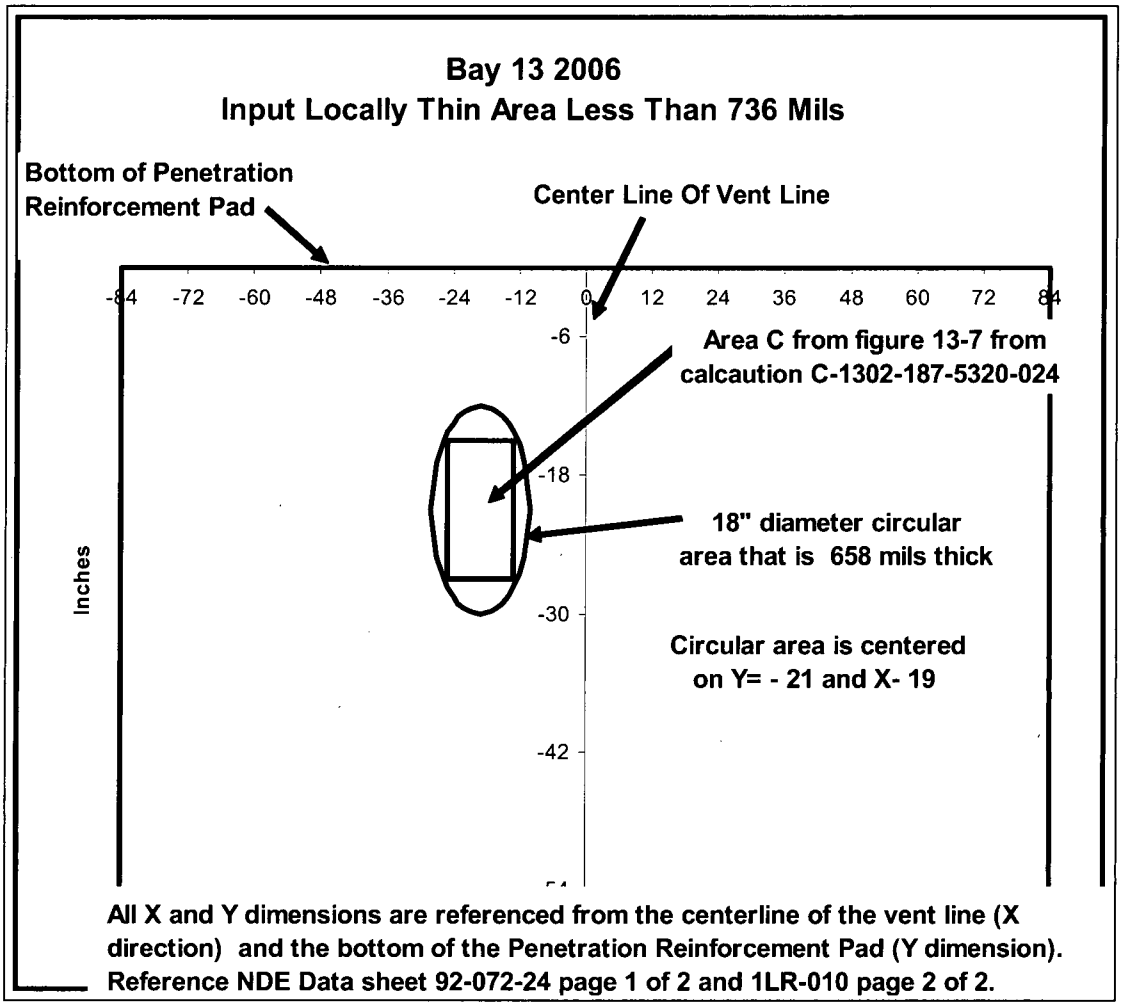

Figure 3-2: Bay 13 2006 [4]

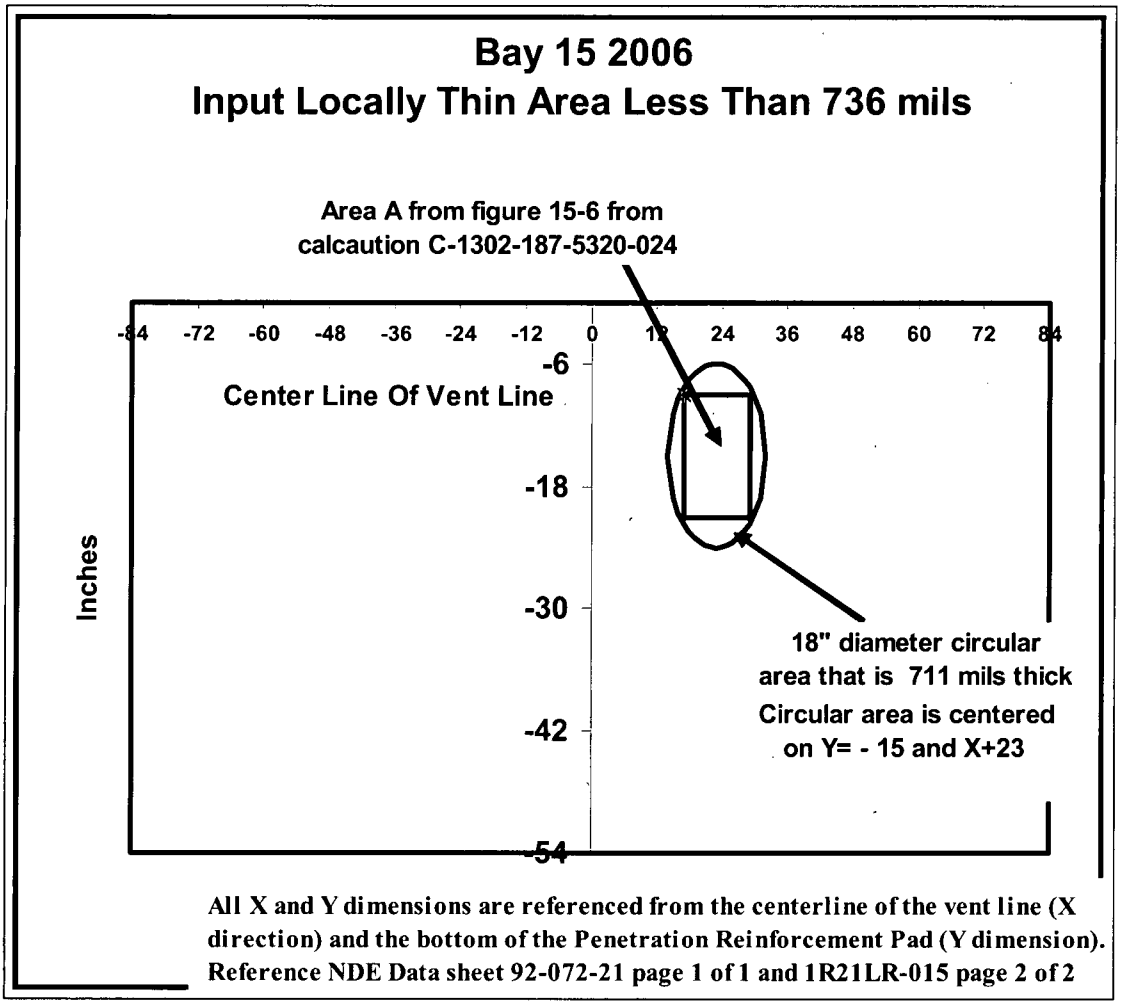

Figure 3-3: Bay 15 2006 [4]

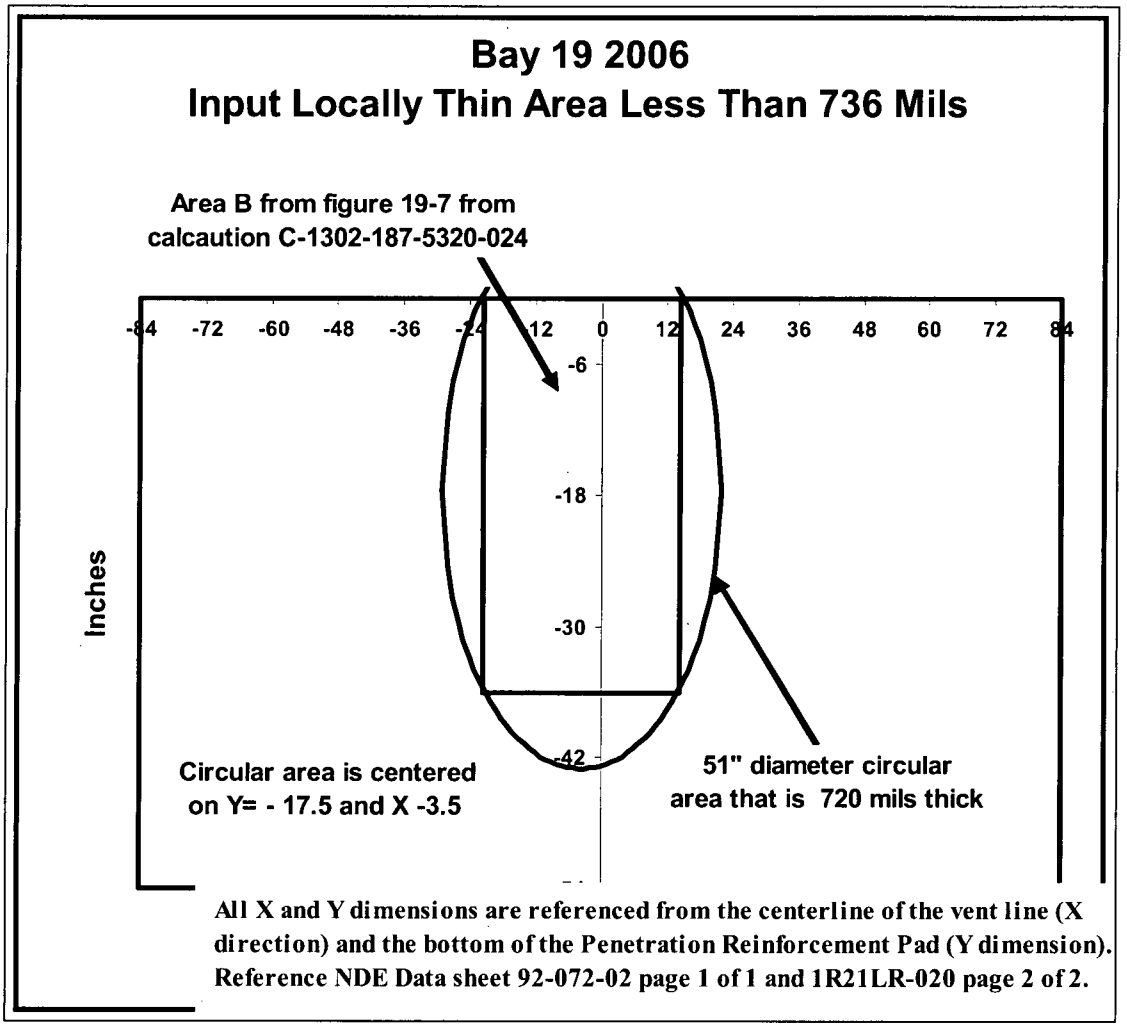

Figure 3-4: Bay 19 2006 [4]

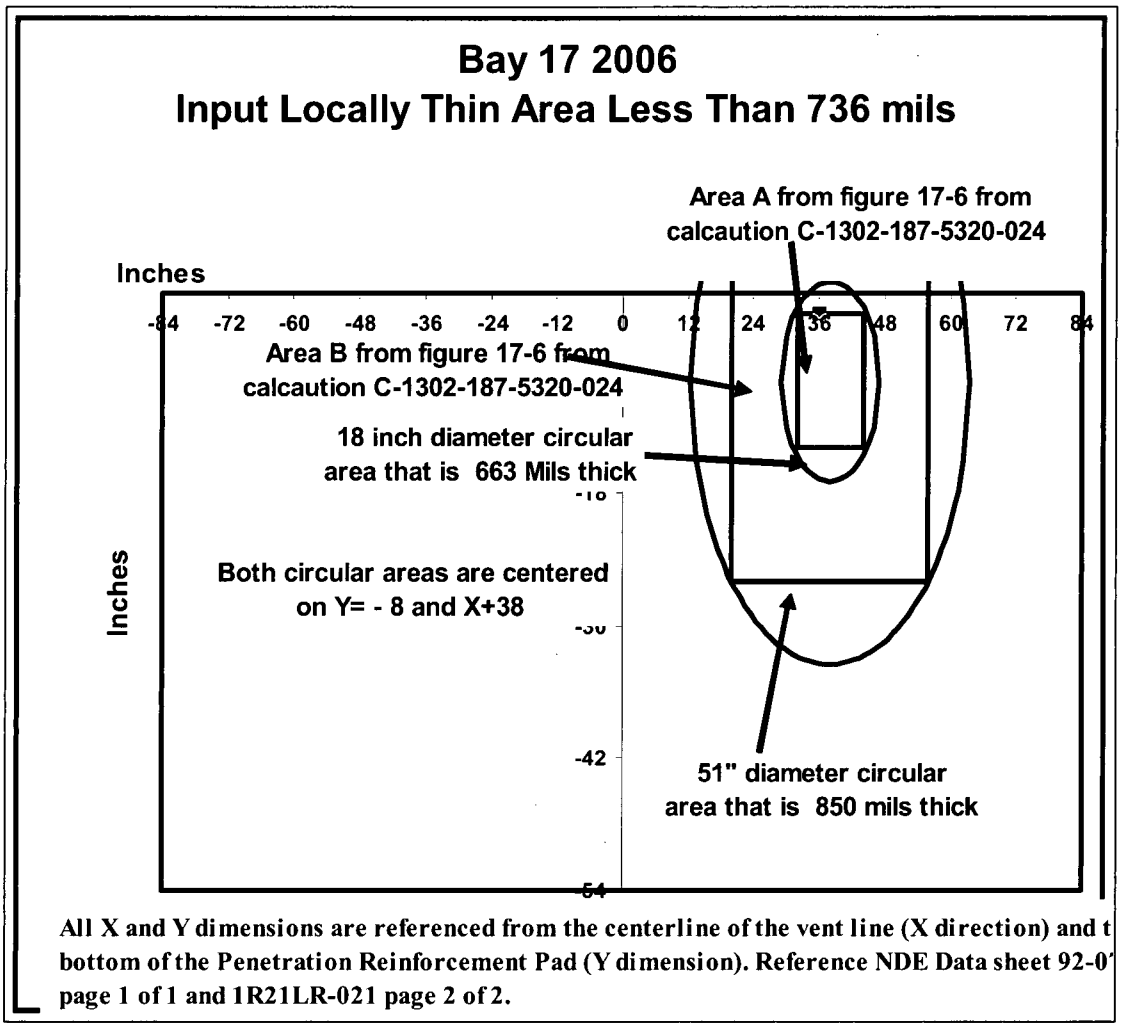

Figure 3-5: Bay 17 2006 [4]

4.0 FINITE ELEMENT MODEL

This section describes the finite element model used for the structural integrity evaluation of the drywell shell, including the ASME Code buckling evaluation and stress analysis. The original design analysis [1, 2, 5] used simplified methods and assumptions to estimate the margins in the drywell. The availability of advanced analyses techniques and computation capability allows for the use of a more realistic representation of the drywell shell and associated components. The finite element model includes, in significant detail, modeling all of the components discussed in Section 2.0. The inclusion of this level of detail allows the model to account for the asymmetric behavior of the drywell shell.

Of special interest in the modeling of the drywell was the representation of the drywell wall thicknesses. This includes the wall thicknesses measured in the sandbed regions and in other locations. Section 3.0 describes the wall thickness observed in the drywell shell (sandbed and elsewhere), and how these thickness measurements were incorporated into the finite element model.

4.1 Finite Element Modeling

All dimensions (except for wall thicknesses) for developing the model were obtained from the Chicago Bridge & Iron (CB&I) drawings listed in Reference 3. Material properties designations were also obtained from these drawings. Material property values are obtained from References 6 to 10. The materials for the major components in the drywell are summarized in Table 4-1.

The finite element model of the Oyster Creek drywell is shown in Figure 4-1 through Figure 4-17. The entire geometry is created using area entities in a 3-D space at the mid-thickness location of the parts. The global Cartesian coordinate system for the geometry is arranged such that the global X-axis is in the plan view 0° azimuth (East) position, and the global Y-axis is in the plan view 90° azimuth (South) position.

Real, type, and material numbering in ANSYS [25] were used to distinguish the different components. Real numbers are for the thicknesses, type numbers for the assemblies, and material numbers for the different material associated with the entire drywell assembly.

Details of the drywell modeling are presented in Figure 4-4 through Figure 4-17. Figure 4-4 shows the cut-out view of the top head/cylindrical/knuckle region of the drywell and the details inside the drywell. Figure 4-5 presents the details of the flange stiffeners and gussets. Figure 4-6 shows the knuckle component with the upper weld pads. Figure 4-7 shows the star truss details inside the cylindrical shell. Figure 4-8 shows the other details inside the cylindrical portion of the drywell. The different shading or color in the above and subsequent figures represents the different 'real' properties used to define the thickness. It should be noted that, even if the sections have the same thickness, they are defined by different 'real' property identification numbers and they would appear in different color or shade in the figures.

Figure 4-9 and Figure 4-10 shows the isometric view and cut-out view of the spherical region of the drywell, showing the upper beam support, lower beam support, stiffeners, vent pipes, and equipment hatch/personnel lock. Figure 4-11 shows the details of weld pads and vent pipe flanges. Figure 4-12 and Figure 4-13 show the sandbed region locally thinned areas and the identification numbers, of individual bays.

Figure 4-14 shows the typical modeling of penetrations with reinforcing plates. Figure 4-15 shows the typical modeling of a penetration with an insert plate. The insert plate is a thicker plate that is inserted into an opening in the drywell shell where the mid-thickness of the insert plate is at the same radial distance as the drywell shell. The reinforcing plate is referred to a plate that is placed on the outside surface of the drywell shell.

Figure 4-16 presents the modeling of the trenches. Figure 4-17 presents the modeling of the vent pipe and deflector plate.

The model has more than 406,000 elements and approximately 400,000 nodes. The typical sizes of the elements in different regions of the drywell are summarized in Table 4-2. The finite element mesh is presented in Figure 4-18 through Figure 4-20. The mesh for each locally thinned area is presented in Figure 4-21 through Figure 4-25.

The key guidelines and assumptions used in generating the finite element model are as follows:

1. All shell radial locations (radial position of shell element nodes) were based on the midpoint of the nominal shell thickness.
2. Gusset plates for the guiding pins were not included in the model. These gusset plates were designed to provide more support for the guiding pins for the purpose of installation of the top head. In addition, there are only 4 gusset plates for the guiding pins versus 96 pairs of gusset plates for the top head bolts. It is judged that the 96 pairs of gusset plates, without the 4 gusset plates for the guiding pins, would provide a conservative representation of the stresses in the upper/lower flange.
3. Transitions zones are created for joints that go from one shell thickness to another. The thickness of these transition zones are the average thickness of the adjacent two shells. These are applicable mostly for the penetration insert plates which have a greater thickness than the drywell shell.
4. For penetrations with reinforcing plates, the welds are assigned the same materials as the pipe; the shell thickness of the weld are set to the throat thickness of the weld callout; the radial distance of the reinforcing plates is from mid-thickness of the drywell wall to mid-thickness of the reinforcing plate.
5. For penetrations with insert plates, the transition zones are assigned the same materials as the insert plate.
6. The vertical location of the lower flange bolting ring and outer water seal ring are at the midpoint thicknesses.
7. For the star truss assembly, the modeling included the male lug with the base plate and the inside truss assembly.

8. The manhole details in the star truss insert plates and in the top head, and the access openings in the star truss insert plates were not modeled. These details are not significant in the overall stress and buckling evaluation of the drywell analysis.
9. The lifting lugs were not modeled because they are not used during normal operation.
10. Fillet radii were not modeled due to the use of shell elements. Also, the corner radius of the insert plates for the small diameter penetrations was not modeled. This is conservative due to being modeled as square corners in the insert plates.
11. For the weld pads at the knuckle region, the space between the reinforcement pad and the shell is modeled from the surface of the shell to the distance equal to the size of the fillet weld (as opposed to mid-thickness to mid-thickness.)
12. The contact between the upper flange and lower flange was modeled as an integral connection due to the use of shell elements and it's limitation in the capabilities to model accurately the contact behavior between the upper and lower flanges. The complexity of the contact behavior between the upper flange and lower flanges under the bolt preload and the operational loads can only be modeled by contact elements between the flanges with the use of solid elements for the flanges.
13. The flange bolts were modeled as beam elements. No preload was applied to the bolts, due to the limitations as described in items (8) and (12).
14. Penetrations that are 3" or smaller are not specifically modeled. Instead, only their reinforcing plates or insert plates are modeled to account for the added stiffness of the plates. Based on the Code Requirements, these small penetrations do not require area of reinforcement indicating that local high stress is not a concern.
15. At penetrations the pipes are truncated at 3" from the drywell shell. The length was selected using the gap between the drywell shell and the reactor building concrete wall as a guideline and applied to both inside and outside of the drywell.
16. The sandbed region is between elevations 8'-11 ¼" and 12'-3". However, the sandbed region does not extend into the insert plates of the vent lines, Figure 4-12.
17. Per Reference 4, each bay within the sandbed region has two general thicknesses: one above elevation 11'-0" and one below that elevation (see Table 3-2). Also, the locally thinned areas within the sandbed region are of circular pattern and have different

thicknesses from the sandbed region. They are explicitly modeled and shown in Figure 4-13.

18. For penetrations with reinforcing plates, the vessel shell-to-plate interface is taken at the mid-thickness level, and the fillet weld connection is represented by an area ring with the weld throat thickness, Figure 4-14.
19. For penetrations with insert plates, the vessel shell-to-plate connection is taken at the mid-thickness level, and the thickness transition is represented by a ring area with a thickness equivalent to the average thickness between the shell and the plate, Figure 4-15.
20. The equipment/personnel hatch is simplified to a cylinder with two flange rings connected to the hatch cylinder. The two doors inside the hatch are not modeled. Instead, they are represented by two circular discs. The other internals are also not modeled due to their complexities. This simplification is appropriate because the main objective in this evaluation is to study the effect of the reduced thickness in the sandbed region on the buckling. The equipment hatch is also separated from the sandbed region by the vent pipes and the insert plates. Therefore, the effect on stress due to any simplification in the modeling of the equipment hatch will be local to the drywell shell region next to the equipment hatch (which is not an evaluation area of interest).
21. Per Reference 11, there are concrete excavation trenches in Bay 5 and Bay 17, Figure 4-16. The Bay 17 Trench is 20" wide [11] and is conservatively assumed to extend to the sandbed region bottom elevation at 8'-11 ¼".
22. The Bay 5 trench portion that is below the sandbed region is 10.5" wide (maximum) and 6.5" along the inside contour of the vessel shell [11]. The 6.5" contour length translates to an approximately 4" elevation change to the vessel mid-surface.

    Note, per Reference 11, the trench portion within the sandbed region is documented as 20" wide. However, since this portion is within the sandbed region and not subject to any boundary conditions and it is surrounded by the concrete and would not experience high stress the trench is simplified to have a constant width of 10.5" in the geometry.

23. The perforated deflector plates of the vent pipes are simplified as solid spherical discs Figure 4-17. Their density and stiffness will be adjusted accordingly based simply on the ratio of the hole area to the whole plate area to account for the effect of perforation holes.

The vent header/downcomer is modeled to include its stiffness effect on the rest of the drywell structure. It is not intended for any stress or buckling evaluation.

The finite element software used to generate the model is ANSYS Rev. 8.1 [12] and Rev. 11 [25] finite element program was used for stress and buckling analyses.

Table 4-1: Major Components and Dimensions

Component	Elevation/Height	Dimensions	Thickness	Material	Drawing No. 9-0971	Note
Top Head	El. 107'-10 3/16" at top	IR: 16'-5 15/16" SR: 29'-4 21/32"	1-3/16"	A212 B FBX to A300	Sht. 7, Rev. 5	2:1 ellipse
Top Head Flange Assembly Cylindrical Shell	Ht.: 7'-3"	IR: 16'-5 15/16"	1 ½"	A212 B FBX to A300	Sht. 7, Rev. 5 Sht. 29, Rev. 7	
Top Head Flange Assembly Upper Stiffener	El. 96'-9" Top Face	IR: 16' 3/8"	2 ¼" 5 ½ wide	A212 B FBX to A300	Sht. 29, Rev. 7	
Top Head Flange Assembly Flange	Ht. 2.25" El. 96'-9" Top Face	CLD:397.25"	2 ¼" 5 ½ wide	A212 B FBX to A300	Sht. 29, Rev. 7	
Cylindrical Shell Flange	Ht. 2.25" El. 94'-9" Top Face	CLD:397.25"	2 ¼" 4 ¼" wide	A212 B FBX to A300	Sht. 29, Rev. 7	
Eye Bolts			2 ½" Dia.	A320 L7	Sht. 29, Rev. 7	
Cylindrical Shell Stiffener	El. 92'-10.75" Top Face	OD: 34' 4 ½"	2.75" wide	A212 B FBX to A300	Sht. 29, Rev. 7	
Cylindrical Shell	Ht. 20'4-7/32"	IR:16'-6"	0.64"	A212 B FBX to A300	Sht. 2, Rev. 10 Sht. 7, Rev. 5	
Cylindrical Shell Stabilizers	El. 82'-9"	OD: 5'-3"	2 ¼"	A212 B FBX to A300	Sht. 36, Rev. 4	
Knuckle Section	Top: 71'-10 25/32" Bottom: 65'-2 7/16"		2 5/8"	A212 B FBX to A300	Sht. 6,Rev. 3	

Table 4-1: Major Components and Dimensions (cont'd)

Component	Elevation/Height	Dimensions	Thickness	Material	Drawing No. 9-0971	Note
Spherical Shell	El. 65'-2 7/16" at top El. 50'-11 1/8" at middle El. 2'-3" at bottom	IR 35'	Top: 0.72" Middle: 0.77" Bottom: 1.154" Next to Hatch: 1.0625"	A212 B FBX to A300	Sht. 1, Rev. 2 Sht. 2, Rev. 10	Equator El at 37'-3"
Welding Pads	El. 66'-3 5/32" El. 61'-1 31/32" El. 54'- 9"	8"∅ (x15) 8" ∅ (x20) 8" ∅ (x24)	0.5" 0.5" 0.5"	A212 B FBX to A300	Sht. 32, Rev. 2	
Upper Beam Supports	El. 49'-3"		T-beam 8"x2", 12"x5/8"	A201 B FBX A212 B FBX to A300	Sht. 35, Rev. 4	
Lower Beam Seats	EL. 21'-5 7/8"	22" ∅ Reinforcing Plate	1"	A212 B FBX to A300	Sht. 34, Rev. 4	
Personnel Lock & Eq. Hatch	El. 27' 6"	ID 10'-0"		A212 B FBX to A300	Sht. 40, Rev. 2 Sht. 100, Rev.2 Sht. 101, Rev. 2	
Bottom Head			0.676"	A212 B FBX to A300	Sht. 1, Rev. 2 Sht. 3, Rev. 2 Sht. 5, Rev. 3	
Vent Penetrations	El. 15'- 7.25"	ID 7'-10"	2-7/8" and 2.5"	A212 B FBX to A300	Sht. 2, Rev.10 Sht. 21, Rev. 2	
Vent Line Jet Deflector		5'∅	2 ½"	USS T1	Sht. 38, Rev. 1	
Vent Lines	Inclined at ≅ 38° Angle	ID 6'-6"	0.25"	A212 B FBX to A300	Sht. 61, Rev. 6 Sht. 62, Rev. 3	
Vent Headers	El. 1'-10 1/8"	ID 4'-7"	0.25"	A212 B FBX to A300	Sht. 1, Rev. 2 Sht. 61, Rev. 6	
Vent Downcomers		OD 2'	¼" and ½"	A212 B FBX to A300		

Table 4-2: Typical Mesh Size

Region	General Mesh Size (inch)
Local Thinning Area	0.75
Sandbed Region	1.5
Mid Spherical Shell	3
Knuckle Region	3
Cylindrical Shell	3
Top Dome	6
6" or smaller penetrations	2.5
8" or larger penetrations	5
Vent Pipe	6
Vent Header	10
Equipment Hatch	6
Bottom Spherical Shell (within concrete)	12

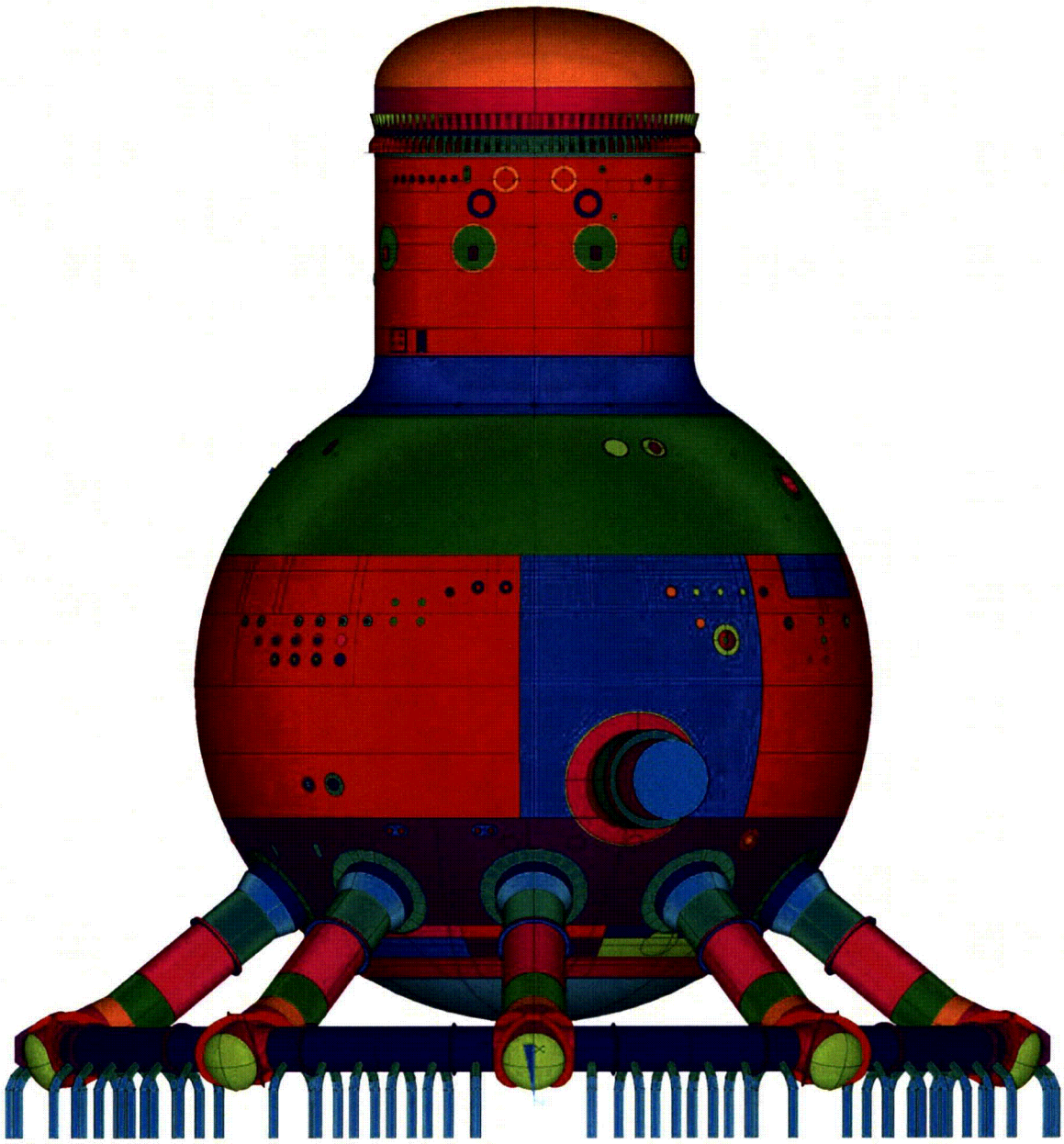

Figure 4-1: Elevation View of Model Assembly

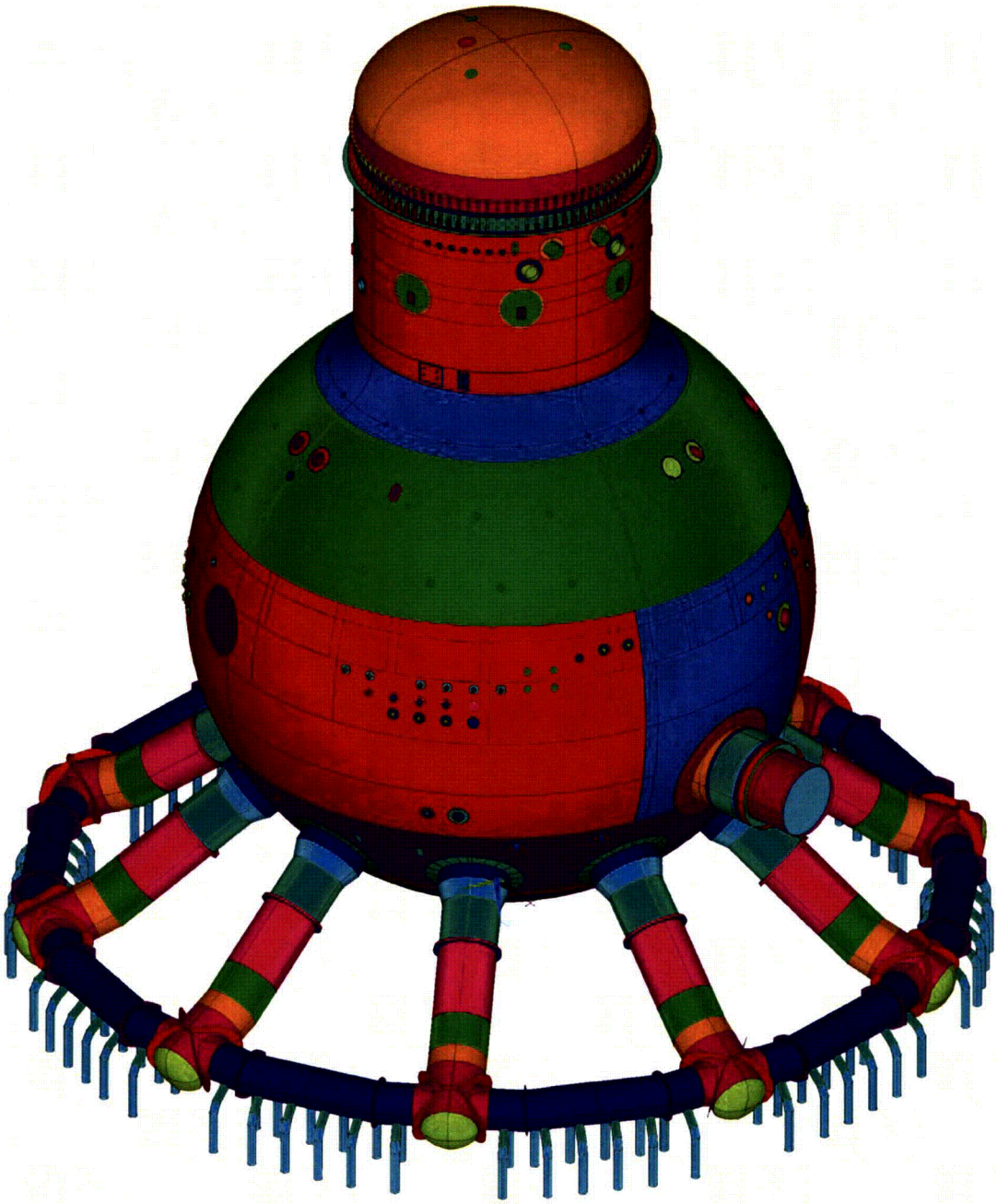

Figure 4-2: Isometric View of Model Assembly

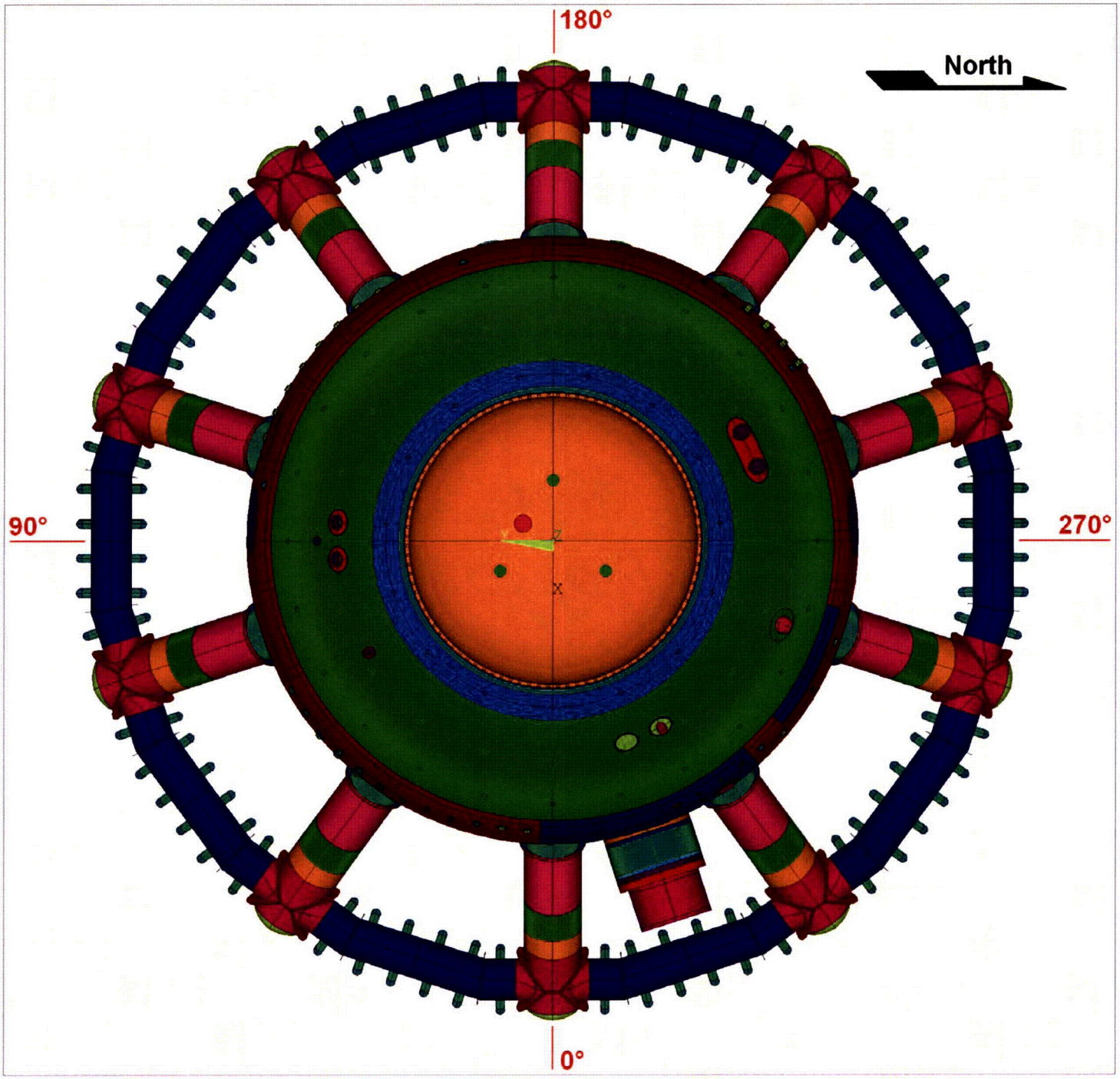

Figure 4-3: Top View of Model Assembly

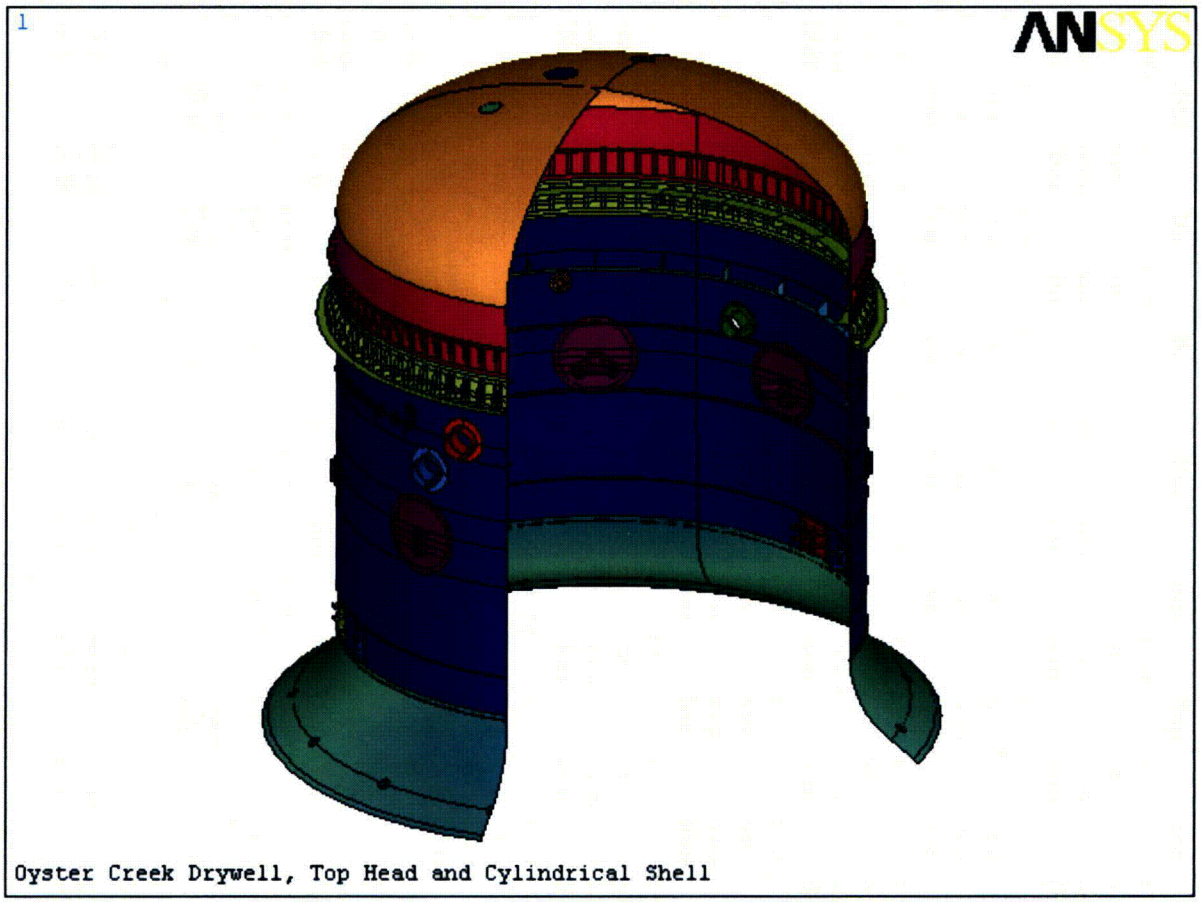

Figure 4-4: Over all Cut-out View of the Top Head and Cylindrical Shell

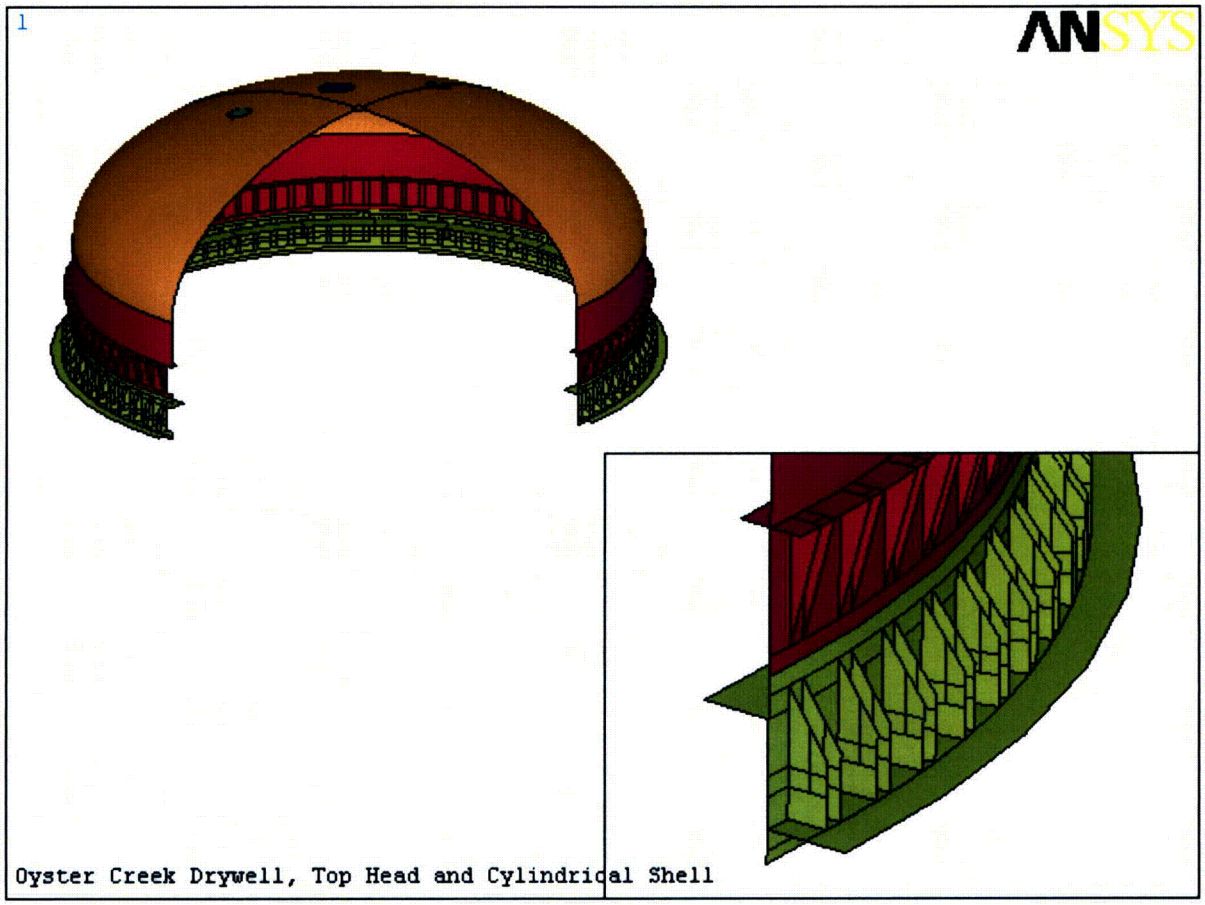

Figure 4-5: Elliptical Dome, Top Flange and Bottom Flange Assembly

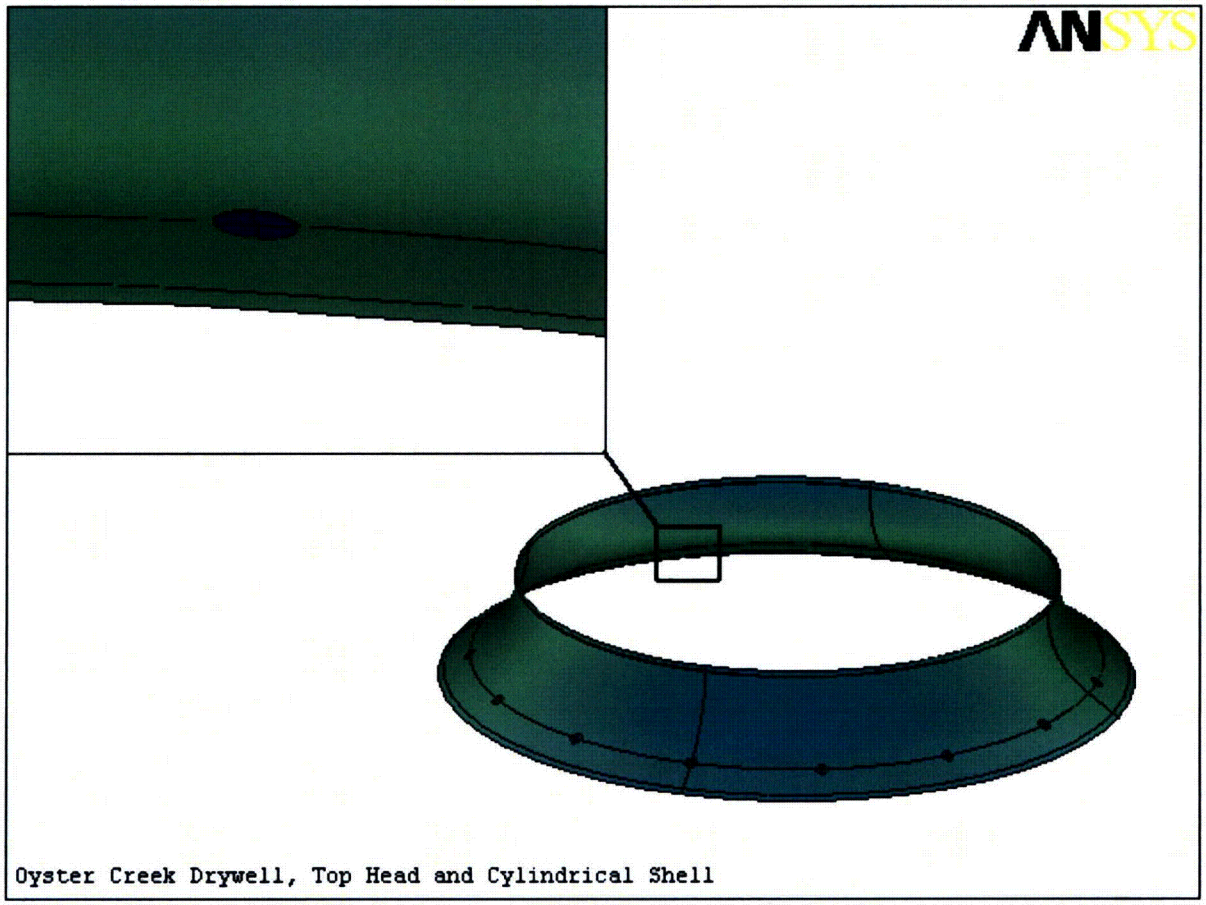

Figure 4-6: Knuckle Region Assembly Showing Weld Pad

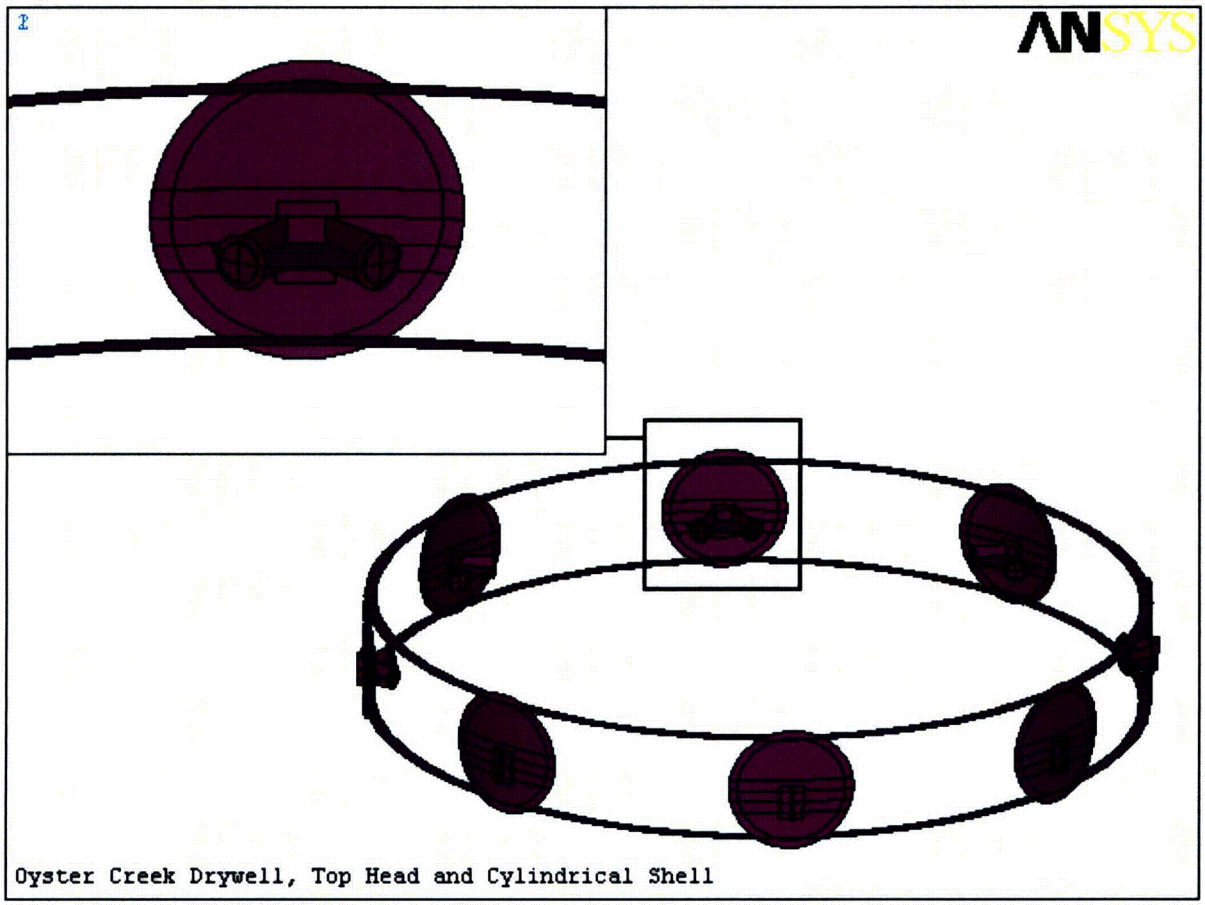

Figure 4-7: Stabilizer ("Star Truss") Assembly

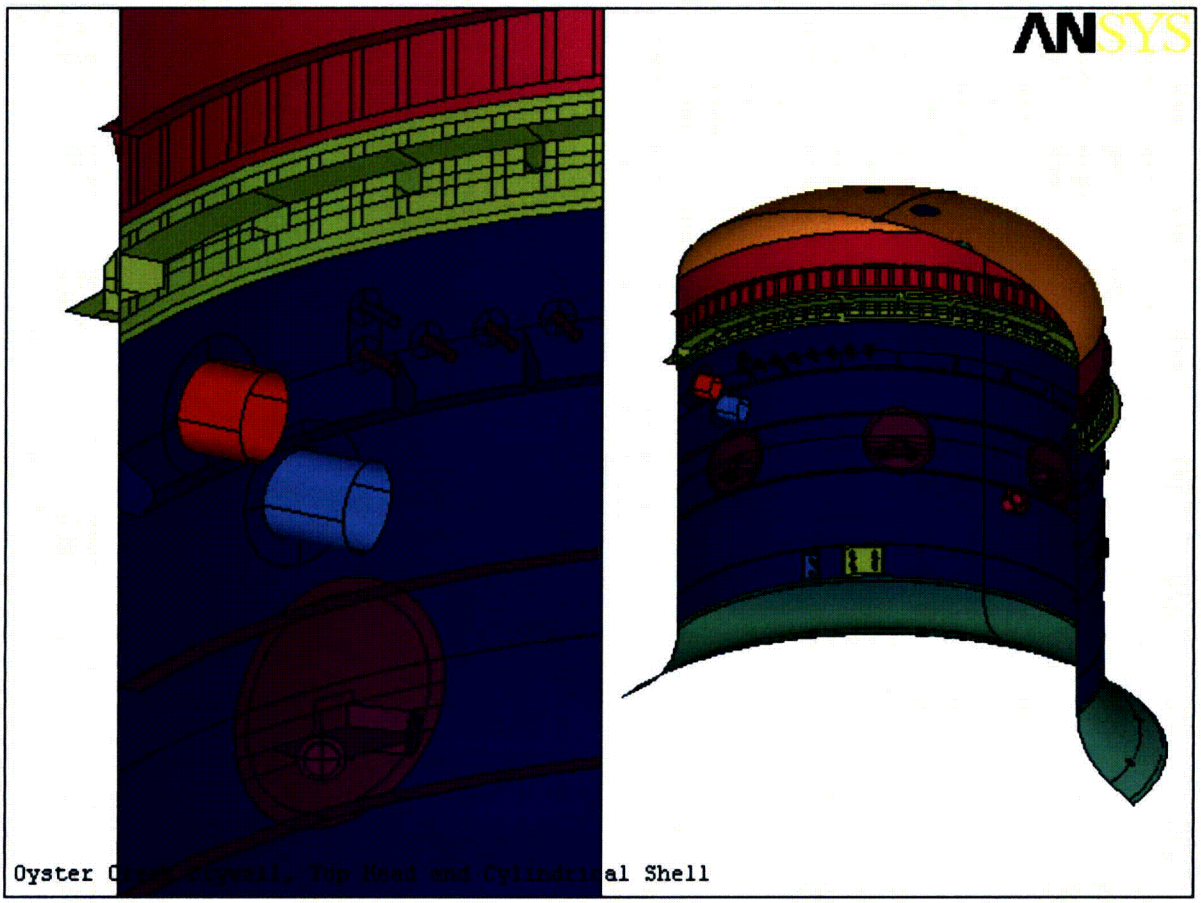

Figure 4-8: Cut out View of Cylindrical Shell Showing Inside Details

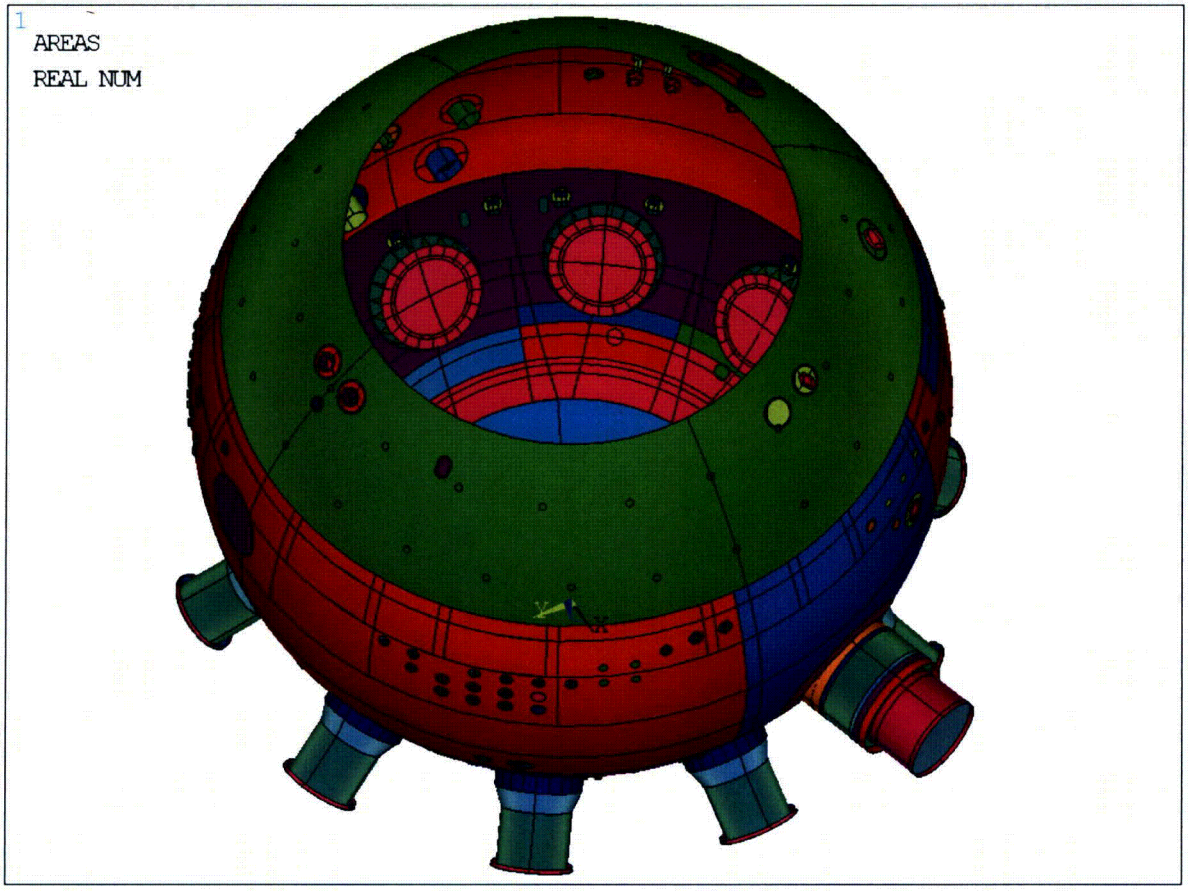

Figure 4-9: Isometric View of Inside of Spherical Shell

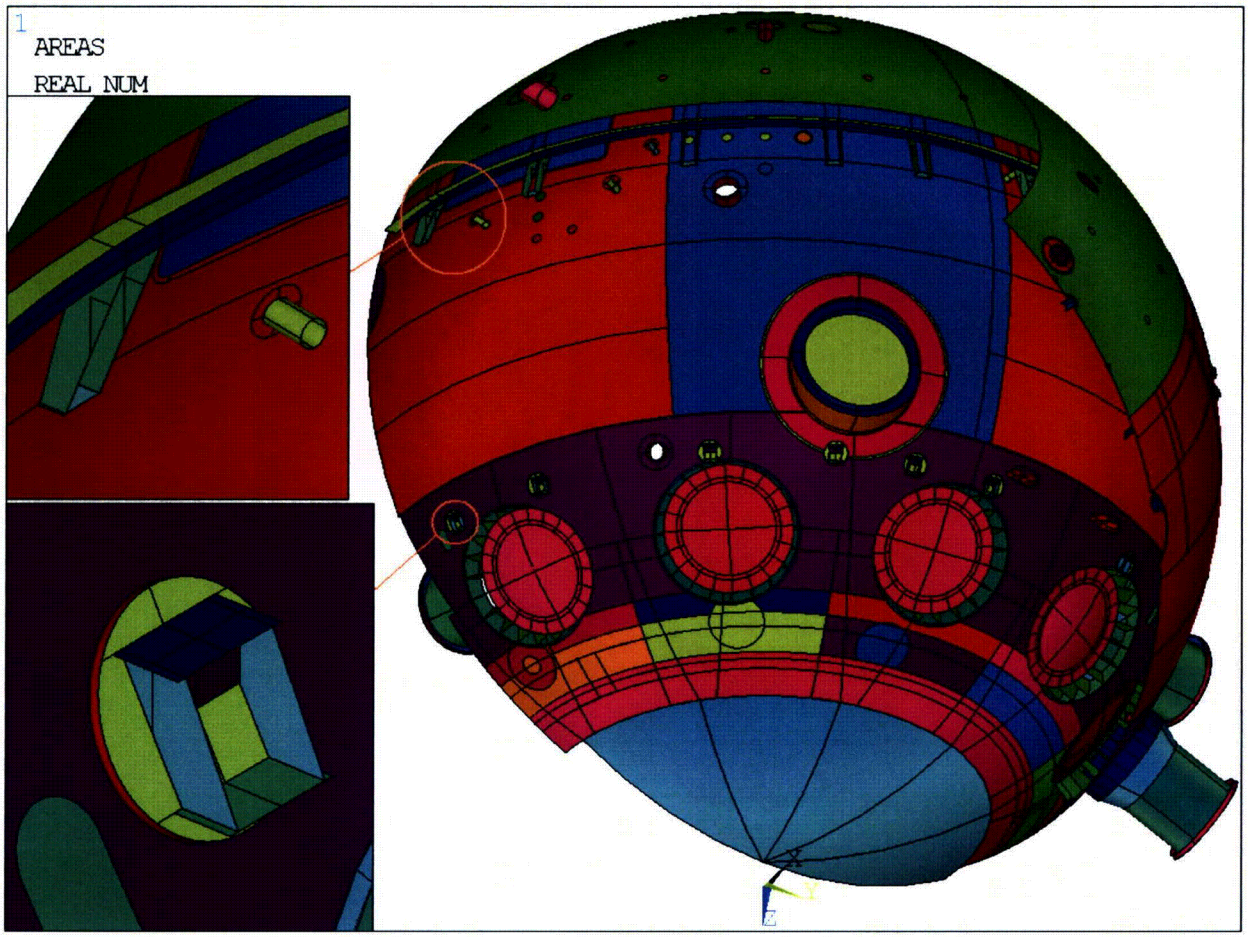

Figure 4-10: Sectional View of Spherical Shell

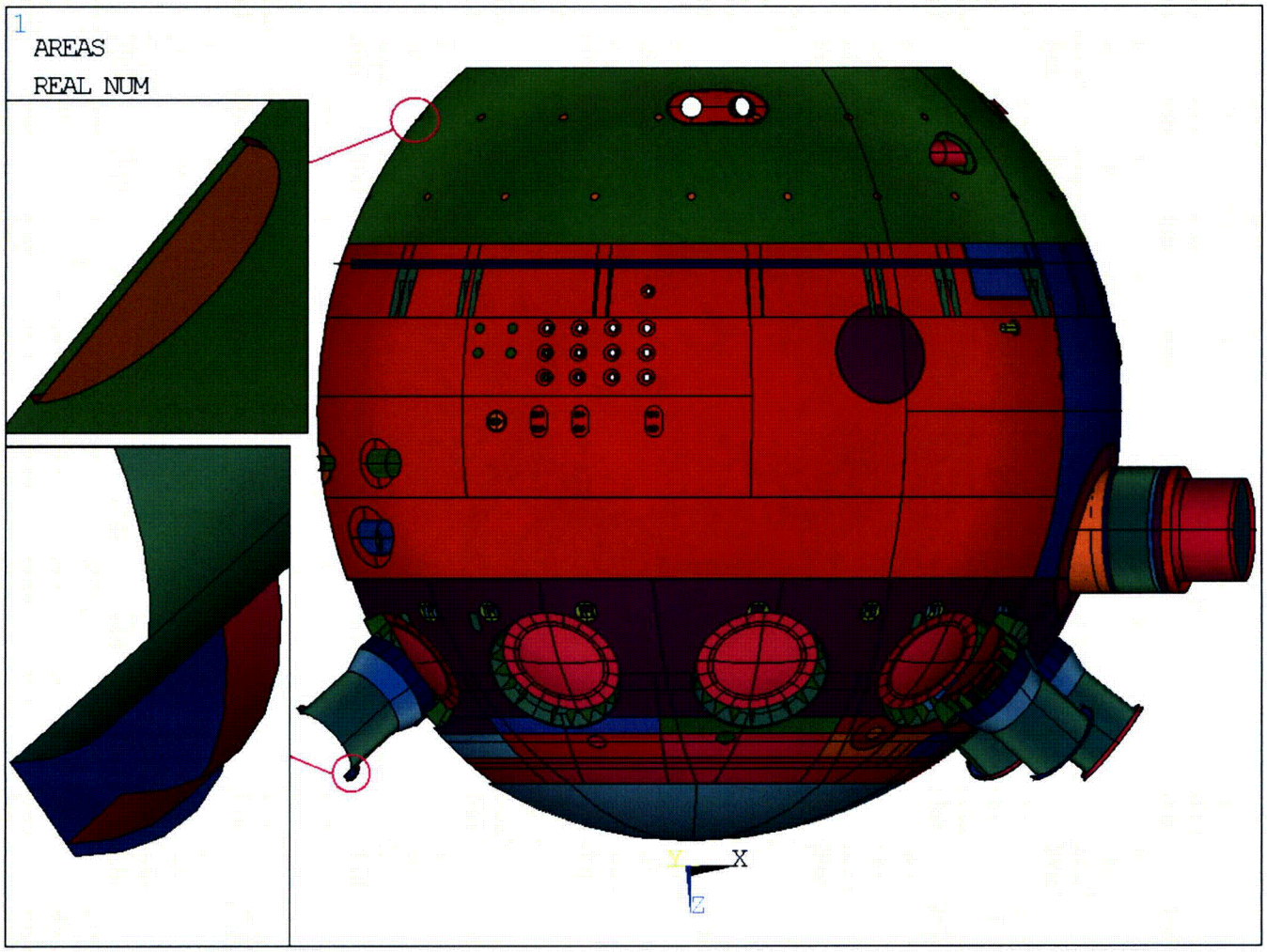

Figure 4-11: Sectional View Showing Welding Pads and Vent Pipe Flanges

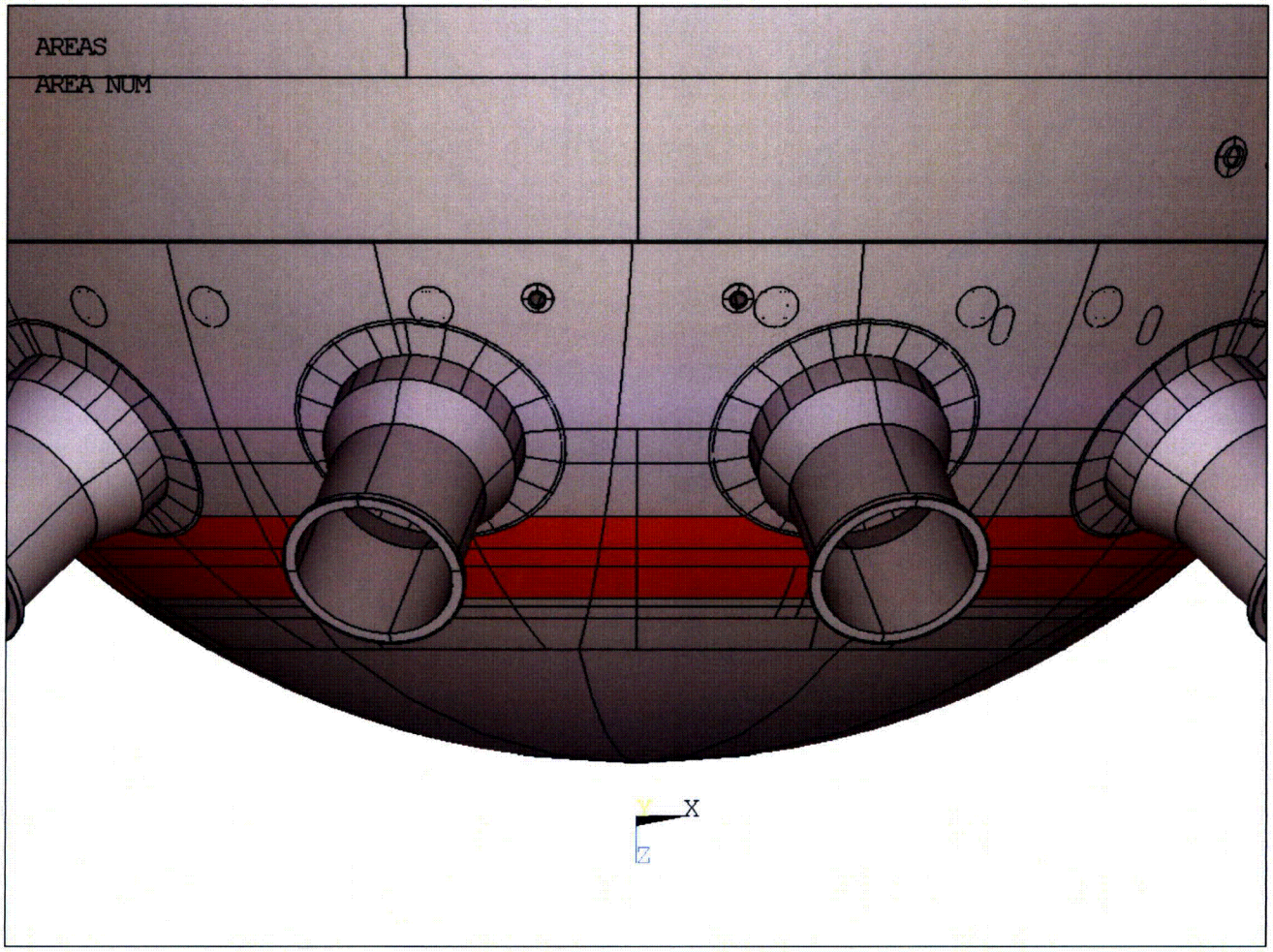

Figure 4-12: Sandbed Region

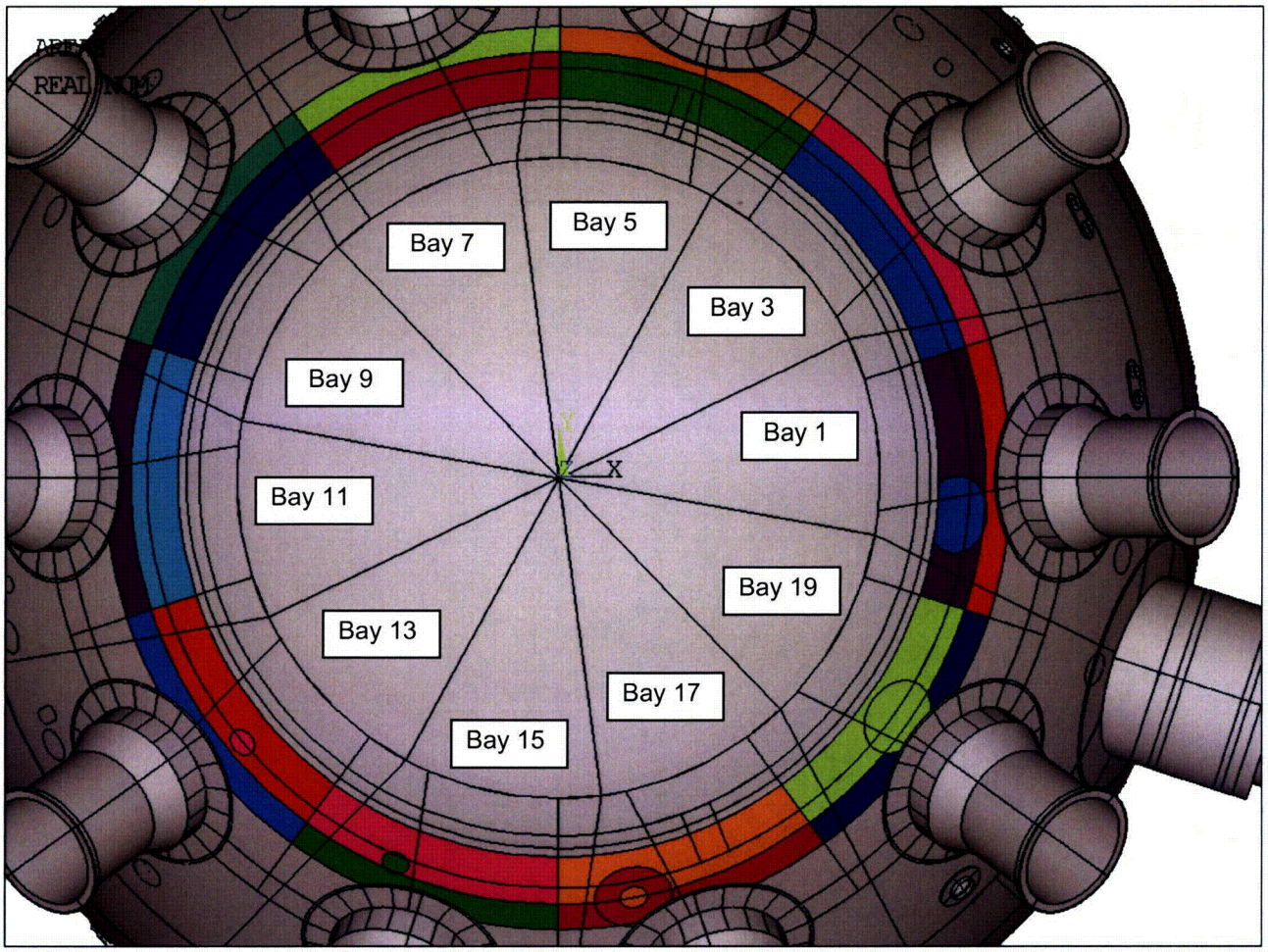

Figure 4-13: Sandbed Region including Locally Thinned Areas

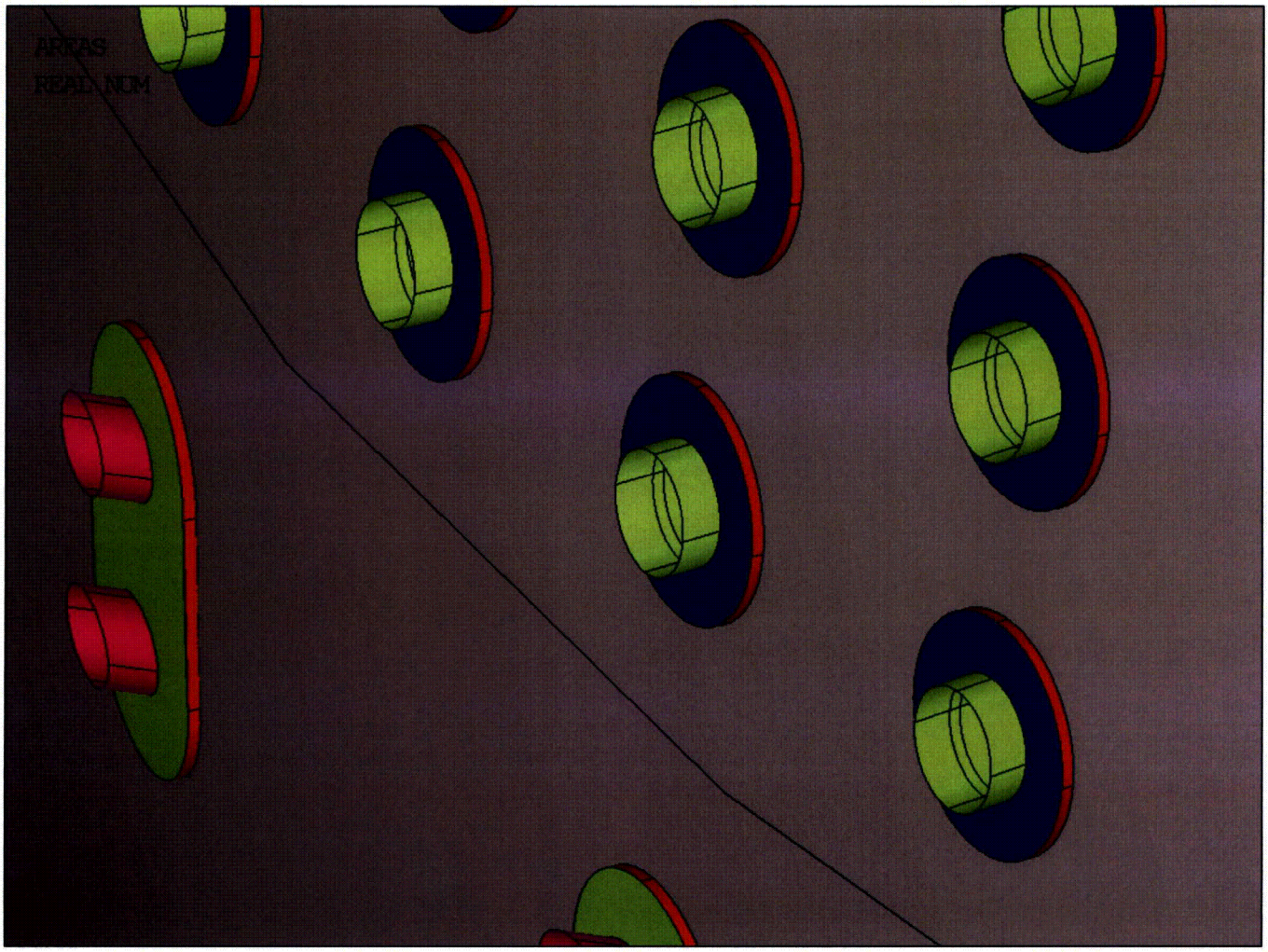

Figure 4-14: Penetrations with Reinforcing Plates

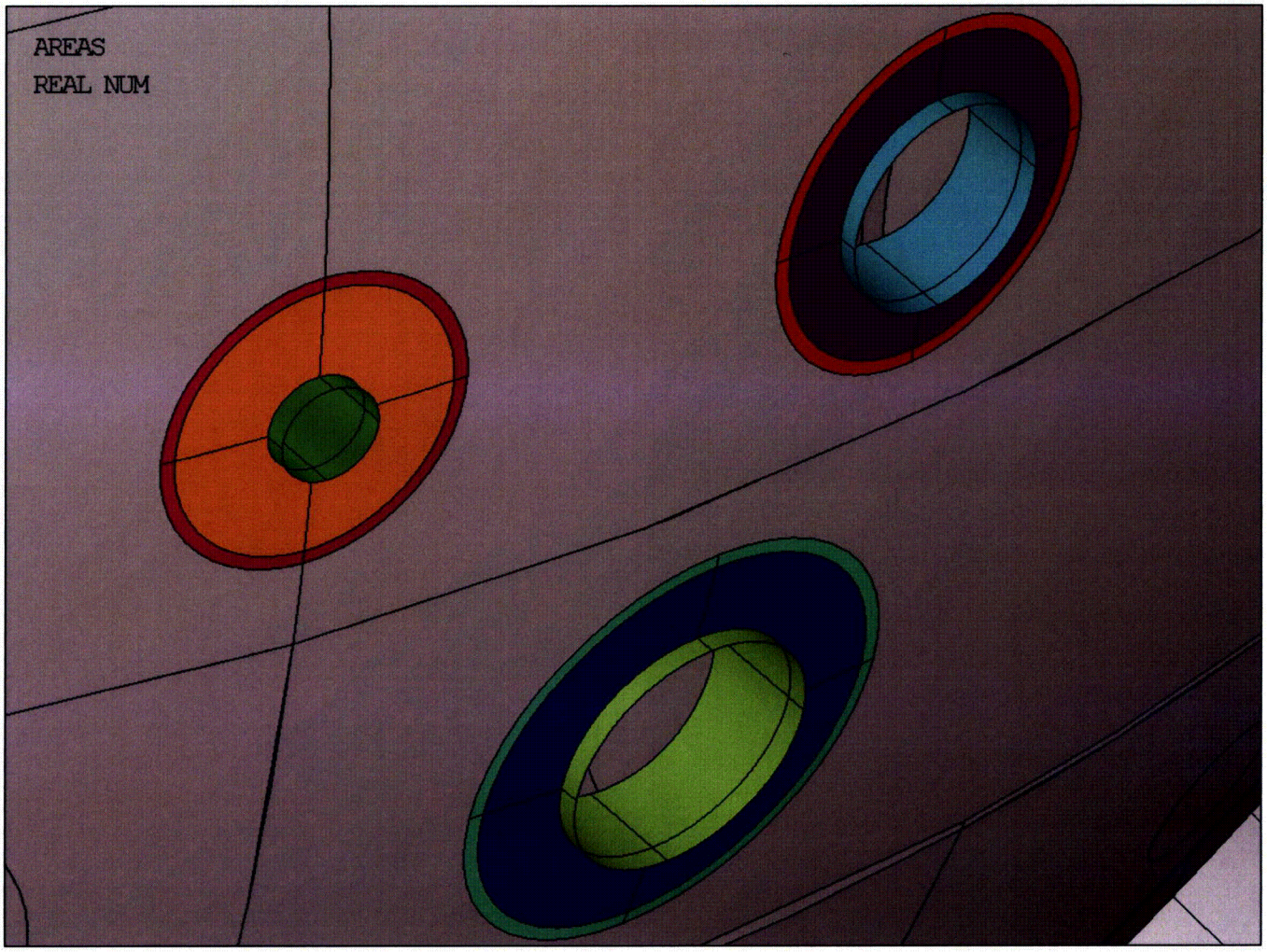

Figure 4-15: Penetrations with Insert Plates

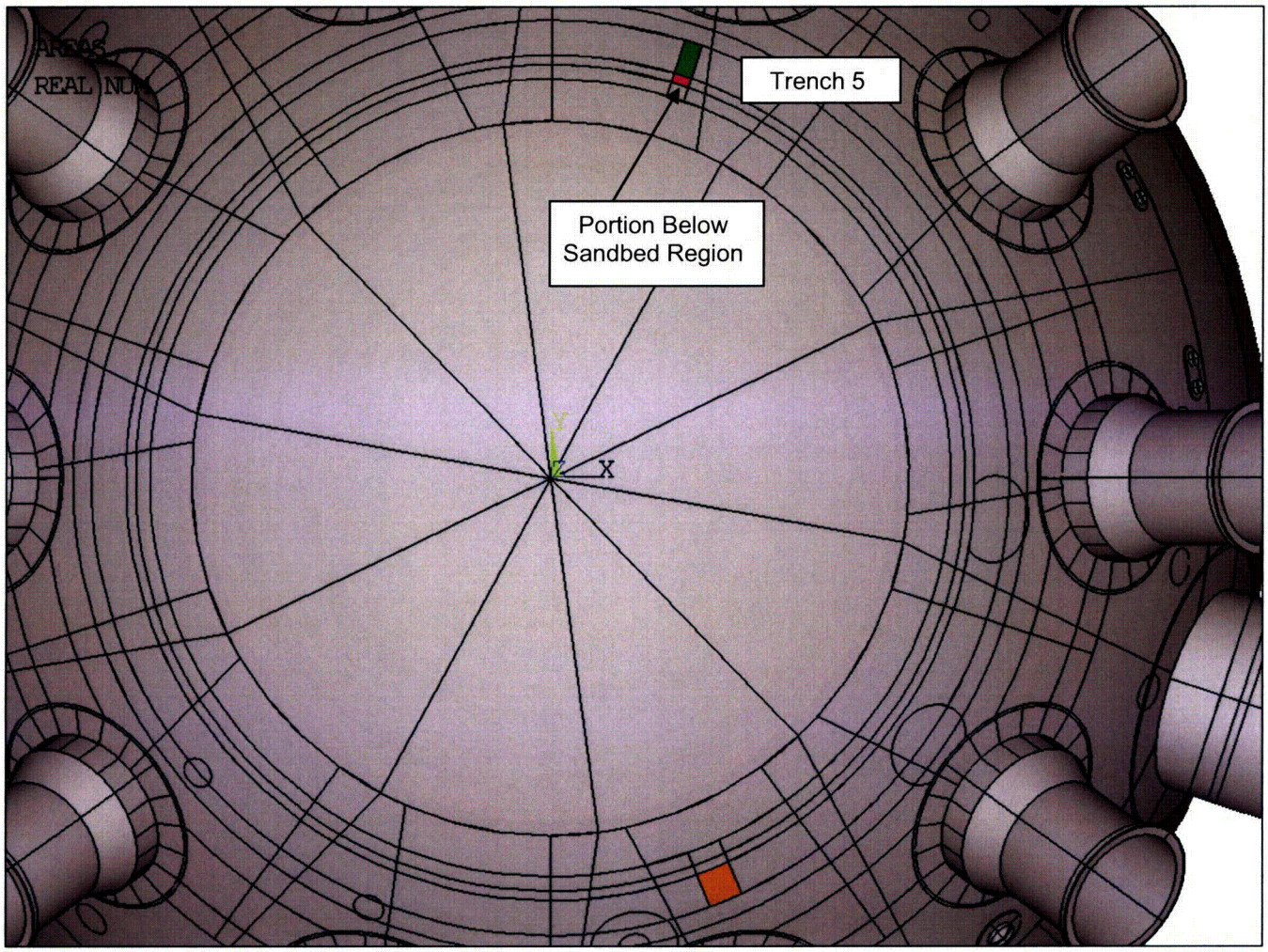

Figure 4-16: Trench 5 and Trench 17 Excavations

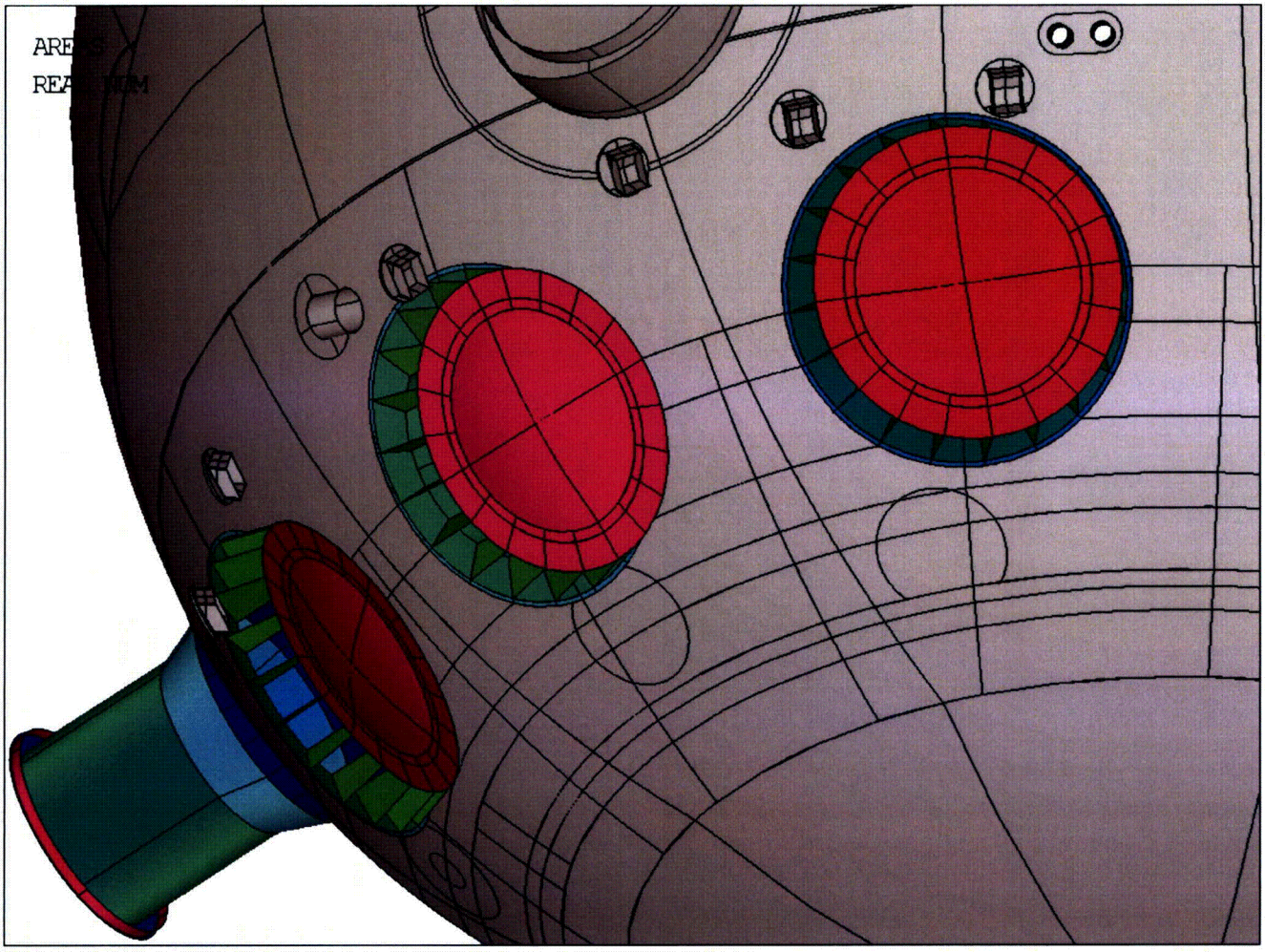

Figure 4-17: Vent Pipe Deflector Plates

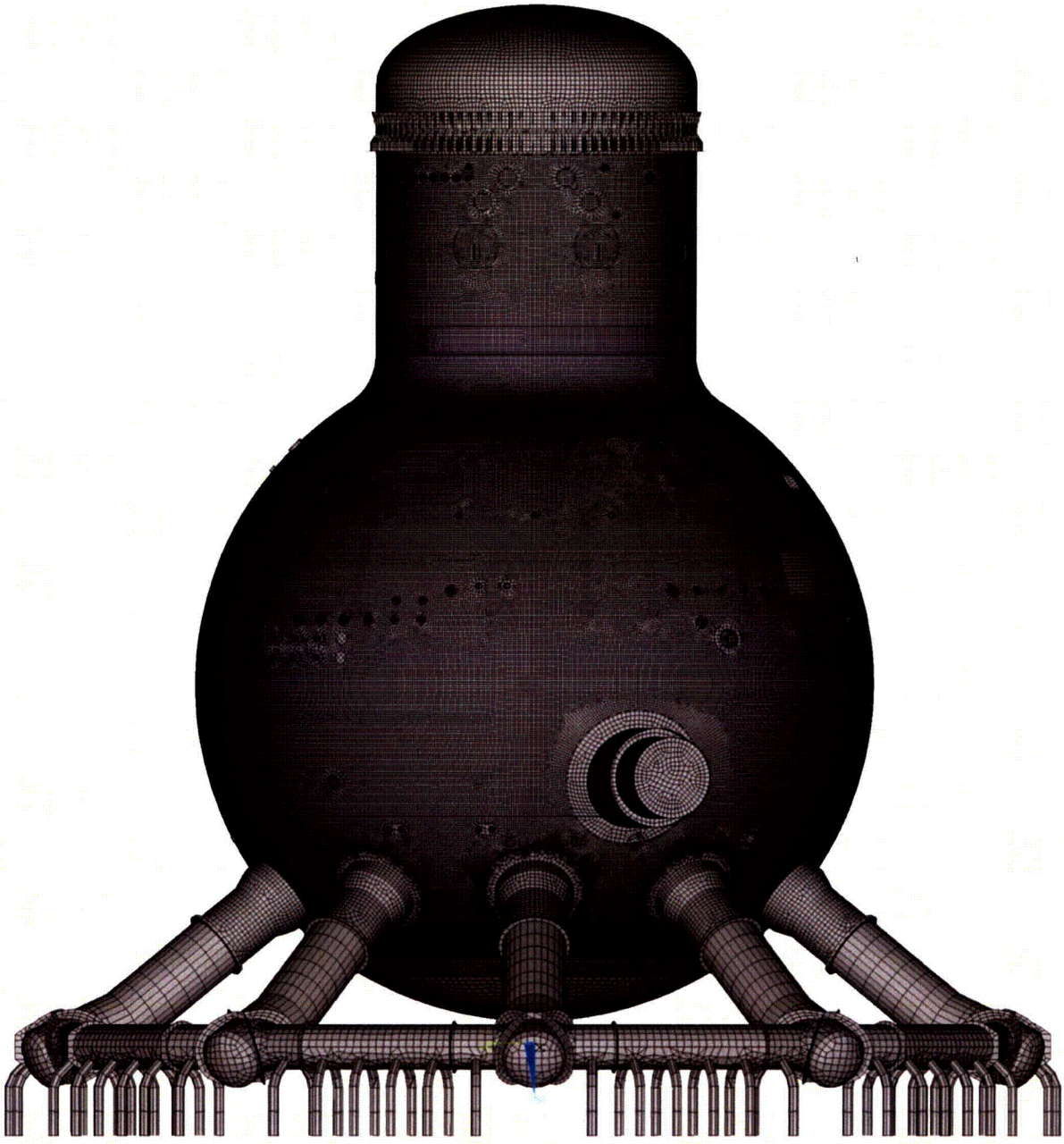

Figure 4-18: Elevation View of Finite Element Model

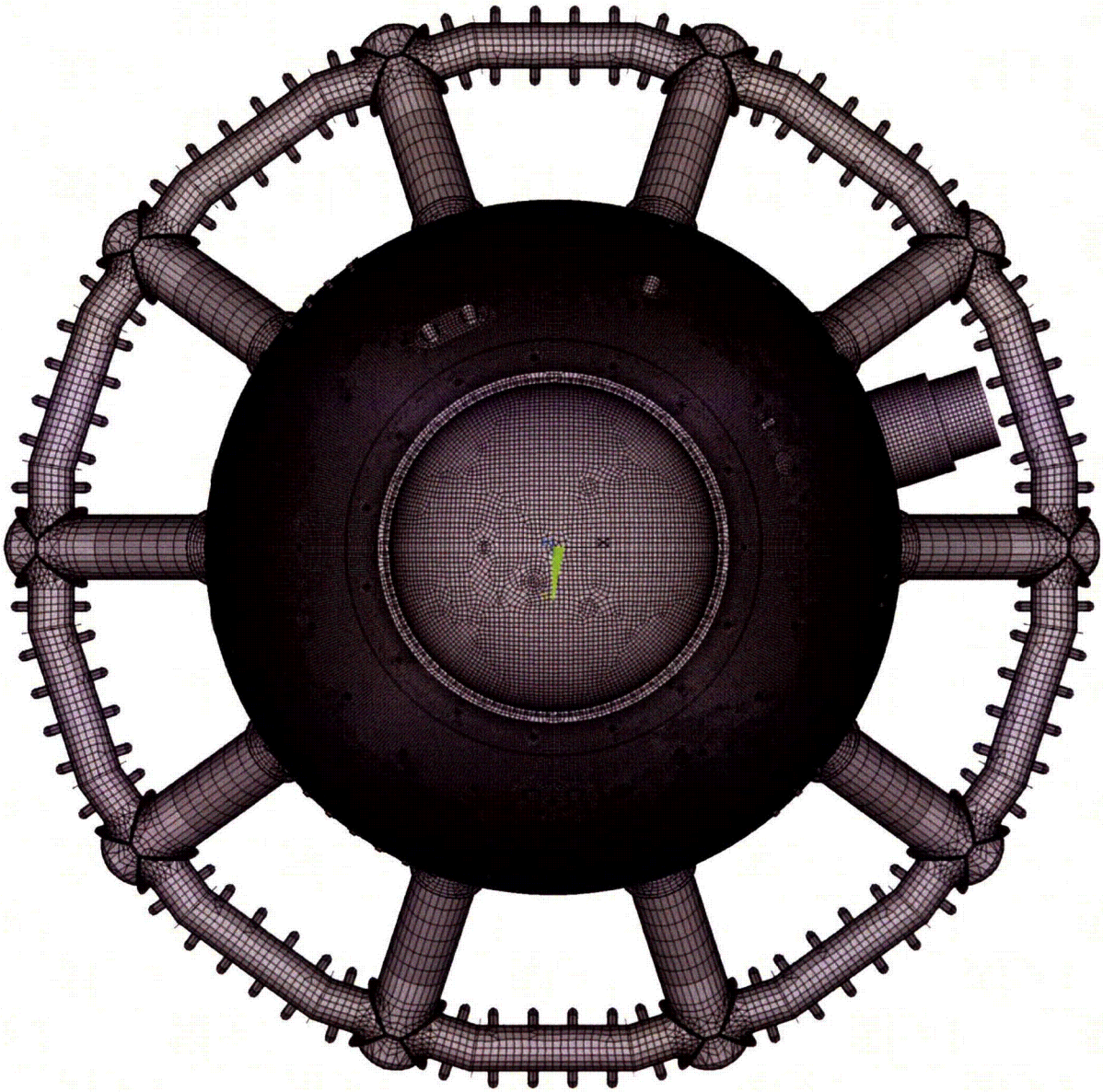

Figure 4-19: Top View of Finite Element Model

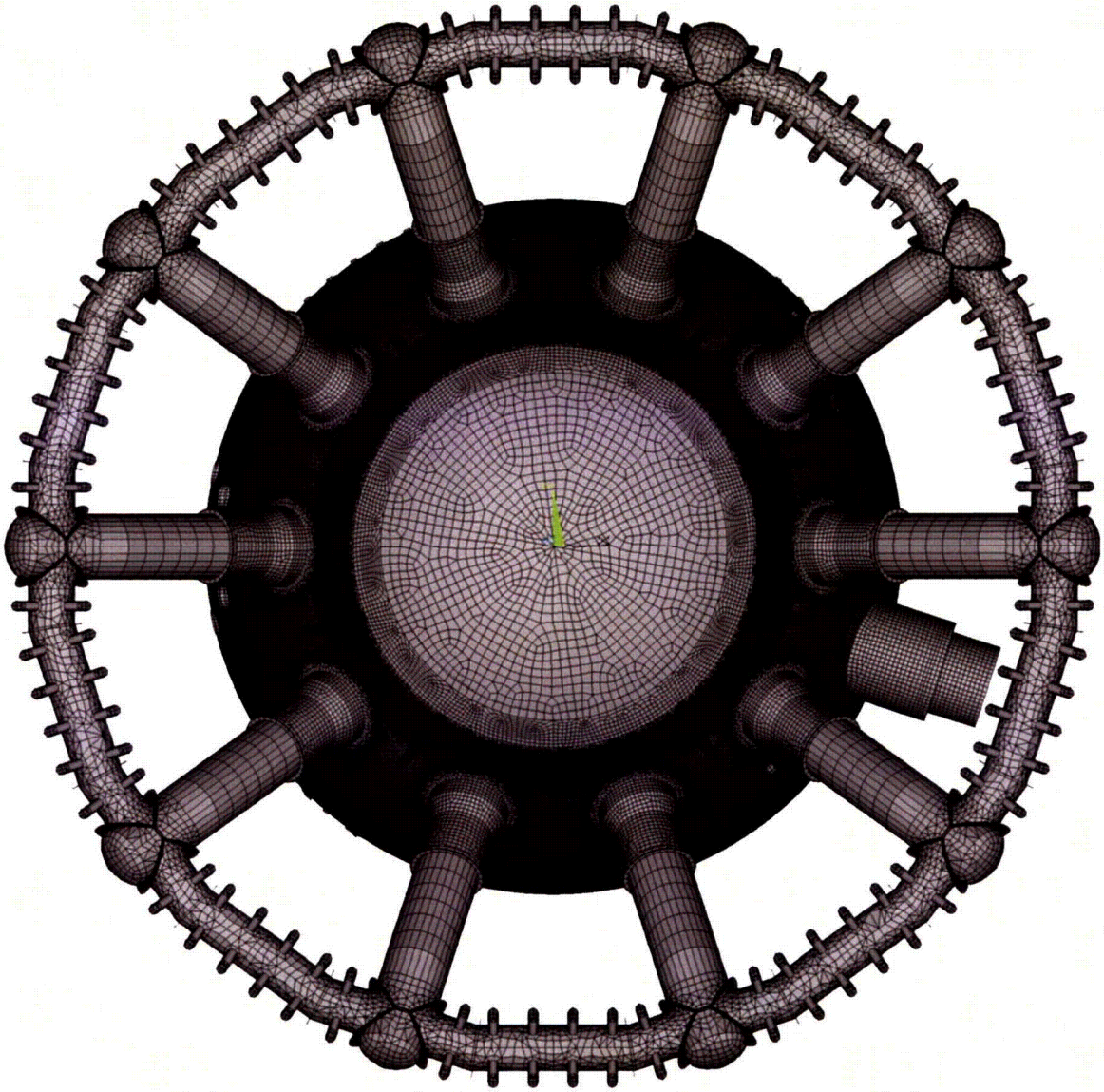

Figure 4-20: Bottom View of the Finite Element Mode

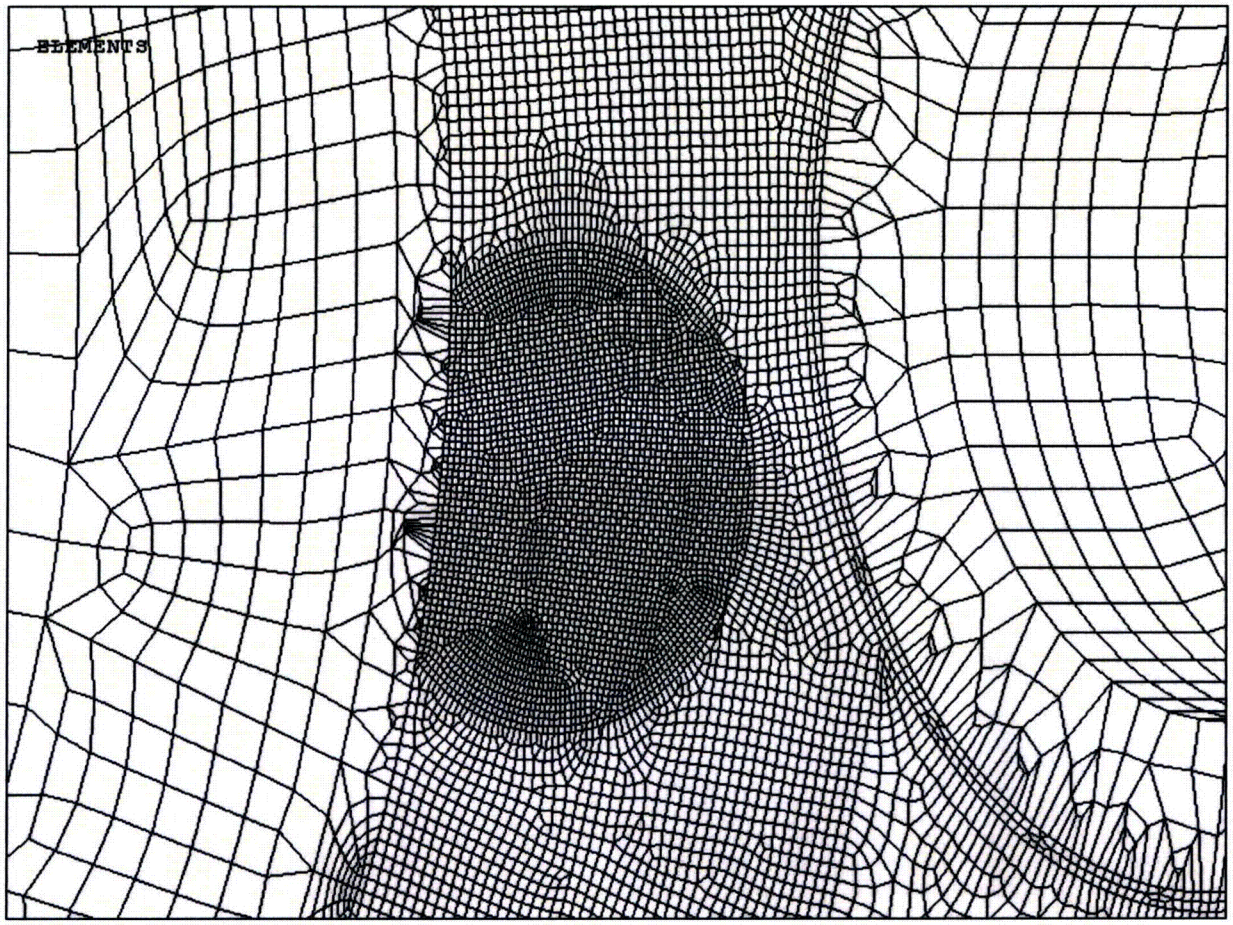

Figure 4-21: Locally Thinned Area in Bay 1

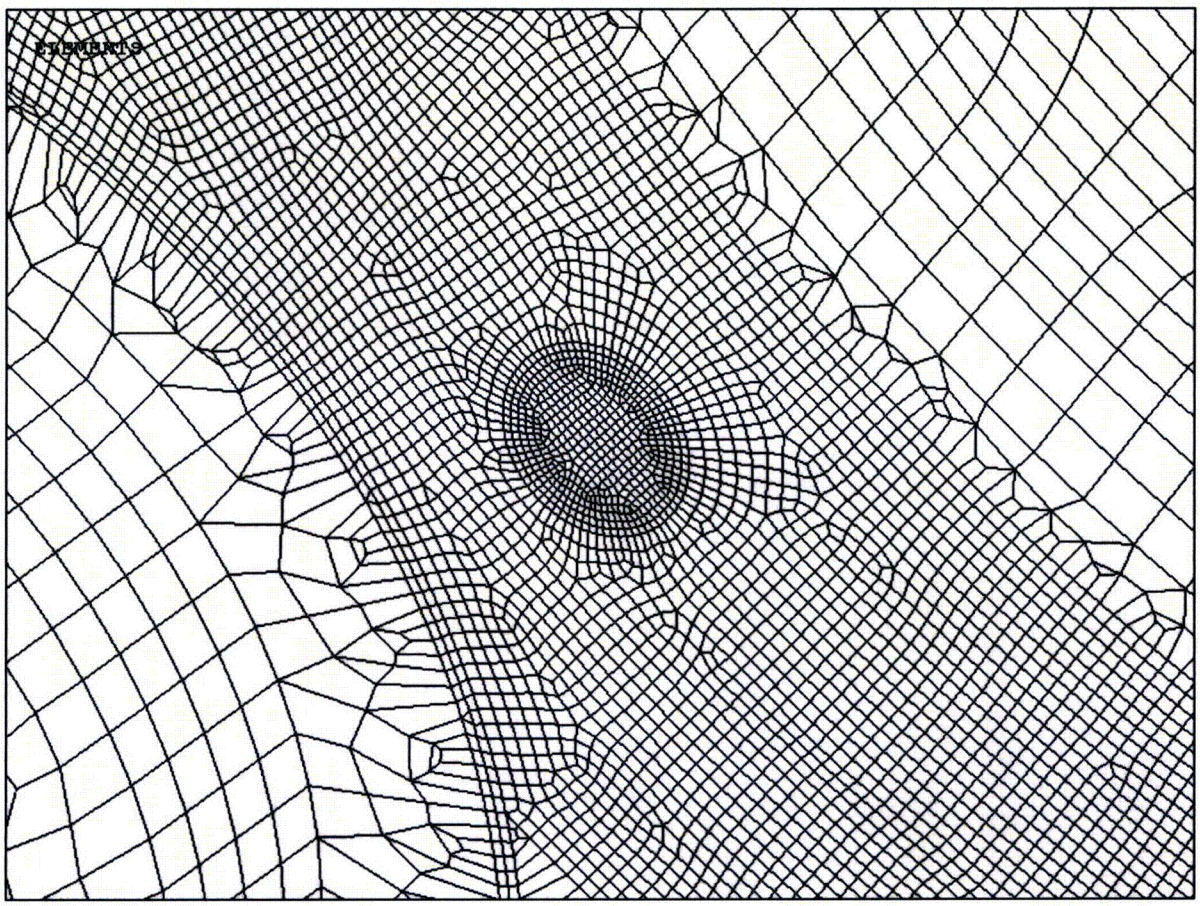

Figure 4-22: Locally Thinned Area in Bay 13

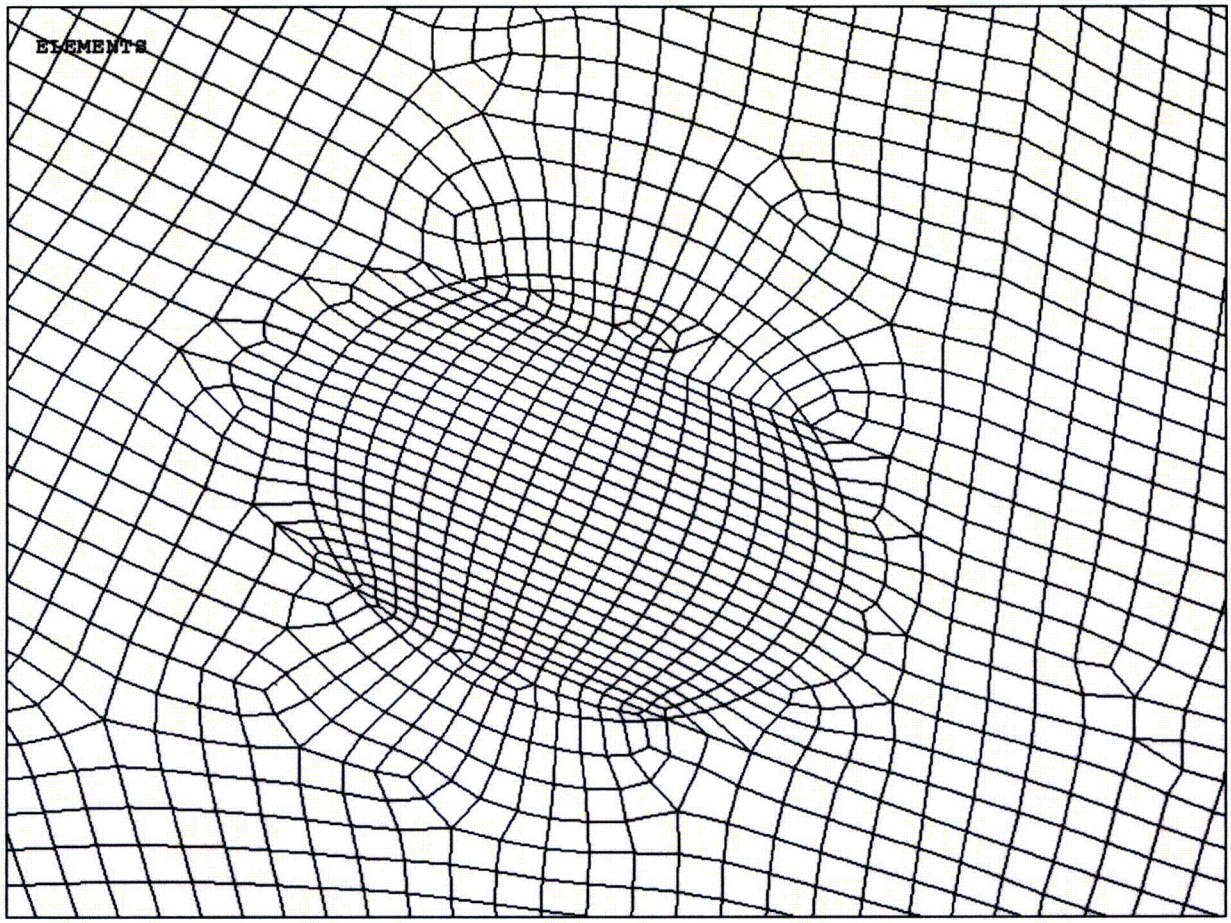

Figure 4-23: Locally Thinned Area in Bay 15

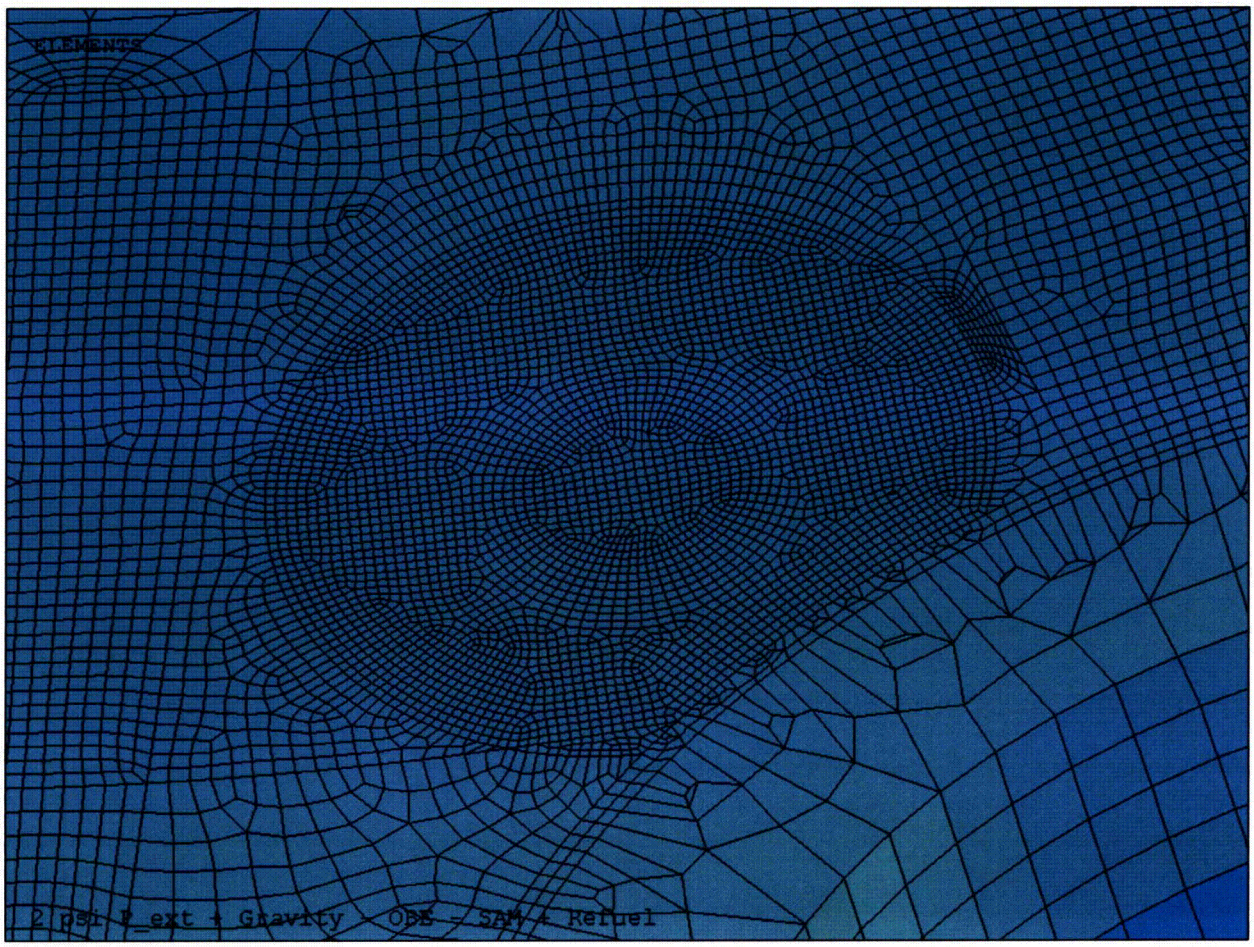

Figure 4-24: Locally Thinned Area in Bay 17

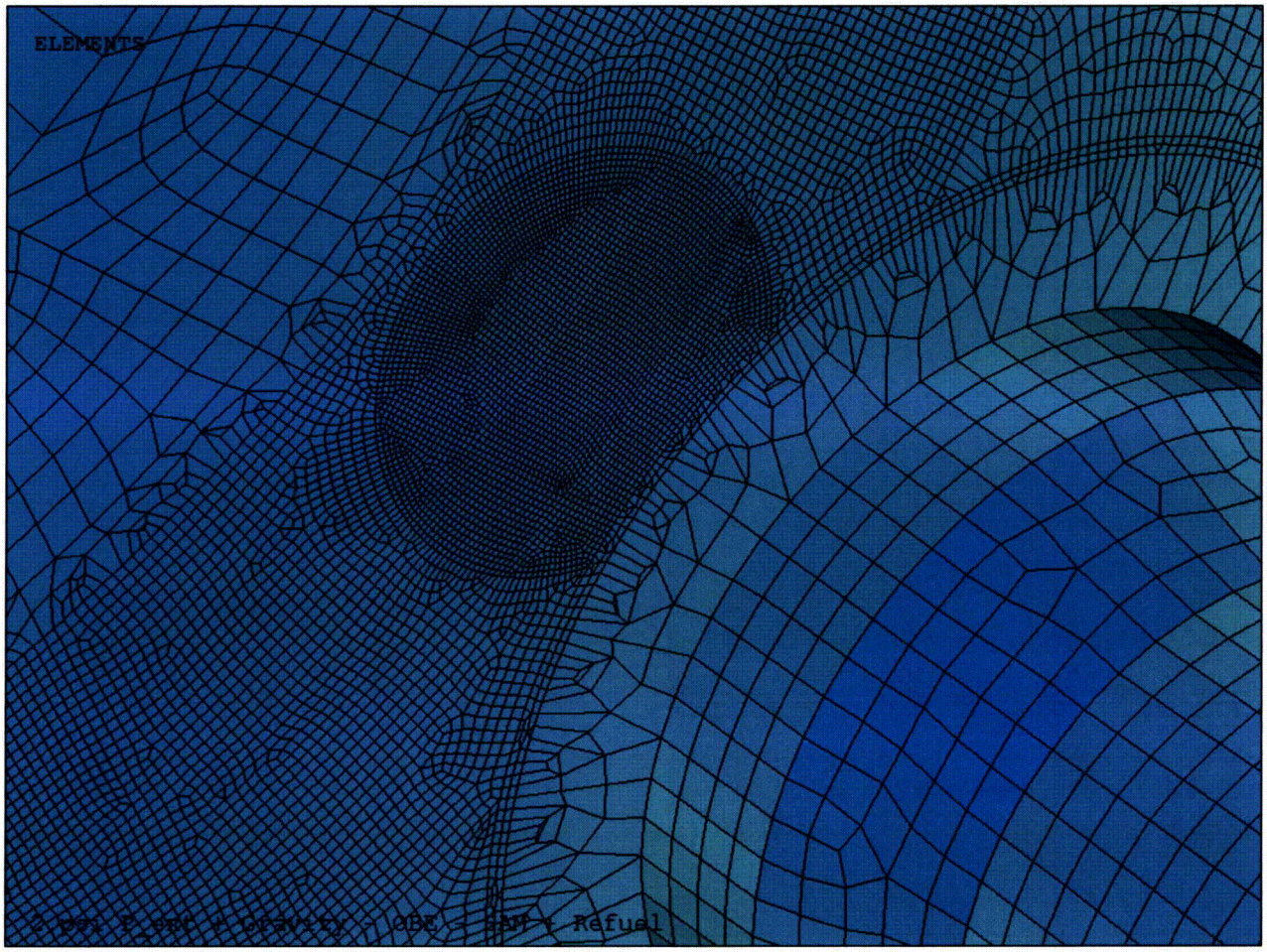

Figure 4-25: Locally Thinned Area in Bay 19

5.0 LOADING

This section describes the loadings and load combinations to be used in the Oyster Creek Drywell analysis.

The loadings are divided into the following categories:

a. Operating Pressure and Thermal
b. Gravity Loads
c. Mechanical and Live Loads
d. Penetration Dead Weight Loads
e. Penetration Piping Loads
f. Hydrostatic Loads
g. Seismic Loads

5.1 System Description and Operation

The primary containment system is to accommodate, with a minimum of leakage, the pressure and temperature resulting from the break of any primary coolant system [5]. The primary containment consists of a drywell and a suppression chamber, as shown in Figure 1-1. The drywell houses the reactor vessel, reactor coolant system and other components associated with the reactor system. It is a 70' diameter spherical shell with a 33' diameter by 23' high cylindrical steel shell. The suppression chamber is a steel shell in the shape of torus located below and around the base of the drywell. It has a torus diameter of 101', a chamber diameter of 30' and is filled with water to a depth of about 12 ft. The two chambers are connected through 10 vent pipes, 6'-6" in diameter, equally spaced around the base of the drywell. The vent pipes are connected to a header inside the suppression chamber. The header is 4'-7" in diameter. There are 120 downcomers, 2' in diameter, uniformly space around the header and extended below the water surface in the torus.

Whenever the reactor is at operating temperature and pressure, the drywell is maintained at atmospheric pressure and cooled to maintain gas temperature below 150 °F and water in the suppression chamber not to exceed 100 °F.

If there is a loss of coolant accident (LOCA), the release water/steam will flow from the drywell through the vent pipes to the suppression chamber water, resulting in essentially complete condensation of the steam with a rapid drop in pressure. Gas forced into the suppression pool with the steam will cause a pressure rise in the gas volume above the pool. With heat dissipation occurring by condensation in the drywell and suppression chamber, in addition to the cooling from the spray system, the drywell pressure may decay to below that of the suppression chamber. At a low differential pressure (less than 1.0 psi), the vacuum breakers open, allowing gas to transfer into the drywell to equalize the pressure between the drywell and the suppression chamber.

5.2 Original Design Parameters

Based on Section II, 1.2.4, p II-6, in Reference 5, the design parameters are based on experience gained from the Bodega Bay tests conducted by Pacific Gas and Electric Gas Company at Moss Landing in 1962:

1. Drywell and connecting vent system tubes are designed for 62 psig internal pressure at 175 °F and/or 35 psig at 281 °F (corresponding to saturation temperature), and an external pressure of 2 psig at 205 °F.

2. Suppression chamber is designed for an internal pressure of 35 psig at 150°F and an external pressure of 1 psig at 150 °F.

3. Drywell is designed to withstand a local hot spot temperature of 300 °F with a surrounding shell temperature of 150 °F concurrent with the design pressure of 62 psig.

Per Section I, 5.0 of Reference 5, the design basis accident assumes a complete circumferential break of one of the main 24" recirculation loops or other equivalent size pipe breaks that would results in the peak containment pressure. The accident is assumed to take place when the reactor

is operating at full power with normal water level in the reactor. It is assumed that the coolant flows out of both open ends of the pipe into the drywell.

Under the above postulated conditions, the blow down would result in a maximum drywell pressure of 33 psig at 275 °F and a maximum suppression chamber pressure of 20 psig at a temperature of 150 °F. The time-pressure and time-temperature curve for the blow down and decay in the drywell are obtained from Reference 5 (Figures I-2 and I-3, Pages I-5 and I-6) and shown in Figure 5-1 and Figure 5-2.

The above is the description of the tests and accident conditions used in the formulating of the original design parameters. The actual design pressure and temperature is further described in Section 5.3.4.

5.3 Original Design Loadings

Based on Section III, 2.3 in Reference 5, the design loadings for the drywell, suppression chamber and interconnecting elements include:

a. Loads caused by temperature and internal or external pressure conditions.
b. Gravity loads from the vessels, appurtenances and equipment supports.
c. Horizontal and vertical seismic loads acting on the structures.
d. Live loads.
e. Vent thrusts.
f. Jet forces on downcomer pipes.
g. Water loadings under normal and flooding conditions.
h. The weight of contained gas in the vessels.
i. The effect of unrelieved deflection under temporary concrete loads during construction.
j. Restraint due to compressible material.
k. Wind loads on the structure during erection.

5.3.1 Description of Loads

The following descriptions of loads are obtained and condensed from Reference 5, (Section III 2.3.1).

5.3.1.1 Pressure and Temperature under Normal Operating Conditions

During reactor operation, the drywell, torus and vent system will be subjected to temperatures up to 150 °F, at atmospheric pressure.

5.3.1.2 Pressures and Temperatures under Accident Conditions

Per Reference 5, the drywell and the vent system are designed for an internal pressure of 62 psig coincident with at temperature of 175 °F, and for an internal pressure of 35 psig coincident with a temperature of 281 °F. The 35 psig and 281 °F have been considered to prevail for a period of 4 to 5 days as a design condition.

The actual design pressure and temperature is further described in Section 5.3.4.

5.3.1.3 Jet Forces

The drywell shell and closure head are design to withstand jet forces from any direction within the drywell. The magnitudes and locations of the jet forces are summarized in Table 5-1. These jet forces consist of steam and/or water at 300 °F maximum in the impingement area. The jet forces do not occur simultaneously. However, a jet force is considered to occur coincident with internal design pressure and a temperature of 150 °F.

The spherical and cylindrical parts of the drywell are backed up by reinforced concrete with compressible material and an air gap between the outside of the drywell and the concrete to allow for thermal expansion. It is assumed that local yielding will take place, but it has been established that a rupture will not occur. This assumption is discussed more fully in Section III-

2.4 of Reference 5, with supporting data available in "Expansion of the Drywell Containment Vessel", a report prepared by Burns and Roe, Inc., following the expansion operation conducted at the site. This report has been included in Appendix III-2.4 of Reference 5.

Where the shell is not backed up by concrete (closure head), the primary stresses resulting from the combination of loads previously defined does not exceed 0.9 times the yield point of the material at temperature. However, the primary plus secondary stresses are limited to three times the allowable stress values given in Table UCS-23, Section VIII, ASME Boiler and Pressure Code, [7]. Supporting data is available in the report, "Loads on Spherical Shells", prepared by Chicago Bridge and Iron (CB&I), following a series of load tests on spherical plates. The report has been included in Appendix III-2-4 of Reference 5.

The suppression chamber and vent system are designed to withstand jet force reactions associated with the design basis loss of coolant accident. The design reaction on each 24" diameter downcomer pipe is 21,000 pounds. Stresses resulting from these reactions are limited to ASME Code allowables.

5.3.1.4 Gravity Loads to be Applied to the Drywell Vessel

The gravity loads are:

a. The weight of the steel shell, jet deflector, vents and other appurtenances.
b. Loads from structural members used to support equipment.
c. An allowance for the weight of the compressible material applied to the exterior of the vessel and as described in the Burns & Roe, Inc. report "Expansion of the Drywell Containment Vessel," attachment to Reference 5.
d. The live load on the access opening: 11 tons or 150 pounds per square foot, whichever is the more severe.
e. The live load for the depth of water on the water seal at the top flange of the drywell with the drywell hemispherical head removed.
f. The weight of contained gas during the test.

g. Dead and live loads on the welding pads provided on the inside of the containment sphere shoulders, spaced at 8' center in each direction. Permanent loads are 200 lbs on each pad, with 800 lbs of live load on any two adjacent pads.
h. A temporary load due to the pressure of fluid concrete which was placed directly against the compressible material attached to the exterior of the drywell and vents. The fluid concrete pressure was controlled by limiting the rate of placement per hour in order to have pressure limit of 3 psi on the compressible material.

5.3.1.5 Seismic Loads

A lateral static coefficient equal to 22%, and a vertical static coefficient equal to 10% of the permanent gravity load were assumed as acting simultaneously with each other.

This load was taken concurrently with permanent gravity loads, accident pressure conditions and other lateral as shown in Figure 5-3and Figure 5-4, [5]. These values were based on studies and criteria described in Section II-5.0 of Reference 5.

It should be noted that the lateral static seismic loads were replaced with the response spectrum seismic loads as described in a later section.

5.3.2 Load Combinations Used in the Design of the Drywell and Vent System

Per Reference 5 (Section III, 2.3.2), the following load combinations are defined and repeated here verbatim:

5.3.2.1 Case I – Initial Test Condition at Ambient Temperature at Time of Test

a. Gravity load of vessel and appurtenances
b. Design Pressure
c. The weight of contained air
d. Lateral load due to wind or seismic forces whichever is more severe

e. Vent thrusts
f. Vertical seismic load

5.3.2.2 Case II – Final Test Condition at Ambient Temperature at Time of Test

a. Gravity load of vessel and appurtenances
b. Gravity load from equipment supports
c. Gravity load of compressible material
d. Gravity load of welding pads
e. Design pressure
f. Seismic loads
g. Effect of unrelieved deflection under temporary concrete load
h. Restraint due to compressible material
i. Vent thrusts

5.3.2.3 Case III – Normal Operating Condition at Operating Temperature Range of 50 °F to 150 °F

a. Gravity load of vessel and appurtenances
b. Gravity load from equipment supports
c. Gravity load of compressible material
d. Seismic loads
e. Vent thrusts
f. Restraint due to compressible material
g. Gravity load on welding pads
h. Effect of unrelieved deflection under temporary concrete load
i. External pressure of 2 psig
j. Live load on personnel air lock

5.3.2.4 Case IV – Refueling Condition with Drywell Hemispherical Head Removed, at Operating Temperature Range of 50 °F to 150 °F

a. Gravity load of vessel and appurtenances
b. Gravity load from equipment supports
c. Gravity load of compressible material
d. Gravity and live load on welding pads
e. Water load on water seal at top flange of drywell
f. Seismic loads
g. Effect of unrelieved deflection under temporary concrete load
h. Restraint due to compressible material
i. Vent thrusts
j. External pressure of 2 psig
k. Live load on access opening

5.3.2.5 Case V – Accident Condition at Temperature List Below

a. Gravity load of vessel and appurtenances
b. Gravity load from equipment supports
c. Gravity load of compressible material
d. Gravity load on welding pads
e. Seismic loads
f. Design Pressure: Maximum positive pressure of 62 psig at 175 °F, decaying to 35 psig at maximum temperature at 281 °F, to maximum negative pressure of 2 psig at 205 °F.
g. Effect of unrelieved deflection under temporary concrete load
h. Restraint due to compressible material
i. Vent thrusts
j. Jet forces

Item (f) is for the original design used in Reference 5. The actual design pressure and temperature is further described in Section 5.3.4.

5.3.3 Load Conditions and Combinations Used in Oyster Creek Drywell Evaluation

The original loading conditions and load combinations were defined in the 1960's during the design of the drywell. Since that time, there have been updates and modifications to the original Final Safety Analysis Report (FSAR) [13]. Therefore, the loading conditions and combinations as presented in the original design report are modified and updated to reflect the current conditions and analysis for the wall thickness conditions of the Oyster Creek Drywell. The load combinations are further discussed in Section 7.0.

5.3.4 Design Pressure and Temperature

Per Reference 5, Section II - 1.2.4, Item (a), page II-6, the drywell was originally designed for a pressure of 62 psig at 175 °F and /or 35 psig at 281°F, and an external pressure of 2 psig at 205 °F.

Per Section 6.2.1.1.1, FSAR [13], the drywell was originally designed for a pressure of 62 psig. The design pressure was reduced to 44 psig according to Reference 15 in the FSAR, (p 6.2-2) [13]

In addition, it is stated in Item (a), page 6.2-4 of FSAR [13] that the drywell and connecting vent system tubes are designed for 44 psig internal pressure at 292°F and/or 35 psig at 281°F (the corresponding saturation temperature), and an external pressure of 2 psig at 205°F.

Therefore, the design pressure and temperature for the current evaluation of Oyster Creek Drywell is set at 44 psig at 292°F.

5.3.5 Operating Pressure and Temperature

The operating pressure and temperature were not explicitly defined together in the References. In Section 6.2.1.1.1, p. 6.2-2 of FSAR [13], it is stated that the primary containment is normally kept near atmospheric pressure, without mentioning the temperature.

In the same Section of the FSAR, it is also stated that the Containment System is normally kept at near atmospheric pressure but as a basis for calculation, an upper limit of 2 psig internal pressure was assumed.

It is mentioned that the initial conditions in the drywell for an accident condition are 150 °F, 15.0 psia and 100% relative humidity, (FSAR [13] Section 6.2.1.3.3, item b, p 6.2-13). It is stated in FSAR [13], Section 6.2.1.3.6, p.2-15 that the Oyster Creek primary containment design considers loads and load combinations corresponding to normal operating temperatures up to 150 °F at close to atmospheric pressure. It is also stated in the same Section that, during normal operations, the calculated bulk drywell temperature is usually near or a few degrees above 135 °F.

In addition, Section 1.2.4, Item (a) in Reference 5 provides a design condition of an external pressure of 2 psig at 205 °F.

Therefore, the operating pressure and temperature of the Oyster Creek Drywell is set an external pressure of 2 psig at 150 °F.

5.3.6 Gravity and Live Loads

The gravity loads and live loads are addressed together in this section because they are treated as quasi-static load in the analysis.

Per Reference 5, the drywell is designed to withstand the gravity loads as identified in Section 5.3.1.4. The only load that is not considered in the current evaluation is the temporary load defined in item (h) of Section 5.3.1.4.

Items (a), in Section 5.3.1.4, are incorporated in the model as the density of the materials and the application is discussed in the finite element modeling.

Items (b) and (e) in Section 5.3.1.4 are obtained from Reference 5 and are shown in Figure 5-12 and Figure 5-4. Loads P1, P2, P3 and P4 are for the refueling operation only. Loads P5, P7 and P8 are at the upper and lower beam supports. These are considered as belonging to item (b). Loads P6 are from the reactor vessel through the biological shield wall and transmitting through the concrete to the building foundation. Therefore, load P6 is not used in the drywell analysis.

The seismic loads were identified as either operating or refueling conditions as shown in the column 'Remark' in Table 5-2. The P5, P7, P8 and P9 are grouped together as Mechanical/Live Loads. The P1, P2, P3, P4 and P6 are grouped together as Refuel loads. These two load groups are used in the load combinations in Section 6.4. They are used in both Refueling (Levels A&B) and Post-Accident Flooding (Level C) load combination. They are not distinguished as SSE or OBE and used as Mechanical/Live loads or Refueling loads in the load combinations.

One load that is not included in Table 5-2 is the horizontal earthquake load of 2,150,000 lbs that is transmitted to the drywell shell tangentially by 5 beams on each side of the vertical axis of the drywell, Figure 5-4 (Plan C-C). These are the beams most nearly perpendicular to the direction of the earthquake.

In Reference 1 (page 1D1), it is shown that the forces P1 and P2 are acting at the top gusset and the forces P3 and P4 are acting at the intersection between the drywell shell and the bottom stiffener, as illustrated in Figure 5-5.

For Item (c), it is stated in Reference 5, Section III - 2.4.4, page III-25 that the gap between the drywell and the concrete building is 3 inches. This gap is filled with compressible material. From Appendix III-2.4, Item 1, Section 4.9 of Reference 5, it is stated that the foamed asbestos fiber-magnestite cement product was selected to fill the expansion space around the drywell vessel. In Section 7.1 of Appendix III-2.4, Item 1, of Reference 5, it is stated that the dry density of the compressible material is 8 pounds per cubic foot. It corresponded to a wet density at the spray nozzle of 29 pounds per cubic foot at the spray nozzle. For the analysis of the Oyster Creek drywell, a dry density of 8 lbs/ft^3 is used. This load is assumed to be distributed in the drywell shell.

For Item (d), from Reference 3(r), the width of the floor is 6'. From Reference 3(ac), the length of the floor is 29 9/16" x 4 = 118.25 inches (9.8542 ft). The total area of floor space is 6'x 9.8542' =59.125 ft^2. With 150 lb/ft^2, the total force is 8868.75 lbs, which is less than 11 tons (24,640 lbs). Therefore, a live load of 11 tons for the access opening is used in the analysis.

For Item (f), the weight of contained air is only included during the initial test condition, as defined in Reference 4, Section 2.3.2.1. It is stated in Reference 3, Section 1.6.3.2, Table II-2, that the drywell air volume is 180,000 ft^3. The air is assumed to compose of about 80% Nitrogen and 20% Oxygen. Using a density of 0.0812 lbm/ft^3 at 80°F for oxygen and 0.0713 lbm/ft^3 at 80°F for nitrogen, the density of air is calculated to be 0.0812*0.2+0.0713*0.8 = 0.0733 lbm/ft^3. The total weight of air in the drywell is 0.0733x180,000 = 13,194 lb. The weight of contained air is only included in the test conditions according to Reference 3.

For item (g), a dead and live load of 1000 lbs at each weld pad is used.

The vent thrust loads are due to the end cap effect of the vent pipe from internal/external pressure, as described in the FSAR [43]. The vent thrust load is applied as an axial force on the vent pipe at the bellow location interfaced with the torus, based on the end cap effect duet to the pressure. For the refueling condition, this is the end cap effect of a 2 psi external pressure. For the post accident flooding condition, the vent thrust load is much more significant due to the

presence of the water inside the drywell. The vent thrust load from the hydrostatic pressure due to the water head is included in the analysis.

5.3.7 Vent Thrust

Per interpretation of Reference 41, the vent thrust load is due to the end cap effect of internal/external pressure.

5.4 Penetrations

From Reference 3, there are 208 penetrations on the drywell. The location and size of these penetrations are presented in Table 5-3. The number of penetrations by grouping in size is summarized in Table 5-4. It should be noted that there are 10 vent openings but grouped as a single opening in Reference 3(b).

The Oyster Creek drywell was designed according to the ASME, Boiler and Pressure Vessel Code, Section VIII, 1962 Edition, [7]. In order to provide a guidance in modeling the penetrations in the finite element model, and since Reference 7 does not have any rule for opening, a latter edition of Section VIII [15] is used to determine the maximum opening size that does not require reinforcement.

Article AD-510 of Reference 15 states that a single opening has a diameter not exceeding $0.2\sqrt{(R_m t)}$ or if there are two or more openings within any circle of diameter $2.5\sqrt{(R_m t)}$, then the sum of the diameter of such unreinforced opening shall not exceed $0.25\sqrt{(R_m t)}$. Based on the mean radius and nominal wall thickness in the cylindrical and spherical region of the drywell, the diameter of reinforced opening at these regions are calculated and presented in Table 5-5.

If the openings meet the Section VIII rules, they do not require any area reinforcement. Usually these openings are small in diameter that they do not cause any significant local stress that addition reinforcement is required. Thus no area reinforcement is necessary for these small openings. Therefore, those openings that do not require area reinforcement are not included in

details in the finite element model. For the drywell, any openings less than 2.25 inches, 2.55 inches and 3.12 inches are not modeled in details in the finite element model for the cylindrical, upper spherical and lower spherical regions of the drywell, respectively.

5.5 Penetration Piping Loads

Among all the penetrations in the Oyster Creek drywell, only a small number of penetrations are provided with the piping loads acting on the penetrations from the piping analyses. These penetrations are shown in Table 5-6.

5.6 Hydrostatic Loads

5.6.1 Refueling Conditions

During refueling conditions, water is filled from the elevation of the water seals between the reactor vessel and the drywell. The water level is at 118'-3" [2]. Outside the drywell, the water seal is at an elevation 92-10 ¾" [3]. Inside the drywell, the water seal is at an elevation 5 ¾" [3] below the top surface of bottom flange which is at 94'-9" [3].

5.6.2 Post Accident Flooding Conditions

The flood stage is at the elevation 74'-6". The total water head for the flood stage is 92'-0", measured from the bottom of the torus. This water head creates a hydrostatic pressure on the drywell shell. The hydrostatic pressure is calculated based on the water depth measured from the water surface.

5.7 Seismic Loads

The original seismic design for the Oyster Creek Nuclear Generating Station critical structures and equipment is based on dynamic analysis using acceleration response spectrum curves which

were based on a peak ground acceleration of 0.11 g for the Operating Basis Earthquake (OBE) and 0.22g for the Safe Shutdown Earthquake (SSE) [17].

For the current drywell evaluation, the seismic analysis is performed using a response spectrum. The response spectrum is obtained from References 16 and 18.

5.7.1 Response Spectrum

5.7.1.1 Operating Basis Earthquake

The Oyster Creek drywell is embedded into concrete on the interior below elevation 10'-3" and constrained in the circumferential direction at the star truss male lug mid elevation at 82'-2" (from 81'-5 1/4" to 82'-10 3/4"), on the outside of the drywell [3]. The response spectrum at the elevation of 82'-9' is used since this is the closest elevation that the response spectrum results are available. The horizontal acceleration response spectra in the North-South direction, East-West direction, and the Vertical direction at these two elevations are presented in Figure 5-6 to Figure 5-11. Based on the guideline in Reference 19, OBE spectra with 2% damping was selected.

All response spectra have significant response in the 1 to 10 Hz region. Above the significant frequency region (i.e. >10 Hz), the magnitude of the acceleration response is less than 0.25g

5.7.1.2 Post-Accident Earthquake with Flooded Drywell

To account for the effect of water in the flooded drywell in the post-accident condition, a re-analysis of the soil-structure-interaction of the drywell was performed [18] to generate a new set of seismic response spectrum for the flooded condition. The response spectra for the three directions are presented in Figure 5-12 and Figure 5-13 for the elevations 10'-3" and 82'-9", respectively. The figures also included the SSE spectra without the water in the drywell for comparison. At 10'-3" elevation, the flooded spectra in the two horizontal directions are essentially the same as the non-flooded OBE spectra. In the vertical direction, the flooded spectrum shows a significant decrease in g level in the 1 Hz to 10 Hz range. The difference is

due to the change in the locations on the base mat (elevation 10'-3") where the spectra are computed. Both analyses include the effect of rocking of the mat. The original analysis included the envelope of the spectra for locations on the mat that extended to the edge of the reactor building walls. The revised analysis included this same rocking effect but only enveloped the points out to the radius of the containment shell. At 82'-9" elevation, the flooded spectra in all three directions are very similar to the non-flooded OBE spectra.

For both the operating basis earthquake and the post-accident earthquake with flooded drywell, the maximum envelope response spectra from the spectrum for the two elevations (10'-3" and 82-9") were used in the analysis for each of the three loading directions (i.e. E-W, N-S and vertical). The results from these three load directions (which were analyzed individually) were combined by square root of the sum of the square (SRSS) to obtain the stress results for the OBE and flooded SSE load cases. The enveloped spectra were applied to all the support locations.

5.7.2 Seismic Anchor Movements

5.7.2.1 Operating Basis Earthquake

During a seismic event, the reactor building would experience a relative displacement between the drywell constraint at 82'-2" and the reactor building base. The relative displacement is obtained using the following approaches:

I. Using Reactor Building Relative Displacements.

II. Using Drywell Maximum Relative Displacements.

III. Using Drywell Time History Displacements.

Approach I: Using Reactor Building Relative Displacements

The reactor building relative displacements are taken from Reference 20, Table 2.1.3, on Page 6. The Upper Bound displacements for the N-S and E-W directions are determined, and the SRSS displacement of the two sets is computed for this approach.

To obtain the displacements at 10'-3", the displacement will be interpolated between the displacements at 9' and at 23.5'. To obtain the displacement at 82'-2", the displacement will be extrapolated from the displacements at 63.5' and 74.0'.

The results are summarized in Table 5-7.

Approach II: Using Drywell Maximum Relative Displacements

The Drywell maximum relative displacements are taken from Reference 20, Table 3-1(b), on Pages 34 & 37, for Nodes 11 & 57, respectively. With reference to Figure 2-3 on Page 22, the 10'-3" elevation corresponds to Node 11, and the elevation 82'-2" corresponds to Node 57.

The maximum relative displacements for Nodes 11 & 57 in the N-S and E-W directions are determined, and the SRSS displacement of the two sets is computed for this approach. The results are summarized in Table 5-7.

Approach III: Using Drywell Time History Displacements

The Drywell time history displacements are taken from Reference 20, for Nodes 11 & 57, as identified in Reference 20, on page 22; the 10'-3" elevation corresponds to Node 11, and the elevation 82'-3" corresponds to Node 57.

These time history displacements carry directional signs, denoting that the phasing of the nodal displacements between the two locations is taken into consideration. The maximum relative displacements between two nodes are computed for each time period. The maximum amplitude for the N-S & E-W directions is established, and the SRSS value of the two is computed for this approach. . The results are summarized in Table 5-7.

All three approaches show that the Seismic Anchor Movement (SAM) values are quite similar: 0.062", 0.067", and 0.068" for Approaches I, II, and III, respectively.

Approach I is the smallest, and the least accurate due to the interpolation and extrapolation used in the methodology.

Approach II is a reasonable approach, assuming that the phasing of the maximum relative displacements for the two nodes occur at the same time.

Approach III is the most accurate approach. It takes into consideration the phasing of the two nodal displacements at all time steps. Moreover, this approach predicts the largest SAM movement of 0.068".

The SAM movement from Approach III will be used in the drywell analysis. The seismic anchor movement in the three directions in the global coordinate system will be applied all together in one load case. This SAM case will then be used in the final combination as +SAM or –SAM.

5.7.2.2 Post Accident Basis

The relative seismic anchor movements at the star truss elevation are obtained from Reference 18 and presented in Table 5-8. The relative anchor displacements are provided for the best estimate (BE), upper bound (UB) and lower bound (LB) for all three global directions. The maximum relative displacements are from the LB in the two horizontal directions with 0.095" in the North-South (X) direction and 0.087" in the East-West (Y) direction.

5.7.3 Critical Damping Values

Per Reference 19, the modal damping values expressed as a percentage of critical damping shown in Table 5-9 should be used for viscous modal damping for all modes considered in an elastic spectral or time-history dynamic seismic analysis of the Seismic Category I structures or components. The modal damping values specified in Table 5-9 are for use in the dynamic analyses for operating basis earthquake and safe shutdown earthquake.

In the evaluation of Oyster Creek Drywell, 2% damping is used for OBE and 4% damping is used for SSE.

Table 5-1: Jet Force Loads [5]

Location	Maximum Jet Forces	Interior Area Subjected to Jet Force
Spherical Part of Drywell	566,000 lbs	3.14 ft^2
Cylindrical and Sphere to Cylindrical Transition	466,000 lbs	2.54 ft^2
Closure Head	16,000 lbs	0.09 ft^2

Table 5-2: Gravity and Live Loads [5]

Load	Elevation	Static (lbs)	Earthquake (lbs)	Remarks	Note
P1	102'-10"	15,000	3,800	Refueling operation only	Horizontal load
P2	102'-10"	14,000	3,500	Refueling operation only	Vertical load
P3	82'-2"	15,000	3,800	Refueling operation only	Horizontal load
P4	82'-2"	15,000	3,800	Refueling operation only	Vertical load
P5	47'-1 ½"	43,200	10,800	Normal operation	Vertical load
P6	12'-3"	6,600,000	1,650,000	Refueling operation only	Vertical load
		6,040,000	1,510,000	Normal operation	Vertical load
P7	23'-6"	13,700	14,100	All operating conditions	Vertical load
P8	23'-6"	6,100	1,500	All operating conditions	Vertical load
P9	12'-3"	0	343,000	All operating conditions	Horizontal load
	42'-1 ½"	--	2,150,000	See Figure 5-4, Plan C-C	Horizontal load

Table 5-3: Drywell Penetrations

#	Custom	CB&I Mk	Size	Azimuth Deg-Min	Elevation	Detail Dwg#	Spare	Pntr Type	Pen Thk(in)	Rfr Plt Thk(in)	Rfr Plt D/L(in)	Weld Vsl/Plt	Weld Pen/Plt	Pntr Matl.	Reinf Plt Matl
1	X- 1	100-A	Lock	342-0	27'-6"	100/40		n/a						A212-B	A212-B
2	X- 2A	23-X 2A	36	171-19	27'-0"	23		3	1.75	1.75	61.875	FP	FP/FW-3/8	A212-B	A212-B
3	X- 2B	15-N36-1	36	188-45	27'-0"	15		1/2	1.75	0.875	61.75	FW-5/8	FP/FW-3/8	A201-B	A212-B
4	X- 3A	19-N24-1R	24	10-30	90'-0"	19		1/2	1.25	0.875	34.5	FW-1/2	FP/FW-3/8	A201-B	A212-B
5	X- 3B	19-N24-1L	24	349-30	90'-0"	19		1/2	1.25	0.875	34.5	FW-1/2	FP/FW-3/8	A201-B	A212-B
6	X- 4A	23-X 4A	30	167-30	33'-0"	23		3	1.5	1.75	48.625	FP	FP/FW-3/8	A201-B	A212-B
7	X- 4B	15-N30-1	30	192-30	33'-0"	15		1/2	1.5	0.875	48.75	FW-5/8	FP/FW-3/8	A201-B	A212-B
8	X- 5A	19-N24-2R	24	19-30	87'-5"	19		1/2	1.125	0.875	36.25	FW-1/2	FP/FW-3/8	A201-B	A212-B
9	X- 5B	19-N24-2L	24	340-30		19		1/2	1.125	0.875	36.25	FW-1/2	FP/FW-3/8	A201-B	A212-B
10	X- 6	28-X 6	6	150-0	87'-9"	28		3	0.432	1.75	16	FP	PP-1/2/FW-3/8	A201-B	A212-B
11	X- 7	18-N26-1	26	325-0	42'-0"	18		1/2	1.5	0.875	40.5	FW-5/8	PP-1/2/FW-3/8	A201-B	A212-B
12	X- 8	26-X 8	26	290-15	58'-3"	26		3	1.5	1.75	50.625	FP	FP	A201-B	A212-B
13	X- 9	25-X 9	22	85-0	62'-0"	25		3	1.125	1.75	38.5	FP	FP	A201-B	A212-B
14	X-10	25-X10	22	95-0	62'-0"	25		3	1.125	1.75	38.5	FP	FP	A201-B	A212-B
15	X-11	17-N18-1	18	114-0	43'-6"	17	Yes	1/2	0.938	0.875	23.75	FW-5/8	PP-1/2/FW-3/8	A201-B	A212-B
16	X-12A	25-X12A	22	240-0	62'-0"	25		3	1.125	1.75	23.563	FP	FP	A201-B	A212-B
17	X-12B	25-X12B	22	250-0	62'-0"	25		3	1.125	1.75	23.563	FP	FP	A201-B	A212-B
18	X-13A	22-X13A	1	94-0	43'-9"	22		3	0.179	1.25	96	FP	FP/FW-1/4	A312-T304	A212-B
19	X-13B	22-X13B	1	266-30	43'-9"	22		3	0.179	1.25	96	FP	FP/FW-1/4	A312-T304	A212-B
20	X-14A	22-X13A	1	94-0	43'-9"	22		3	0.179	1.25	96	FP	FP/FW-1/4	A312-T304	A212-B
21	X-14B	22-X13B	1	266-30	43'-9"	22		3	0.179	1.25	96	FP	FP/FW-1/4	A312-T304	A212-B
22	X-15	13-N2-1	2	300-0	40'-0"	13		3	0.218	0.875	8.5	FW-9/16	FW-1/4	A333-O	A212-B
23	X-16	13-N2-1	2	305-0	40'-0"	13		3	0.218	0.875	8.5	FW-9/16	FW-1/4	A333-O	A212-B
24	X-17	16-N 8-8	8	82-30	21'-3"	16		1/2	0.5	0.875	15.25	FW-9/16	PP-3/8/FW-3/8	A333-O	A212-B
25	X-17	16-N 8-8	8	97-30	21'-3"	16		1/2	0.5	0.875	15.25	FW-9/16	PP-3/8/FW-3/8	A333-O	A212-B
26	X-18	27-X18	18	190-0	86'-0"	27		3	0.938	1.75	30	FP	FP	A201-B	A212-B
27	X-19	16-N18-2	18	314-30	21'-3"	16		1/2	0.938	0.875	32.5	FW-9/16	PP-3/8/FW-3/8	A201-B	A212-B
28	X-20A	12-N8-4	8	5-0	47'-6"	12		1/2	0.5	0.75	15.75	FW-9/16	PP-3/8/FW-3/8	A333-O	A212-B
29	X-20B	12-N8-4	8	10-0	47'-6"	12		1/2	0.5	0.75	15.75	FW-9/16	PP-3/8/FW-3/8	A333-O	A212-B
30	X-21	12-N8-5	8	310-0	43'-9"	12		1/2	0.5	0.875	15.75	FW-9/16	PP-3/8/FW-3/8	A333-O	A212-B
31	X-22A	X-22A	24	0-0	14'-0"	70		3						A201-B	A212-B
32	X-22B	X-22B	24	72-0	14'-0"	70		3						A201-B	A212-B
33	X-22C	X-22C	24	108-0	14'-0"	70		3						A201-B	A212-B
34	X-22D	X-22D	24	144-0	14'-0"	70		3						A201-B	A212-B
35	X-22E	X-22E	24	216-0	14'-0"	70		3						A201-B	A212-B
36	X-22F	X-22F	24	252-0	14'-0"	70		3						A201-B	A212-B
37	X-22G	X-22G	24	288-0	14'-0"	70		3						A201-B	A212-B
38	X-23	12-N6-5	6	330-0	43'-0"	12	Yes	1/2	0.432	0.875	13	FW-9/16	PP-3/8/FW-3/8	A333-O	A212-B
39	X-24	12-N6-4	6	15-0	47'-0"	12		1/2	0.432	0.875	13	FW-9/16	PP-3/8/FW-3/8	A333-O	A212-B
40	X-24	28-X24	6	101-0	47'-0"	28		3	0.432	1.75	16	FP	PP-3/8/FW-1/2	A333-O	A212-B
41	X-24	28-X24	6	162-0	47'-0"	28		3	0.432	1.75	16	FP	PP-3/8/FW-1/2	A333-O	A212-B
42	X-24	12-N6-4	6	234-0	47'-0"	12		1/2	0.432	0.875	13	FW-9/16	PP-3/8/FW-3/8	A333-O	A212-B
43	X-24	12-N6-4	6	315-0	47'-0"	12		1/2	0.432	0.875	13	FW-9/16	PP-3/8/FW-3/8	A333-O	A212-B
44	X-25	12-N6-2	6	30-0	44'-0"	12		1/2	0.432	0.875	13	FW-9/16	PP-3/8/FW-3/8	A333-O	A212-B
45	X-26	12-N6-2	6	35-0	44'-0"	12	Yes	1/2	0.432	0.875	13	FW-9/16	PP-3/8/FW-3/8	A333-O	A212-B
46	X-27	12-N6-2	6	40-0	44'-0"	12		1/2	0.432	0.875	13	FW-9/16	PP-3/8/FW-3/8	A333-O	A212-B
47	X-27	12-N6-2	6	45-0	44'-0"	12		1/2	0.432	0.875	13	FW-9/16	PP-3/8/FW-3/8	A333-O	A212-B
48	X-27	12-N6-2	6	55-0	44'-0"	12		1/2	0.432	0.875	13	FW-9/16	PP-3/8/FW-3/8	A333-O	A212-B
49	X-27	12-N6-2	6	60-0	44'-0"	12		1/2	0.432	0.875	13	FW-9/16	PP-3/8/FW-3/8	A333-O	A212-B
50	X-31	12-N8-3	8	50-0	42'-0"	12		1/2	0.5	0.875	15.75	FW-9/16	PP-3/8/FW-3/8	A333-O	A212-B
51	X-31	12-N8-3	8	45-0	42'-0"	12		1/2	0.5	0.875	15.75	FW-9/16	PP-3/8/FW-3/8	A333-O	A212-B
52	X-31	12-N8-3	8	40-0	42'-0"	12		1/2	0.5	0.875	15.75	FW-9/16	PP-3/8/FW-3/8	A333-O	A212-B
53	X-31	12-N8-3A	8	35-0	42'-0"	12	Yes	1/2	0.5	0.875	15.75	FW-9/16	PP-3/8/FW-3/8	A333-O	A212-B
54	X-28	12-N8-2	8	220-0	40'-0"	12		1/2	0.5	0.875	15.75	FW-9/16	PP-3/8/FW-3/8	A333-O	A212-B
55	X-31	12-N8-2	8	30-0	40'-0"	12		1/2	0.5	0.875	15.75	FW-9/16	PP-3/8/FW-3/8	A333-O	A212-B
56	X-31	12-N8-2	8	45-0	40'-0"	12		1/2	0.5	0.875	15.75	FW-9/16	PP-3/8/FW-3/8	A333-O	A212-B
57	X-31	12-N8-2	8	40-0	40'-0"	12		1/2	0.5	0.875	15.75	FW-9/16	PP-3/8/FW-3/8	A333-O	A212-B
58	X-31	12-N8-2A	8	35-0	40'-0"	12	Yes	1/2	0.5	0.875	15.75	FW-9/16	PP-3/8/FW-3/8	A333-O	A212-B
59	X-28	12-N8-2	8	224-40	40'-0"	12		1/2	0.5	0.875	15.75	FW-9/16	PP-3/8/FW-3/8	A333-O	A212-B
60	X-28	12-N8-2	8	229-20	40'-0"	12	Yes	1/2	0.5	0.875	15.75	FW-9/16	PP-3/8/FW-3/8	A333-O	A212-B

Table 5-3: Drywell Penetrations (cont'd)

#	Custom	CB&I Mk	Size	Azimuth Deg-Min	Elevation	Detail Dwg#	Spare	Pntr Type	Pen Thk(in)	Rfr Plt Thk(in)	Rfr Plt D/L(in)	Weld Vsl/Plt	Weld Pen/Plt	Pntr Matl.	Reinf Plt Matl
61	X-28	12-N8-2	8	234-0	40'-0"	12	Yes	1/2	0.5	0.875	15.75	FW-9/16	PP-3/8/FW-3/8	A333-O	A212-B
62	X-29	12-N8-3	8	220-0	42'-0"	12		1/2	0.5	0.875	15.75	FW-9/16	PP-3/8/FW-3/8	A333-O	A212-B
63	X-29	12-N8-3	8	224-40	42'-0"	12		1/2	0.5	0.875	15.75	FW-9/16	PP-3/8/FW-3/8	A333-O	A212-B
64	X-29	12-N8-3	8	229-20	42'-0"	12	Yes	1/2	0.5	0.875	15.75	FW-9/16	PP-3/8/FW-3/8	A333-O	A212-B
65	X-29	12-N8-3	8	234-0	42'-0"	12	Yes	1/2	0.5	0.875	15.75	FW-9/16	PP-3/8/FW-3/8	A333-O	A212-B
66	X-30	12-N8-6	8	220-0	44'-0"	12		1/2	0.5	0.875	15.75	FW-9/16	PP-3/8/FW-3/8	A333-O	A212-B
67	X-30	12-N8-6	8	224-40	44'-0"	12		1/2	0.5	0.875	15.75	FW-9/16	PP-3/8/FW-3/8	A333-O	A212-B
68	X-30	12-N8-6	8	229-20	44"-0"	12		1/2	0.5	0.875	15.75	FW-9/16	PP-3/8/FW-3/8	A333-O	A212-B
69	X-30	12-N8-6	8	234-0	44'-0"	12		1/2	0.5	0.875	15.75	FW-9/16	PP-3/8/FW-3/8	A333-O	A212-B
70	X-32	12-N8-7	8	120-0	36'-0"	12		1/2	0.5	0.875	15.75	FW-9/16	PP-3/8/FW-3/8	A333-O	A212-B
71	X-32	12-N8-7	8	125-0	36'-0"	12		1/2	0.5	0.875	15.75	FW-9/16	PP-3/8/FW-3/8	A333-O	A212-B
72	X-32	12-N8-7	8	130-0	36'-0"	12	Yes	1/2	0.5	0.875	15.75	FW-9/16	PP-3/8/FW-3/8	A333-O	A212-B
73	X-32	12-N8-7	8	135-0	36'-0"	12	Yes	1/2	0.5	0.875	15.75	FW-9/16	PP-3/8/FW-3/8	A333-O	A212-B
74	X-32	12-N8-1	8	110-0	38'-0"	12		1/2	0.5	0.875	15.75	FW-9/16	PP-3/8/FW-3/8	A333-O	A212-B
75	X-32	12-N8-1	8	115-0	38'-0"	12		1/2	0.5	0.875	15.75	FW-9/16	PP-3/8/FW-3/8	A333-O	A212-B
76	X-32	12-N8-1	8	120-0	38'-0"	12		1/2	0.5	0.875	15.75	FW-9/16	PP-3/8/FW-3/8	A333-O	A212-B
77	X-32	12-N8-1	8	125-0	38'-0"	12	Yes	1/2	0.5	0.875	15.75	FW-9/16	PP-3/8/FW-3/8	A333-O	A212-B
78	X-32	12-N8-1	8	130-0	38'-0"	12	Yes	1/2	0.5	0.875	15.75	FW-9/16	PP-3/8/FW-3/8	A333-O	A212-B
79	X-32	12-N8-1	8	135-0	38'-0"	12		1/2	0.5	0.875	15.75	FW-9/16	PP-3/8/FW-3/8	A333-O	A212-B
80	X-32	12-N8-1	8	140-0	38'-0"	12		1/2	0.5	0.875	15.75	FW-9/16	PP-3/8/FW-3/8	A333-O	A212-B
81	X-32	12-N8-1	8	145-0	38'-0"	12		1/2	0.5	0.875	15.75	FW-9/16	PP-3/8/FW-3/8	A333-O	A212-B
82	X-32	12-N8-2	8	110-0	40'-0"	12		1/2	0.5	0.875	15.75	FW-9/16	PP-3/8/FW-3/8	A333-O	A212-B
83	X-32	12-N8-2	8	115-0	40'-0"	12		1/2	0.5	0.875	15.75	FW-9/16	PP-3/8/FW-3/8	A333-O	A212-B
84	X-32	12-N8-2	8	120-0	40'-0"	12		1/2	0.5	0.875	15.75	FW-9/16	PP-3/8/FW-3/8	A333-O	A212-B
85	X-32	12-N8-2	8	125-0	40'-0"	12		1/2	0.5	0.875	15.75	FW-9/16	PP-3/8/FW-3/8	A333-O	A212-B
86	X-32	12-N8-2	8	130-0	40'-0"	12		1/2	0.5	0.875	15.75	FW-9/16	PP-3/8/FW-3/8	A333-O	A212-B
87	X-32	12-N8-2	8	135-0	40'-0"	12		1/2	0.5	0.875	15.75	FW-9/16	PP-3/8/FW-3/8	A333-O	A212-B
88	X-32	12-N8-2	8	140-0	40'-0"	12		1/2	0.5	0.875	15.75	FW-9/16	PP-3/8/FW-3/8	A333-O	A212-B
89	X-32	12-N8-2	8	145-0	40'-0"	12		1/2	0.5	0.875	15.75	FW-9/16	PP-3/8/FW-3/8	A333-O	A212-B
90	X-33	12-N8-7	8	140-0	36'-0"	12		1/2	0.5	0.875	15.75	FW-9/16	PP-3/8/FW-3/8	A333-O	A212-B
91	X-34	12-N8-7	8	145-0	36'-0"	12		1/2	0.5	0.875	15.75	FW-9/16	PP-3/8/FW-3/8	A333-O	A212-B
92	X-36	12-N8-6	8	290-0	44'-0"	12		1/2	0.5	0.875	15.75	FW-9/16	PP-3/8/FW-3/8	A333-O	A212-B
93	X-37	16-N 8-9	8	8-0	22'-3"	16	Yes	1/2	0.5	0.875	15.25	FW-9/16	PP-3/8/FW-3/8	A333-O	A212-B
94	X-37	16-N 8-9	8	10-30	22'-3"	16		1/2	0.5	0.875	15.25	FW-9/16	PP-3/8/FW-3/8	A333-O	A212-B
95	X-37	16-N 8-9	8	25-30	22'-3"	16		1/2	0.5	0.875	15.25	FW-9/16	PP-3/8/FW-3/8	A333-O	A212-B
96	X-37	16-N 8-9	8	28-0	22'-3"	16	Yes	1/2	0.5	0.875	15.25	FW-9/16	PP-3/8/FW-3/8	A333-O	A212-B
97	X-38	27-X38	3	209-0	73'-9"	27		3	0.3	1.75	16	FP	PP-3/8/FW-1/2	A333-O	A212-B
98	X-38	27-X38	3	212-0	73'-9"	27		3	0.3	1.75	16	FP	PP-3/8/FW-1/2	A333-O	A212-B
99	X-38	27-X38	3	215-0	73'-9"	27		3	0.3	1.75	16	FP	PP-3/8/FW-1/2	A333-O	A212-B
100	X-38	27-X38	3	209-0	72'-11"	27		3	0.3	1.75	16	FP	PP-3/8/FW-1/2	A333-O	A212-B
101	X-38	27-X38	3	212-0	72'-11"	27		3	0.3	1.75	16	FP	PP-3/8/FW-1/2	A333-O	A212-B
102	X-38	27-X38	3	215-0	72'-11"	27		3	0.3	1.75	16	FP	PP-3/8/FW-1/2	A333-O	A212-B
103	X-39	27-X39	3	55-30	73'-9"	27		3	0.3	1.75	16	FP	PP-3/8/FW-1/2	A333-O	A212-B
104	X-39	27-X39	3	61-30	73'-9"	27		3	0.3	1.75	16	FP	PP-3/8/FW-1/2	A333-O	A212-B
105	X-39	27-X39	3	55-30	72'-11"	27		3	0.3	1.75	16	FP	PP-3/8/FW-1/2	A333-O	A212-B
106	X-39	27-X39	3	61-30	72'-11"	27		3	0.3	1.75	16	FP	PP-3/8/FW-1/2	A333-O	A212-B
107	X-40	12-N3-9	3	210-0	42'-0'	12		1/2	0.3	0.875	9.75	FW-9/16	FW-3/8	A333-O	A212-B
108	X-40	12-N3-9	3	215-0	42'-0"	12		1/2	0.3	0.875	9.75	FW-9/16	FW-3/8	A333-O	A212-B
109	X-40	12-N3-9	3	300-0	42'-0"	12		1/2	0.3	0.875	9.75	FW-9/16	FW-3/8	A333-O	A212-B
110	X-40	12-N3-1	3	20-0	44"-0"	12		1/2	0.3	0.875	9.75	FW-9/16	FW-3/8	A333-O	A212-B
111	X-40	12-N3-1	3	25-0	44"-0"	12		1/2	0.3	0.875	9.75	FW-9/16	FW-3/8	A333-O	A212-B
112	X-40	12-N3-1	3	210-0	44"-0"	12		1/2	0.3	0.875	9.75	FW-9/16	FW-3/8	A333-O	A212-B
113	X-40	12-N3-1	3	215-0	44"-0"	12		1/2	0.3	0.875	9.75	FW-9/16	FW-3/8	A333-O	A212-B
114	X-40	12-N3-1	3	300-0	44"-0"	12		1/2	0.3	0.875	9.75	FW-9/16	FW-3/8	A333-O	A212-B
115	X-40	12-N3-2	3	20-0	46'-0"	12		1/2	0.3	0.875	9.75	FW-9/16	FW-3/8	A333-O	A212-B
116	X-40	12-N3-2	3	23-0	46'-0"	12		1/2	0.3	0.875	9.75	FW-9/16	FW-3/8	A333-O	A212-B
117	X-41	13-N3-6	3	47-0	19'-9"	13		1/2	0.218	0.875	10.25	FW-9/16	FP/FW-1/4	A333-O	A212-B
118	X-41	13-N3-6	3	61-0	19'-9"	13		1/2	0.218	0.875	10.25	FW-9/16	FP/FW-1/4	A333-O	A212-B
119	X-41	13-N3-6	3	191-0	19'-9"	13		1/2	0.218	0.875	10.25	FW-9/16	FP/FW-1/4	A333-O	A212-B
120	X-41	13-N3-6	3	205-0	19'-9"	13		1/2	0.218	0.875	10.25	FW-9/16	FP/FW-1/4	A333-O	A212-B

Table 5-3: Drywell Penetrations (cont'd)

#	Custom	CB&I Mk	Size	Azimuth Deg-Min	Elevation	Detail Dwg#	Spare	Pntr Type	Pen Thk(in)	Rfr Plt Thk(in)	Rfr Plt D/L(in)	Weld Vsl/Plt	Weld Pen/Plt	Pntr Matl.	Reinf Plt Matl
121	X-41	13-N3-6	3	277-0	19'-9"	13		1/2	0.218	0.875	10.25	FW-9/16	FP/FW-1/4	A333-O	A212-B
122	X-41	13-N3-7	3	47-0	20'-6"	13		1/2	0.218	0.875	10.25	FW-9/16	FP/FW-1/4	A333-O	A212-B
123	X-41	13-N3-7	3	61-0	20'-6"	13		1/2	0.218	0.875	10.25	FW-9/16	FP/FW-1/4	A333-O	A212-B
124	X-41	13-N3-7	3	191-0	20'-6"	13		1/2	0.218	0.875	10.25	FW-9/16	FP/FW-1/4	A333-O	A212-B
125	X-41	12-N3-7	3	205-0	20'-6"	13		1/2	0.218	0.875	10.25	FW-9/16	FP/FW-1/4	A333-O	A212-B
126	X-41	12-N3-7	3	277-0	20'-6"	13		1/2	0.218	0.875	10.25	FW-9/16	FP/FW-1/4	A333-O	A212-B
127	X-42	26-X42-43	3	58-30	61'-9"	26		3	0.3	1.75	16	FP	FP	A333-O	A212-B
128	X-43	26-X42-43	3	58-30	62'-4"	26	Yes	3	0.3	1.75	16	FP	FP	A333-O	A212-B
129	X-44	17-N3-13	3	25-0	91'-0"	17	Yes	1/2	0.5	0.875	9	FW-9/16	FW-3/8	A333-O	A212-B
130	X-44	17-N3-12A	3	335-0	91'-0"	17	Yes	1/2	0.5	0.875	9	FW-9/16	FW-3/8	A333-O	A212-B
131	X-45	14-N6-7A	6	219-19	35'-10.25"	14		1/2	0.432	0.875	16.625	FW-9/16	FP	A333-O	A212-B
132	X-45	14-N6-9A	6	225-05	35'-10.25"	14		1/2	0.432	0.875	16.625	FW-9/16	FP	A333-O	A212-B
133	X-45	14-N6-6A	6	235-03	35'-10.25"	14		1/2	0.432	0.875	16.625	FW-9/16	FP	A333-O	A212-B
134	X-45	24-X45	6	213-08	36'-5"	24		3	0.432	1.75	21	FP	PP-3/8/FW-1/2	A333-O	A212-B
135	X-45	14-N6-7	6	219-19	36'-11.75"	14		1/2	0.432	0.875	16.625	FW-9/16	PP-3/8/FW-3/8	A333-O	A212-B
136	X-45	14-N6-9	6	225-05	36'-11.75"	14		1/2	0.432	0.875	16.625	FW-9/16	PP-3/8/FW-3/8	A333-O	A212-B
137	X-45	14-N6-6	6	235-03	36'-11.75"	14		1/2	0.432	0.875	16.625	FW-9/16	PP-3/8/FW-3/8	A333-O	A212-B
138	X-46	28-X46	3	120-0	86'-0"	28	Yes	3	0.3	1.75	16	FP	PP-3/8/FW-1/2	A333-O	A212-B
139	X-46	17-N3-12A	3	330-0	86'-0"	17	Yes	1/2	0.3	0.875	9	FW-9/16	FW-3/8	A333-O	A212-B
140	X-47	12-N3-5	3	320-0	47'-0"	12	Yes	1/2	0.3	0.875	9.75	FW-9/16	FW-3/8	A333-O	A212-B
141	X-47	12-N3-5	3	325-0	47'-0"	12	Yes	1/2	0.3	0.875	9.75	FW-9/16	FW-3/8	A333-O	A212-B
142	X-47	12-N3-5	3	330-0	47'-0"	12	Yes	1/2	0.3	0.875	9.75	FW-9/16	FW-3/8	A333-O	A212-B
143	X-47	28-X47	3	335-0	47'-0"	28	Yes	3	0.5	1.75	16	FP	PP-3/8/FW-1/2	A333-O	A212-B
144	X-49	21-A	94	'ent Opening	15'-7.25"	21		3	2.5	2.875	105.25	FP	FP		
145	X-50	24-X50	3	284-0	47'-0"	24		3	0.3	1.75	14.125	FP	PP-3/8/FW-1/2	A333-O	A212-B
146	X-50	24-X50	3	286-0	47'-0"	24		3	0.3	1.75	14.125	FP	PP-3/8/FW-1/2	A333-O	A212-B
147	X-50	24-X50	3	288-0	47'-0"	24		3	0.3	1.75	14.125	FP	PP-3/8/FW-1/2	A333-O	A212-B
148	X-50	24-X50	3	290-0	47'-0"	24		3	0.3	1.75	14.125	FP	PP-3/8/FW-1/2	A333-O	A212-B
149	X-50	24-X50	3	292-0	47'-0"	24		3	0.3	1.75	14.125	FP	PP-3/8/FW-1/2	A333-O	A212-B
150	X-50	24-X50	3	294-0	47'-0"	24		3	0.3	1.75	14.125	FP	PP-3/8/FW-1/2	A333-O	A212-B
151	X-50	24-X50	3	296-0	47'-0"	24		3	0.3	1.75	14.125	FP	PP-3/8/FW-1/2	A333-O	A212-B
152	X-50	24-X50	3	298-0	47'-0"	24		3	0.3	1.75	14.125	FP	PP-3/8/FW-1/2	A333-O	A212-B
153	X-50	24-X50	3	300-0	47'-0"	24		3	0.3	1.75	14.125	FP	PP-3/8/FW-1/2	A333-O	A212-B
154	X-50	24-X50	3	302-0	47'-0"	24		3	0.3	1.75	14.125	FP	PP-3/8/FW-1/2	A333-O	A212-B
155	X-50	24-X50	3	304-0	47'-0"	24	Yes	3	0.3	1.75	14.125	FP	PP-3/8/FW-1/2	A333-O	A212-B
156	X-50	24-X50	3	306-0	47'-0"	24	Yes	3	0.3	1.75	14.125	FP	PP-3/8/FW-1/2	A333-O	A212-B
157	X-50	24-X50	3	308-0	47'-0"	24	Yes	3	0.3	1.75	14.125	FP	PP-3/8/FW-1/2	A333-O	A212-B
158	X-50	24-X50	3	284-0	48'-6"	24		3	0.3	1.75	14.125	FP	PP-3/8/FW-1/2	A333-O	A212-B
159	X-50	24-X50	3	286-0	48'-6"	24	Yes	3	0.3	1.75	14.125	FP	PP-3/8/FW-1/2	A333-O	A212-B
160	X-50	24-X50	3	288-0	48'-6"	24	Yes	3	0.3	1.75	14.125	FP	PP-3/8/FW-1/2	A333-O	A212-B
161	X-50	24-X50	3	290-0	48'-6"	24	Yes	3	0.3	1.75	14.125	FP	PP-3/8/FW-1/2	A333-O	A212-B
162	X-50	24-X50	3	292-0	48'-6"	24	Yes	3	0.3	1.75	14.125	FP	PP-3/8/FW-1/2	A333-O	A212-B
163	X-50	24-X50	3	294-0	48'-6"	24	Yes	3	0.3	1.75	14.125	FP	PP-3/8/FW-1/2	A333-O	A212-B
164	X-50	24-X50	3	296-0	48'-6"	24	Yes	3	0.3	1.75	14.125	FP	PP-3/8/FW-1/2	A333-O	A212-B
165	X-50	24-X50	3	298-0	48'-6"	24	Yes	3	0.3	1.75	14.125	FP	PP-3/8/FW-1/2	A333-O	A212-B
166	X-50	24-X50	3	300-0	48'-6"	24	Yes	3	0.3	1.75	14.125	FP	PP-3/8/FW-1/2	A333-O	A212-B
167	X-50	24-X50	3	302-0	48'-6"	24	Yes	3	0.3	1.75	14.125	FP	PP-3/8/FW-1/2	A333-O	A212-B
168	X-50	24-X50	3	304-0	48'-6"	24	Yes	3	0.3	1.75	14.125	FP	PP-3/8/FW-1/2	A333-O	A212-B
169	X-50	24-X50	3	306-0	48'-6"	24		3	0.3	1.75	14.125	FP	PP-3/8/FW-1/2	A333-O	A212-B
170	X-51A	X51-A	24	0-0	10'-2"	70		3						A201-B	A212-B
171	X-51B	X51-B	24	72-0	10'-2"	70		3						A201-B	A212-B
172	X-51C	X51-C	24	108-0	10'-2"	70		3						A201-B	A212-B
173	X-51D	X51-D	24	144-0	10'-2"	70		3						A201-B	A212-B
174	X-51E	X51-E	24	216-0	10'-2"	70		3						A201-B	A212-B
175	X-51F	X51-F	24	252-0	10'-2"	70		3						A201-B	A212-B
176	X-51G	X51-G	24	288-0	10'-2"	70		3						A201-B	A212-B
177	X-52	20-X52	24	120-0	DRYWELL HI	20		n/a		1.5					A201-B
178	X-53	X-53	36	35-0 & 275-(	10'-2"	65		3						A201-B	A212-B
179	X-56	X-56	8	36-0	10'-2"	68		3						A333-O	A212-B
180	X-57	X-57	8	324-0	10'-2"	68		3						A333-O	A212-B

Table 5-3: Drywell Penetrations (concluded)

#	Custom	CB&I Mk	Size	Azimuth Deg-Min	Elevation	Detail Dwg#	Spare	Pntr Type	Pen Thk(in)	Rfr Plt Thk(in)	Rfr Plt D/L(in)	Weld Vsl/Plt	Weld Pen/Plt	Pntr Matl.	Reinf Plt Matl
181	X-58	X-58	1			64 & 78								A333-O	A212-B
182	X-59	17-N3-13A	3	25-0	90'-0"	17	Yes	1/2	0.3	0.875	9	FW-9/16	FW-3/8	A333-O	A212-B
183	X-60	17-N3-12A	3	30-0	90'-0"	17	Yes	1/2	0.3	0.875	9	FW-9/16	FW-3/8	A333-O	A212-B
184	X-60	17-N3-12A	3	35-0	90'-0"	17	Yes	1/2	0.3	0.875	9	FW-9/16	FW-3/8	A333-O	A212-B
185	X-60	17-N3-12A	3	40-0	90'-0"	17	Yes	1/2	0.3	0.875	9	FW-9/16	FW-3/8	A333-O	A212-B
186	X-60	17-N3-12A	3	45-0	90'-0"	17	Yes	1/2	0.3	0.875	9	FW-9/16	FW-3/8	A333-O	A212-B
187	X-60	17-N3-12A	3	50-0	90'-0"	17	Yes	1/2	0.3	0.875	9	FW-9/16	FW-3/8	A333-O	A212-B
188	X-60	17-N3-12A	3	55-0	90'-0"	17	Yes	1/2	0.3	0.875	9	FW-9/16	FW-3/8	A333-O	A212-B
189	X-60	17-N3-12A	3	60-0	90'-0"	17	Yes	1/2	0.3	0.875	9	FW-9/16	FW-3/8	A333-O	A212-B
190	X-61	12-N6-3	6	55-0	42'-0"	12		1/2	0.432	0.875	13	FW-9/16	PP-3/8/FW-3/8	A333-O	A212-B
191	X-62	14-N6-10	6	315-0	90'-0"	14		1/2	0.432	0.875	16.625	FW-9/16	PP-3/8/FW-3/8	A333-O	A212-B
192	X-63	26-X63	14	330-0	62'-0"	26		3	0.75	1.75	35	FP	FP	A201-B	A212-B
193	X-63	26-X63	14	340-0	62'-0"	26		3	0.75	0.75	35	FP	FP	A201-B	A212-B
194	X-64	26-X64	24	CL	2'-3"	20		n/a		1.25					A201-B
195	X-65	X-65	20	180-0	10'-2"	65		3						A201-B	A212-B
196	X-66	18-N16-1	16	38-0	27'-0"	18		1/2	0.875	0.875	28.75	FW-5/8	PP-1/2/FW-3/8	A201-B	A212-B
197	X-67	18-N10-1	10	44-0	27'-0"	18	Yes	1/2	0.593	0.875	20	FW-5/8	PP-1/2/FW-3/8	A333-O	A212-B
198	X-68A	X-68A	16	300-0	45 BEL; CL	67		3						A201-B	A212-B
199	X-68B	X-68A	16	102-20	45 BEL; CL	67		3						A201-B	A212-B
200	X-69	X-69	16	60-0	45 BEL; CL	67		3						A201-B	A212-B
201	X-70	33-X70	16	100-0	79'-6"	33		3	0.875	1.75	28	FP	FP/FW-3/8	A201-B	A212-B
202	X-71	33-X71	8	90-0	99'-6"	33		3	0.5	1.75	17	FP	PP-3/8/FW-3/8	A333-O	A212-B
203	X-72	33-X72	14	180-0	33'-0"	33		3	0.75	1.75	42	FP	FP/FW-3/8	A201-B	A212-B
204	X-73	39-X73	3	45-0	72'-6"	39		3	0.3	1.75	16	FP	PP-3/8/FW-1/2	A333-O	A212-B
205	X-73	39-X73	3	45-0	73'-6"	39		3	0.3	1.75	16	FP	PP-3/8/FW-1/2	A333-O	A212-B
206	X-73	39-X73	3	225-0	72'-6"	39		3	0.3	1.75	16	FP	PP-3/8/FW-1/2	A333-O	A212-B
207	X-73	39-X73	3	225-0	73'-6"	39		3	0.3	1.75	16	FP	PP-3/8/FW-1/2	A333-O	A212-B
208	X-74	81-X74	20	115-06	7'-1.75"	81									

Note: Pntr Type : Penetration Type
1/2: Type 1 or Type 2 Penetration (Reinforcing Plate)
3: Type 3 Penetration (Insert Plate)

Table 5-4: Penetrations by Size

Penetration Size (in)	Number of Penetrations
1	5
2	2
3	77
6	22
8	55
10	1
14	3
16	5
18	3
20	2
22	4
24	20
26	2
30	2
36	3
94	1 (10 Vent Openings)
Lock	1
Total	208

Table 5-5: Penetration Size for Reinforcement Requirement

Region	Cylindrical Shell	Upper Spherical Shell	Lower Spherical Shell
Inside Diameter (in)	396	420	420
Nominal Wall Thickness (in)	0.64	0.77	1.154
Mean Radius (in)	198.32	210.39	210.58
$0.2*\sqrt{(R_m t)}$ (in)	2.25	2.55	3.12

Table 5-6: Penetrations with Piping Loads

Penetration ID	Description
X2 A, B	Main Steam
X3 A, B	Isolation Condenser – A Steam
X4 A, B	Feedwater
X5 A, B	Isolation Condenser – A Condensate Return
X7	Shutdown Cooling Supply
X8	Shutdown Cooling Return
X9	Cleanup Supply
X10	Cleanup Return
X12 B	Core Spray Supply
X18	Ventilation Intake
X19	Ventilation Exhaust
X63	Containment Spray Supply
X70	Core Spray Supply

Table 5-7: OBE Seismic Anchor Movements at Star Truss Male Lug Elevation Calculated From Reference 20

Direction	Approach I	Approach II	Approach III
North – South	0.040	0.045	0.046
East - West	0.047	0.050	0.050
SRSS	0.062	0.067	0.068

Table 5-8: Post Accident Seismic Anchor Movements at Star Truss Male Lug Elevation, [20]

Direction	Max Relative Disp. (in)		
	Lower Bound	Upper Bound	Best Estimate
North-South	0.095	0.080	0.087
East-West	0.087	0.086	0.083
Vertical	0.001	0.001	0.001

Table 5-9: Damping Values (Percent of Critical Damping) [19]

Structural or Component	Operating Basis Earthquake or ½ Safe Shutdown Earthquake[1]	Safe Shutdown Earthquake
Equipment and large-diameter piping system[2], pipe diameter greater than 12"	2	3
Small diameter piping systems, diameter equal to or less than 12"	1	2
Weld Steel Structures	2	4
Bolted Steel Structures	4	7
Prestressed Concrete Structures	2	5
Reinforced Concrete Structures	4	7

Note:

1. In the dynamic analysis of active components as defined in Regulatory Guide 1.61, these values should also be used for SSE.
2. Includes both material and structural damping. If the piping system consists of only one or two spans with little structural damping, use values for small diameter piping.

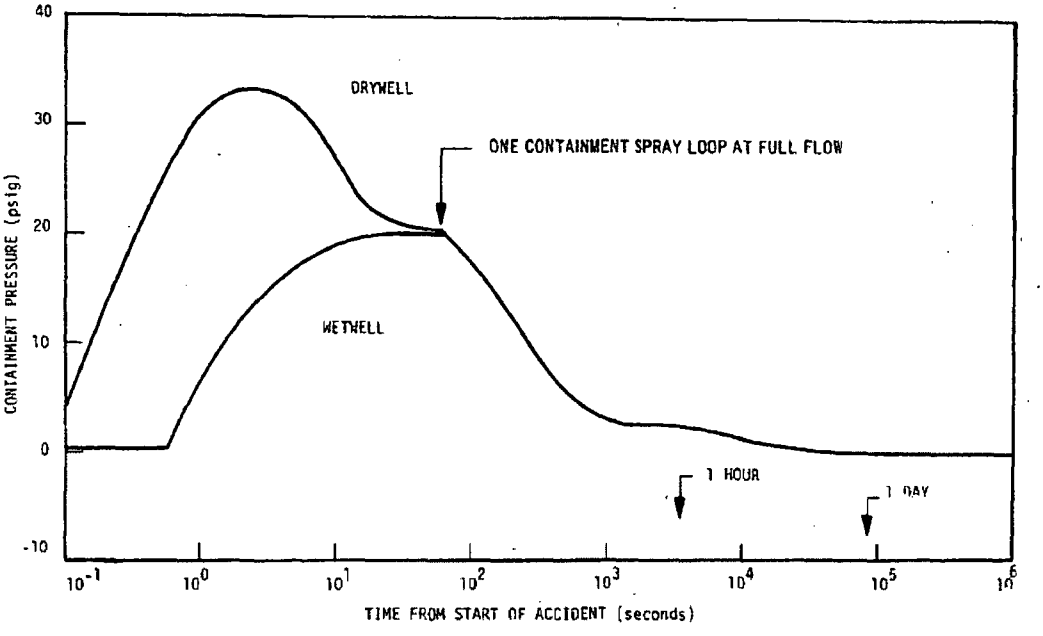

Figure 5-1: Primary Containment Pressure Following Recirculation Line Break

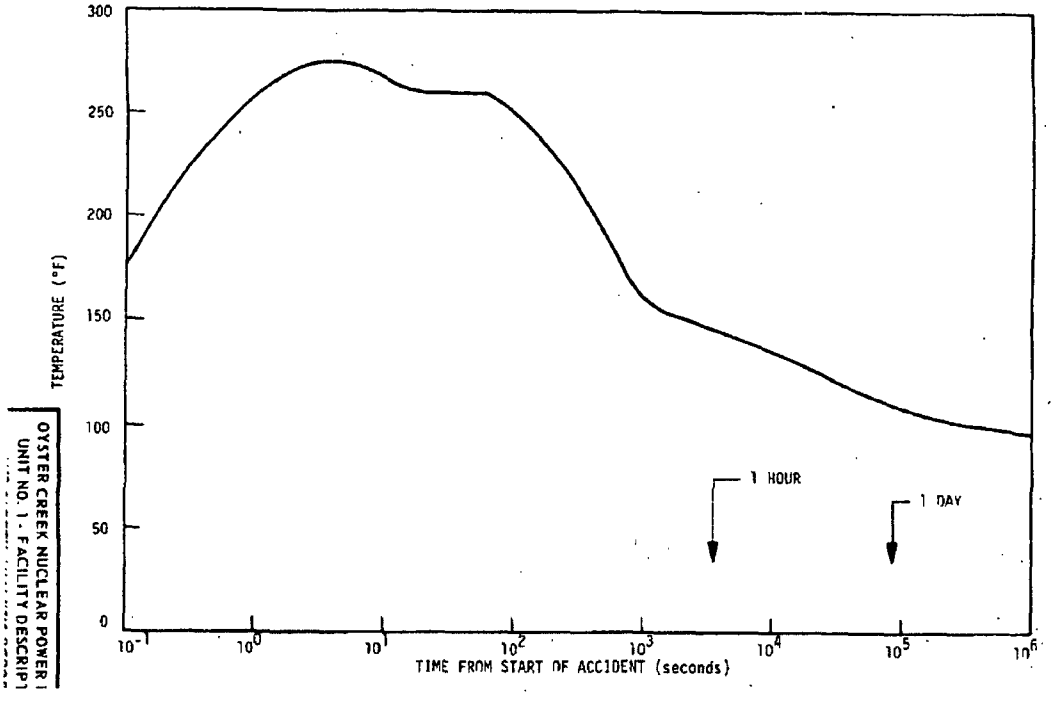

Figure 5-2: Drywell Temperature Response Following Recirculation Line Break

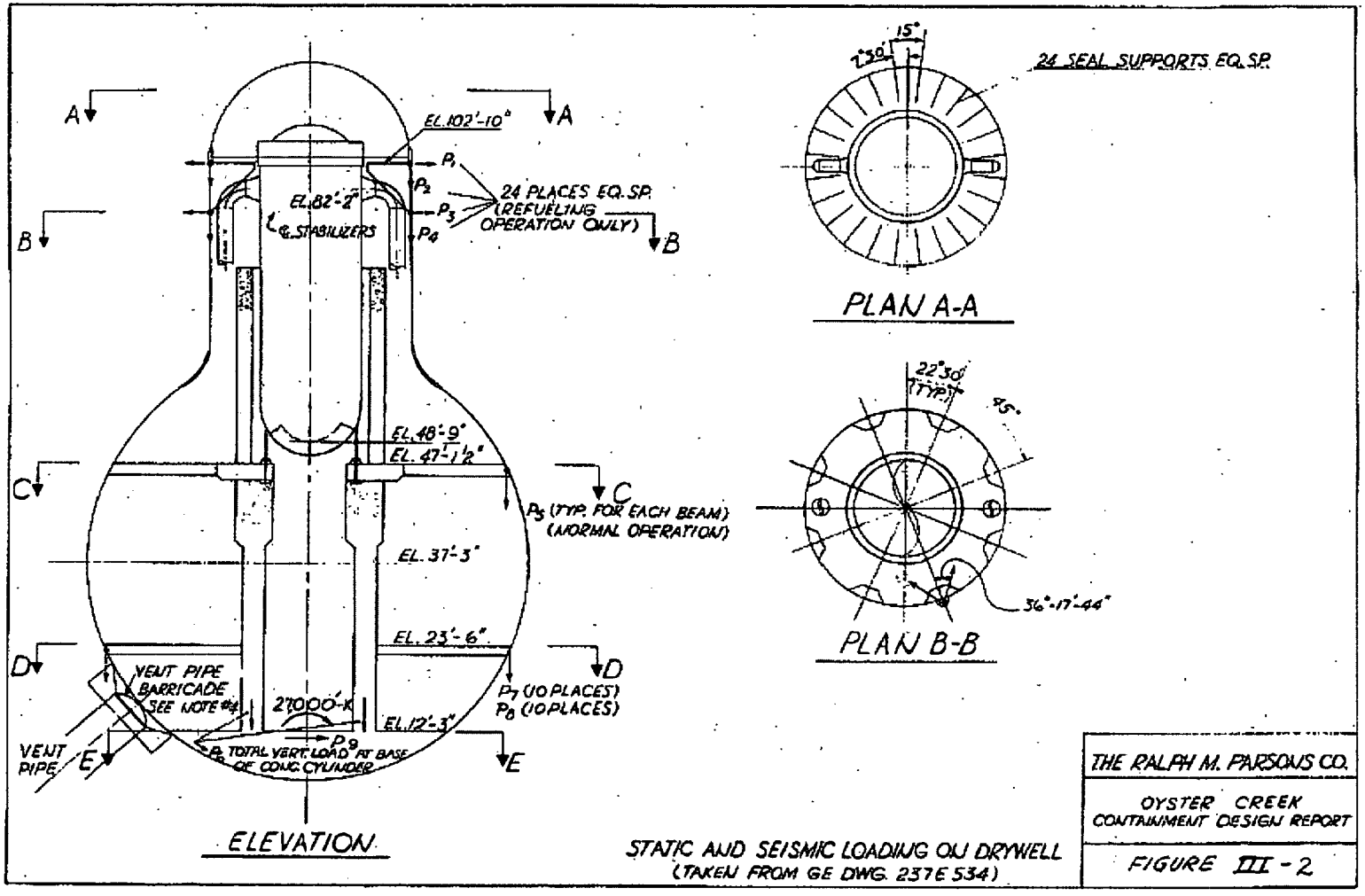

Figure 5-3: Static and Seismic Loading on Drywell [5]

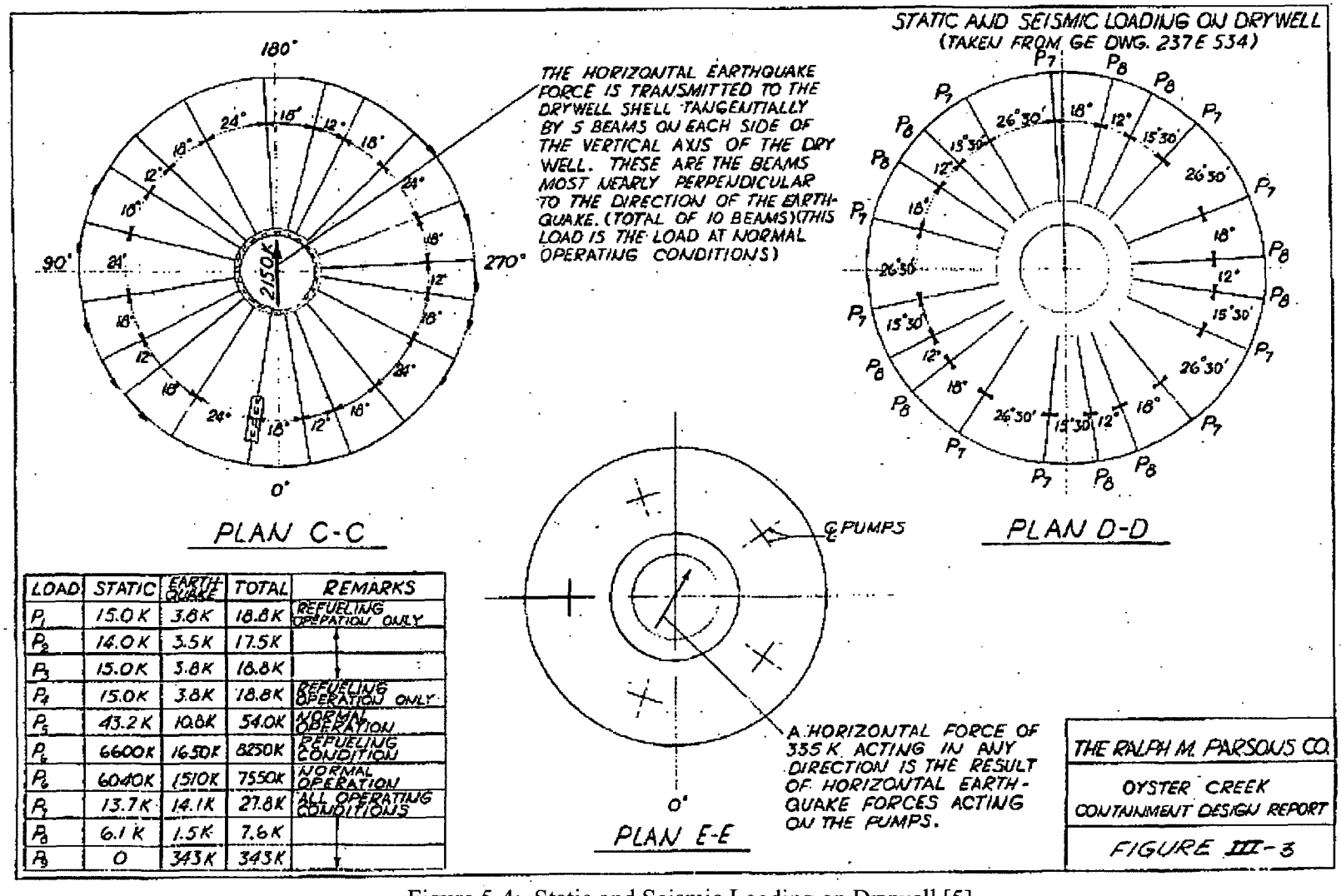

LOAD	STATIC	EARTHQUAKE	TOTAL	REMARKS
P_1	15.0K	3.8K	18.8K	REFUELING OPERATION ONLY
P_2	14.0K	3.5K	17.5K	
P_3	15.0K	3.8K	18.8K	
P_4	15.0K	3.8K	18.8K	REFUELING OPERATION ONLY
P_5	43.2K	10.8K	54.0K	NORMAL OPERATION
P_6	6600K	1650K	8250K	REFUELING CONDITION
P_7	6040K	1510K	7550K	NORMAL OPERATION
P_8	13.7K	14.1K	27.8K	ALL OPERATING CONDITIONS
P_9	6.1K	1.5K	7.6K	
P_{10}	0	343K	343K	

Figure 5-4: Static and Seismic Loading on Drywell [5]

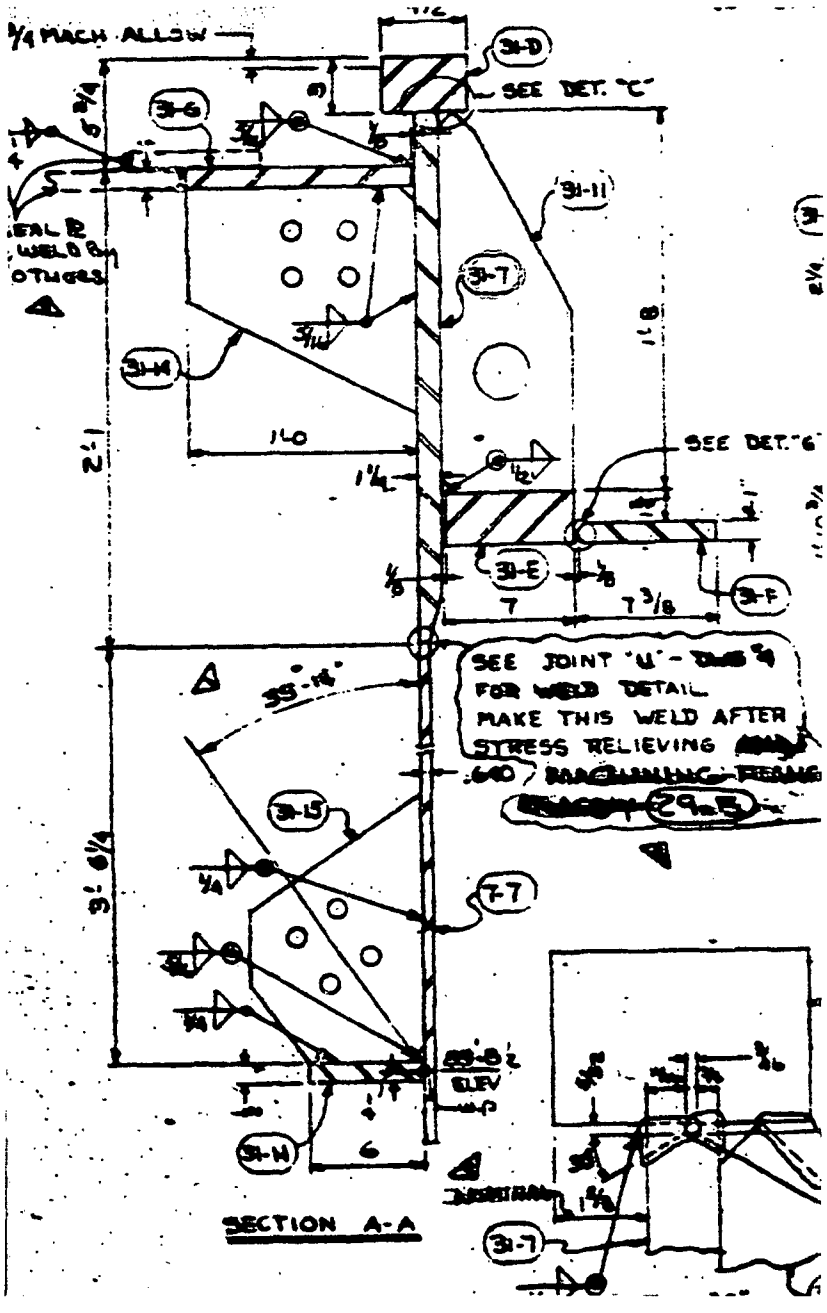

Figure 5-5: Application of Loads P1, P2, P3 and P4 From Reference 1

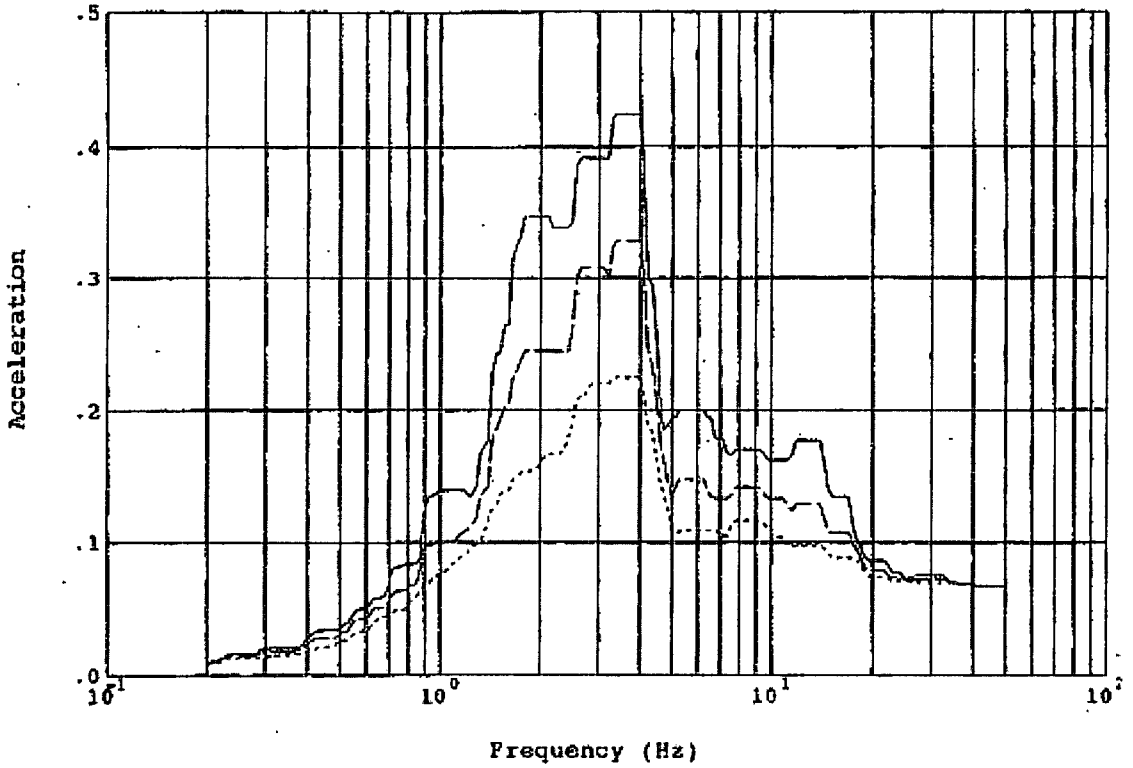

Figure 5-6: Seismic Response Spectra, OBE, Elevation , 10'-3", N-S Direction

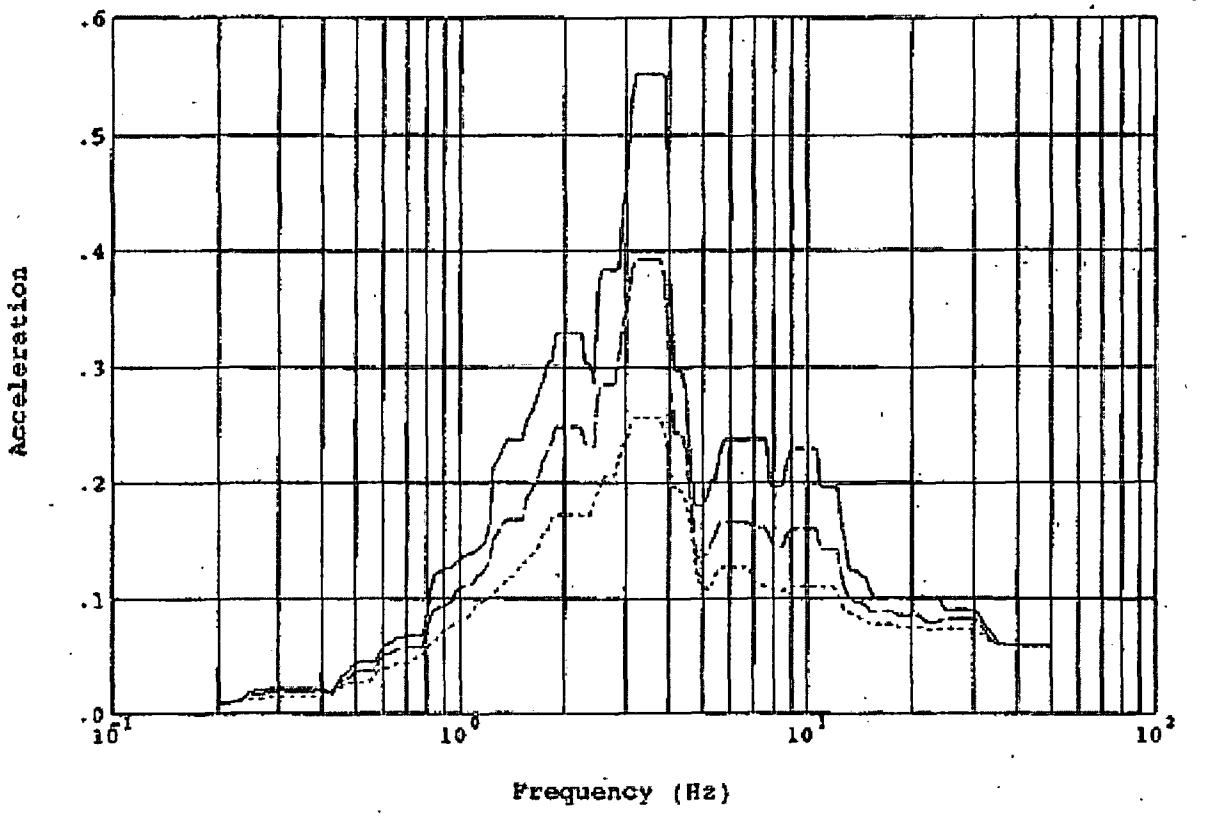

Figure 5-7: Seismic Response Spectra, OBE, Elevation 10'-3", E-W Direction

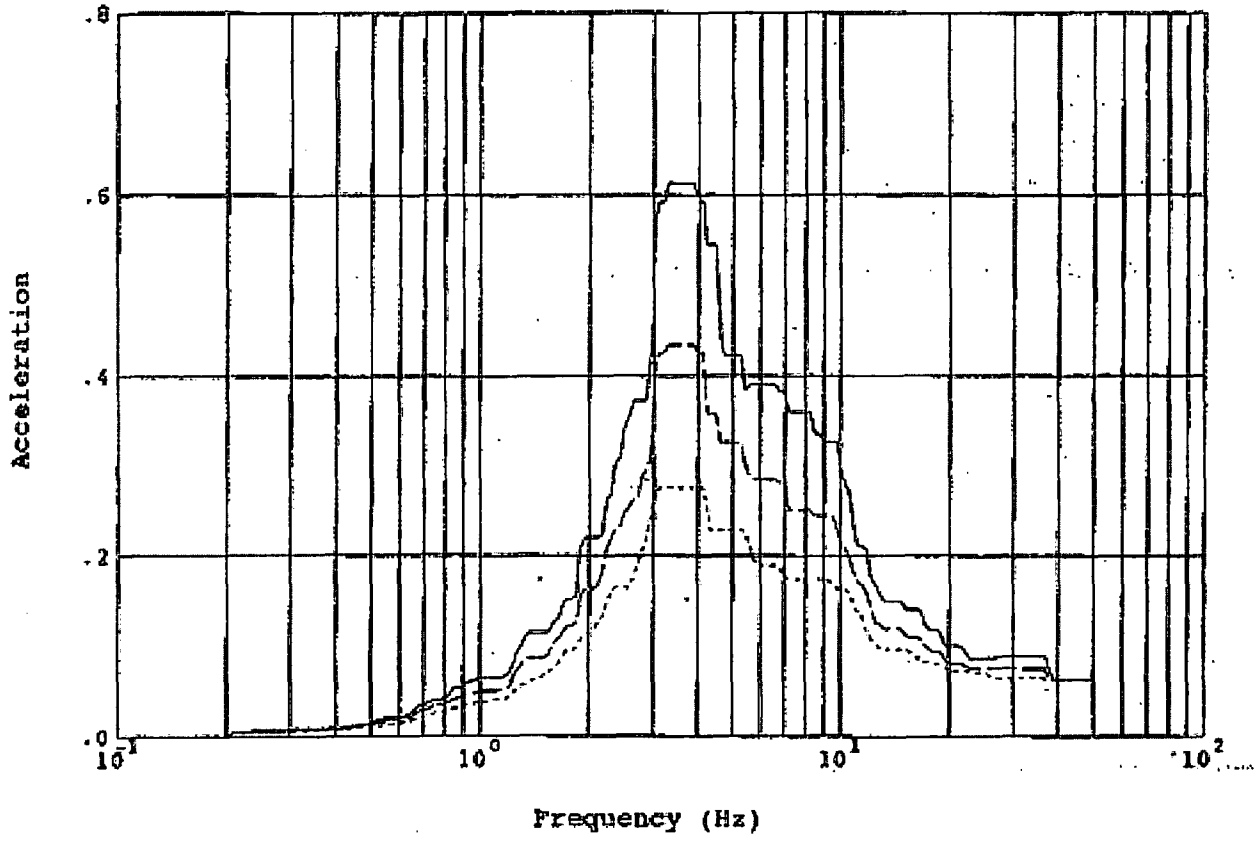

Figure 5-8: Seismic Response Spectra, OBE, Elevation 10'-3", Vertical Direction

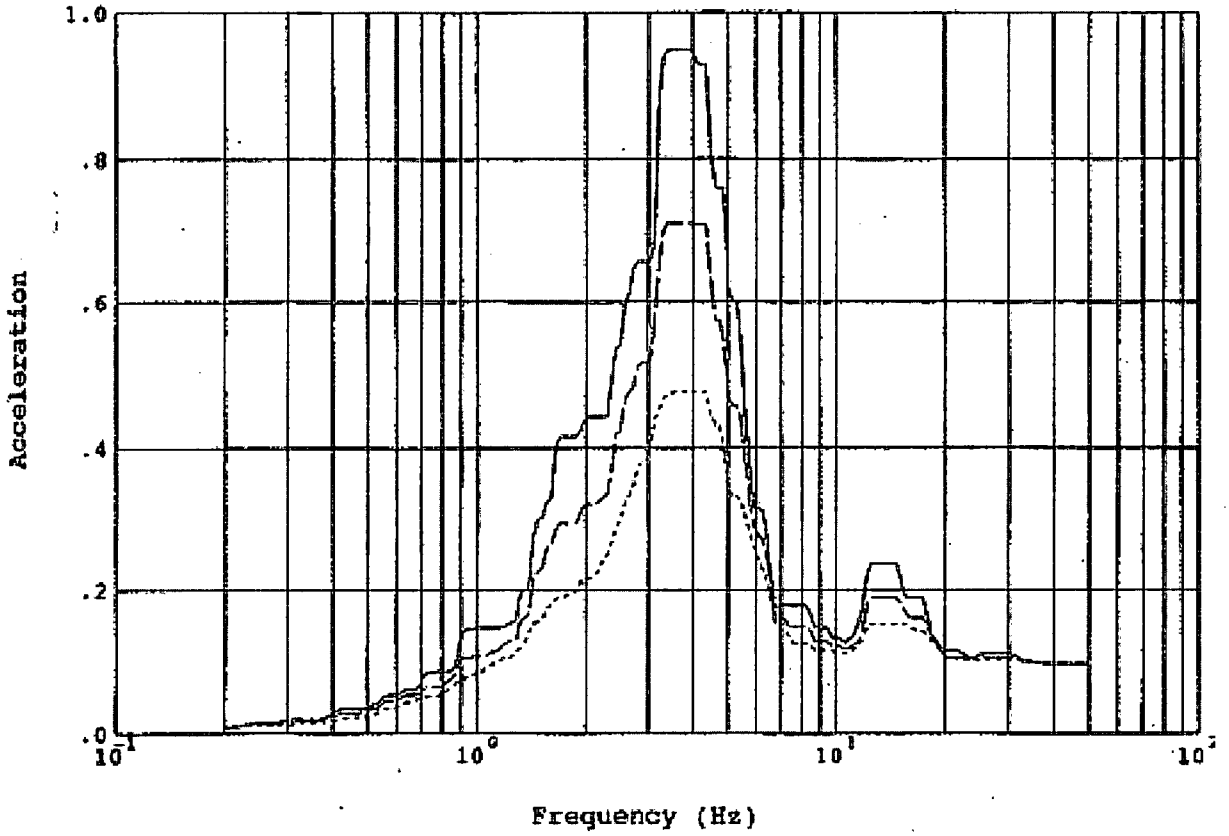

Figure 5-9: Seismic Response Spectra, OBE, Elevation 82'-9", N-S Direction

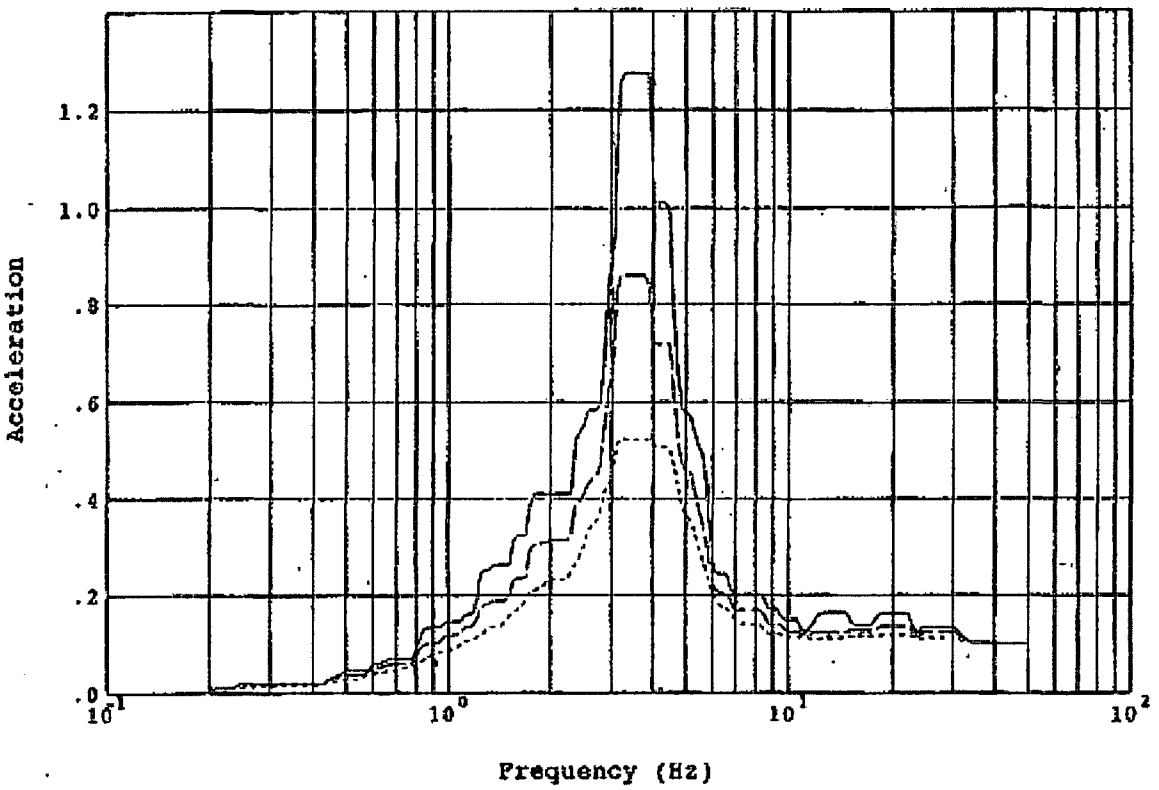

Figure 5-10: Seismic Response Spectra, OBE, Elevation 82'-9", E-W Direction

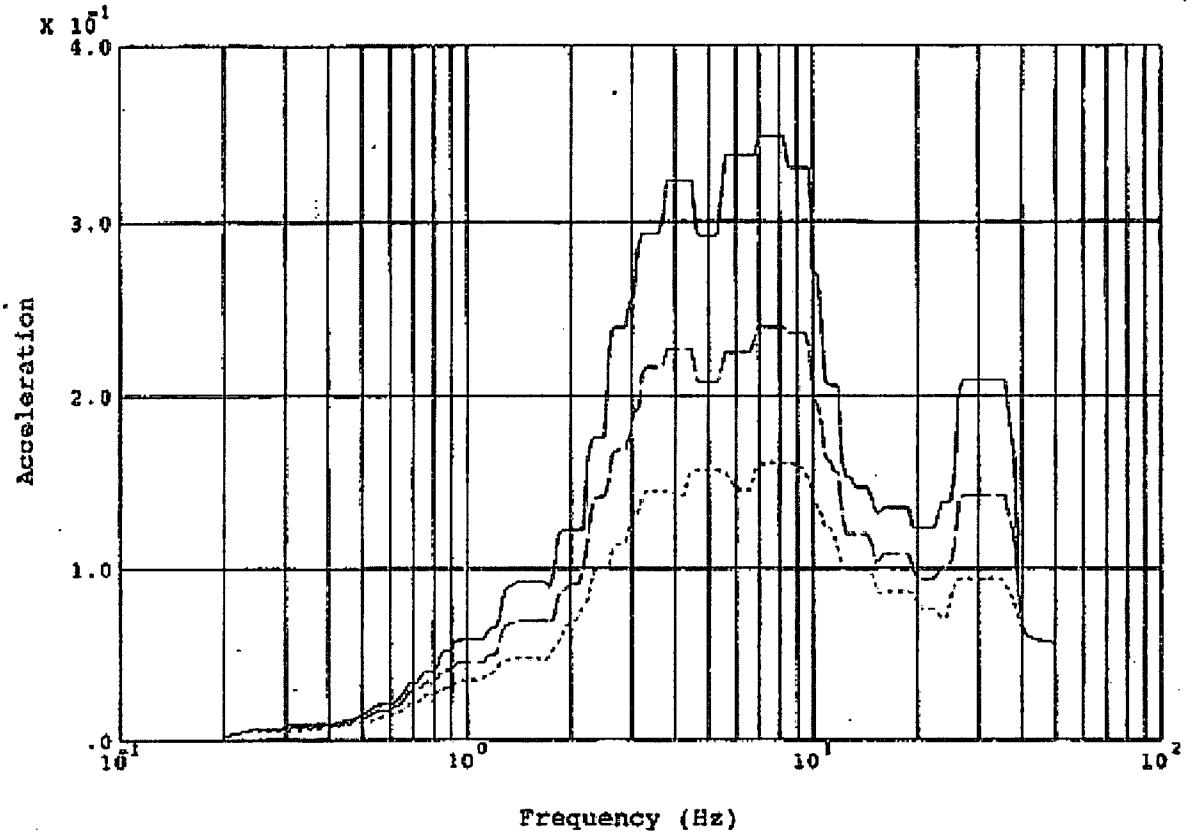

Figure 5-11: Response Spectra, OBE, Elevation 82'-9", Vertical Direction

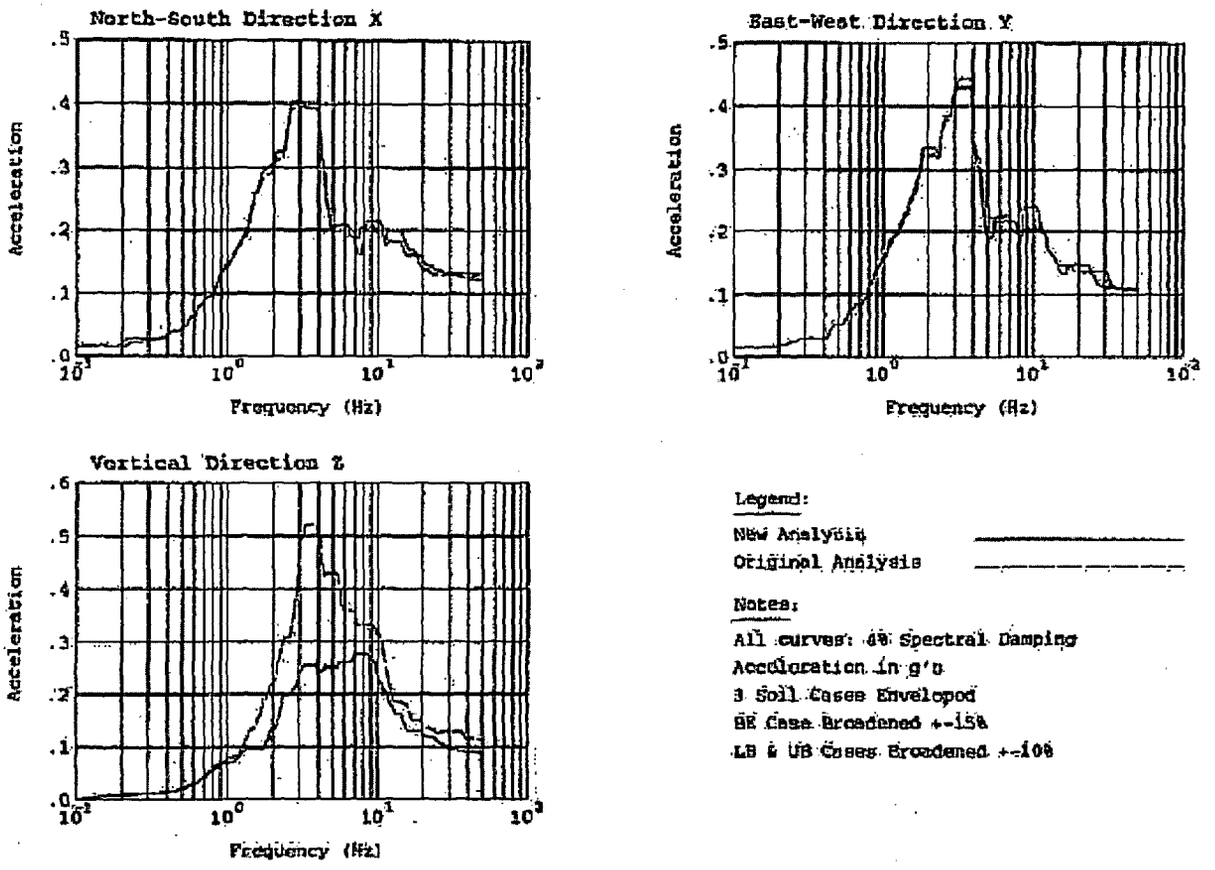

Figure 5-12: Flooded Response Spectra, at Drywell Elevation 10'-3"

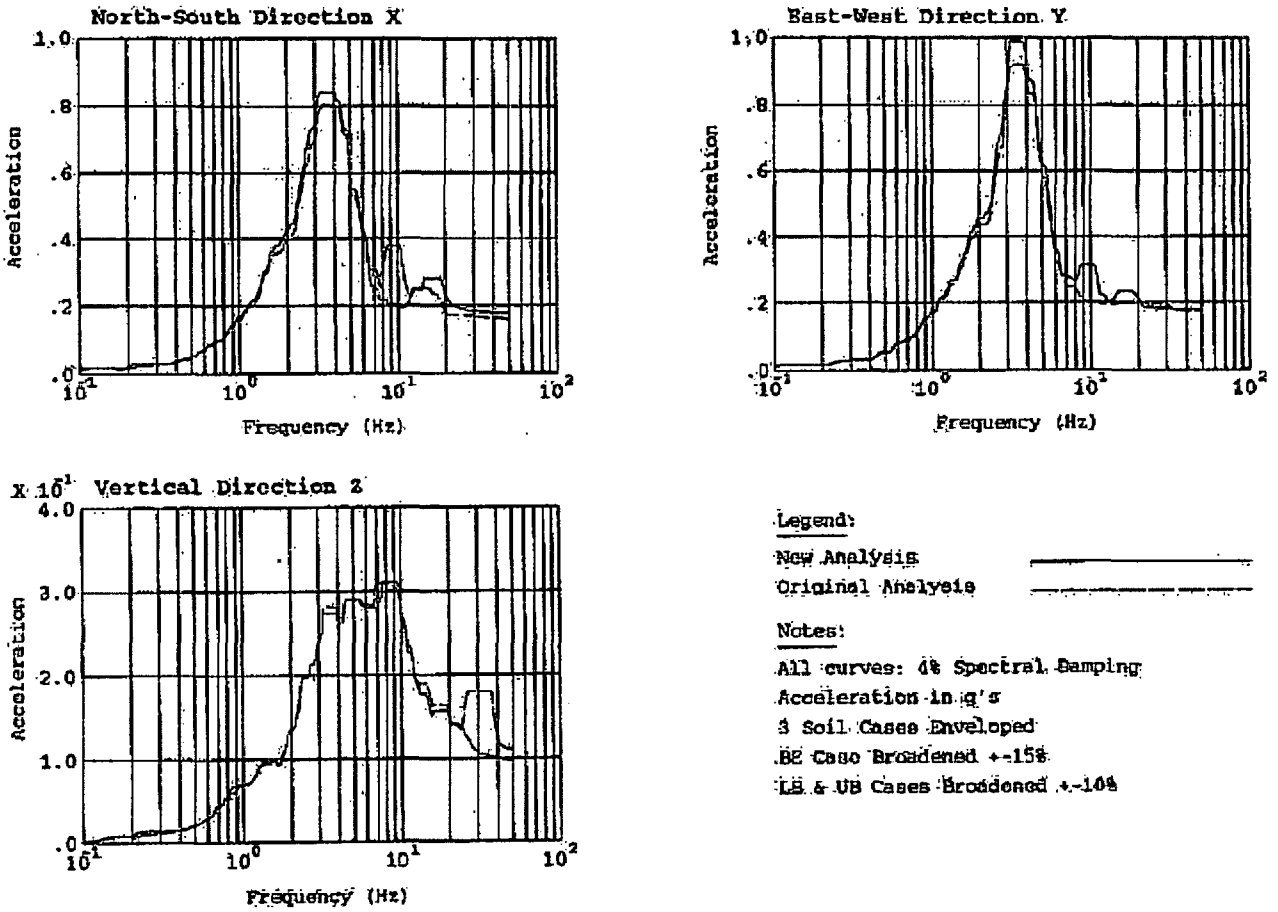

Figure 5-13: Flooded Response Spectra, at Drywell Elevation 82'-9"

6.0 FINITE ELEMENT STRESS ANALYSIS

The section describes the stress analyses of the Oyster Creek Drywell under different loading conditions using the finite element model described in Section 4.0. The results from these analyses will be used in subsequent load combinations and ASME Code evaluation in Section 7.0.

6.1 LOADING INPUT

The loading input is described in Section 5.0, and the individual load cases are shown in Table 6-1. The individual load cases are defined based on the type of applied loads and the load combinations that are required for the subsequent ASME Class MC Code evaluation.

6.2 ASSUMPTIONS

The following assumptions are used in the analysis (note that other assumptions are made in the body of the report):

(a) No bolt preloads were considered as described in Section 4.1.

(b) The top head and the cylindrical shell are assumed to be integrally connected as described in Section 4.1.

(c) The gap between the male lug in the star truss and the reactor building concrete wall is assumed to be closed. This is the gap in the circumferential direction. The gap is about 0.01 inches to the spacers which are inserted in between the male lug and the reactor building concrete wall. Assuming the gap is closed would provide constraint to the movement of the drywell and cause a higher stress in the local vicinity of the male lug and star truss insert plate. This assumption is conservative since the spacers may not be as rigid as the concrete wall and might easily be deformed to allow some movement of the male lug in the circumferential direction.

(d) Star truss load is not included because the star truss assembly design is to transmit the loads from the reactor /reactor internals and biological shield wall directly to the reactor building concrete wall such that it causes no significant stress in the drywell shell.

(e) The reactor building concrete wall is assumed to be rigid compared to the drywell shell since the concrete wall is much thicker.

(f) The concrete floor inside and outside the drywell are assumed to be rigid based on the thickness of the concrete .

(g) Since the as-measured wall thicknesses were used in the analytical model, the manufacturing tolerance on shell thickness was not considered in the analysis.

6.3 BOUNDARY CONDITIONS

6.3.1 Bottom Head Structural and Thermal Boundary Conditions

The Bottom Head of the Oyster Creek Drywell is embedded in the concrete as shown in Figure 6-1 and Figure 6-2. It is shown that the elevation of the concrete inside the drywell is 10'-3". On the outside of the bottom head of the drywell, the concrete elevation is 8'-11 ¼", at the bottom of sand bed region (Figure 6-2).

There is a caulk perimeter inside the drywell which reaches a higher elevation, Figure 6-1 and Figure 6-6. The elevation at the top of the caulk perimeter is 11'-0", shown in Figure 6-3, with an upper curb at 12'-3", Figure 6. Also it is shown that the concrete in the curb region was removed at the two trenches located at azimuth 72° and about 292° (Bay 5 and 17), Figure 6-6 and Figure 6-7.

In addition to the drywell bottom head being embedded in the concrete, the drywell is also supported by the drywell skirt and reinforced by the stiffener plate, Figure 6-1. The top of the stiffener plate is at an elevation 8'-9". Both the drywell skirt and the stiffener plate are embedded in the concrete.

Based on the above information, a section of drywell shell between elevation 8'-11 ¼" and 12'-3" has concrete on the inside but not on the outside.

For the thermal boundary condition, at steady state operating condition, the drywell shell temperature is 150 °F, above elevation 11'-0", top of concrete caulk perimeter [Section 6.2.1.3.3, Reference 13]. It is assumed that the concrete is at ambient temperature of 70 °F, below the elevation 8'-11 ¼". The steady state operating temperature distribution between the elevation 11'-0" and 8'-11 ¼" is established through heat conduction by running a thermal steady state solution, assuming no heat convection through the concrete and the air in the sand bed region. The thermal boundary conditions are shown in Figure 6-4.

For the structural boundary condition, it is assumed that, at the bottom head, there is no bonding between the concrete and the drywell (similar to previous evaluations). In the region where there is concrete on the inside and outside of the bottom shell, the concrete will prevent movement into the concrete in the radial direction, either towards or away from the center of the spherical drywell. Therefore, it is reasonable to restrict the radial movement for the portion of the bottom head with concrete on both sides of the shell but allows movement in the meridional direction as illustrated in Figure 6-5, from elevation 8' 11 ¼" and below. In addition, at the location of the skirt, a constraint is imposed on the displacement in the vertical and horizontal directions. The basis is that both the concrete and the skirt which are anchored inside the concrete provide sufficient constraint in the movement of the shell at either direction. For the curb region, between elevation 8'-11 ¼" and top of the curb (12'-13"), there is only concrete on the inside. Under the condition of internal pressure in the design condition, assuming no bonding between the shell and the concrete, the bottom head shell could deflect away from the concrete in the curb region. Therefore, no constraint boundary condition will be imposed in the curb region. This would provide conservatism with regards to stress since it allows the shell in the curb region to deform more than would be expected. This argument or assumption is also applicable to the case of an external pressure in the operating condition. In this case, the shell will deform inward as if the concrete inside is not present.

Similar assumptions and arguments on the structural boundary conditions can also be applied to the trench regions in Bay 5 and Bay 17. In Bay 5, the displacement boundary conditions are illustrated in Figure 6-6. The shell is allowed to displace and rotate in all three directions starting from the bottom of the trench which is at about elevation 8'-9". Figure 6-7 presents the displacement boundary conditions in Bay 17. The shell is allowed to displace and rotate in all three directions starting from the bottom of the sandbed region at elevation 8'-11 ¼".

The application of the displacement boundary conditions in the bottom head of the drywell is shown in Figure 6-8.

6.3.2 Star Truss Boundary Conditions

There are 8 star truss assemblies spaced evenly around the circumference in the cylindrical portion of the drywell, at an elevation of 82'-2". Each star truss has two truss members (10" pipe double extra strong) connecting the biological shield wall to the drywell star truss reinforcing plate, Figure 6-9. The truss members are welded onto the top plate of the shield wall. On the outside of the star truss reinforcing plate, there is a male lug which is situated into a slot plate embedded into the concrete wall of the reactor building, Figure 6-10. The purpose of the star truss components is to transmit the forces from the drywell internals (i.e. reactor vessel) to the reactor building directly without loading the drywell shell. In an independent study, it was shown that, one truss member is in tension while the other one in the same assembly is in compression such that there is essentially no resulting bending moment and radial forces on the drywell shell. The only net force is in the circumferential direction of the drywell. This circumferential force is resisted by the concrete wall of the reactor building through the male lug on the outside of the star truss reinforcing plate, when it comes into contact within the slot in the reactor building concrete wall after the gap is closed.

In the finite element model, a displacement constraint in the circumferential direction at the male lug of the star truss is imposed to simulate the restraint when the male lug comes into contact with the reactor building concrete wall within the slot, Figure 6-11. For the welded connection

between the truss member and the shield wall, no displacement constraint was applied in the finite element model at this location.

6.3.3 Vent Header Boundary Conditions

The vent header/downcomer is supported by vertical columns at the bottom of the stiffener at both ends of the vent header segment, Figure 6-12. The corresponding structural constraint in the finite element model is shown in Figure 6-13. The constraint is only in the vertical direction. The stiffener is allowed to move in the two lateral directions.

6.4 ANALYSIS LOAD CASES

The analysis load cases are summarized in Table 6-1. Each load case is described in the following sections. These load cases are defined based on Reference 5.

6.4.1 Pressure / Temperature

Load Cases 1 and 2 are the steady state thermal cases, with a steady state uniform temperature in the drywell at 292 °F and 150 °F, respectively, all with the embedded portion of drywell at a uniform temperature of 70°F.

Load Cases 3 and 4 are the load cases with an internal pressure of 44 psi and an external pressure of 2 psi, respectively.

Since the vent headers/downcomers are inside the suppression chamber, it was assumed that the pressure inside the vent headers/downcomers is the same as the pressure inside the suppression chamber. Therefore, there is no pressure applied inside the vent headers/downcomers in the model below the vent pipe bellow location.

6.4.2 Gravity Loads

6.4.2.1 Drywell Shell

The gravity load of the shell is input as the weight density of the material.

6.4.2.2 Compressible Material

To model the gravity load due to the compressible material, the density of the drywell steel should be adjusted according to the following:

$$\rho_{additon} = \frac{\rho_{cm}}{\rho_{steel}} \frac{t_{cm}}{t_{steel}}$$

where ρ_{cm} = density of compressible material

ρ_{steel} = density of drywell steel

t_{cm} = thickness of the compressible material

t_{steel} = thickness of the drywell steel

Since $\rho_{cm} = 8$ lb/ft^3, assuming, $\rho_{steet} = 490$lb/ft^3, $t_{cm} = 3$ in, therefore, the additional fraction of steel density lumped to the drywell shell is $0.049/t_{steel}$, expressed as fraction of the steel density. This will be different at various regions of the drywell (i.e. cylindrical, knuckle, spherical and bottom head), due to the differences in the drywell wall thickness.

6.4.2.3 Piping Gravity Loads on Penetrations

Piping loads from gravity, thermal and seismic were provided for some of the penetrations on the drywell. For other penetrations, no loading was provided, likely because of the absence of significant loading or stress. However, it is considered prudent to include some consideration for the weight/mass of the piping/penetrations near the drywell. In addition, it is possible that an

isolation valve is in the vicinity of the drywell penetrations. For large nominal pipe size, the weight of this isolation valve could be substantial.

To account for the effect of the gravity loads from the attached piping and valves on the penetrations, an estimation of these gravity loads is made. This estimation is based on a common piping support configuration.

In Reference 30, guidelines are provided for the piping support spacing based on pipe size and its carried content. The suggested pipe support spacing from Table 121.1.4 in Reference 39 is reproduced in Table 6-2 for nominal pipe sizes of 1 inch to 24 inches for either water service or steam, gas/air service. In practice, the support spacing could be less due to the presence of other mechanical components and loading conditions.

To assess the gravity weight of the piping span between the pipe supports acting on the penetration, the following assumptions were made.

(a) The penetration location was assumed as an anchor point or a support location.
(b) The closest pipe supports inside the drywell and outside the drywell are assumed to be at the distance of maximum span from the penetration.
(c) The weight from half of the maximum span of the piping on either side of the drywell penetration was assumed to be taken up by the penetration.
(d) The content of the piping system was water.
(e) The weight of the pipe insulation was not included.
(f) The isolation valve is assumed to be next to the drywell penetration and that the valve weight was all taken up by the drywell penetration.
(g) The isolation valve was assumed to be a motor operated stainless steel gate valve. The weight of the motor operated stainless steel gate valve was assumed to be twice as heavy as the manual operated stainless steel gate valve.

These assumptions provide an upper bound of the gravity loads from the attached piping systems and valves acting on the penetrations. The basis for this being an upper bound is that the maximum support spacing is used to determine the piping gravity loads and that the gravity load from the valve is not taken by any adjacent support, especially since pipe supports are provided for the isolation valves in large pipe in close proximity. In addition, the content inside the piping was assumed to be water even though some of these piping may contain air during operation. Table 5-4 presents a summary of number of penetrations at different penetration sizes in the Oyster Creek Drywell. There are external piping loads provided for penetration sizes 24 inches and larger. Gravity loads are estimated for penetrations with sizes less than 24 inches.

Table 6-3 presents the pipe weight and the water weight according to pipe size, [30]. The valve weight is obtained from Reference 32. Table 6-5 also presents the total weight (or mass) for each penetration size. This total weight includes the weight of the pipe, its content for the maximum span and the valve weight.

In the finite element model, these weights are modeled using mass elements on the nodes around the edges of the areas modeling the penetrations. These penetration weights are used on the gravity and seismic analyses.

The penetrations that required inclusion of valve/pipe weight are summarized in Table 6-4. It is based on the data provided in References 33 and 34. The general guidelines are:

(a) Valve/piping deadweight load are not included for the penetrations where the applied piping loads are available from piping analyses.
(b) No valve weights are included for the electrical penetrations. The electrical penetrations are identified in Reference 34.
(c) The pipe and water weight were used for the electrical penetrations. The water weight was used to simulate the cable weight in side the electrical penetrations.
(d) The spare and abandoned penetrations do not include the valve/piping deadweight loads.

(e) The vent pipes and manhole do not included the valve/piping deadweight loads.

For the penetrations with the external applied piping loads available, only the loads from the piping gravity load case were used in this load case.

6.4.2.4 Gravity of Air

The weight of the contained air is calculated to be 13,194 lb in Section 5.3.6. Compared to the total weight of the system, this weight is considered to be small and insignificant. Also, the weight of gas is considered only for the test condition, Section 5.3.2.1. Therefore, the weight of the air is not included in the analysis.

6.4.3 Mechanical and Live Loads

This load case included the loads from the Parson's report [5], external piping loads, weld pad loads (dead and live), and hatch/air lock live loads as described in Section 5.0.

The external piping loads are applied using a pilot node at the center of the penetrations. The weld pad loads were applied as a distributed force over the entire weld pad in the model. The hatch/air lock live loads were applied as a distributed force over the bottom portion of the hatch in the model.

The moment at the bottom of the pedestal was assumed to transmit through the concrete floor into the bottom skirt and the reactor building concrete ground.

The horizontal earthquake load of 2150K at the elevation of 47' 1 ½" was assumed to be evenly distributed on the drywell shell along the length of the upper beam support.

6.4.4 Refueling Loads

The refueling loads include the water load at the water seal as shown in Parson's report, [5]. These refueling loads were applied at the 25 gussets in the lower and upper flanges. The loads were identified as a concentrated force at a location as identified in Figure 5-5. In order to eliminate excessive conservatism, these concentrated forces were applied as distributed loads in the gussets as shown in Figure 6-14. This is a better representation of the refueling loads because the loads are due to the weight of the water above the water seal.

In this load case, the top head, including the beam elements for the bolts were removed from the finite element model.

6.4.5 Flood Loads

The flood load was applied using internal pressure as a function of water depth, with zero hydrostatic pressure at elevation of 74'-6".

In this load case, the top head, including the beam elements for the bolts were included in the finite element model.

6.4.6 Jet Loads

As documented in Reference 5, the jet loads were considered in three different locations: spherical shell, cylindrical shell and top head.

The jet load was classified as a Level D condition. This load case was evaluated as described in Section 5.3.1.3.

6.4.7 Seismic Anchor Movements

The relative displacement for the reactor building between elevations 82'-9" and 10'-3" during a seismic event was analyzed as a seismic anchor movement. This relative displacement is at the star truss male lug elevation where the drywell is restrained in the circumferential direction by the reactor building.

Conservatively, the displacement in the reactor building is used as a seismic anchor movement for the drywell, assuming the reactor and the drywell move together in the same direction.

The seismic anchor movements for OBE were obtained from Section 5.7.2.1. The north-south displacement is 0.046 inches. The east-west displacement is 0.05 inches. These displacements were applied to the male lugs on the outside of the star truss reinforcing plates.

The SSE seismic anchor movements for the flooded condition were obtained from Section 5.7.2.2. The north-south displacement is 0.095 inches. The east-west displacement is 0.087 inches.

6.4.8 Modal Analysis / Response Spectrum

A modal analysis was performed to obtain the structural frequencies of the drywell. A preliminary evaluation demonstrated that the vent headers/downcomers produce many modes in the low frequency range. Since the vent headers/downcomers are not in the current scope of evaluation (but to include the stiffness effect on the drywell), the mode frequencies were obtained without the downcomers in the modal frequency evaluation.

The dynamic response of the steel containment structure can be significantly different if the structure is filled with water as opposed to being empty during normal conditions. It is a typical industry practice and commonly used analytical technique in the plant seismic analysis using finite element analysis to include the added mass that accounts for the effect of the enclosed

water on the drywell dynamics in the post accident event. These added water masses can be modeled by increasing the mass density of the drywell steel in the model.

The flood elevation is at 74'-6", (Reference 5, Figure III-9, page III-37). The flood volume can be estimated as a combination of spherical volume and knuckle volume. The equation for the volume of a partial spherical shell is obtained from Reference 35.

Using these data as input, the calculation of water mass is summarized in Table 6-5. The water mass is 8,850,440 lbm. This water mass is accounted for by adjusting the metal density in the model.

In this calculation, the flooded volume is taken as 80% of the drywell volume. In Reference 40, it was shown that the space for flood water is about 78% of the drywell space up to the flood elevation. Therefore the estimate of added water mass is comparable.

The added water mass is included only for the post-accident flooded case but not during the normal operating and refueling conditions.

All the modes between 1 Hz to 50 Hz were extracted. This selection is based on the response spectra shown in Figure 5-6 to Figure 5-13.

A single point response spectrum analysis was performed. The enveloped response spectrum between the two elevations of 10'-3" and 82'-9" were used.

The response spectrum analyses were performed individually using the two horizontal (E-W direction, N-S direction) spectra and the vertical spectrum. The modal combination was performed using the Rosenblueth Correlation Coefficient for closely spaced modes as required in Regulatory Guide 1.92. The reference from Oyster Creek design or licensing basis documents (i.e. FSAR Section 3.7.2.3, Update 10, page 3.7-4, 04/97) may refer to an earlier revision of the

same Regulatory Guide. The stresses due to each response spectrum were combined using SRSS (square root of sum of the square) to obtain the resultant stresses for the seismic load case.

The use of damping ratio follows the guideline of Reg Guide 1.61 [19]. For welded steel structures, the critical damping is 2% for operating basis earthquake (OBE) and 4% for safe shutdown earthquake (SSE). In the latest revision of Reg Guide 1.61 [31], for welded steel structures, the critical damping is 3%. Therefore, using 2% critical damping for OBE is conservative.

6.5 ANALYSIS RESULTS

6.5.1 Pressure

6.5.1.1 44 psi Internal Pressure

The overall membrane stresses due to an internal pressure of 44 psi are presented in Figure 6-15 (a). It is shown that the maximum stress is at a penetration in the middle spherical shell. This maximum stress is highly localized and will be treated accordingly in the ASME Code stress evaluation.

The surface stresses are presented in Figure 6-15 (b) and (c). It is shown that all the thinned bay regions have high stress. The maximum surface stress is in the locally thinned area in Bay 1, right below the vent pipe.

6.5.1.2 2 psi External Pressure

The overall membrane stresses are presented in Figure 6-16 (a), with the bending stresses in Figure 6-16 (b) and (c) for the top and bottom surfaces, respectively.

The maximum stress occurs at the same penetration location as in the 44 psi internal pressure case but at a much lower magnitude. The maximum membrane stress is in the cylindrical region instead of Bay 1 in the 44 psi internal pressure case.

6.5.2 Thermal

The steady state temperature distribution for the drywell at 150 °F and 292 °F with the bottom head at 70°F are shown in Figure 6-17.

The steady state thermal stresses at 150 °F and 292 °F are presented in Figure 6-18 and Figure 6-19, respectively. Disregarding the stresses in the vent header and downcomers, the maximum thermal stress is essentially at the concrete floor elevation in the bottom head region where the temperature decreases from the steady state temperature to the assumed temperature of 70 °F for the drywell embedded in the concrete.

6.5.3 Gravity Loads

The membrane and surface stress distribution due to the gravity loads is presented in Figure 6-20. The maximum stress is near the equipment hatch/personnel lock. This is due to the large dead load inside the personnel lock and equipment hatch.

6.5.4 Mechanical and Live Loads

The application of mechanical and live loads is shown in Figure 6-21.

The stress intensities due to the mechanical and live loads are presented in Figure 6-22. It is shown that the highest stress intensity is at the star truss male lug.

6.5.5 Refueling

The stress intensity distribution due to refueling is presented in Figure 6-23. The maximum stress is at the lower stiffener in the cylindrical portion of the drywell. It is one of the two elevations where the water loads were applied. Also the knuckle region shows a higher stress compared to the cylindrical or spherical portion of the drywell.

6.5.6 Flooding

The hydrostatic pressure loading due to water flooding is presented in Figure 6-24. It is shown that at the bottom of the drywell at the concrete floor level, the hydrostatic pressure due to the water head is about 28 psi.

The stress intensity distribution in the drywell bottom head is shown in Figure 6-25. The high stress area is in the sandbed thinned regions. This is attributed to a combination of high hydrostatic pressure and the thinned wall thickness in the sandbed region.

6.5.7 OBE Seismic Anchor Movements

The stress intensity distribution due to the seismic anchor movements at the star truss is presented in Figure 6-26. The maximum stress occurred in the star truss component where the anchor movement was applied. There is also high stress at the bottom of the drywell due to the cantilever effect.

6.5.8 Seismic Loads

6.5.8.1 Modal Analysis

A mode frequency analysis was performed for both refueling and flooding conditions. For the refueling conditions, the top head was not included in the model. For the flooding condition, the added water mass was included in the model.

In addition, due to the numerous modes occurring in the downcomers which are not part of the current evaluation, they were excluded in the model in order to obtain the mode frequencies for the drywell in a reasonable number of extracted modes.

6.5.8.1.1 Refueling

The modal frequencies for the refueling condition are presented in Table 6-6. The first significant mode frequency in the drywell is the 5th mode at 12.54 Hz. This mode is essentially a breathing mode of the cylindrical and knuckle portion of the drywell.

In Table 6-6, it is shown that these modal frequencies are closely spaced. The results on modal participation factor and effective masses are summarized in Table 6-7. The highest participation factor is in the 5th and 15th modes for the global X (N-S) and Y (E-W) direction. For the global Z direction, the highest participation factor is in the 10th mode. The first 107 modes account for 90% cumulative mass as required by Reference 36.

6.5.8.1.2 Flooding

The modal frequencies for the flooding condition are summarized in Table 6-8. The first two mode frequencies are 3.15 Hz and 5.54 Hz. These two modes are in the vent pipes inside the suppression chamber. The first significant mode frequency in the drywell is the 3rd mode at 5.706 Hz. This mode is a combination of breathing and bending modes of the top cylindrical portion of the drywell with some circumferential wave mode at the star truss elevation.

Due to the large added masses for the water inside the drywell, the 120th mode frequency is 15.895 Hz. These mode frequencies are also closely spaced. The results on modal participation factor and effective masses are summarized in Table 6-9. The most significant modes frequencies are in the 2nd to 4th modes except for the global z-axis rotation which is at the 14th

mode. For the vertical direction, the highest participation factor is in the 2nd mode. The first 47 modes account for 90% cumulative mass as required by Reference 36.

6.5.8.2 Response Spectrum Analysis

6.5.8.2.1 Refueling

The stress intensity due to OBE E-W response spectrum is presented in Figure 6-27. The highest stress intensity location is at a penetration (X71) in the upper spherical shell. The stress intensity due to OBE N-S response spectrum is presented in Figure 6-28. The highest stress intensity location is at the equipment hatch /personnel lock. The stress intensity to OBE vertical response spectrum is presented in Figure 6-29. The highest stress intensity location is also at the equipment hatch/personnel lock. The resultant stress from the square root sum of the square of the three response spectrum evaluation is shown in Figure 6-30. The highest stress locations are in the penetration and Lock/Hatch.

6.5.8.2.2 Flooding SSE

The stress intensity due to the flooding SSE E-W response spectrum is presented in Figure 6-31. The highest stress intensity location is at the star truss in upper spherical shell. The stress intensity due to SSE N-S response spectrum is presented in Figure 6-32. The highest stress intensity location is also at the star truss location. The stress intensity to Flooding SSE vertical response spectrum is presented in Figure 6-33. The highest stress intensity location is at the sand bed region. The resultant stress from the square root sum of the square of the three response spectrum stress is shown in Figure 6-34. The highest stress location is at the star truss.

6.5.9 External Piping OBE Loads

The external piping OBE loads include both seismic inertia and seismic anchor movements by the external piping system acting on the drywell penetrations. The stress intensity distribution is presented in Figure 6-35.

6.5.10 External Piping SSE Loads

The external piping SSE loads include both seismic inertia and seismic anchor movements by the external piping system acting on the drywell penetrations. The stress intensity distribution is presented in Figure 6-36.

6.5.11 External Piping Thermal Loads

The external piping thermal loads included all the normal operating thermal loads from the attached piping. The stress intensity distribution is presented in Figure 6-37.

6.5.12 Flooding SSE Seismic Anchor Movements

The stress distribution due to Flooding SSE Seismic Anchor Movements is presented in Figure 6-38.

Table 6-1: Analysis Load Cases

Case	ID	Description
1	Thrm1	Uniform 292 °F at the drywell, uniform 70°F at the embedded bottom head and steady state distribution in between
2	Thrm2	Uniform 150 °F at the drywell, uniform 70°F at the embedded bottom head and steady state distribution in between
3	Prs1	Internal Pressure 44 psi and vent thrust
4	Prs2	External Pressure 2 psi and vent thrust
5	Grvty	Gravity loads included: (a) Gravity of shell (b) Gravity of compressible material (c) Gravity of penetrations (d) Gravity of hatch/lock (e) Gravity of external piping loads
6	Mch/Live	Mechanical/live loads included: (a) Weld pads loads (dead and live loads) (b) Parson's loads
7	Refuel	Refueling loads
8	Flood	Flooding loads – water level at 74"-6" with a water head of 92'-0"
9	Jet	Jet force load (a) Spherical shell at deflector plate (b) Cylindrical shell at start truss (c) Top head
10	SAM	Seismic anchor movement at star truss
11	OBE	Operating basis earthquake response spectrum
12	SSE	Safe shutdown earthquake response spectrum with flood water added mass
13	EPOBE	External piping loads - OBE and SAM
14	EPSSE	External piping loads – SSE and SAM
15	EPThrm	External piping loads – Thermal
16	SSESAM	SSE seismic anchor movement at start truss

Table 6-2: Suggested Pipe Support Spacing [39]

Nominal Pipe Size (in)	Suggested Maximum Span in Feet	
	Water Service	Steam Gas or Air Service
1	7	9
2	10	13
3	12	15
4	14	17
6	17	21
8	19	24
12	23	30
16	27	35
20	30	39
24	32	42

Table 6-3: Total Gravity Loads on Penetration due to Attached Piping and Valve

Size	Span (ft)	Pipe Wt. (lb/ft)	Water Wt. (lb/ft)	Valve Wt. (lbs)	Total Wt (lbs)	
					w/o valve	w/ valve
1	7	2.172	0.311	87.8	17.38	105.18
2	10	5.022	1.28	155.4	63.02	218.42
3	12	10.25	2.864	291.8	157.37	449.17
6	17	28.57	11.29	1069.6	677.62	1747.22
8	19	43.39	19.8	1876.8	1200.61	3077.41
10	21	64.33	31.1	2781	2004.03	4785.03
14	25	106.13	53.2	5338.6	3983.25	9321.85
16	27	136.46	69.7	6242.8	5566.32	11809.12
18	28.5	170.75	88.5	9831	7388.63	17219.63

Table 6-4: Nozzles with Applied Valve Weight

Customer Mk	CBI Marking	Valve Wt	Customer Mk	CBI Marking	Valve Wt	Customer Mk	CBI Marking	Valve Wt	Customer Mk	CBI Marking	Valve Wt	Customer Mk	CBI Marking	Valve Wt	Customer Mk	CBI Marking	Valve Wt
X- 1	100-A	n/a	X-24	28-X24	(2)	X-32	12-N8-1	(2)	X-41	13-N3-6	(1)	X-50	24-X50	Yes	X-70	33-X70	No
X- 2A	23-X 2A	No	X-24	12-N6-4	(2)	X-32	12-N8-2	(2)	X-41	13-N3-7	(1)	X-50	24-X50	Yes	X-71	33-X71	Yes
X- 2B	15-N36-1	No	X-24	12-N6-4	(2)	X-32	12-N8-2	(2)	X-41	13-N3-7	(1)	X-50	24-X50	Yes	X-72	33-X72	No
X- 3A	19-N24-1R	No	X-25	12-N6-2	Yes	X-32	12-N8-2	(2)	X-41	13-N3-7	(1)	X-50	24-X50	Yes	X-73	39-X73	Yes
X- 3B	19-N24-1L	No	X-26	12-N6-2	spare	X-32	12-N8-2	(2)	X-41	12-N3-7	(1)	X-50	24-X50	Yes	X-73	39-X73	Yes
X- 4A	23-X 4A	No	X-27	12-N6-2	(2)	X-32	12-N8-2	(2)	X-41	12-N3-7	(1)	X-50	24-X50	Yes	X-73	39-X73	Yes
X- 4B	15-N30-1	No	X-27	12-N6-2	(2)	X-32	12-N8-2	(2)	X-42	26-X42-43	Yes	X-50	24-X50	Yes	X-73	39-X73	Yes
X- 5A	19-N24-2R	No	X-27	12-N6-2	(2)	X-32	12-N8-2	(2)	X-43	26-X42-43	spare	X-50	24-X50	Yes	X-74	81-X74	n/a
X- 5B	19-N24-2L	No	X-27	12-N6-2	(2)	X-32	12-N8-2	(2)	X-44	17-N3-13	spare	X-50	24-X50	Yes			
X- 6	28-X 6	No	X-28	12-N8-2	(2)	X-33	12-N8-7	(2)	X-44	17-N3-12A	spare	X-51A	X51-A	n/a			
X- 7	18-N26-1	No	X-28	12-N8-2	(2)	X-34	12-N8-7	(2)	X-45	14-N6-7A	Yes	X-51B	X51-B	n/a			
X- 8	26-X 8	No	X-28	12-N8-2	spare	X-36	12-N8-6	(2)	X-45	14-N6-9A	Yes	X-51C	X51-C	n/a			
X- 9	25-X 9	No	X-28	12-N8-2	spare	X-37	16-N 8-9	spare	X-45	14-N6-6A	Yes	X-51D	X51-D	n/a			
X-10	25-X10	No	X-29	12-N8-3	(2)	X-37	16-N 8-9	(2)	X-45	24-X45	Yes	X-51E	X51-E	n/a			
X-11	17-N18-1	Yes	X-29	12-N8-3	(2)	X-37	16-N 8-9	(2)	X-45	14-N6-7	Yes	X-51F	X51-F	n/a			
X-12A	25-X12A	Yes	X-29	12-N8-3	spare	X-37	16-N 8-9	spare	X-45	14-N6-9	Yes	X-51G	X51-G	n/a			
X-12B	25-X12B	No	X-29	12-N8-3	spare	X-38	27-X38	Yes	X-45	14-N6-6	Yes	X-52	20-X52	n/a			
X-13A	22-X13A	Yes	X-30	12-N8-6	(2)	X-38	27-X38	Yes	X-46	28-X46	spare	X-53	X-53	n/a			
X-13B	22-X13B	Yes	X-30	12-N8-6	spare	X-38	27-X38	Yes	X-46	17-N3-12A	spare	X-56	X-56	n/a			
X-14A	22-X13A	Yes	X-30	12-N8-6	spare	X-38	27-X38	Yes	X-47	12-N3-5	spare	X-57	X-57	n/a			
X-14B	22-X13B	Yes	X-30	12-N8-6	(2)	X-38	27-X38	Yes	X-47	12-N3-5	spare	X-58	X-58	n/a			
X-15	13-N2-1	Yes	X-31	12-N8-3	(2)	X-38	27-X38	Yes	X-47	12-N3-5	spare	X-59	17-N3-13A	Yes			
X-16	13-N2-1	Yes	X-31	12-N8-3	(2)	X-39	27-X39	No	X-47	28-X47	spare	X-60	17-N3-12A	Yes			
X-17	16-N 8-8	(1)	X-31	12-N8-3	(2)	X-39	27-X39	No	X-49	21-A	(3)	X-60	17-N3-12A	Yes			
X-17	16-N 8-8	(1)	X-31	12-N8-3A	(2)	X-39	27-X39	No	X-50	24-X50	Yes	X-60	17-N3-12A	Yes			
X-18	27-X18	No	X-31	12-N8-2	(2)	X-39	27-X39	No	X-50	24-X50	Yes	X-60	17-N3-12A	Yes			
X-19	16-N18-2	No	X-31	12-N8-2	(2)	X-40	12-N3-9	Yes	X-50	24-X50	Yes	X-60	17-N3-12A	Yes			
X-20A	12-N8-4	Yes	X-31	12-N8-2	(2)	X-40	12-N3-9	Yes	X-50	24-X50	Yes	X-60	17-N3-12A	Yes			
X-20B	12-N8-4	Yes	X-31	12-N8-2A	(2)	X-40	12-N3-9	Yes	X-50	24-X50	Yes	X-60	17-N3-12A	Yes			
X-21	12-N8-5	No	X-32	12-N8-7	(2)	X-40	12-N3-1	Yes	X-50	24-X50	Yes	X-61	12-N6-3	No			
X-22A	X-22A	n/a	X-32	12-N8-7	(2)	X-40	12-N3-1	Yes	X-50	24-X50	Yes	X-62	14-N6-10	Yes			
X-22B	X-22B	n/a	X-32	12-N8-7	(2)	X-40	12-N3-1	Yes	X-50	24-X50	Yes	X-63	26-X63	No			
X-22C	X-22C	n/a	X-32	12-N8-7	(2)	X-40	12-N3-1	Yes	X-50	24-X50	Yes	X-63	26-X63	spare			
X-22D	X-22D	n/a	X-32	12-N8-1	(2)	X-40	12-N3-1	Yes	X-50	24-X50	Yes	X-64	26-X64	n/a			
X-22E	X-22E	n/a	X-32	12-N8-1	(2)	X-40	12-N3-2	Yes	X-50	24-X50	Yes	X-65	X-65	n/a			
X-22F	X-22F	n/a	X-32	12-N8-1	(2)	X-40	12-N3-2	Yes	X-50	24-X50	Yes	X-66	18-N16-1	No			
X-22G	X-22G	n/a	X-32	12-N8-1	(2)	X-41	13-N3-6	(1)	X-50	24-X50	Yes	X-67	18-N10-1	Yes			
X-23	12-N6-5	No	X-32	12-N8-1	(2)	X-41	13-N3-6	(1)	X-50	24-X50	Yes	X-68A	X-68A	n/a			
X-24	12-N6-4	(2)	X-32	12-N8-1	(2)	X-41	13-N3-6	(1)	X-50	24-X50	Yes	X-68B	X-68A	n/a			
X-24	28-X24	(2)	X-32	12-N8-1	(2)	X-41	13-N3-6	(1)	X-50	24-X50	Yes	X-69	X-69	n/a			

Note: Valve weight is not included in those penetrations with external piping loads available.
n/a: penetrations are either manhole or in compression pool
(1): abandoned
(2): power and control cables, no valve weight considered.
(3): vent pipe

Table 6-5: Calculation of Added Water Mass

Elevation (ft) / Note		Radius (ft) / Note		Volume (ft^3)	80% Volume (ft^3)	Nodal Volume (ft^3)	Nodal Mass (by Height) (lbf)	Area (ft^2)	Nodal Area (ft^2)	Nodal Mass (by area) (lb)
10.250		22.271		12,485.7	9,988.6	9,988.6	622,288	1,347.0	1,347.0	895,436
16.375	mid level	28.093		17,406.3	13,925.1			1,347.0		
22.500		31.740		25,441.9	20,353.5	34,278.6	2,135,555	1,621.8	2,968.8	1,973,614
29.875	mid level	34.214		27,962.3	22,369.8			1,621.8		
37.250		35.000	sphere equator	20,208.9	16,167.1	38,536.9	2,400,852	1,163.7	2,785.5	1,851,761
42.542	mid level	34.598		19,278.0	15,422.4			1,163.7		
47.833		33.362		27,571.0	22,056.8	37,479.2	2,334,955	1,942.6	3,106.2	2,064,985
56.667	mid level	29.120		17,641.1	14,112.9			1,876.6		
65.200	top of sphere	21.067		414.0	331.2			48.7		
65.500		20.850	linear interpolation	3,682.4	2,946.0	17,390.0	1,083,399	459.6	2,384.9	1,585,466
68.500	mid level	18.683		2,919.5	2,335.6			409.2		
71.500		16.517		20.1	16.1	4,388.3	273,392	3.0	720.8	479,179
71.523	top of knuckle region	16.500		2,545.8	2,036.7			308.6		
74.500	Flood Level	16.500								
77.125	mid level									
82.750										
88.750	mid level									
94.750										
			total =	177,577.1	142,061.6	142,061.6	8,850,440	13,313	13,313	8,850,440

Table 6-6: Refueling Mode Frequencies

Mode	Freq (Hz)	Mode	Freq (Hz)	Mode	Freq (Hz)
1	6.56970	41	27.1142	81	33.3562
2	7.12277	42	27.1660	82	33.4728
3	10.5437	43	27.2675	83	33.5383
4	10.6930	44	27.3915	84	33.7958
5	12.5429	45	27.7476	85	34.0030
6	13.9016	46	27.9721	86	34.3143
7	13.9232	47	27.9806	87	34.4872
8	16.0208	48	27.9860	88	34.7242
9	16.6904	49	28.3099	89	34.9543
10	18.4379	50	28.4232	90	34.9747
11	19.1820	51	28.5390	91	34.9879
12	19.3356	52	28.7480	92	35.0986
13	19.3561	53	28.9255	93	35.1014
14	19.8672	54	29.3505	94	35.1038
15	20.5301	55	29.3603	95	35.1049
16	20.9963	56	29.5962	96	35.1087
17	21.2506	57	29.8211	97	35.1112
18	21.2722	58	30.0008	98	35.1126
19	21.8368	59	30.0818	99	35.1173
20	22.3490	60	30.0967	100	35.1202
21	22.5510	61	30.1638	101	35.1476
22	22.6618	62	30.3430	102	35.2594
23	22.6890	63	30.5471	103	35.6192
24	23.0071	64	30.8054	104	35.6386
25	23.2269	65	31.0185	105	35.7394
26	23.4080	66	31.5174	106	35.8608
27	24.8731	67	31.6577	107	36.3911
28	25.3126	68	31.7922	108	36.4337
29	25.6547	69	31.8067	109	36.8865
30	25.7843	70	31.9815	110	36.8886
31	25.9508	71	32.0099	111	37.6037
32	26.1642	72	32.0999	112	37.7367
33	26.2338	73	32.3243	113	37.8077
34	26.3907	74	32.3969	114	38.1862
35	26.4866	75	32.5507	115	38.2728
36	26.5146	76	32.7912	116	38.5118
37	26.5951	77	32.8755	117	38.5938
38	26.7416	78	32.8819	118	38.6111
39	26.8291	79	32.9022	119	38.7440
40	26.9840	80	33.2996	120	39.3166

Table 6-7: Summary of Participation Factor and Effective Masses for Refueling

DoF	Highest Participation Factor		90% Cumulative Mass	
	Mode	Freq (Hz)	Mode	Freq (Hz)
X Displacement	5th	12.54	86th	34.31
Y Displacement	15th	20.53	107th	36.39
Z Displacement	10th	18.44	28th	25.31
X Rotation	15th	20.53	107th	36.39
Y Rotation	19th	21.84	86th	34.31
Z Rotation	1st	6.57	44th	27.39

Table 6-8: Flooding Mode Frequencies

Mode	Freq (Hz)	Mode	Freq (Hz)	Mode	Freq (Hz)
1	3.150	41	12.784	81	14.953
2	5.543	42	12.833	82	14.956
3	5.706	43	12.910	83	15.000
4	5.793	44	12.960	84	15.037
5	5.922	45	12.980	85	15.065
6	5.927	46	13.184	86	15.118
7	6.740	47	13.356	87	15.200
8	6.745	48	13.462	88	15.220
9	7.051	49	13.611	89	15.248
10	8.245	50	13.711	90	15.291
11	8.264	51	13.800	91	15.307
12	8.578	52	13.855	92	15.363
13	8.599	53	13.944	93	15.418
14	8.843	54	14.038	94	15.436
15	9.085	55	14.054	95	15.460
16	9.091	56	14.069	96	15.489
17	9.294	57	14.108	97	15.492
18	9.978	58	14.227	98	15.499
19	9.986	59	14.323	99	15.535
20	10.224	60	14.357	100	15.543
21	10.284	61	14.369	101	15.570
22	10.306	62	14.464	102	15.584
23	10.447	63	14.466	103	15.594
24	10.472	64	14.475	104	15.613
25	10.648	65	14.519	105	15.627
26	10.682	66	14.549	106	15.64
27	10.689	67	14.587	107	15.666
28	10.784	68	14.629	108	15.676
29	10.967	69	14.647	109	15.706
30	11.234	70	14.676	110	15.738
31	11.601	71	14.691	111	15.758
32	11.829	72	14.700	112	15.770
33	12.102	73	14.740	113	15.806
34	12.111	74	14.789	114	15.809
35	12.119	75	14.795	115	15.836
36	12.440	76	14.844	116	15.860
37	12.450	77	14.861	117	15.864
38	12.570	78	14.893	118	15.884
39	12.573	79	14.924	119	15.892
40	12.776	80	14.941	120	15.895

Table 6-9: Summary of Participation Factor and Effective Masses for Flooding

DoF	Highest Participation Factor		90% Cumulative Mass	
	Mode	Freq (Hz)	Mode	Freq (Hz)
X Displacement	4th	5.79	46th	13.18
Y Displacement	3rd	5.71	47th	13.36
Z Displacement	2nd	5.54	2nd	5.54
X Rotation	3rd	5.71	42th	18.83
Y Rotation	4th	5.79	43nd	12.91
Z Rotation	14th	8.84	14th	8.84

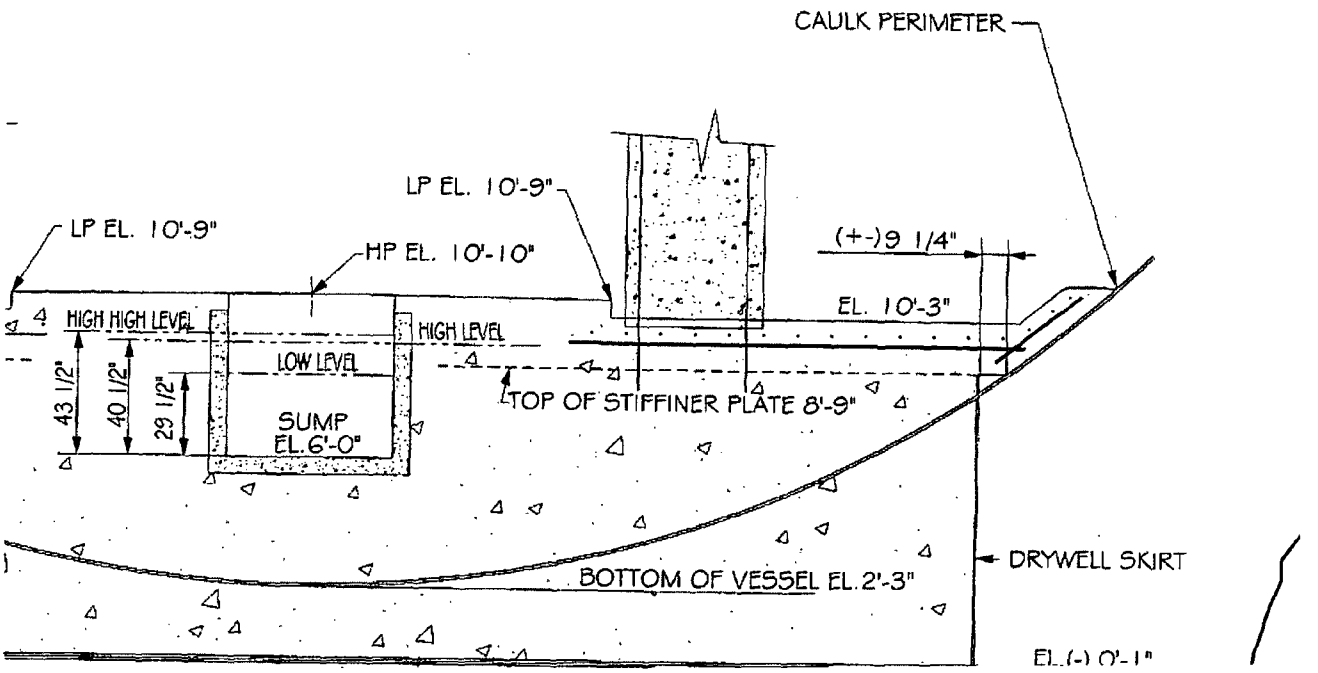

Figure 6-1: Oyster Creek Bottom Head

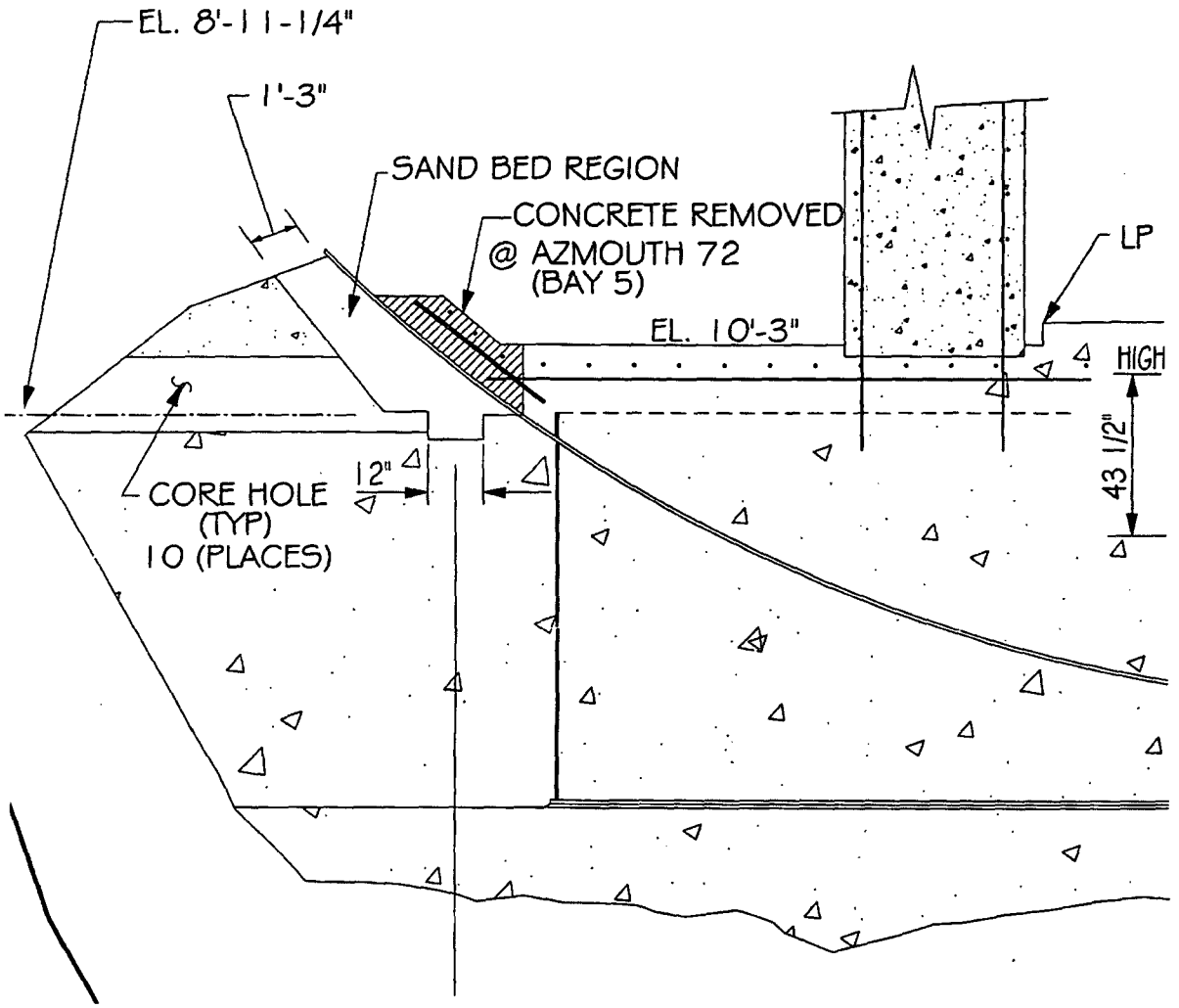

Figure 6-2: Oyster Creek Bottom Head with Sandbed Region

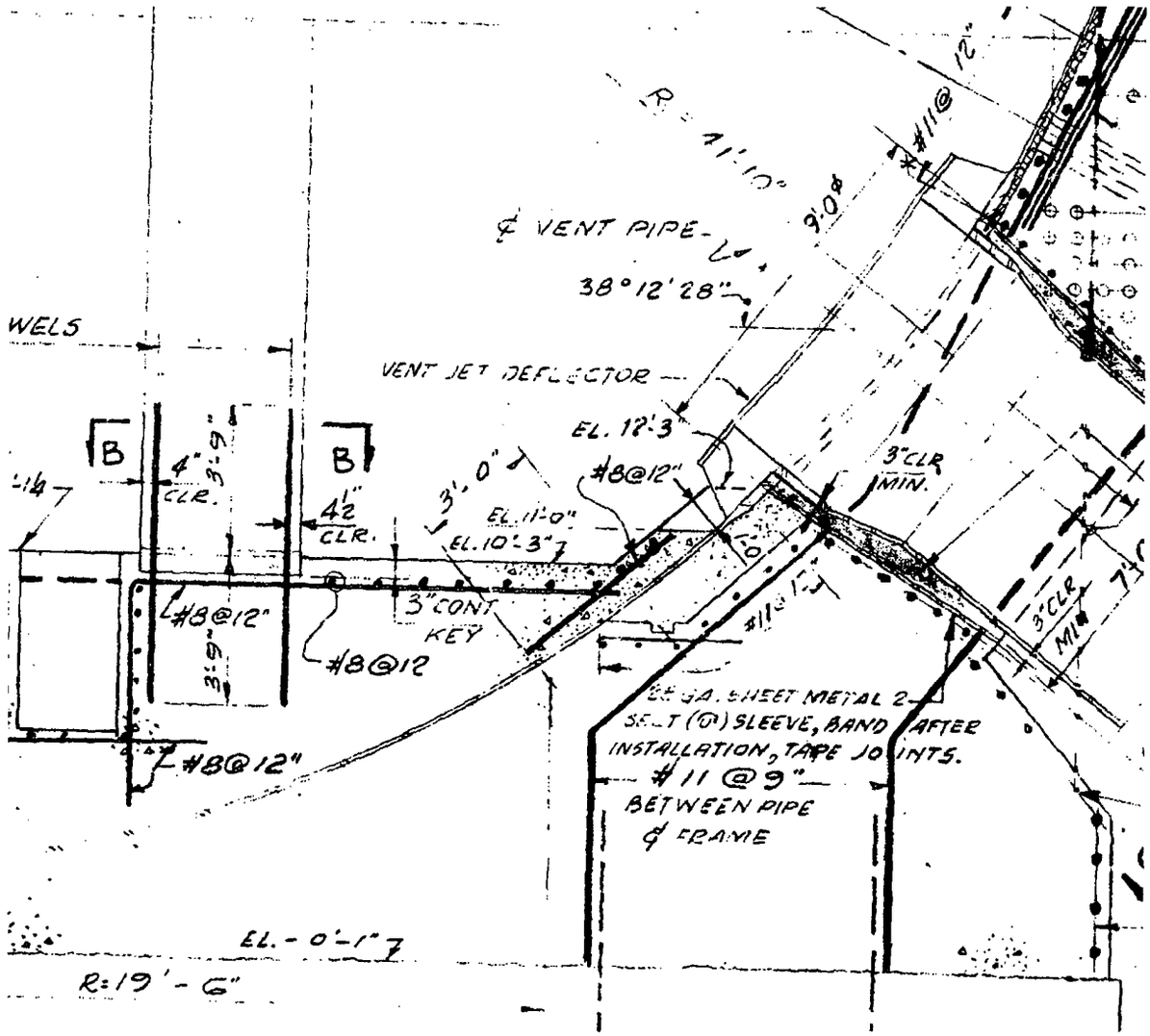

Figure 6-3: Oyster Creek Reactor Building First Floor

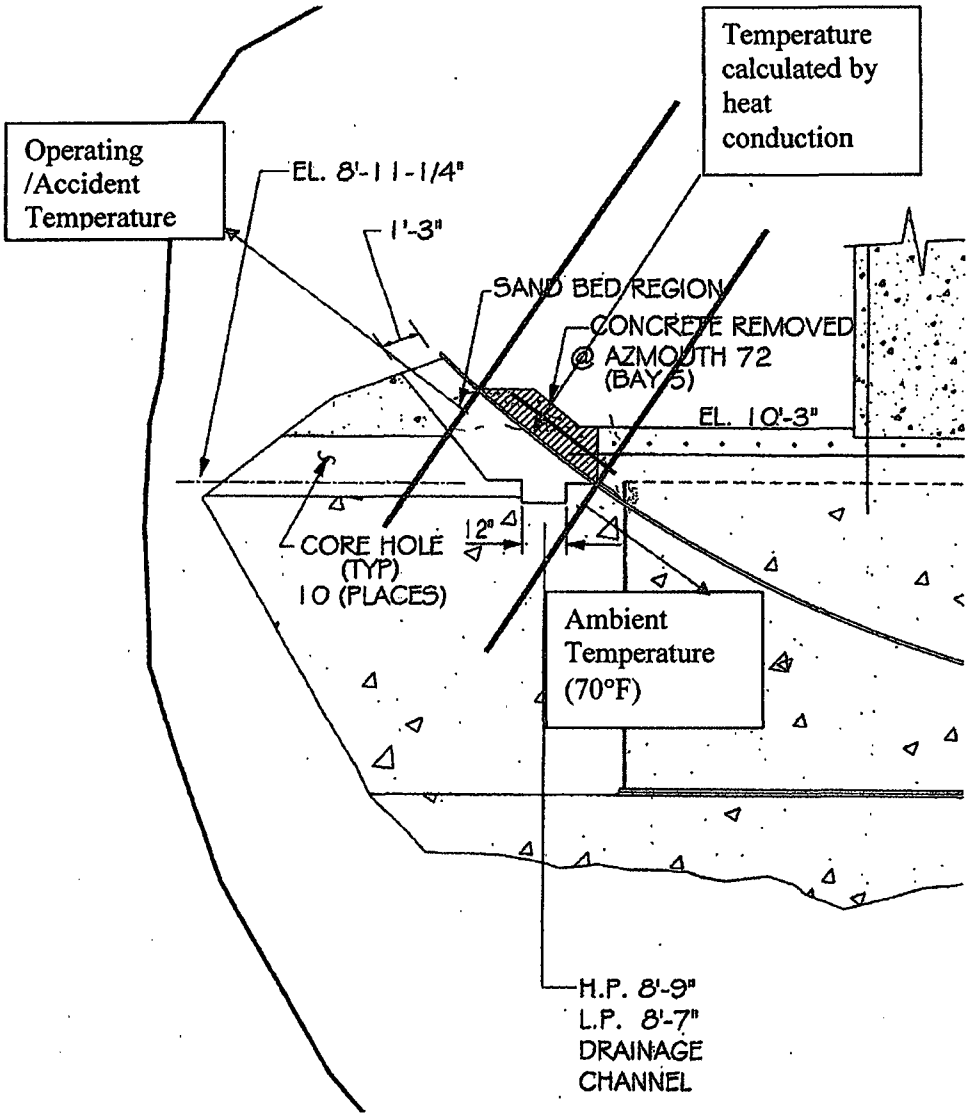

Figure 6-4: Thermal Boundary Conditions

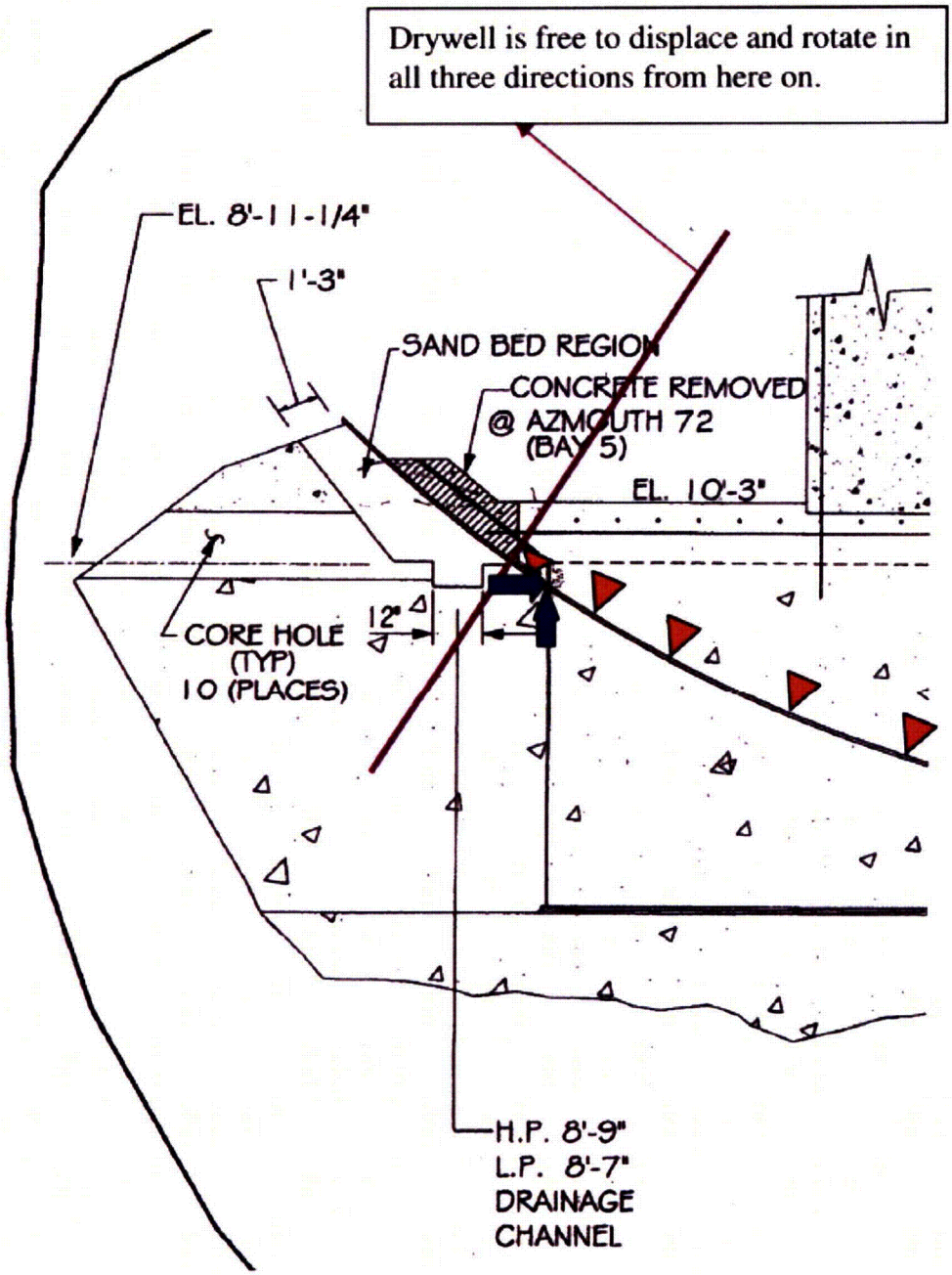

Figure 6-5: Displacement Boundary Condition Illustration

Note: Blue arrows (at skirt) represent displacement constraint in the vertical and circumferential directions at the intersection between the skirt and the bottom head of the drywell.
Red triangles (inside drywell) represent displacement constraint in the radial direction of the bottom head of the drywell.

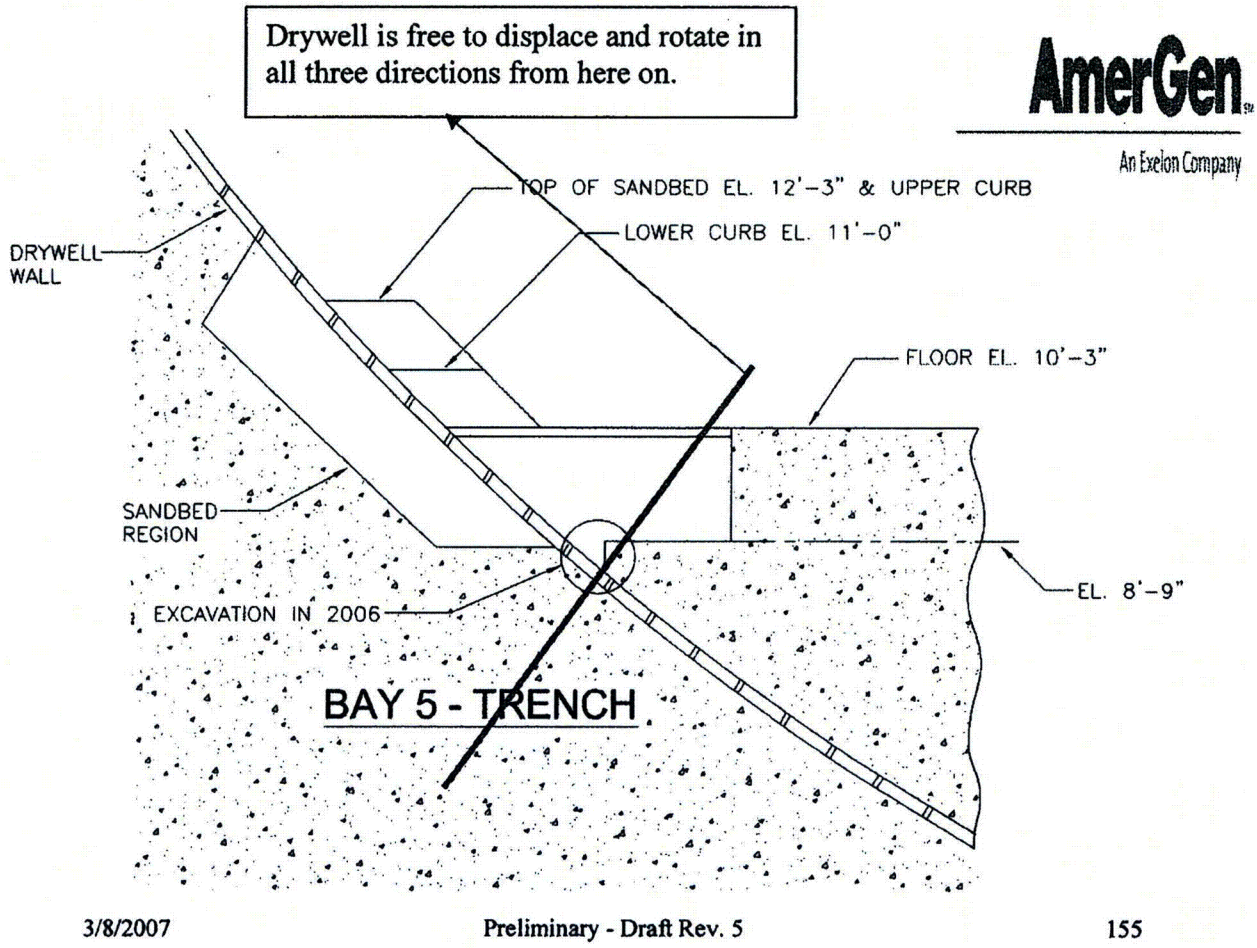

Figure 6-6: Displacement Boundary Condition Illustration in Bay 5

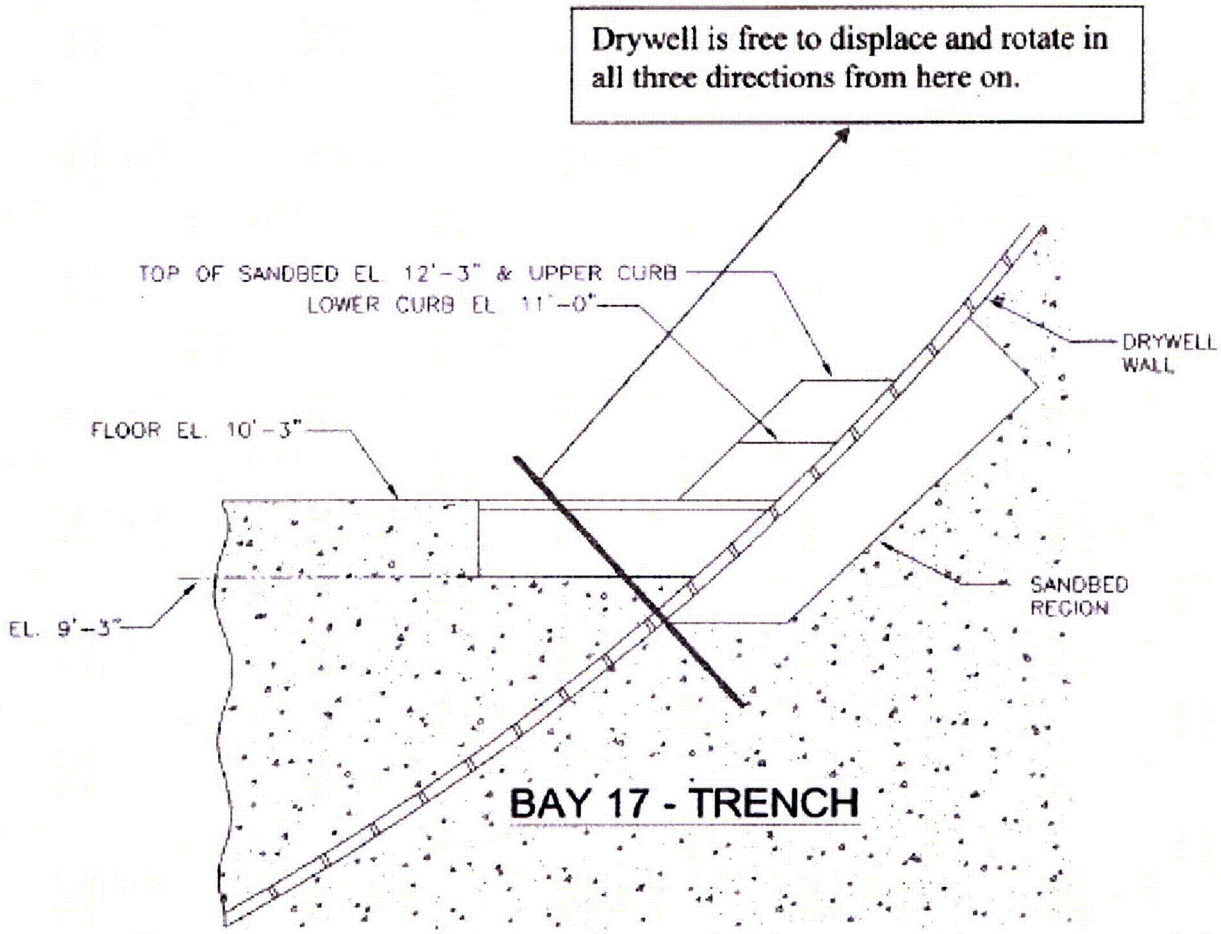

Figure 6-7: Displacement Condition Illustration in Bay 17

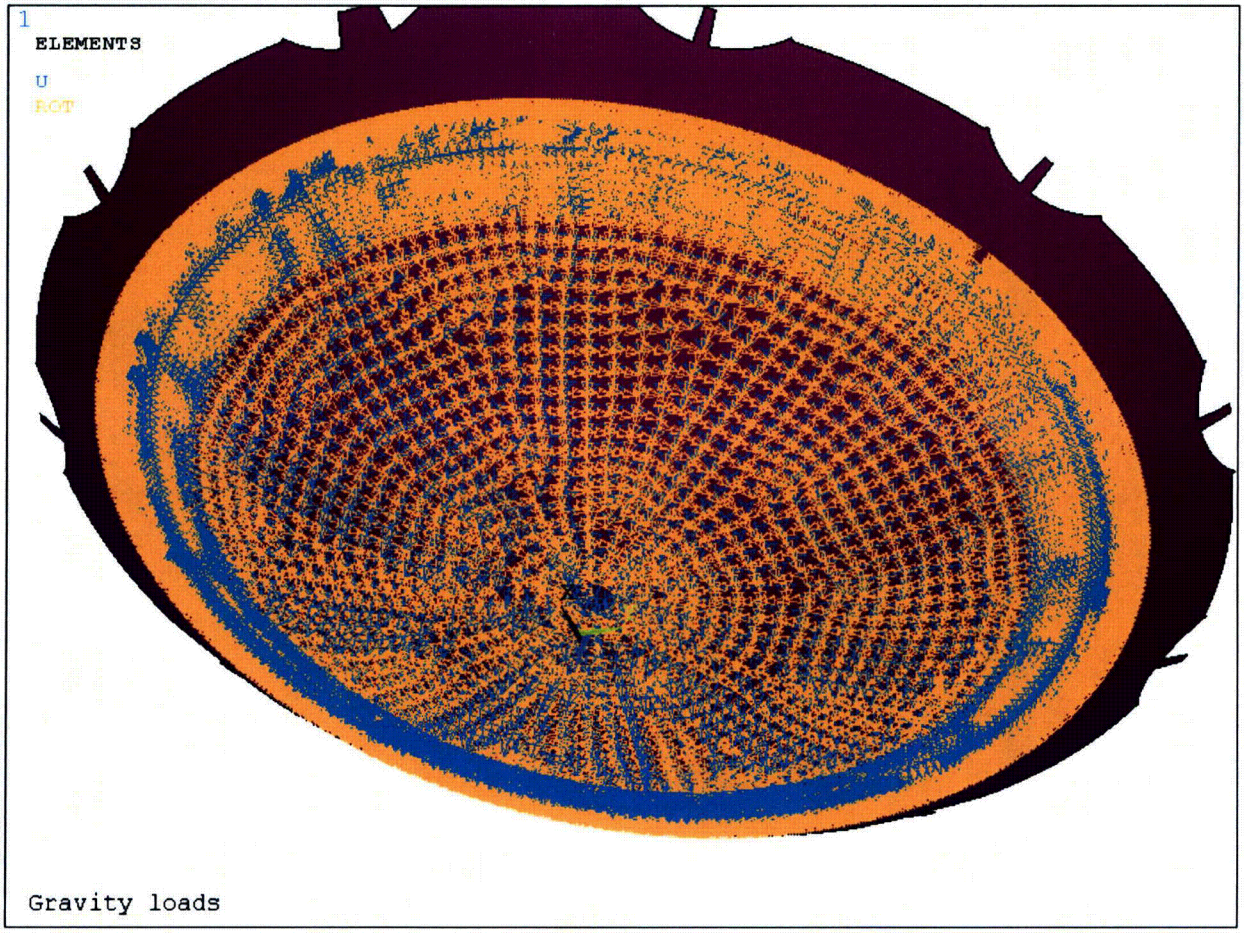

Figure 6-8: Bottom Head Displacement Boundary Condition

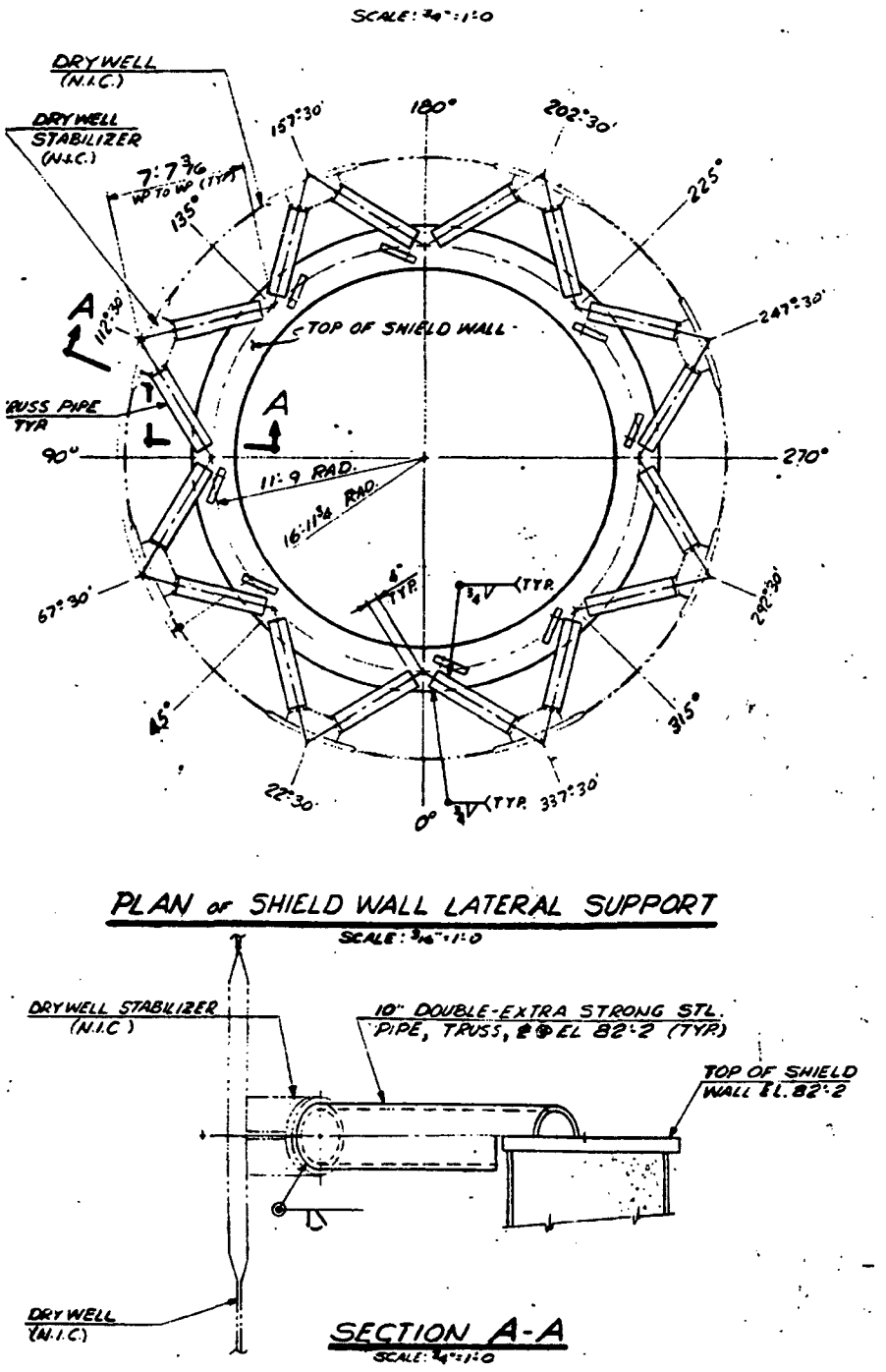

Figure 6-9: Star Truss Connection to Shield Wall

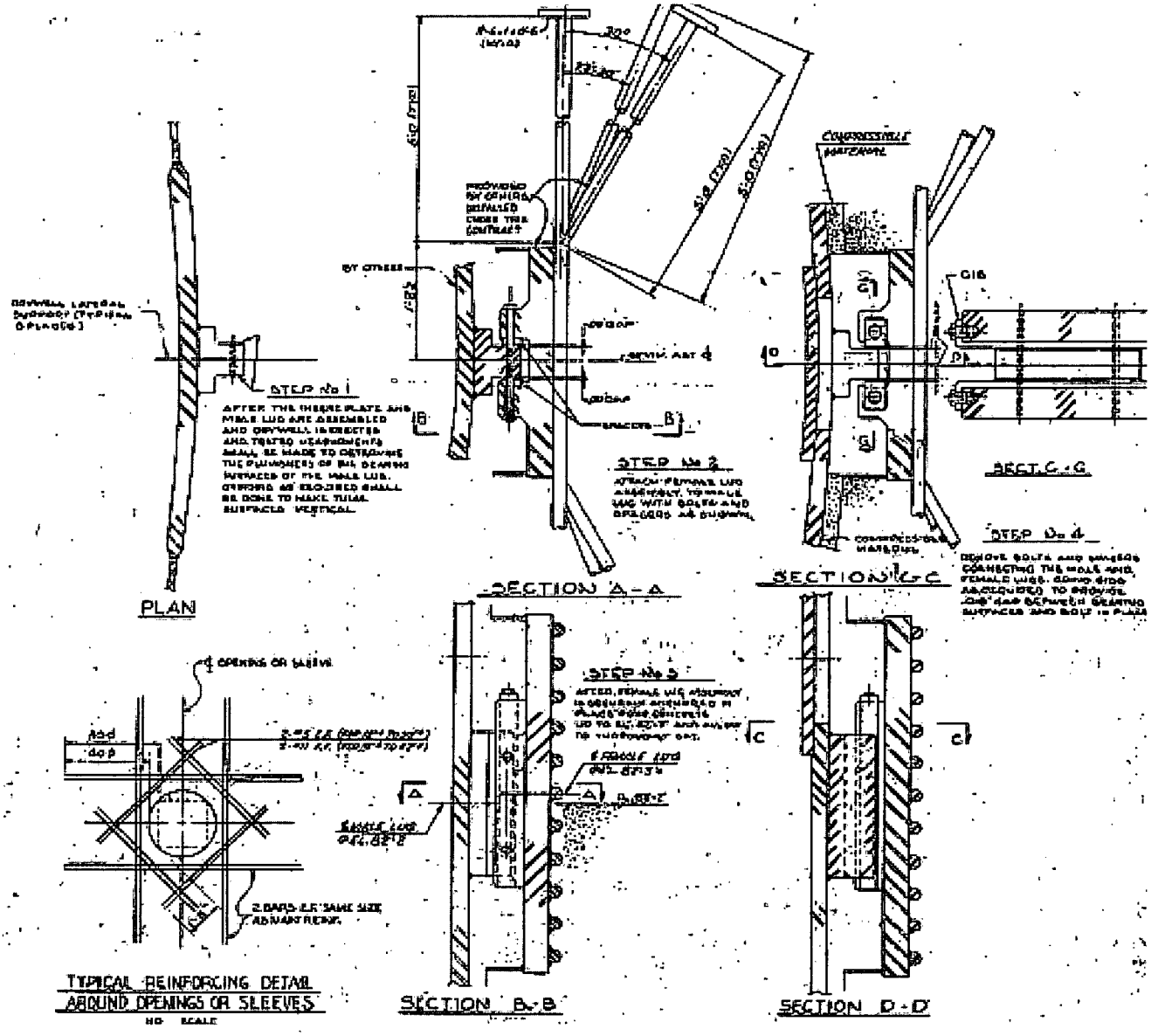

Figure 6-10: Star Truss Male Lug Configuration

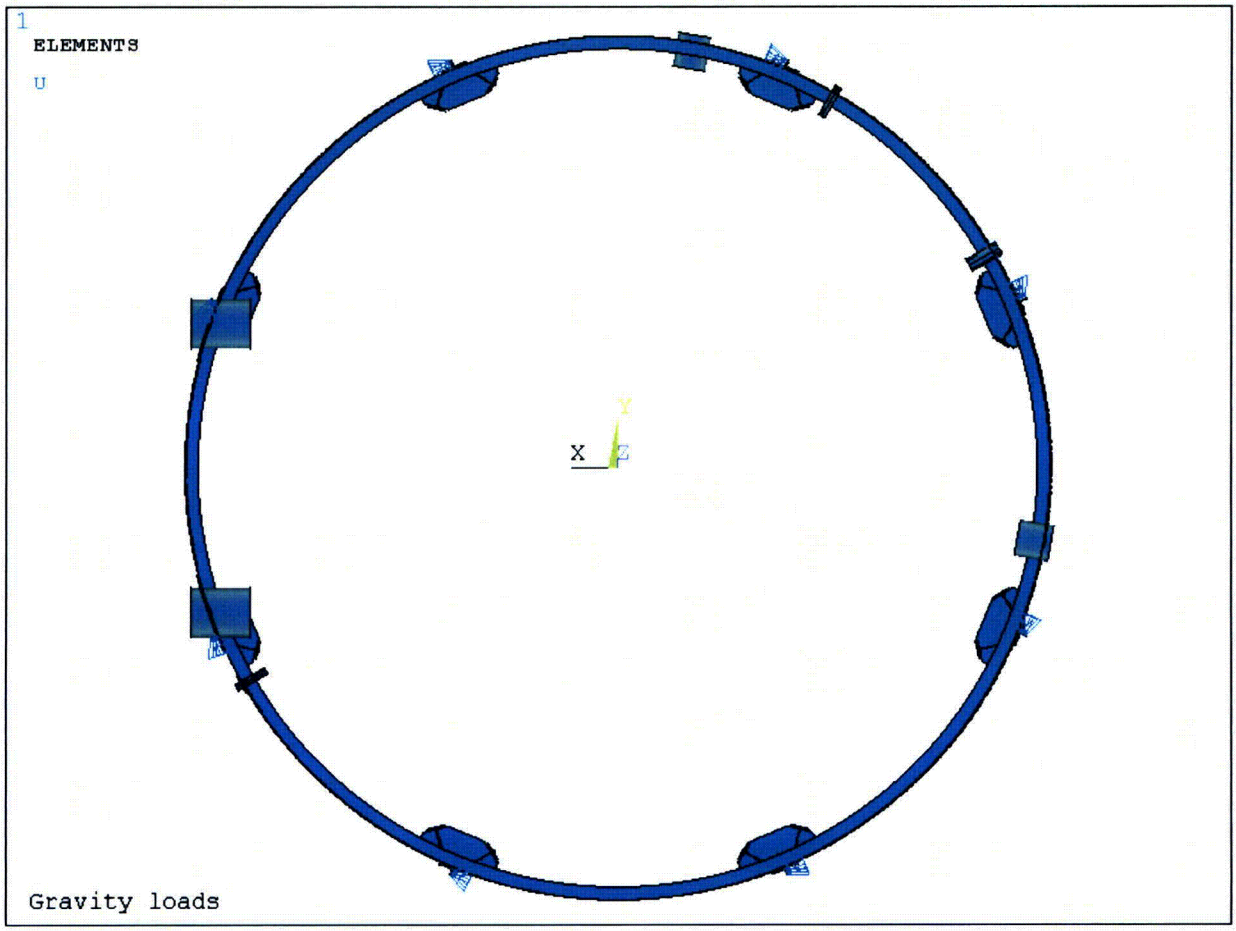

Figure 6-11: Star Truss Displacement Boundary Condition

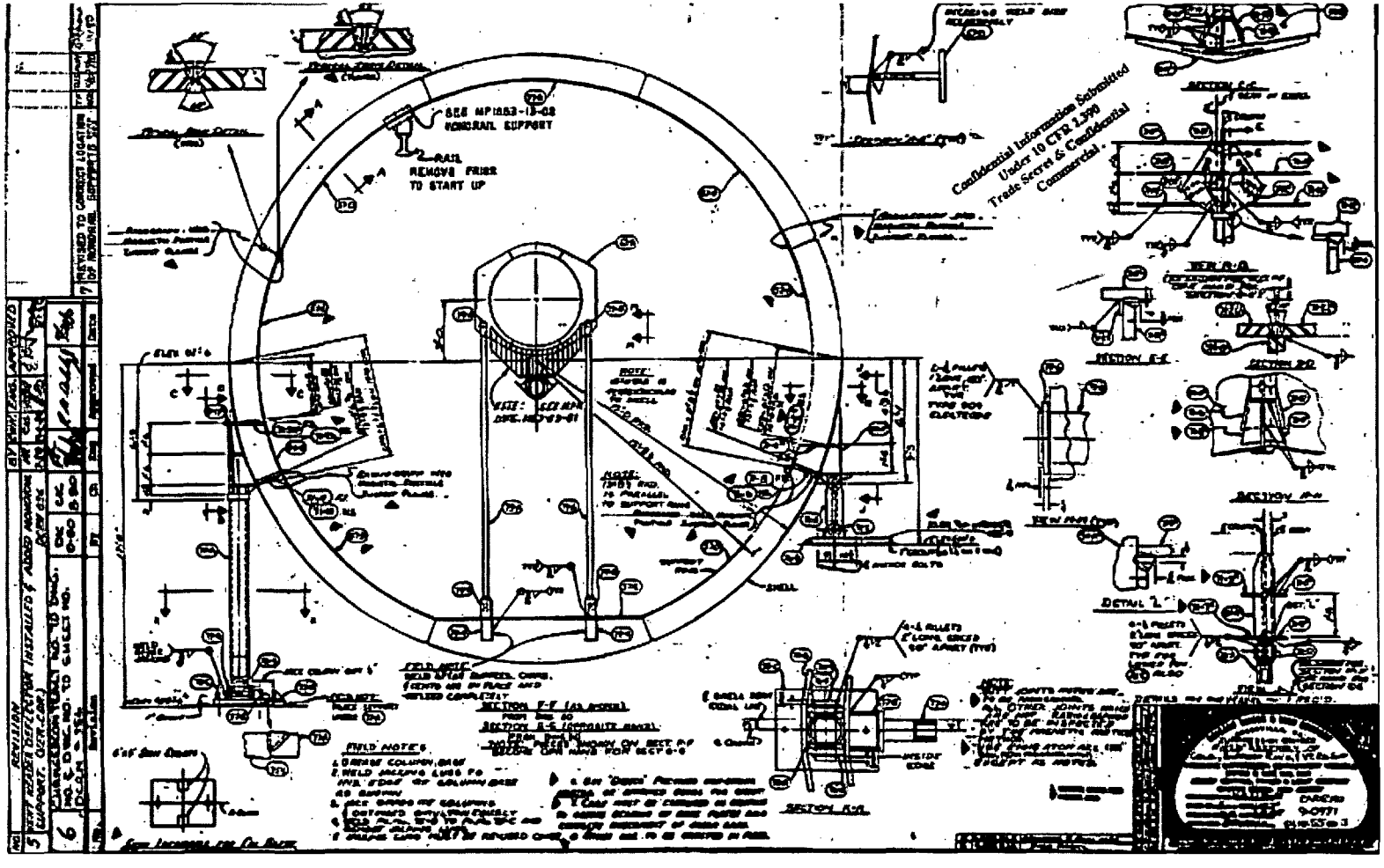

Figure 6-12: Vent Header Displacement Boundary Conditions

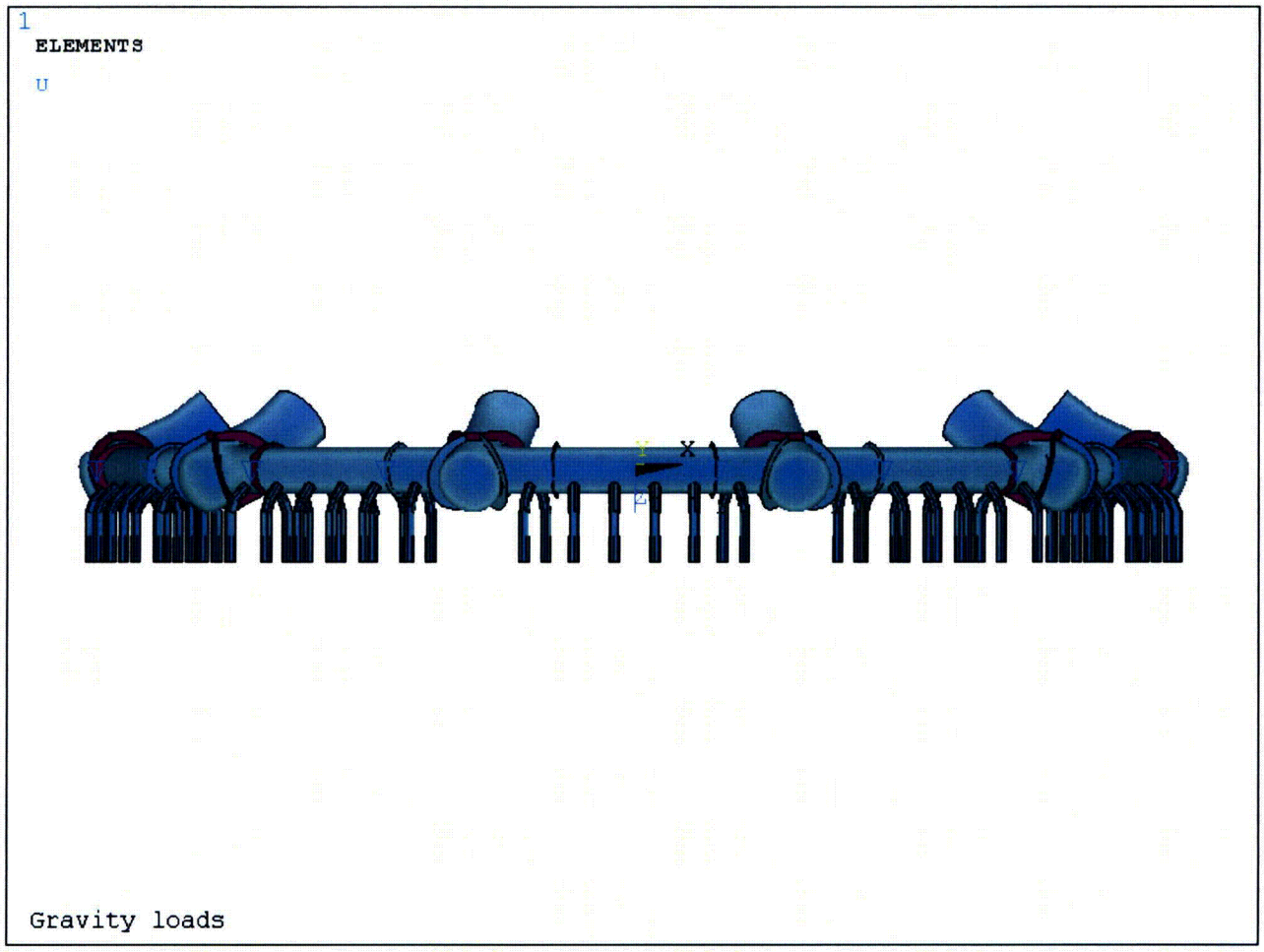

Figure 6-13: Vent Header Displacement Boundary Conditions

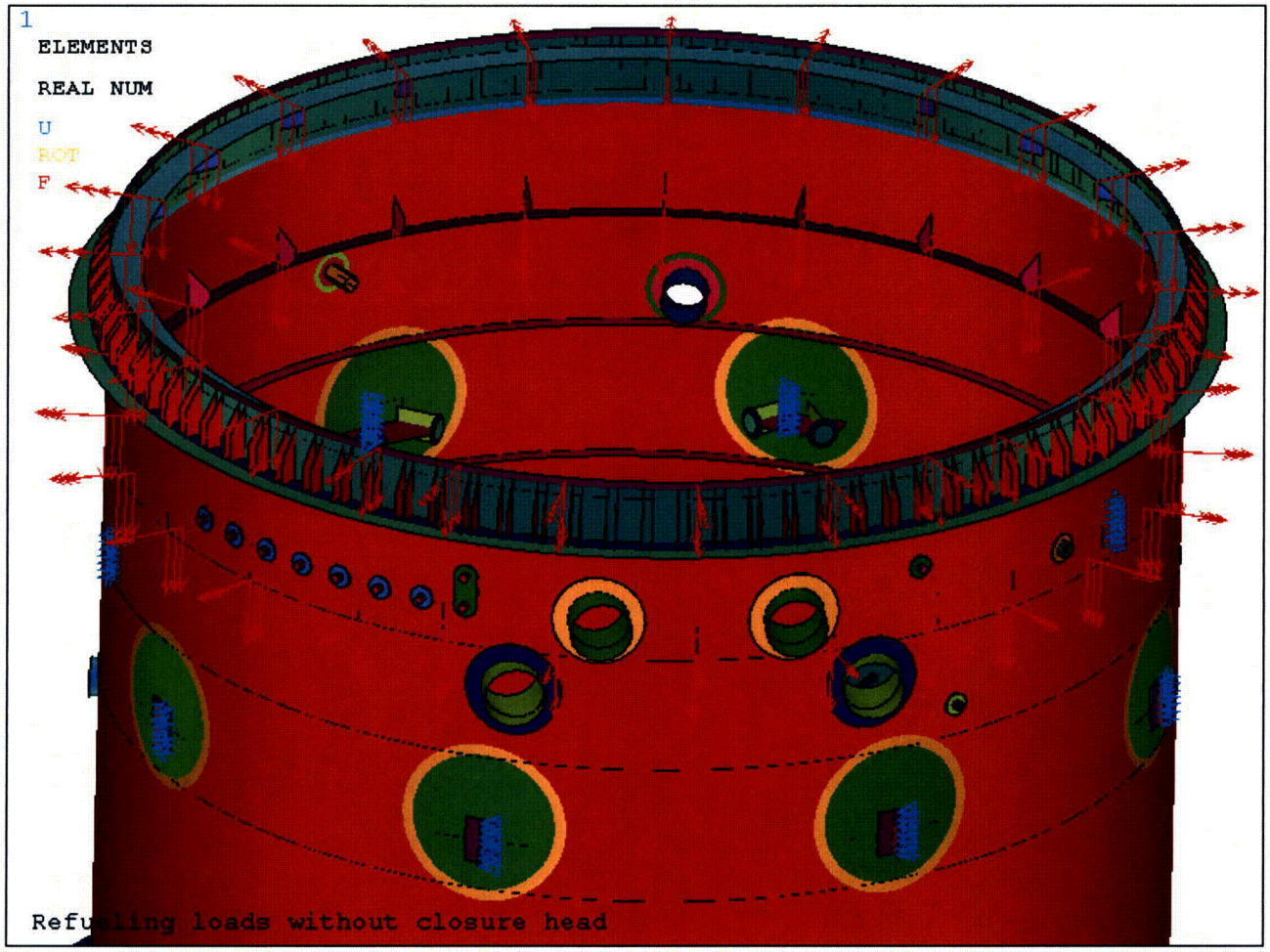

Figure 6-14: Refueling Loads as Applied in the Model

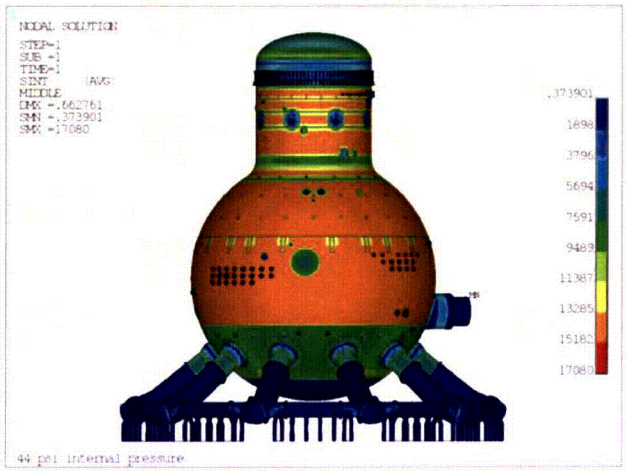

(a) Mid Surface

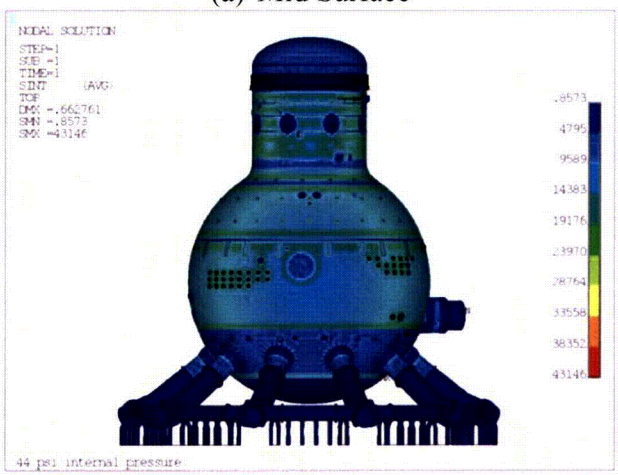

(b) Top Surface

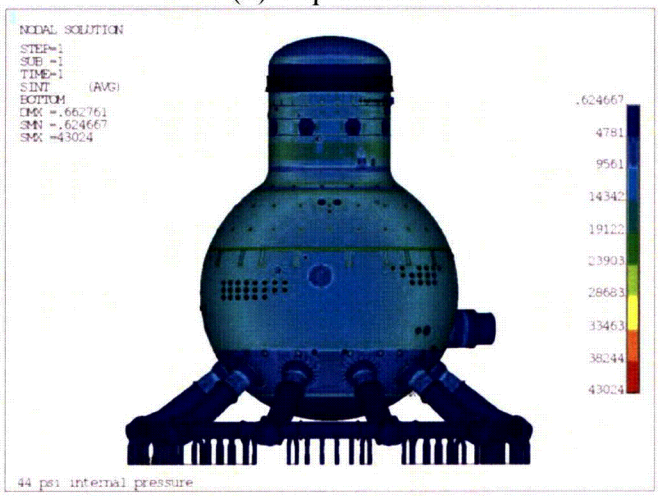

(c) Bottom Surface

Figure 6-15: Stress Intensity Distribution due to 44 psi Internal Pressure

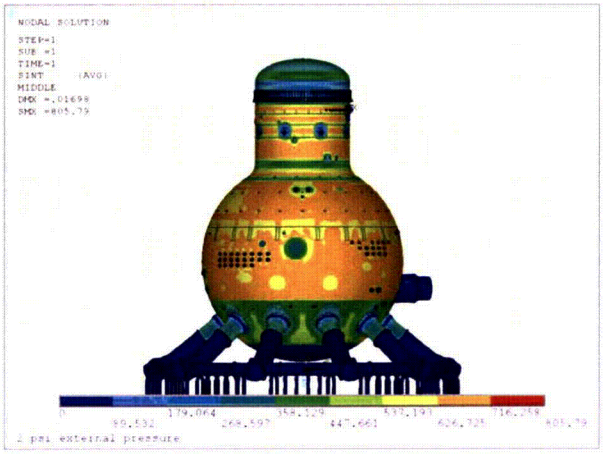

(a) Mid Surface

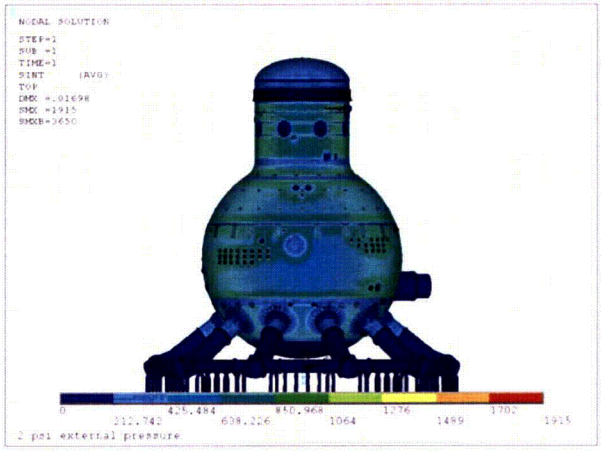

(b) Top Surface

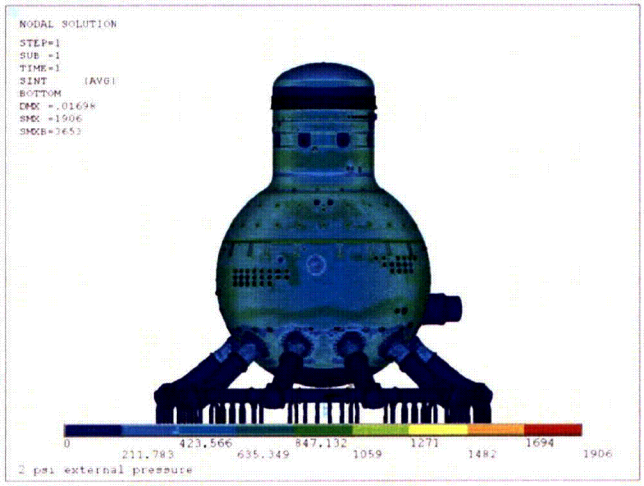

(c) Bottom Surface

Figure 6-16: Stress Intensity Distribution due to 2 psi External Pressure

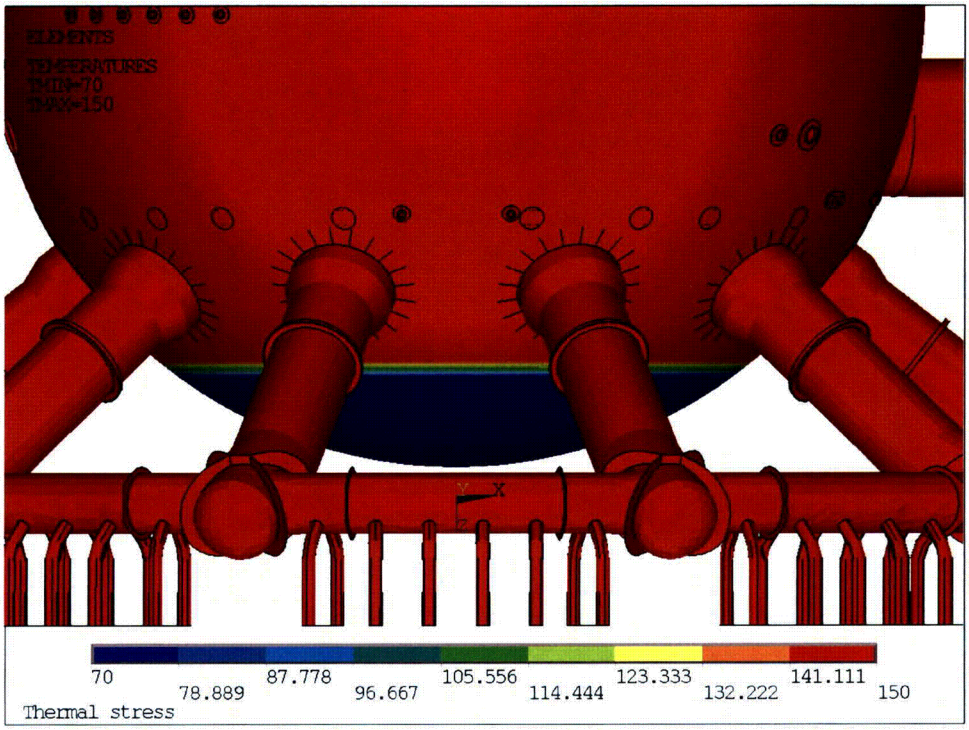

(a) 150 °F

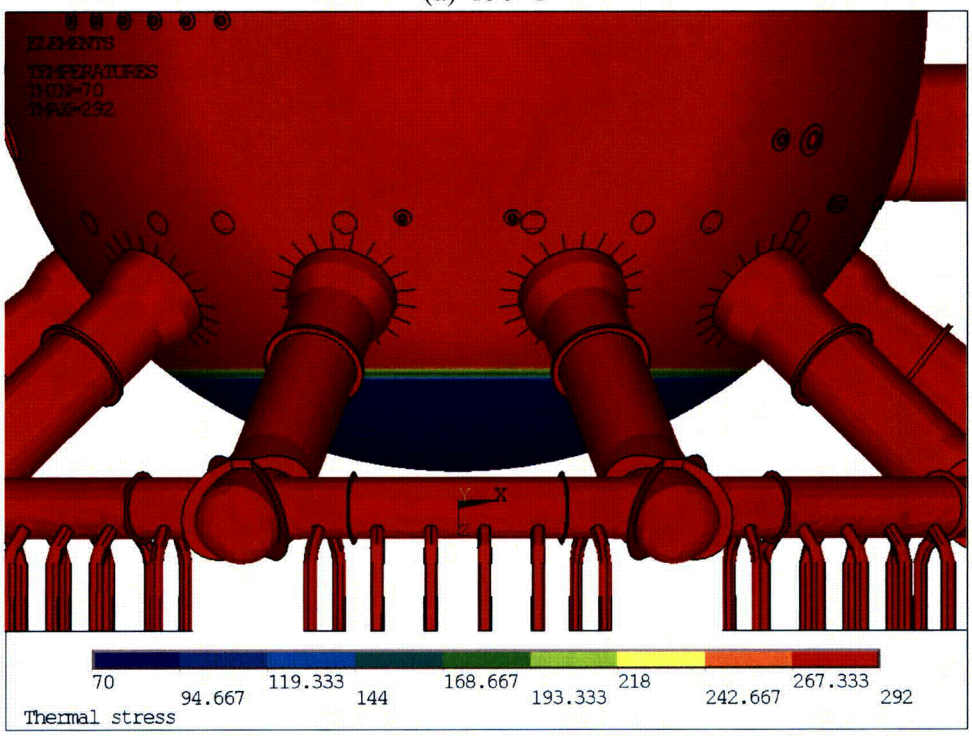

(b) 292 °F

Figure 6-17: Steady State Temperature Distribution

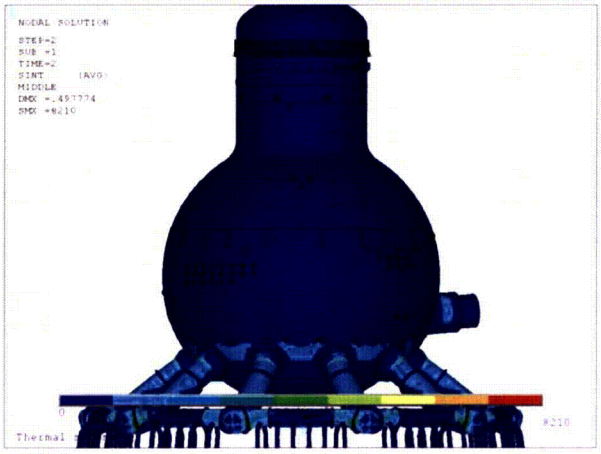

(a) Mid Surface

(b) Top Surface

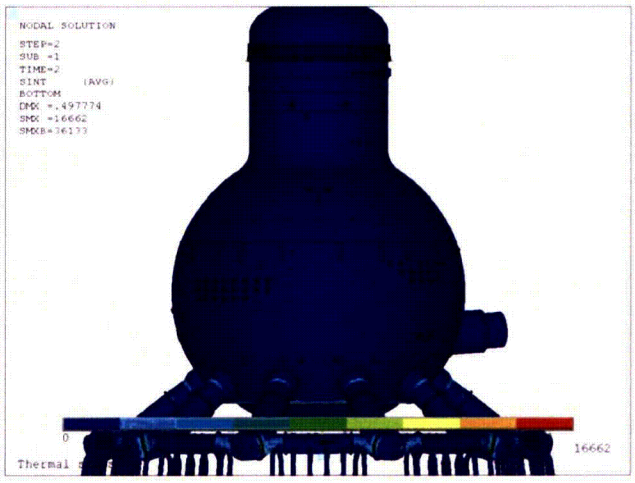

(c) Bottom Surface

Figure 6-18: Stress Intensity Distribution, Steady State Thermal at 150°F

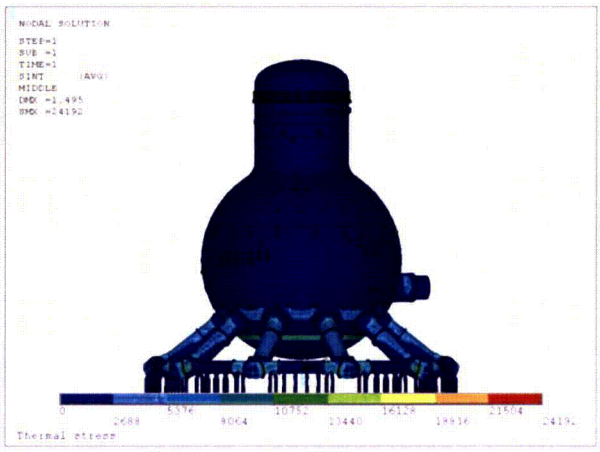

(a) Mid Surface

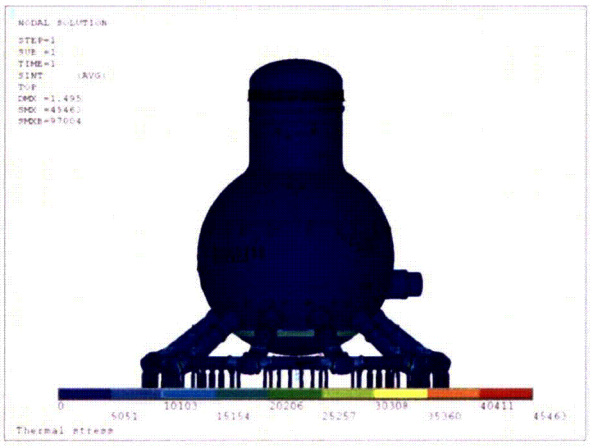

(b) Top Surface

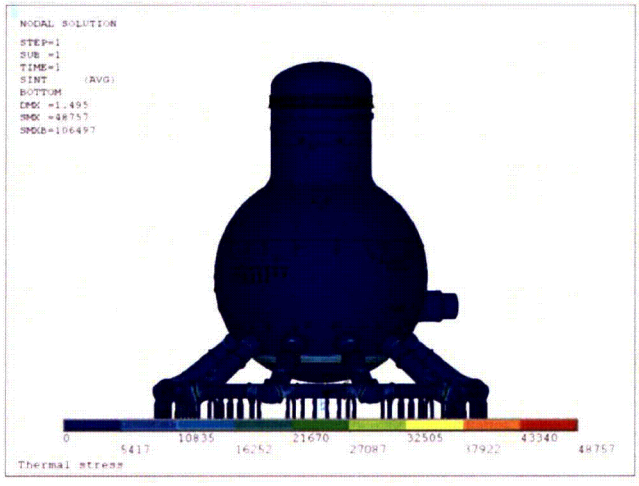

(c) Bottom Surface

Figure 6-19: Stress Intensity Distribution, Steady State Thermal at 292°F

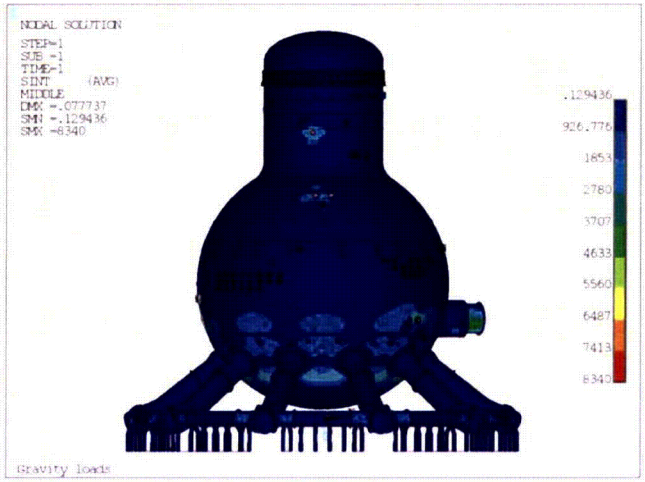

(a) Membrane Stress

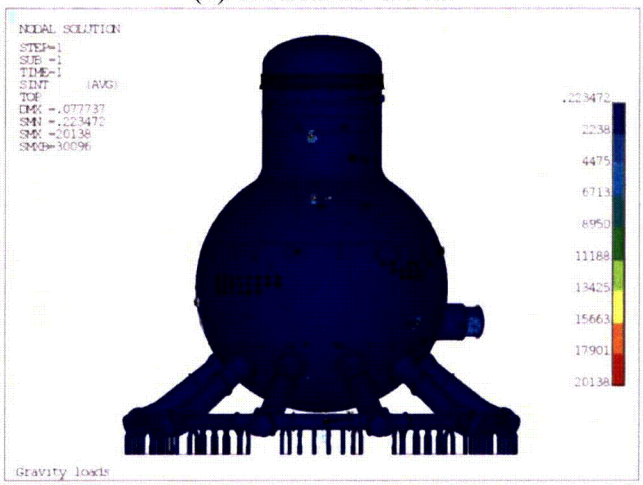

(b) Top Surface

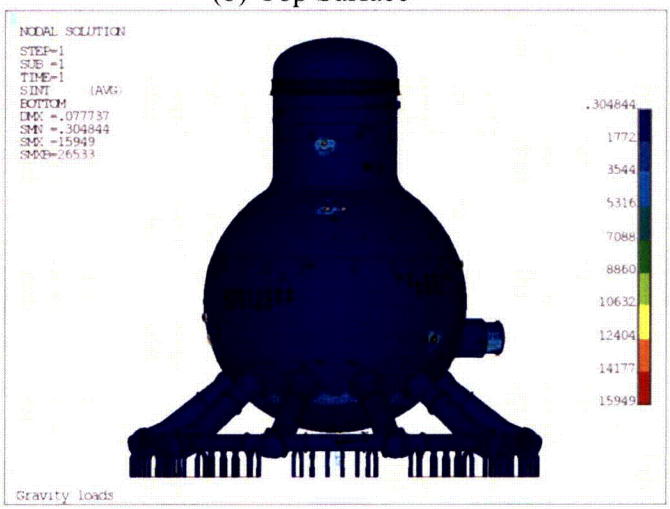

(c) Bottom Surface

Figure 6-20: Stress Intensity Distribution, Gravity Loads

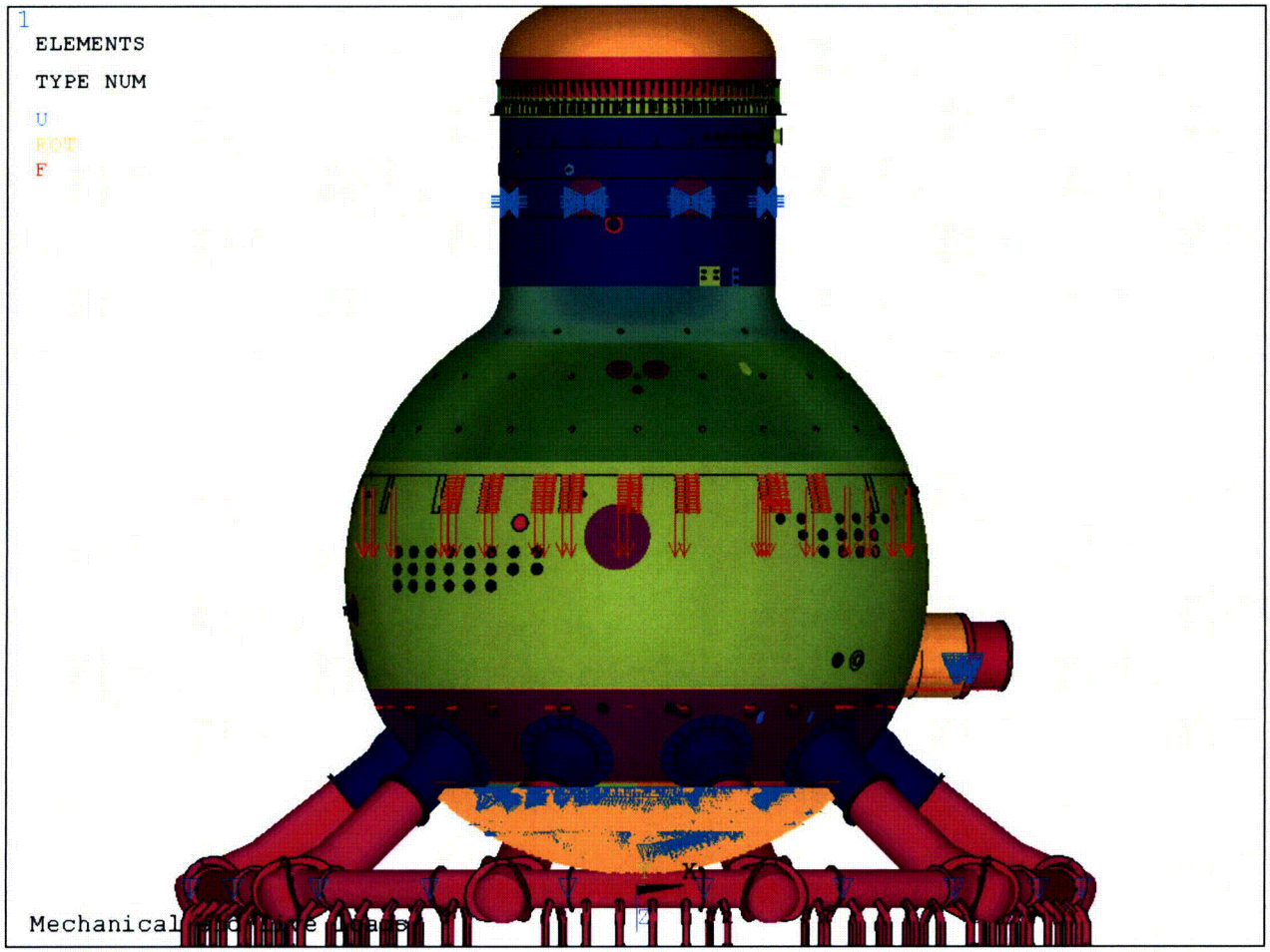

Figure 6-21: Application of Mechanical and Live Loads

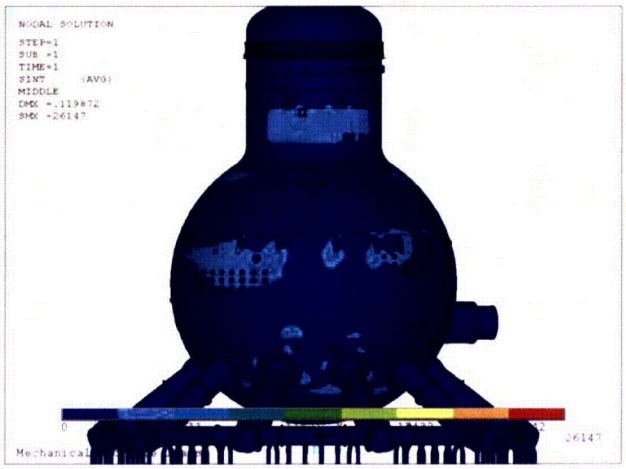

(a) Mid Surface

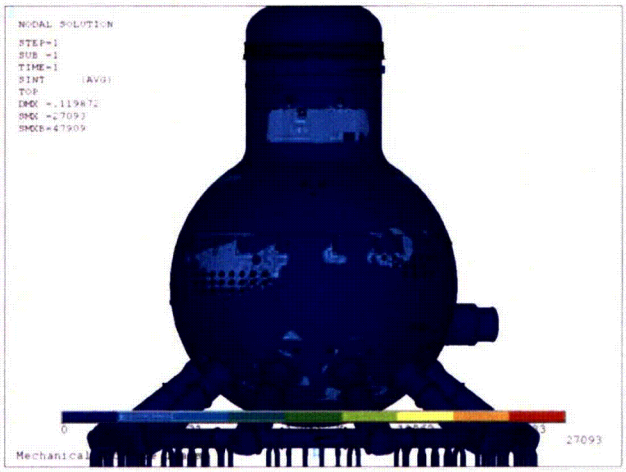

(b) Top Surface

(c) Bottom Surface

Figure 6-22: Stress Intensity Distribution, Mechanical and Live Loads

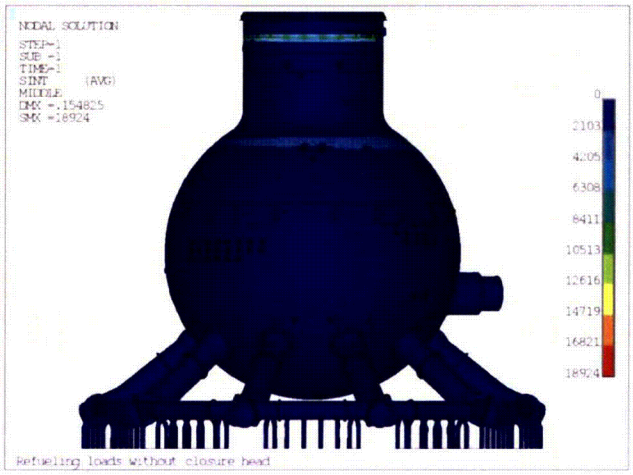

(a) Mid Surface

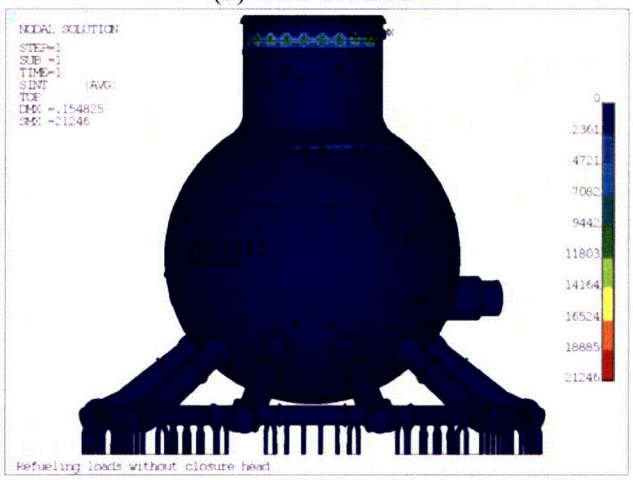

(b) Top Surface

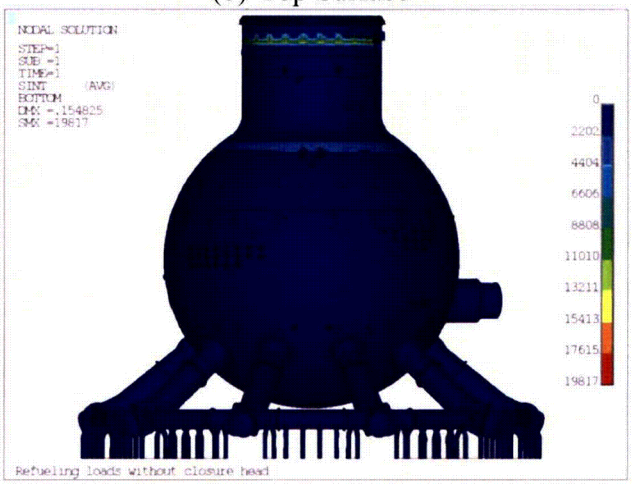

(c) Bottom Surface

Figure 6-23: Stress Intensity Distribution, Refueling

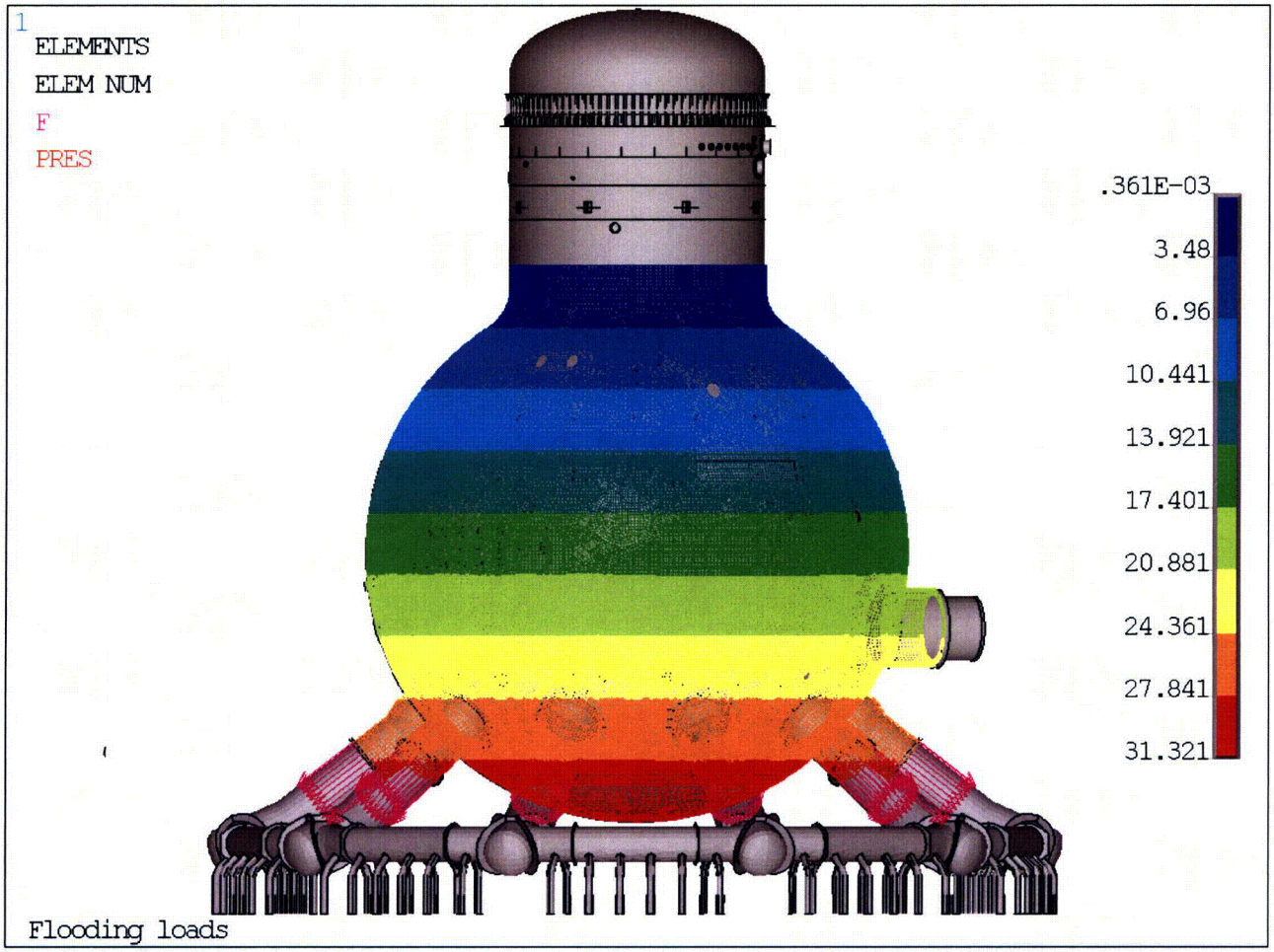

Figure 6-24: Hydrostatic Pressure Distribution due to Flooding

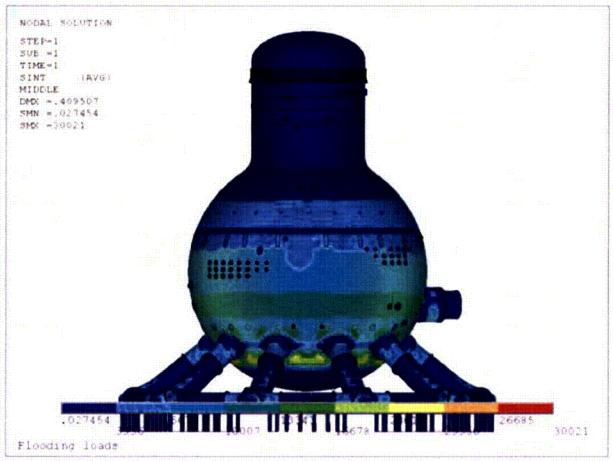

(a) Mid Surface

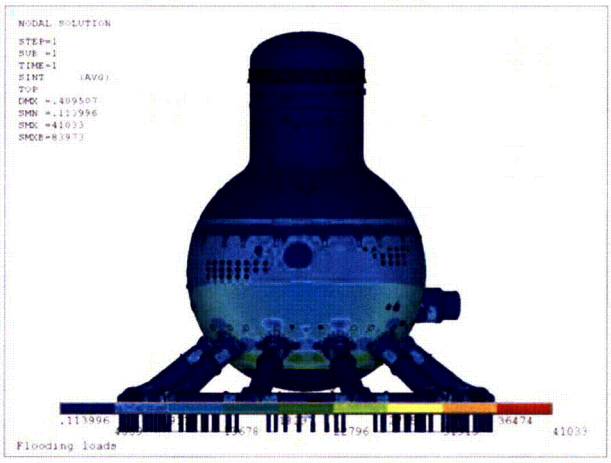

(b) Top Surface

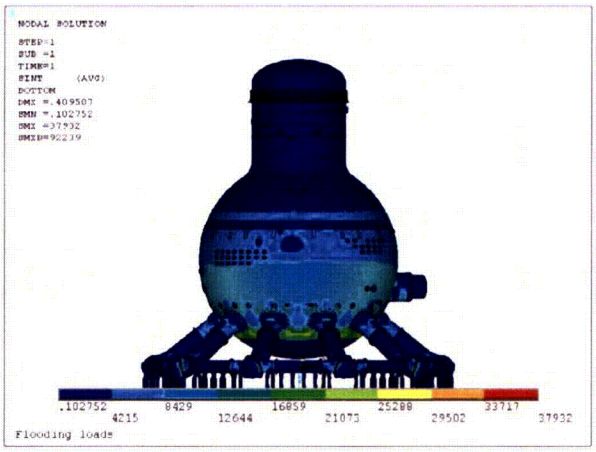

(c) Bottom Surface

Figure 6-25: Membrane Stress Distribution, Flooding

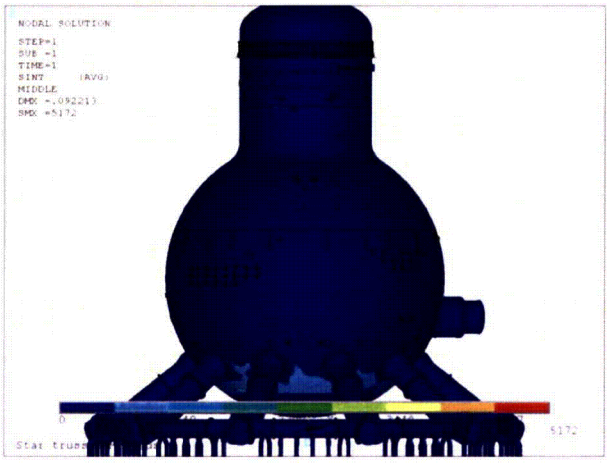

(a) Mid Surface

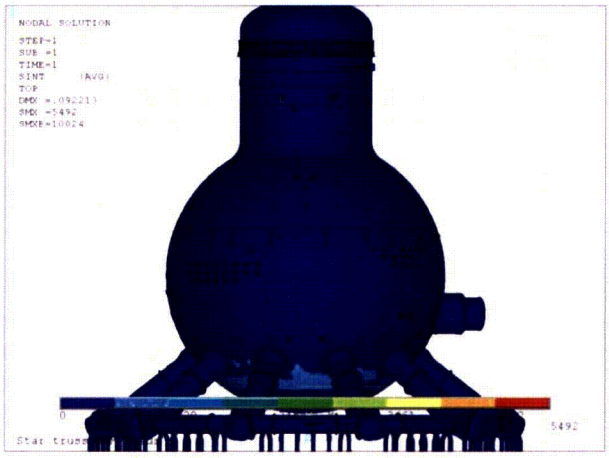

(b) Top Surface

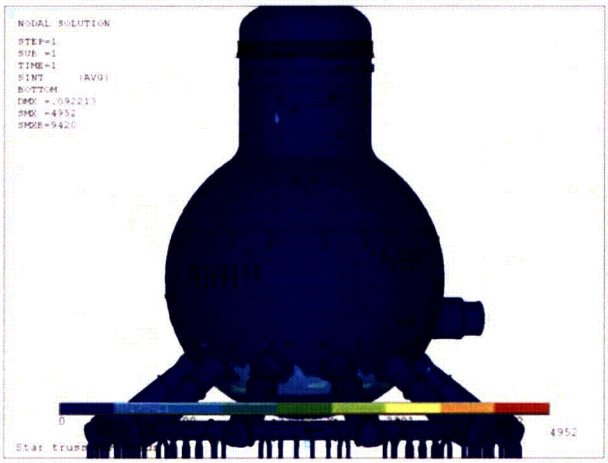

(c) Bottom Surface

Figure 6-26: Stress Intensity Distribution, Seismic Anchor Movements

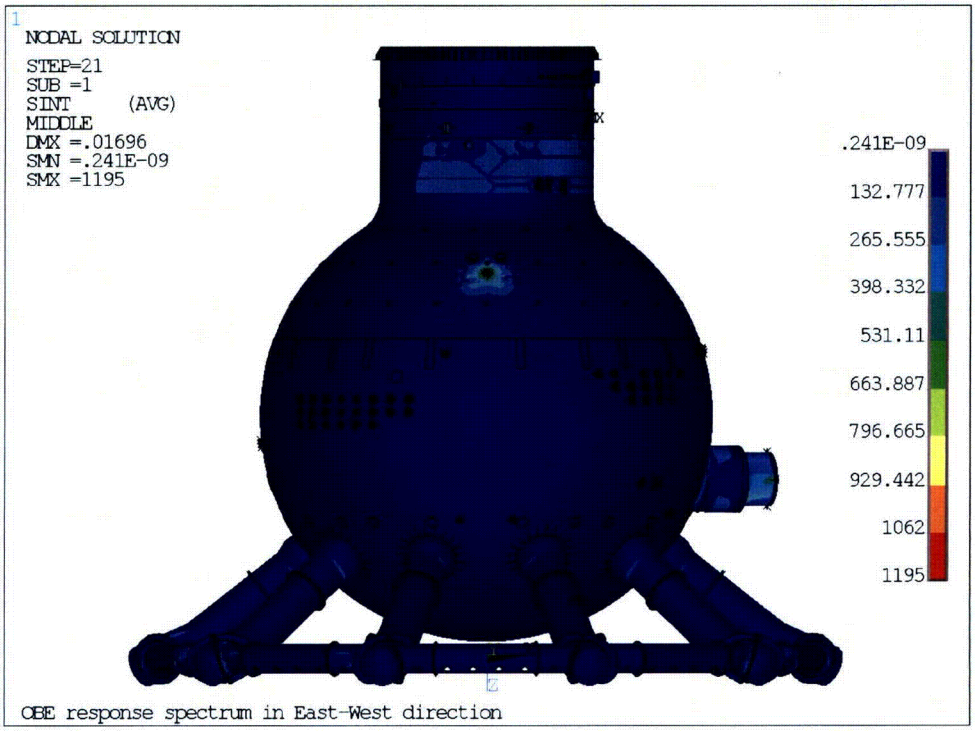

Figure 6-27: Stress Intensity Distribution, OBE E-W Response Spectrum

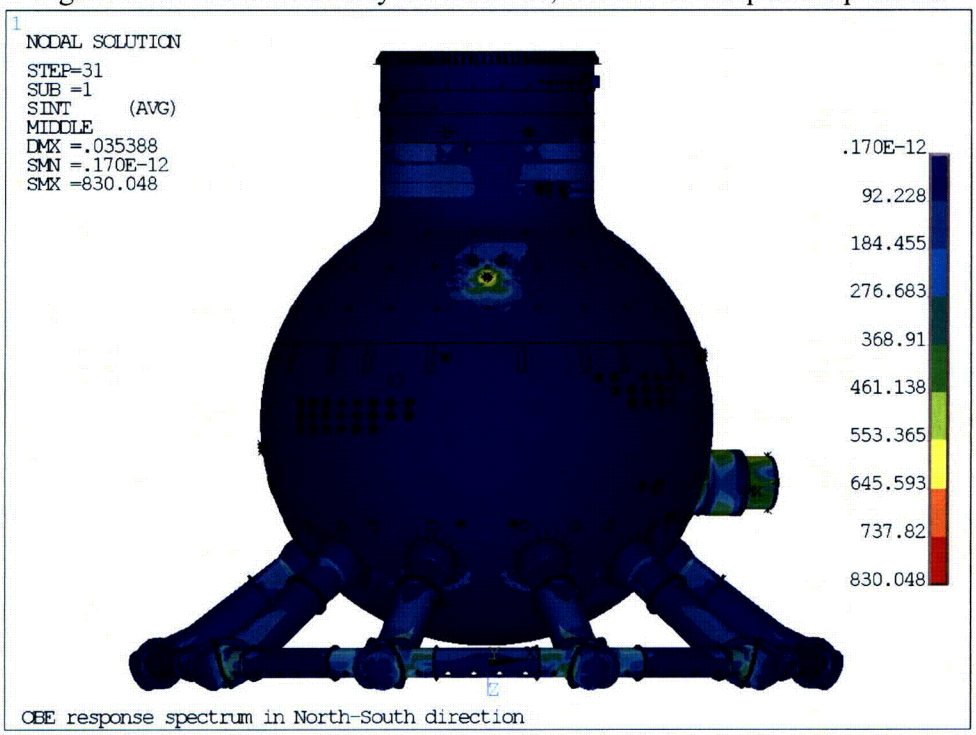

Figure 6-28: Stress Intensity Distribution, OBE N-S Response Spectrum

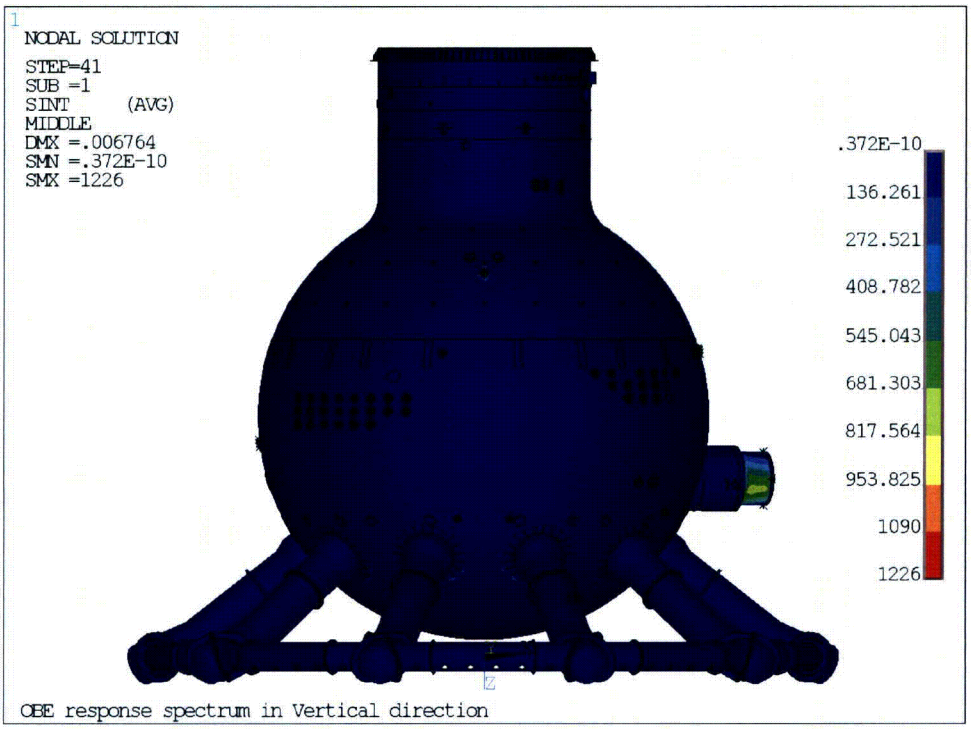

Figure 6-29: Stress Intensity Distribution, OBE Vertical Response Spectrum

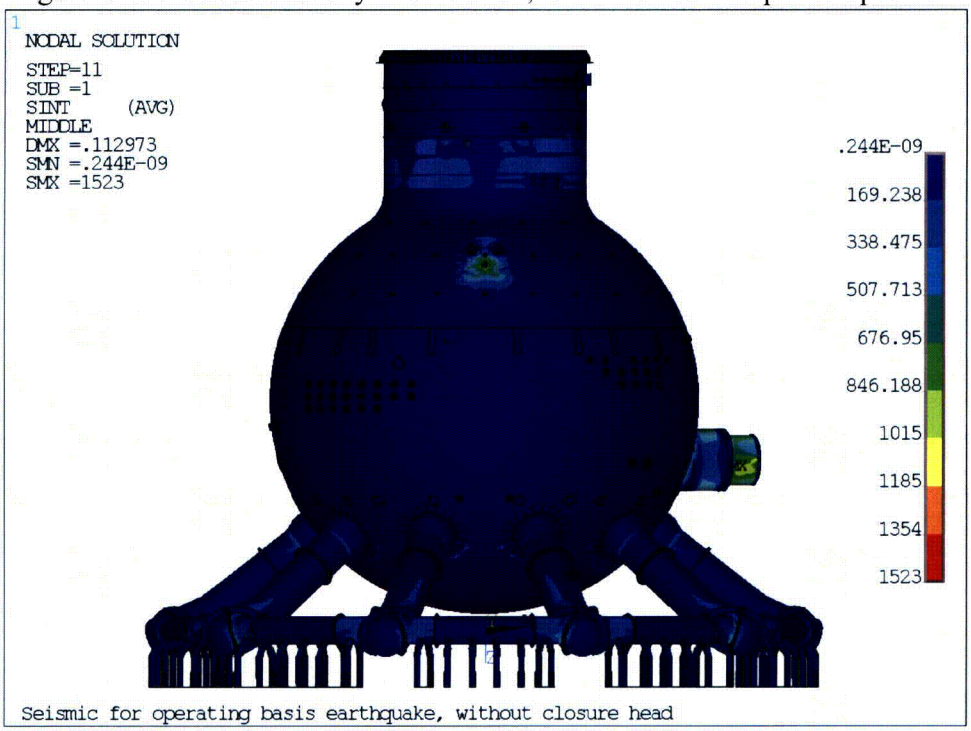

Figure 6-30: Stress Intensity Distribution, OBE Resultant Stress

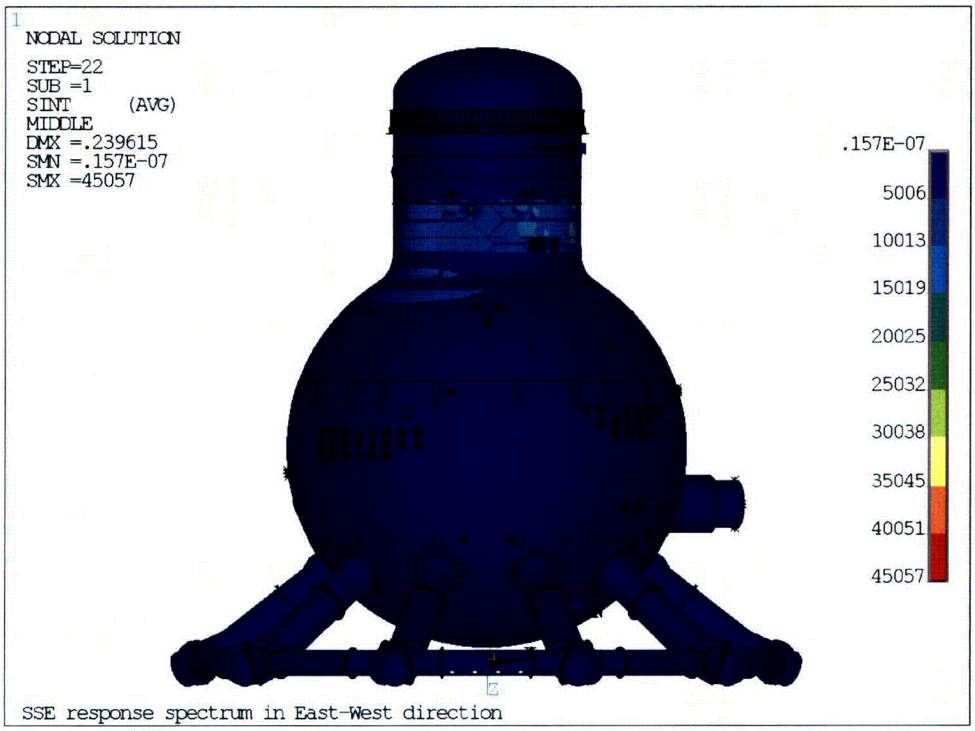

Figure 6-31: Stress Intensity Distribution, Flooding SSE E-WS Response Spectrum

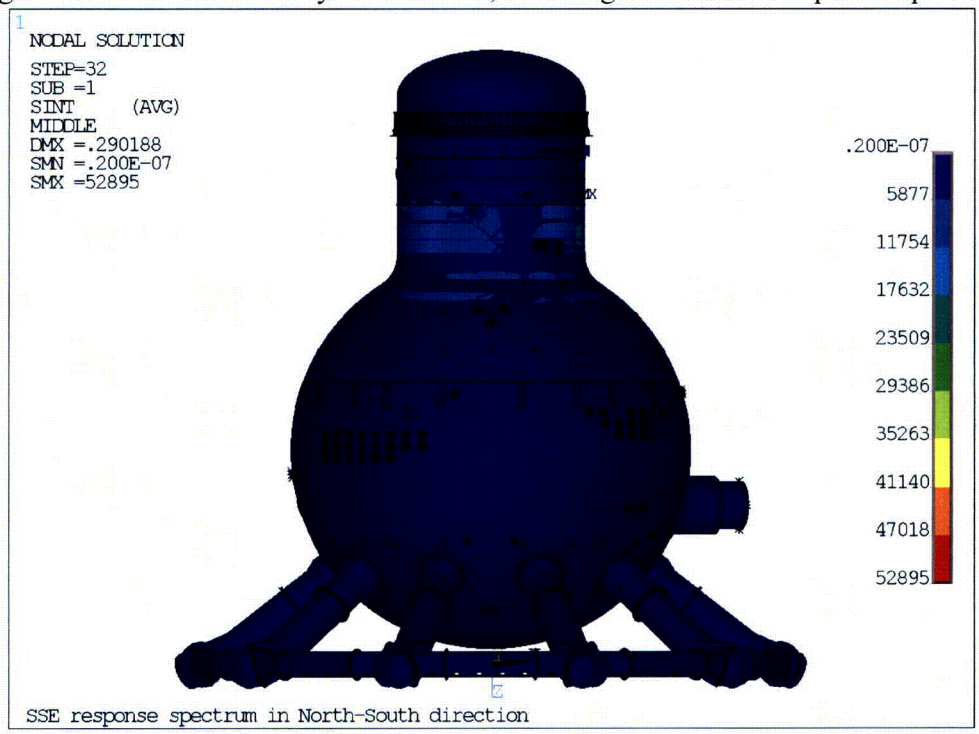

Figure 6-32: Stress Intensity Distribution, Flooding SSE N-S Response Spectrum

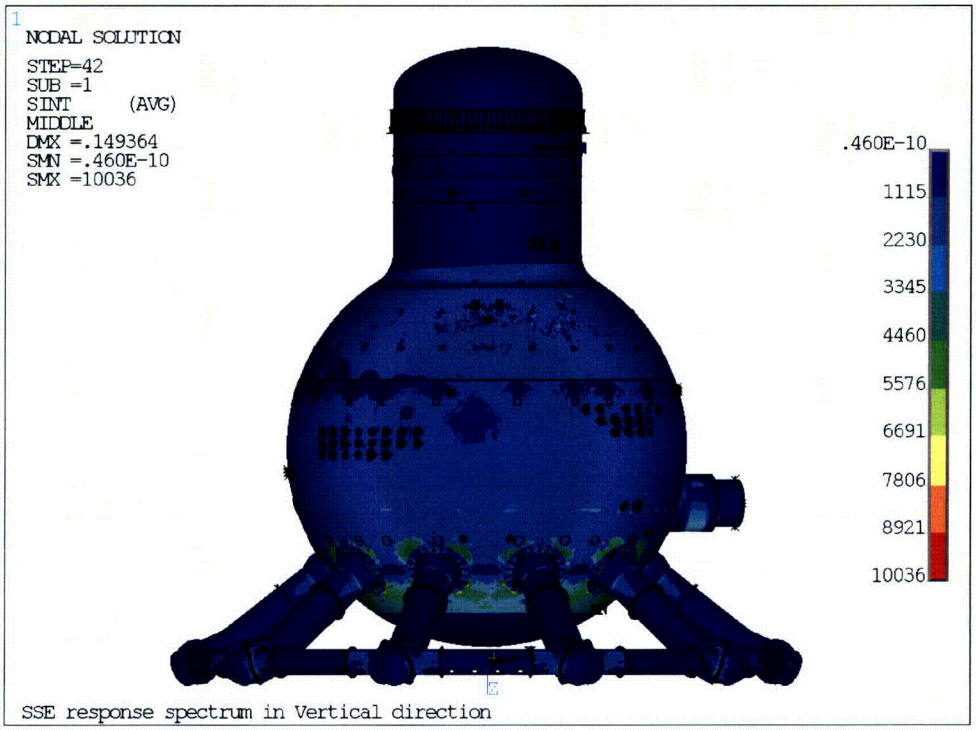

Figure 6-33: Stress Intensity Distribution, Flooding SSE Vertical Response Spectrum

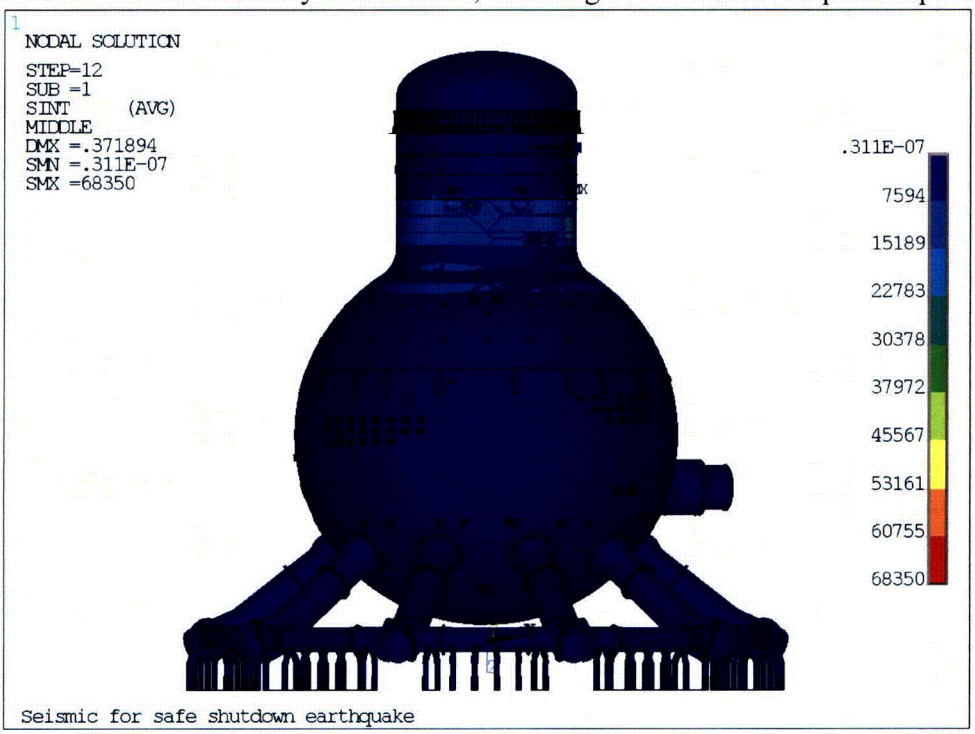

Figure 6-34: Stress Intensity Distribution due to OBE N-S Response Spectrum

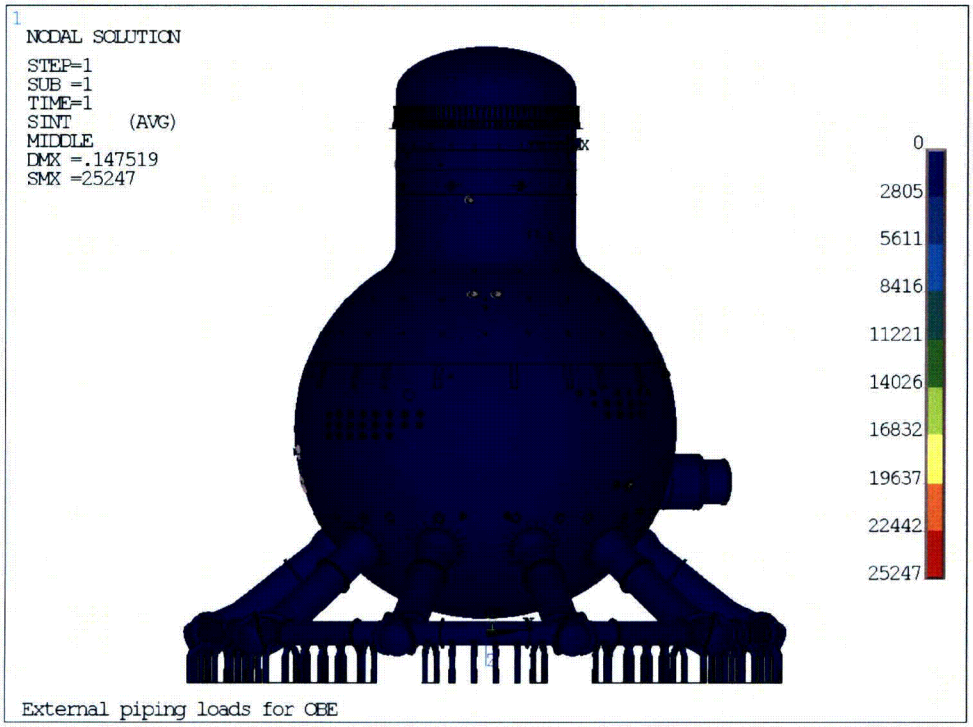

Figure 6-35: Stress Intensity Distribution, External Piping OBE Loads

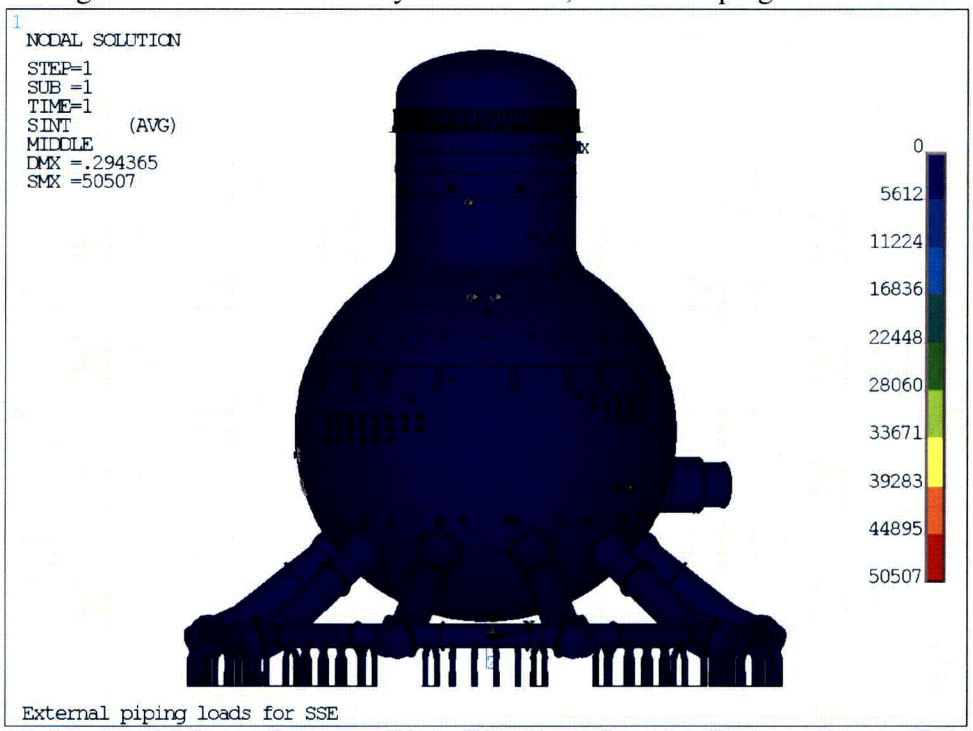

Figure 6-36: Stress Intensity Distribution, External Piping SSE Loads

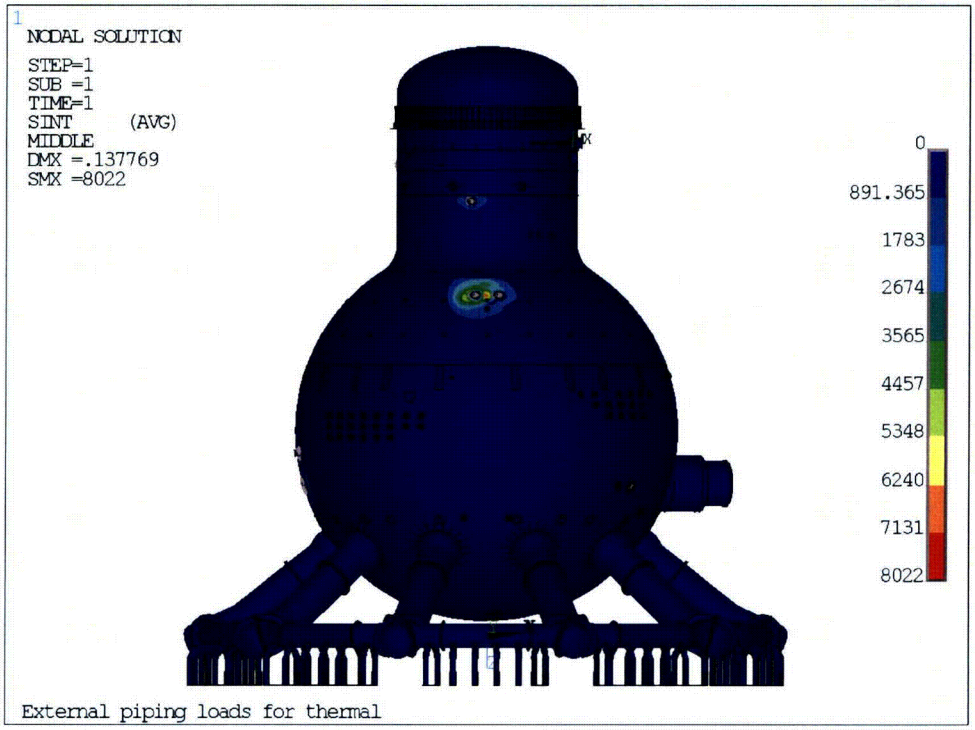

Figure 6-37: Stress Intensity Distribution, External Piping Thermal Loads

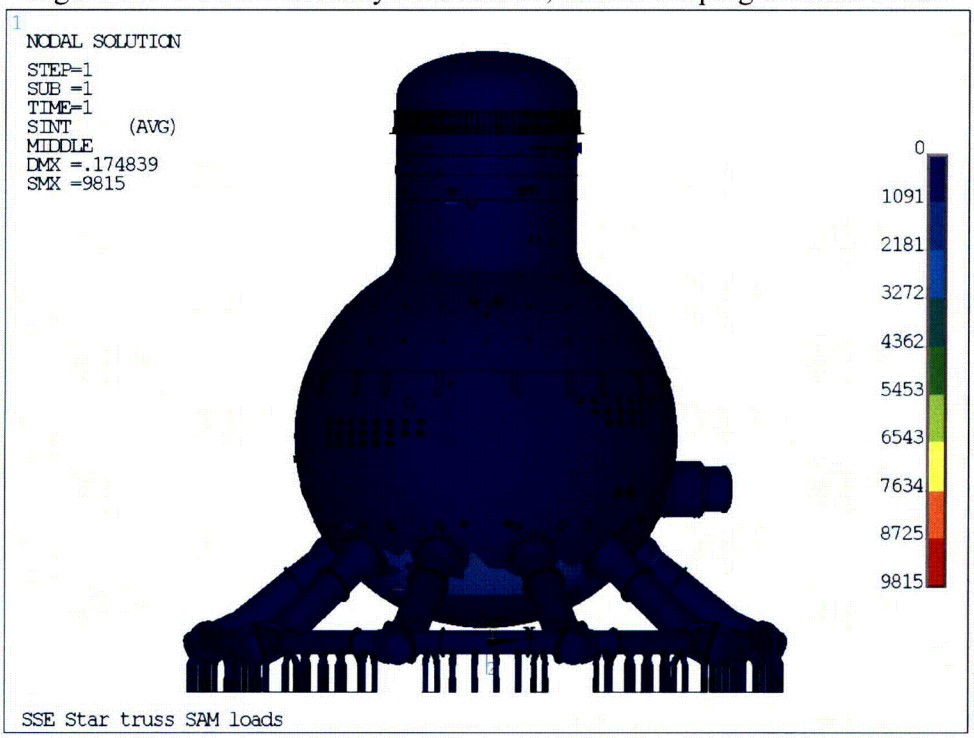

Figure 6-38: Stress Intensity Distribution, Flooding SSE Seismic Anchor Movements

7.0 ASME CODE STRESS EVALUATION

This Section describes the load combinations of individual load cases and the results of the ASME Code Section III, Subsection NE, Class MC components stress evaluation.

7.1 ASME Code Requirements

The original Code of Record is ASME Boiler and Pressure Vessel (B&PV) Code, Section VIII, 1962 Edition, with Nuclear Case Interpretations 1270 N-5, 1274 N-5 and 1272 N-5 [7]. The original Code of Record and Nuclear Case Interpretations do not provide stress intensity limits at different operating conditions, (i.e. post-accident conditions) and the local membrane stress due to the thickness reductions from local to general corrosion effect.

To address the need for guidance for the above areas, the code stress intensity requirements and limits from ASME B&PV Code, Section III, Subsection NE, Class MC Components 1989 Edition including 1991 Winter Addenda [28] is used. This Code of Record was used in previous re-evaluation of Oyster Creek drywell stress analyses [2]. The stress intensity limits which must be satisfied are specified in Subarticle NE-3320, and duplicated in Table 7-1 and Figure 7-1 through Figure 7-4.

7.2 Stress Intensity Allowables

The allowable stress intensity, S_{mc}, for the Oyster Creek drywell materials are presented in Table 7-2. The allowable stress intensities were obtained from Reference 6. If the allowable stress intensity is not available for a material, the allowable value was determined based on the rules provided in Appendix III of Reference 6. The allowable stress intensities for Class MC components are 110% of the values for the same materials in Class 2 and Class 3 components. Also, the material yield strength, S_y and ultimate strength, S_u, are presented in Table 7-3 for completeness.

The stress intensity limits for different stress categories are summarized in Table 7-4 at 150 °F for different service conditions and materials. The classification of different stress categories are provided in Table 7-5.

7.3 Load Combinations

The description of load cases is summarized in Table 7-1. The individual load cases are used for load combinations to obtain the stress during the operating conditions for different levels. An algebraic sum of the individual load cases is used in the load combinations.

The load combinations are summarized in Table 7-6. The load combinations are assigned to different service levels per References 5, 14 and 28. Only the refueling and post-accident flooding conditions are evaluated for ASME Code compliance since they are considered to be the governing cases. As listed in Table 7-6, the load cases used in the load combinations for Levels A and B are identified. It is shown that the LC3, LC4, LC5 and LC6 have more number of load cases than LC1 and LC2. LC5 and LC6 have an additional load case of refueling included compared to LC3 and LC4. In addition, previous evaluation [2] identified that the refueling case is the governing case for service Levels A/B conditions. Therefore, the refueling condition is bounding (i.e. LC5 and LC6) and selected for Code and buckling evaluation.

The flooding case is typically classified as a Level D condition because it follows after the LOCA condition. However, Oyster Creek conservatively evaluates the flooding case as a Level C condition. (Chapter 3 of the Oyster Creek UFSAR defines the allowable stresses to be used for this case. These allowables are the equivalent of the ASME Code Level C allowable stresses.) The load cases used for the flooding condition are similar to the Level C conditions with an extra load case due to flooding loads. Typical Level C conditions usually include a higher pressure, temperature and safe shut down earthquake versus Level A/B but less severe conditions than those used for the Level D conditions. In addition, the flooding introduces a significant hydrostatic pressure at the bottom of the drywell in the sandbed regions. Therefore, the flooding case is bounding and conservative for the ASME Code service level C evaluation.

The jet loads due to loss of coolant accident (LOCA) conditions are considered in the Level D condition [14]. The effect of jet loads was documented in Reference 37 and not evaluated in this report.

7.4 ASME Section III Subsection MC Code Evaluation

Major components in the drywell are identified for ASME Code stress evaluation. These components include:

(a) Top head shell
(b) Cylindrical shell
(c) Stiffeners/gussets in cylindrical shell
(d) Star truss and stiffeners
(e) Knuckle
(f) Spherical Shell
(g) Upper Beam Seat and stiffener
(h) Lower Beam Seat
(i) Vent Pipes
(j) Sandbed Region
(k) Penetrations

Material properties for SA-516 Grade 70 are used for stress evaluations for all the above components, except the Upper Beam Seat, which is made from SA-516 Grade 60.

For those penetrations with the external piping loads available, the code stress evaluation is performed for each penetration. For those penetrations where no penetration loads are available, the penetrations are grouped by penetration size and evaluated as a group (3", 6", 8", 10", 14", and 18"). Penetrations in the suppression chamber, spare or abandoned drywell penetrations or manholes are not included for evaluation.

The personnel lock/equipment hatch is not included because only overall outer shells are included in the model without the detail internals, such as locks, floor, and doors. Also the drywell bolts and pins are not included for Code stress evaluation because the top head and the

cylindrical shell are assumed integrally connected and the bolt preloads are not considered in the model.

Following guidelines are also used for classification of stress categories.

(a) Per NE-3213.9 [28], bending stress at a gross structural discontinuity is classified as secondary stress. These include bending stress due to internal pressure and external load or moment per Table NE-3217-1 [6] near nozzle, other opening, junction with head or flange, knuckle or junction to shell.

(b) Per NE-3213.10 [28], a stress region may be considered local if the distance over which the membrane stress intensity exceeds 1.1 S_{mc} does not extend in the meridional direction more than $\sqrt{(Rt)}$ where R is the minimum midsurface radius of curvature and t is the minimum thickness in the region considered.

(c) Per NE-3221.3, the primary general or local membrane plus primary bend stress intensity is derived from the highest value across the thickness of a section. In addition, Note (2) in Figure NE-3221-1 and Figure NE-3221-3 state that it is for a solid rectangular section.

Among the load combinations presented in Table 7-6, the refueling cases (LC5 and LC6) are the limiting cases in Levels A and B service conditions, because of the additional loads due to the refueling. For Level C, the post-accident flooding case (LC9 and LC10) are the limiting cases. These two load cases are selected as the bounding cases for Code stress allowable evaluation.

The Code evaluations for the different load combinations are provided in the following tables:

- Table 7-7 Refueling Case, Load Combination LC5
- Table 7-8 Refueling Case, Load Combination LC6
- Table 7-9 Post Accident Flooding Case, Load Combination LC9
- Table 7-10 Post Accident Flooding Case, Load Combination LC10

7.5 Fatigue Evaluation

Per NE-3221.5 (a) of Reference 28:

> "If the specified Service Loadings for the component meet all of the requirements of NE-3221.5 (d), no analysis for cyclic service is required. It may be assumed that the limits on peak stress intensities as governed by fatigue have been satisfied by compliance with the applicable requirements for materials, design, fabrication, examination, and testing of this Subsection."

The conditions stipulated in NE-3221.5 (d) [28] are:

(1) Atmospheric-to-Service Pressure Cycle
(2) Normal Service Pressure Fluctuation
(3) Temperature Difference – Startup and Shutdown
(4) Temperature Difference – Similar Material
(5) Temperature Difference – Dissimilar Materials
(6) Mechanical Loads.

In general, these conditions provide a limit on the number of significant service cycles, the maximum fluctuation of the pressure cycles, the maximum temperature difference under different conditions and the maximum mechanical loads applied on component. The detailed steps in evaluating these conditions are provided in NE-3221.5 (d) (1) to NE-3221.5 (d) (6) [28].

In evaluating these conditions, it is assumed that the average temperature of the drywell is 150 °F. This is a reasonable assumption because it is stated in the FSAR Section 3.8.2.3, Sub-Section C, Paragraph 3 [17] that the normal operating temperature ranges from 50 °F 150 °F. The number of significant pressure/temperature fluctuation is assumed to be 200 cycles. This number of pressure/temperature cycles is assumed to include the regular startup/shutdown and leak test cycles. The startup/shown cycle is likely no more than 1 cycle per year and the leak test cycle is about 1 per 10 years. This is judged to be more than sufficient for a license renewal to 60 years. Also instead of an instantaneous coefficient of thermal expansion, an average coefficient of thermal expansion was used.

The evaluation results are summarized in Table 7-11 categorized by the materials existed in the drywell. The values presented in Table 7-11 are the limits that the drywell operating parameters cannot exceed such that a detailed fatigue evaluation is not required. The lower bounded number of atmospheric-to-service pressure cycles is 855. This is more than sufficient for any anticipated number of atmospheric-to-service pressure cycles for 60 years of operation. The pressure fluctuation was calculated to be limited to no higher than 72 psi, which is higher than the design pressure of 44 psi [5]. The limit on temperature difference for startup/shutdown, similar material and dissimilar material cannot be larger than 322 °F. Since the maximum temperature for the drywell is 292 °F [5], the maximum temperature difference is under the limit. The maximum stress intensity from the mechanical loads cannot be higher than 135 ksi, which is larger than the required $3S_{mc}$ limit.

Since all the criteria in NE-3221.5 (d) (1) to NE-3221.5 (d) (28) are satisfied, per NE-3221.5 (d), an analysis for cyclic service is not required.

7.6 Code Reconciliation

The Oyster Creek drywell was designed according to the requirements of the latest edition at the time of design of Section VIII of the ASME Boiler and Pressure Vessel Code with all applicable addenda, Nuclear Code Case Interpretations 1270N-5, 1271N, 1272N-5 and other applicable case interpretations, [5, 13]. At the time of the original design and construction, the latest applicable edition was 1962 edition including Winter 1963 Addenda.

The ASME Code permits the use of later editions and addenda as described in Section III, Subarticle NCA-1140 (b). A detailed justification is provided in Reference 21. This justification includes:

(1) The evolution of the Code requirements for containment vessels
(2) Design, Service, Test and Stress Limits
(3) Classifications of local membrane stress
(4) Materials, fabrication and Examination Issues.

Reference 21 concludes that:

(a) ASME Code Section III did not change the basic considerations in containment design from those contained in Section VIII and Case 1272 N-5, except for the change in the forming tolerance rules. Rules were amplified and clarified. There were detailed changes in requirements without change in concept.
(b) The limits in Section VIII and Case 1272 N-5 were incorporated in Section III, with additional provisions, and the address of local membrane stress limits.

It should be noted that special requirements for jet impingement was introduced in Winter 72 Addenda [21]. The special requirements had been deleted in the 1989 Edition. Instead, guidance is provided in NE-3228.4 for impulse loads in the application of plastic analysis for relaxation of stress limits.

In the treatment of stress limits, although the terminologies used in 1962 Edition Section VIII are different from those used in 1989 Edition Section III, the limits are similar. In Case 1272 N-5 of 1962 Edition Section VIII, the limit on general membrane, local membrane and general bending is 1.5 times the general membrane limit, which is 1.1 times the allowable stress value. In the later Section III Code, the stress allowable is 1.5 S_{mc}.

Table 7-1: Summary of Stress Intensity Limit

TABLE NE-3221-1
SUMMARY OF STRESS INTENSITY LIMITS

	Loading Condition					
Symbol	Design Stress Intensity Limit	Level A Service Stress Intensity Limit	Level B Service Stress Intensity Limit and Level C Service Stress Limit Where the Structure Is Not Integral and Continuous	Level C Service Stress Intensity Limit Where the Structure Is Integral and Continuous, and Level D Service Stress Limit Where the Structure Is Not Integral and Continuous, and at Partial Penetration Welds (1)	Level D Service Stress Intensity Limit Where the Structure Is Integral and Continuous (Elastic Analysis) (2)	Level D Service Stress Intensity Limit Where the Structure is Integral and Continuous (Inelastic Analysis) (2)
P_m	$1.0S_{mo}$	$1.0S_{ma}$	$1.0S_{mc}$	$1.2S_{mc}$ or * $1.0S_y$	S_f	S_f
P_L	$1.5S_{mo}$	$1.5S_{ma}$	$1.5S_{mc}$	$1.8S_{mc}$ or * $1.5S_y$	$1.5S_f$	S_f
$P_L + P_b$ (3)	$1.5S_{mo}$	$1.5S_{ma}$	$1.5S_{mc}$	$1.8S_m$ or * $1.5S_y$	$1.5S_f$	S_f
$P_L + P_b + Q$	N/A (4)	$3.0S_{m2}$	$3.0S_{m2}$ (5)	N/A (4)	N/A (4)	N/A (4)
$P_L + P_b + Q + F$	N/A (4)	S_a	S_a (5)	N/A (4)	N/A (4)	N/A (4)

NOTES:
(1) Limits identified by (*) indicate a choice of the larger of two limits.
(2) S_f is 85% of the general primary membrane allowable permitted in Appendix F. In the application of the rules of Appendix F, S_{m2}, if applicable, shall be as specified in Tables I-1.0.
(3) Values shown are for a solid rectangular section. See NE-3221.3(d) for other than a solid rectangular section.
(4) N/A—No evaluation required.
(5) Evaluation not required for Level C Service.

Table 7-2: Code Allowable Stress Intensities

Material	Allowable Stress Intensities, S_{mc} (ksi)			
	70 °F	100 °F	200 °F	300 °F
SA-516, Grade 70	--	19.3	19.3	19.3
SA-516, Grade 60	--	16.5	16.5	16.5
SA-320, L7[4]	--	27.5	27.5	27.5
USS-T1[1] (SA-514, Grade F)		27.5	27.5	27.5
SA-333, Grade O[2]		15.1	15.1	15.1
SA-333, Grade 1		15.1	15.1	15.1
SA-312, Type 304		18.8	17.8	16.6
SA-276, Type 304[1,3]		18.8	17.8	16.6

Notes:

(1) Stress intensity allowable is based on Appendix III, Article III-3000, Reference 6, using tensile strength of 110 ksi at room temperature.

(2) Stress intensity allowable not available in Reference 28, use the allowable of SA-333, Grade 1

(3) Use the allowable of SA-312, Type 304.

(4) Use the allowable of SA-193 Grade B7.

Table 7-3: Material Strength

Material	Yield Strength S_y (ksi)				Ultimate Strength S_u (ksi)			
	70 °F	**100 °F**	**200 °F**	**300 °F**	**70 °F**	**100 °F**	**200 °F**	**300 °F**
SA-516, Grade 70	38[3]	38	34.6	33.7	70	70	70	70
SA-516, Grade 60	32[3]	32	29.2	28.3	60	60	60	60
SA-320, L7[3]	105[3]	105	98	94.1				
USS-T1 (SA-514, Grade F)	100[2]	(1)	(1)	100[2]				
SA-333, Grade O	(1)	(1)	(1)	(1)	55[4]	(1)	(1)	(1)
SA-333, Grade 1	30.0[3]	30.0	27.3	26.6	55[3]	55	55	55
SA-312, Type 304	30.3[3]	30.3	25.0	22.5	75[3]	75	71	66
SA-276, Type 304[1]	30[2]	(1)	(1)	(1)	(1)	(1)	(1)	(1)

Notes:
(1) Yield strength is not available in Reference 28.
(2) Yield strength is obtained from Reference 22.
(3) Assumed same value at 100 °F.
(4) Assumed same as SA-333, Grade 1.

Table 7-4: Code Allowable Stress Intensities

(a) Service Levels A and B

Matl/Allowable	P_m	P_L	P_L+P_b	P_L+P_b+Q	P_L+P_b+Q+F
	S_{mc}	$1.5S_{mc}$	$1.5S_{mc}$	$3.0S_{ml}$ [1]	S_a
SA-516, Grade 70	19.3	28.95	28.95	57.9	--
SA-516, Grade 60	16.5	24.75	24.75	49.5	--
SA-320, L7	27.5	41.25	41.25	82.5	--
USS-T1 (SA-514, Grade F)	30.25	45.38	45.38	90.75	--
SA-333, Grade O	15.1	22.65	22.65	45.3	--
SA-333, Grade 1	15.1	22.65	22.65	45.3	--
SA-312, Type 304	18.3	27.45	27.45	54.9	--
SA-276, Type 304	18.3	27.45	27.45	54.9	--

Note: 1 S_{ml} is described in note (2) of Figure NE-3231-2 of Reference 28.

(b) Service Level C

Material	P_m			P_L			P_L+P_b		
	$1.2S_{mc}$	$1.0S_y$	(1)	$1.8S_{mc}$	$1.5S_y$	(1)	$1.8S_{mc}$	$1.5S_y$	(1)
SA-516, Grade 70	23.16	36.30	36.30	34.74	54.45	54.45	34.74	54.45	54.45
SA-516, Grade 60	19.80	30.60	30.60	29.70	45.90	45.90	29.70	45.90	45.90
SA-320, L7	33.00	101.50	101.50	49.50	152.25	152.25	49.50	152.25	152.25
USS-T1 (SA-514, Grade F)	36.30	100 [5]	100	54.45	150 [5]	150	54.45	150 [5]	150
SA-333, Grade O	18.12	28.65 [3]	28.65	27.18	42.97 [3]	42.97	27.18	42.97 [3]	42.97
SA-333, Grade 1	18.12	28.65	28.65	27.18	42.97	42.97	27.18	42.97	42.97
SA-312, Type 304	21.96	27.65	27.65	32.94	41.47	41.47	32.94	41.47	41.47
SA-276, Type 304	21.96	27.65 [4]	27.65	32.94	41.47 [4]	41.47	32.94	41.47 [4]	41.47

Notes :
(1) Choice of the larger of two limits.
(2) For P_L+P_b+Q and P_L+P_b+Q+F, evaluation not required for Level C Service.
(3) Assumed same as SA-333, Grade 1.
(4) Assumed same as SA-312, Type 304.
(5) Yield Strength at 100 °F used.

Table 7-4: Code Allowable Stress Intensities (Continued)

(c) Service Level D (from Appendix F of Reference 28)

Matl	P_m			P_L	P_L+P_b
	$2.4S_{mc}$	$0.7S_u$	(1)	$1.5P_m$	$1.5P_m$
SA-516, Grade 70	46.3	49	46.3	69.5	69.5
SA-516, Grade 60	39.6	42	39.6	59.4	59.4
SA-320, L7	66.0	--	66.0	99	99
USS-T1(SA-514, Grade F)	72.6		72.6	108.9	108.9
SA-333, Grade O	36.24	38.5	36.24	54.36	54.36
SA-333, Grade 1	36.24	38.5	36.24	54.36	54.36
SA-312, Type 304	43.92	52.5	43.92	65.88	65.88
SA-276, Type 304	43.92	52.5	43.92	65.88	65.88

Note: (1) lesser of the two limits

Table 7-5: Classification of Stress Category

TABLE NE-3217-1
CLASSIFICATION OF STRESS INTENSITY IN VESSELS FOR SOME TYPICAL CASES[1]

Vessel Component	Location	Origin of Stress	Type of Stress	Classification
Cylindrical or spherical shell	Shell plate remote from discontinuities	Internal pressure	General membrane Gradient through plate thickness	P_m Q
		Axial thermal gradient	Membrane Bending	Q Q
	Junction with head or flange	Internal pressure	Membrane Bending	P_L Q [Note (2)]
Any shell or head	Any section across entire vessel	External load or moment, or internal pressure	General membrane averaged across full section	P_m
		External load or moment	Bending across full section	P_m
	Near nozzle or other opening	External load or moment, or internal pressure	Local membrane Bending Peak (fillet or corner)	P_L Q F
	Any location	Temperature difference between shell and head	Membrane Bending	Q Q
Dished head or conical head	Crown	Internal pressure	Membrane Bending	P_m P_b
	Knuckle or junction to shell	Internal pressure	Membrane Bending	P_L [Note (3)] Q
Flat head	Center region	Internal pressure	Membrane Bending	P_m P_b
	Junction to shell	Internal pressure	Membrane Bending	P_L Q [Note (2)]
Perforated head or shell	Typical ligament in a uniform pattern	Pressure	Membrane (through cross section) Bending (through width of ligament, but gradient through plate) Peak	P_m P_b F
	Isolated or atypical ligament	Pressure	Membrane Bending Peak	Q F F

(Table NE-3217.1 continues on next page)

Table 7-5: Classification of Stress Category (continued)

(NE-3227.5)	reinforcement defined by NB-3334	loads and moments, including those attributable to restrained free end displacements of attached piping	Bending (other than gross structural discontinuity stresses) averaged through nozzle thickness	P_m
	Outside the limits of reinforcement defined by NE-3334	Pressure and external axial, shear, and torsional loads other than those attributable to restrained free end displacements of the attached piping	General membrane stresses	P_m
		Pressure and external loads and moments other than those attributable to restrained free end displacements of the attached piping	Membrane Bending	P_L P_b
		Pressure, and all external loads and moments	Membrane Bending Peak	P_L Q F
	Nozzle wall	Gross structural discontinuities	Local membrane Bending Peak	P_L Q F
		Differential expansion	Membrane Bending Peak	Q Q F
Cladding	Any	Differential expansion	Membrane Bending	F F
Any	Any	Radial temperature distribution [Note (4)]	Equivalent linear stress [Note (5)]	Q
			Nonlinear portion of stress distribution	F
Any	Any	Any	Stress concentration (notch effect)	F

NOTES:
(1) Q and F classifications of stresses refer to other than design condition (Fig. NE-3221-2).
(2) If the bending moment at the edge is required to maintain the bending stress in the middle to within acceptable limits, the edge bending is classified as P_b. Otherwise, it is classified as Q.
(3) Consideration must also be given to the possibility of wrinkling and excessive deformation in vessels with a large diameter–thickness ratio.
(4) Consider possibility of thermal stress ratchet.
(5) Equivalent linear stress is defined as the linear.

Table 7-6: Load Combinations

LC	Level	Conditions	Load Cases
LC1	A	Design/Test	Prs1 + Grvty + OBE + SAM
LC2	A	Design/Test	Prs1 + Grvty – OBE – SAM
LC3	A/B	Normal	Prs2 + Grvty + Mch/Live + OBE + SAM + EPOBE + EPThrm + Thrm2
LC4	A/B	Normal	Prs2 + Grvty + Mch/Live – OBE – SAM – EPOBE + EPThrm + Thrm2
LC5	A/B	Refueling	Prs2 + Grvty + Mch/Live + OBE + SAM + EPOBE + EPThrm + Thrm2 + Refuel
LC6	A/B	Refueling	Prs2 + Grvty + Mch/Live – OBE – SAM – EPOBE + EPThrm + Thrm2 + Refuel
LC9	C	Post-Accident	Prs2 + Grvty + Mch/Live + SSE + SAM(SSE) + EPSSE + Flood
LC10	C	Post-Accident	Prs2 + Grvty + Mch/Live – SSE – SAM(SSE)– EPSSE + Flood

Table 7-7: Code Evaluation, Load Combination LC5, Refueling, Level A/B

Component	P_m	S_{mc}	P_L	P_L+P_b (ksi)		$1.5S_{mc}$	P_L+P_b+Q (ksi)		$3S_{mc}$
	(ksi)	(ksi)	(ksi)	Top	Bot	(ksi)	Top	Bot	(ksi)
Cylindrical Shell	--	19.30	16.10	28.62	28.56	28.95	26.76	27.84	57.9
Stiffeners/Gussets	8.25[2]	19.30	24.76[2]	21.86[1,2]	24.76[1,2]	28.95	33.15	36.30	57.9
StarTruss/Stiffeners	3.28	19.30	26.41	27.47	25.39	28.95	26.71	24.67	57.9
Knuckle	--	19.30	4.17	6.98	4.90	28.95	6.75	4.71	57.9
Spherical Shell	--	19.30	9.97	16.18	11.69	28.95	17.48	11.30	57.9
Upper Beam Seat	--	16.50	7.43	8.98	7.46	24.75	8.77	7.30	49.5
Lower Beam Seat	--	19.30	9.88	14.75	15.38	28.95	14.89	15.39	57.9
Vent Pipe	--	19.30	8.92	9.60	9.18	28.95	9.63	9.02	57.9
Sandbed – Bay 1	--	19.30	10.38	16.99	12.35	28.95	28.67	19.59	57.9
Sandbed – Bay 3	--	19.30	9.94	17.59	12.21	28.95	30.09	19.80	57.9
Sandbed – Bay 5	--	19.30	9.96	15.66	10.48	28.95	29.06	23.14	57.9
Sandbed – Bay 7	--	19.30	10.08	12.67	10.30	28.95	25.49	18.09	57.9
Sandbed – Bay 9	--	19.30	9.20	10.32	10.37	28.95	22.94	16.51	57.9
Sandbed – Bay 11	--	19.30	9.75	9.12	10.88	28.95	20.15	14.76	57.9
Sandbed – Bay 13	--	19.30	10.02	9.74	10.66	28.95	20.79	15.16	57.9
Sandbed – Bay 15	--	19.30	9.71	11.42	10.03	28.95	23.43	16.73	57.9
Sandbed – Bay 17	--	19.30	12.39	14.54	12.39	28.95	26.85	18.45	57.9
Sandbed – Bay 19	--	19.30	11.37	15.98	11.57	28.95	26.50	17.03	57.9
Pen X2A & X2B	--	19.30	6.75	8.97	7.60	28.95	14.66	9.80	57.9
Pen X3A & X3B	--	19.30	9.79	9.79[1]	9.79[1]	28.95	34.98	36.61	57.9
Pen X4A & X4B	--	19.30	5.12	4.98	5.97	28.95	6.82	9.67	57.9
Pen X5A & X5B	--	19.30	10.24	12.01	16.46	28.95	13.46	16.45	57.9
Pen X7	--	19.30	1.91	4.69	5.33	28.95	4.07	4.15	57.9
Pen X8	--	19.30	3.34	5.77	4.59	28.95	8.01	5.43	57.9
Pen X9 & X10	--	19.30	4.19	4.73	4.50	28.95	15.78	11.87	57.9
Pen X12B	--	19.30	4.71	4.93	4.49	28.95	11.10	9.88	57.9
Pen X18	--	19.30	2.72	9.05	6.26	28.95	20.19	13.71	57.9
Pen X63	--	19.30	1.20	2.10	2.54	28.95	18.75	9.61	57.9
Pen X66	--	19.30	4.69	10.15	8.27	28.95	9.99	7.99	57.9
Pen X70	--	19.30	7.12	13.92	9.96	28.95	17.87	12.79	57.9
18" Penetrations	--	19.30	3.58	9.50	6.26	28.95	20.19	13.71	57.9
14" Penetrations	--	19.30	3.45	3.62	3.29	28.95	3.67	3.37	57.9
10" Penetrations	--	19.30	3.82	3.17	4.64	28.95	3.53	4.65	57.9
8" Penetrations	--	19.30	5.25	5.41	6.30	28.95	5.29	6.23	57.9
6" Penetrations	--	19.30	4.79	4.59	5.88	28.95	4.58	5.88	57.9
3" Penetrations	--	19.30	4.36	7.22	6.97	28.95	8.02	7.54	57.9

Notes: (1) Without bending stress at gross structural discontinuity per Section MC, NE-3213.9 [28]
(2) Stress linearization has been used to compute the stresses.

Table 7-8: Code Evaluation, Load Combination LC6, Refueling, Levels A/B

Component	P_m	S_{mc}	P_L	P_L+P_b (ksi)		$1.5S_{mc}$	P_L+P_b+Q (ksi)		$3S_{mc}$
	(ksi)	(ksi)	(ksi)	Top	Bot	(ksi)	Top	Bot	(ksi)
Cylindrical Shell	--	19.30	14.28	14.28[1]	14.28[1]	28.95	53.34	41.59	57.9
Stiffeners/Gussets	6.42	19.30	6.35[2]	15.20[2]	16.97[2]	28.95	53.34	41.59	57.9
Star Truss/Stiffeners	4.50	19.30	21.42[2]	24.95[2]	21.40[2]	28.95	33.28	30.47	57.9
Knuckle	--	19.30	4.43	7.14	5.19	28.95	6.90	5.01	57.9
Spherical Shell	--	19.30	11.97	11.78	13.27	28.95	17.81	13.02	57.9
Upper Beam Seat	--	16.50	7.34	8.82	7.42	24.75	8.61	7.27	49.5
Lower Beam Seat	--	19.30	8.83	15.11	14.28	28.95	15.24	14.13	57.9
Vent Pipe	--	19.30	9.90	10.37	10.24	28.95	10.15	10.17	57.9
Sandbed – Bay 1	--	19.30	8.68	14.93	10.60	28.95	25.51	18.10	57.9
Sandbed – Bay 3	--	19.30	8.03	14.19	10.02	28.95	26.68	17.85	57.9
Sandbed – Bay 5	--	19.30	8.24	11.86	8.12	28.95	25.63	20.29	57.9
Sandbed – Bay 7	--	19.30	9.34	10.74	9.81	28.95	23.88	16.73	57.9
Sandbed – Bay 9	--	19.30	10.23	12.00	11.25	28.95	25.00	17.28	57.9
Sandbed – Bay 11	--	19.30	11.86	12.79	13.02	28.95	24.59	15.81	57.9
Sandbed – Bay 13	--	19.30	12.48	14.15	13.40	28.95	26.14	16.81	57.9
Sandbed – Bay 15	--	19.30	11.37	15.03	12.11	28.95	27.16	17.68	57.9
Sandbed – Bay 17	--	19.30	12.49	15.58	13.09	28.95	28.01	18.42	57.9
Sandbed – Bay 19	--	19.30	9.77	15.26	11.00	28.95	26.87	16.85	57.9
Pen X2A & X2B	--	19.30	6.78	9.07	7.79	28.95	14.77	9.98	57.9
Pen X3A & X3B	--	19.30	8.62	8.62[1]	8.62[1]	28.95	45.24	42.60	57.9
Pen X4A & X4B	--	19.30	5.91	5.59	6.46	28.95	6.45	9.45	57.9
Pen X5A & X5B	--	19.30	7.03	7.60	10.00	28.95	12.11	10.51	57.9
Pen X7	--	19.30	1.60	4.96	5.28	28.95	10.33	9.98	57.9
Pen X8	--	19.30	2.26	3.27	2.38	28.95	10.26	6.43	57.9
Pen X9 & X10	--	19.30	5.61	9.09	8.59	28.95	10.76	8.39	57.9
Pen X12B	--	19.30	5.95	6.48	5.85	28.95	6.83	5.64	57.9
Pen X18	--	19.30	3.47	8.87	8.02	28.95	7.61	4.98	57.9
Pen X63	--	19.30	3.09	11.53	7.11	28.95	28.68	15.32	57.9
Pen X66	--	19.30	3.25	5.85	5.18	28.95	4.83	4.61	57.9
Pen X70	--	19.30	6.02	7.34	7.69	28.95	11.34	9.57	57.9
18" Penetrations	--	19.30	3.47	8.87	8.02	28.95	7.61	6.27	57.9
14" Penetrations	--	19.30	3.63	3.86	3.52	28.95	3.86	3.58	57.9
10" Penetrations	--	19.30	2.59	2.42	2.96	28.95	2.60	3.57	57.9
8" Penetrations	--	19.30	5.66	7.02	6.71	28.95	6.90	6.65	57.9
6" Penetrations	--	19.30	4.70	4.62	5.86	28.95	4.64	5.86	57.9
3" Penetrations	--	19.30	4.80	4.79	5.04	28.95	5.39	5.17	57.9

Notes: (1) Without bending stress at gross structural discontinuity per Section MC, NE-3213.9 [28]
(2) Stress linearization has been used to compute the stresses.

Table 7-9: Code Evaluation, Load Combination LC9, Post-Accident Flooding, Level C

Comp	P_m	S_y	P_L	P_L+P_b (ksi)		$1.5S_y$
	(ksi)	(ksi)	(ksi)	Top	Bottom	(ksi)
Top Head	--	36.30	1.08	1.05	1.17	54.45
Cylindrical Shell	--	36.30	23.83	23.83[1]	23.83[1]	54.45
Stiffeners/Gussets	28.11	36.30	49.80	49.80[1]	49.80[1]	54.45
Star Truss/Stiffeners	5.03	36.30	37.94[2,3]	38.01[2,3]	36.82[2,3]	54.45
Knuckle	--	36.30	12.01	11.42	12.62	54.45
Spherical Shell	--	36.30	37.54	40.37	37.10	54.45
Upper Beam Seat	--	30.60	13.22	18.50	10.57	45.90
Lower Beam Seat	--	36.30	22.16	32.68	27.37	54.45
Vent Pipe	--	36.30	35.08	37.33	32.73	54.45
Sandbed – Bay 1	34.53	36.30	44.03	45.93	46.68	54.45
Sandbed – Bay 3	31.11	36.30	38.71	42.57	40.67	54.45
Sandbed – Bay 5	28.22	36.30	38.41	40.13	43.28	54.45
Sandbed – Bay 7	27.94	36.30	38.84	40.00	37.73	54.45
Sandbed – Bay 9	27.80	36.30	39.00	39.57	38.25	54.45
Sandbed – Bay 11	30.20	36.30	44.60	45.14	44.01	54.45
Sandbed – Bay 13	29.78	36.30	44.04	44.52	43.62	54.45
Sandbed – Bay 15	32.52	36.30	39.63	40.47	38.85	54.45
Sandbed – Bay 17	22.86	36.30	49.15	50.65	50.27	54.45
Sandbed – Bay 19	31.71	36.30	48.34	49.95	47.13	54.45
Pen X2A & X2B	--	36.30	22.26	21.65	22.97	54.45
Pen X3A & X3B	--	36.30	12.62	12.62[1]	12.62[1]	54.45
Pen X4A & X4B	--	36.30	16.95	17.02	16.94	54.45
Pen X5A & X5B	--	36.30	7.35	10.90	11.99	54.45
Pen X7	--	36.30	7.14	10.39	14.21	54.45
Pen X8	--	36.30	10.12	10.29	10.79	54.45
Pen X9 & X10	--	36.30	11.70	12.05	11.69	54.45
Pen X12B	--	36.30	8.82	10.77	13.21	54.45
Pen X18	--	36.30	3.96	12.21	9.79	54.45
Pen X63	--	36.30	5.87	8.45	6.35	54.45
Pen X66	--	36.30	13.39	15.45	22.10	54.45
Pen X70	--	36.30	9.78	16.59	16.83	54.45
18" Penetrations	--	36.30	16.12	14.61	19.68	54.45
14" Penetrations	--	36.30	11.88	12.42	11.34	54.45
10" Penetrations	--	36.30	15.41	14.70	16.75	54.45
8" Penetrations	--	36.30	14.52	12.92	17.96	54.45
6" Penetrations	--	36.30	9.91	9.94	13.10	54.45
3" Penetrations	--	36.30	16.93	16.50	17.43	54.45

Notes: (1) Without bending stress at gross structural discontinuity per Section MC, NE-3213.9 [28]
(2) Stress linearization has been used to compute the stresses.
(3) Shell / solid model stress reduction factor of 0.63 is applied to compute the stresses.

Table 7-10: Code Evaluation, Load Combination LC10, Post Accident Flooding

Comp	P_m	S_y	P_L	P_L+P_b (ksi)		$1.5S_y$
	(ksi)	(ksi)	(ksi)	Top	Bottom	(ksi)
Top Head	--	36.30	0.88	1.31	1.20	54.45
Cylindrical Shell	--	36.30	23.71	23.71[(1)]	23.71[(1)]	54.45
Stiffeners/Gussets	21.16	36.30	49.21	49.21[(1)]	49.21[(1)]	54.45
Star Truss/Stiffeners	6.33	36.30	45.50[(2,3)]	47.55[(2,3)]	44.47[(2,3)]	54.45
Knuckle	--	36.30	11.22	13.51	11.91	54.45
Spherical Shell	--	36.30	39.91	40.19	41.84	54.45
Upper Beam Seat	--	30.60	11.49	12.91	14.11	45.90
Lower Beam Seat	--	36.30	20.59	31.69	26.11	54.45
Vent Pipe	--	36.30	35.82	37.80	34.44	54.45
Sandbed – Bay 1	31.86	36.30	43.99	43.99[(1)]	45.12	54.45
Sandbed – Bay 3	--	36.30	35.33	35.33[(1)]	39.42	54.45
Sandbed – Bay 5	25.32	36.30	36.68	36.68[(1)]	35.64	54.45
Sandbed – Bay 7	26.62	36.30	39.67	39.67[(1)]	39.12	54.45
Sandbed – Bay 9	28.20	36.30	42.27	42.27[(1)]	42.03	54.45
Sandbed – Bay 11	32.76	36.30	48.56	48.56[(1)]	48.11	54.45
Sandbed – Bay 13	32.77	36.30	47.34	47.34[(1)]	46.65	54.45
Sandbed – Bay 15	29.51	36.30	40.99	40.99[(1)]	42.58	54.45
Sandbed – Bay 17	35.42	36.30	50.06	50.06[(1)]	52.63	54.45
Sandbed – Bay 19	33.70	36.30	42.35	42.35[(1)]	42.95	54.45
Pen X2A & X2B	--	36.30	20.86	19.72	22.42	54.45
Pen X3A & X3B	--	36.30	13.64	13.64[(1)]	13.64[(1)]	54.45
Pen X4A & X4B	--	36.30	18.64	17.95	19.31	54.45
Pen X5A & X5B	--	36.30	6.72	9.93	14.61	54.45
Pen X7	--	36.30	7.42	9.93	9.41	54.45
Pen X8	--	36.30	8.07	9.04	8.85	54.45
Pen X9 & X10	--	36.30	9.02	13.78	10.68	54.45
Pen X12B	--	36.30	11.26	15.56	11.49	54.45
Pen X18	--	36.30	4.50	13.30	11.82	54.45
Pen X63	--	36.30	7.05	18.21	10.13	54.45
Pen X66	--	36.30	9.21	11.30	13.55	54.45
Pen X70	--	36.30	7.99	9.19	11.21	54.45
18" Penetrations	--	36.30	15.61	16.57	19.06	54.45
14" Penetrations	--	36.30	12.36	12.87	11.89	54.45
10" Penetrations	--	36.30	10.45	9.42	11.98	54.45
8" Penetrations	--	36.30	10.99	13.63	14.06	54.45
6" Penetrations	--	36.30	10.43	10.67	10.35	54.45
3" Penetrations	--	36.30	16.53	15.80	17.57	54.45

Notes: (1) Without bending stress at gross structural discontinuity per Section MC, NE-3213.9 [28]
(2) Stress linearization has been used to compute the stresses.
(3) Shell / solid model stress reduction factor of 0.63 is applied to compute the stresses.

Table 7-11: Conditions Stipulated for not Requiring Analysis for Cyclic Service per ASME Code Subparagraph NE-3221.5

Criteria		A212 Gr B	A 201 Gr B	A333 Gr O	T1	Type 304
NE-3221.5 (d) (1)	Allowable atmospheric-to-service pressure cycles	2,752	4,533	6,055	855	21,130
NE-3221.5 (d) (2)	Allowable normal service pressure fluctuation	118 psi	138 psi	151 psi	72 psi	161 psi
NE-3221.5 (d) (3)	Allowable temperature difference – start up and shutdown	467 °F	451 °F	405 °F	322 °F	416 °F
NE-3221.5 (d) (4)	Allowable temperature difference – similar material	467 °F	451 °F	405 °F	322 °F	416 °F
NE-3221.5 (d) (5)	Allowable temperature difference – dissimilar material with A201 Gr B	12,926 °F	--	--	--	--
	Allowable temperature difference – dissimilar material with A333 Gr O	3,075 °F	--	--	--	--
	Allowable temperature difference – dissimilar material with T1	1,769 °F	--	--	--	--
	Allowable temperature difference – dissimilar material with Type 304	1,323 °F	--	--	--	--
NE-3221.5 (d) (6)	Allowable stress intensity from mechanical loads	155 ksi	155 ksi	135 ksi	201 ksi	201 ksi

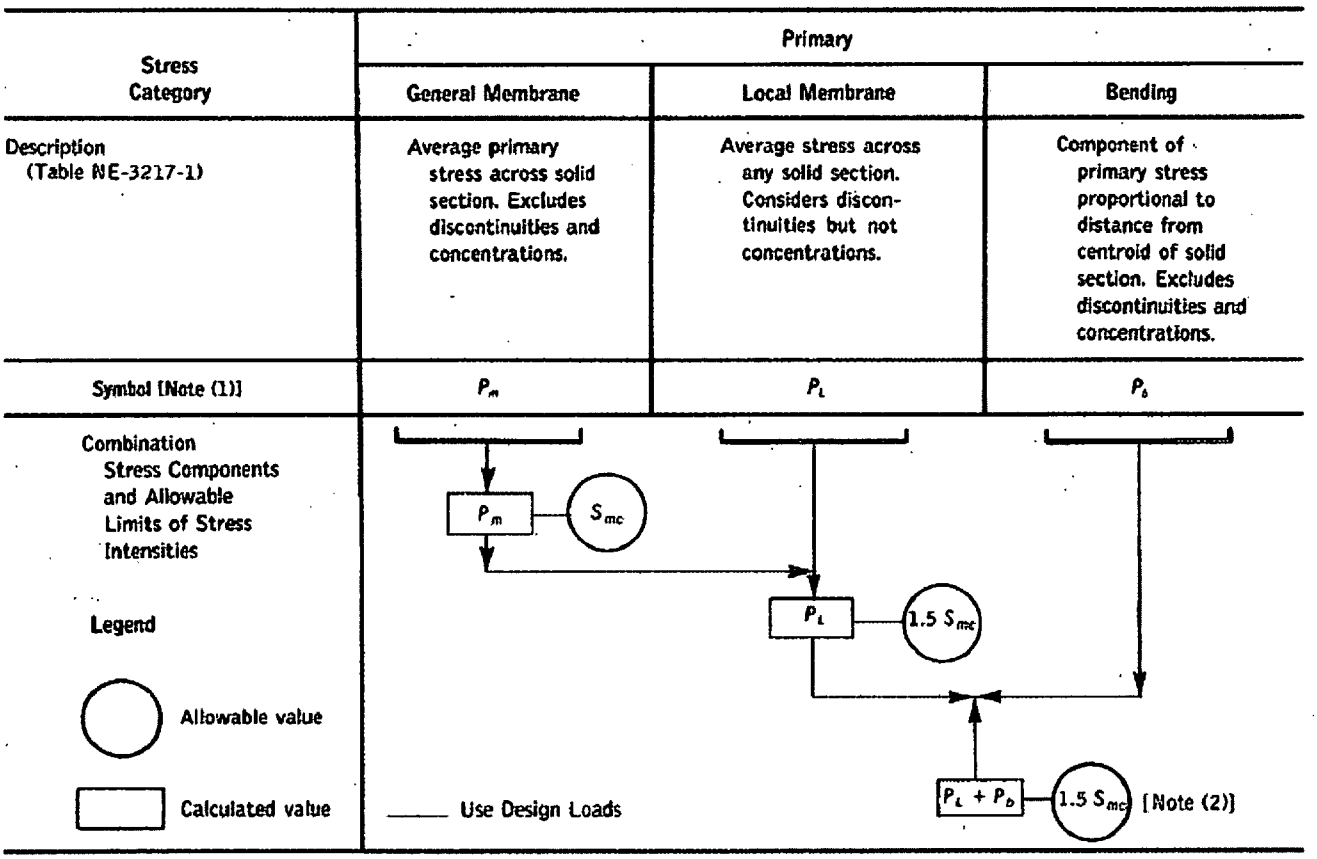

NOTES:

(1) The symbols P_m, P_L, and P_b do not represent single quantities, but rather sets of six quantities representing the six stress components σ_t, σ_s, σ_r, τ_{ts}, τ_{tr}, and τ_{rs}.

(2) Value shown is for a solid rectangular section. See NE-3221.3(d) for other than a solid rectangular section.

FIG. NE-3221-1 STRESS CATEGORIES AND LIMITS OF STRESS INTENSITY FOR DESIGN CONDITIONS

Figure 7-1: Stress Intensity Limits for Design Conditions

Stress	Primary			Secondary	Peak
	General Membrane	Local Membrane	Bending	Membrane Plus Bending	
Description (Table NE-3217-1)	Average primary stress across solid section. Excludes effects of discontinuities and concentrations.	Average stress across any solid section. Considers effects of discontinuities but not concentrations.	Component of primary stress proportional to distance from centroid of solid section. Excludes effects of discontinuities and concentrations.	Self-equilibrating stress necessary to satisfy continuity of structure. Occurs at structural discontinuities. Excludes local stress concentrations.	(1) Increment added to primary or secondary stress by a concentration (notch). (2) Certain thermal stresses which may cause fatigue but not distortion.
Symbol [Note (1)]	P_m	P_L	P_b	Q	F
Combination of stress components and allowable limits of stress intensities					

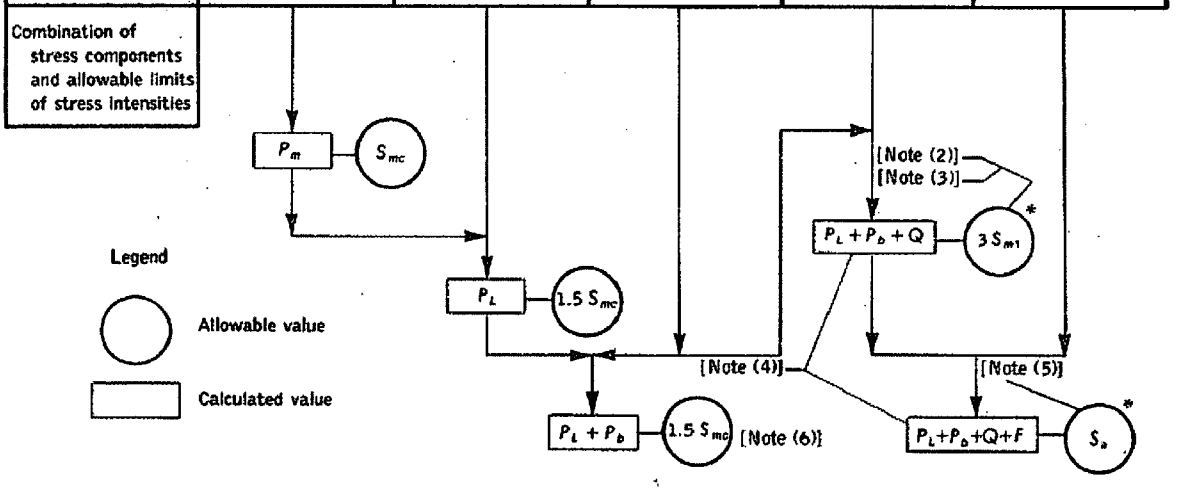

NOTES:

(1) The symbols P_m, P_L, Q, and F do not represent single quantities, but sets of six quantities representing the six stress components σ_t, σ_l, σ_r, τ_{tl}, τ_{lr}, and τ_{rt}.

(2) When the secondary stress is due to a temperature transient at the point at which the stresses are being analyzed, the value of S_{m1} shall be taken as the average of the tabulated S_{m1} values for the highest and the lowest temperatures of the metal during the transient. When part or all of the secondary stress is due to mechanical load, the value of S_{m1} shall not exceed the value for the highest temperature of metal during the transient.

(3) Special rules for exceeding 3 S_{m1} are provided in NE-3228.3.

(4) The stresses in category Q are those parts of the total stress that are produced by thermal gradients, structural discontinuities, and they do not include the primary stresses that may also exist at the same point. However, it should be noted that a detailed stress analysis frequently gives the combination of primary and secondary stresses directly and, when appropriate, the calculated value represents the total of $P_m + P_b + Q$ and not Q alone. Similarly, if the stress in category F is produced by a stress concentration, the quantity F is the additional stress produced by the notch over and above the nominal stress. For example, if a point has a nominal stress intensity P_m and has a notch with a stress concentration factor K, then $P_m \leq S_{m1}$, $P_b = Q$, $Q = 0$, $F = P_m(K\text{-}1)$, and the peak stress intensity equals $P_m + P_m(K\text{-}1) = KP_m$. However, P_L is the total membrane stress that results from mechanical loads, including discontinuity effects, rather than a stress increment. Therefore, the P_L value always includes the P_m contribution.

(5) S_a is obtained from the fatigue curves, Figs. 1-9.0. The allowable stress intensity for the full range of fluctuations is $2S_a$.

(6) Value shown is for a solid rectangular section. See NE-3221.3(d) for other than a solid rectangular section.

* Evaluation not required for level C Service limits.

FIG. NE-3221-2 STRESS CATEGORIES AND LIMITS OF STRESS INTENSITY FOR LEVEL A AND B SERVICE LIMITS; AND FOR LEVEL C SERVICE LIMITS WHERE THE STRUCTURE IS NOT INTEGRAL AND CONTINUOUS

Figure 7-2: Stress Intensity Limits for Levels A and B

Stress Category		Primary	
	General Membrane	Local Membrane	Bending
Description (Table NE-3217-1)	Average primary stress across solid section. Excludes effects of discontinuities and concentrations.	Average stress across any solid section. Considers effects of discontinuities but not concentrations.	Component of primary stress proportional to distance from centroid of solid section. Excludes effects of discontinuities and concentrations.
Symbol (Note (1))	P_m	P_L	P_b
Combination of stress components and allowable limits of stress intensities.			

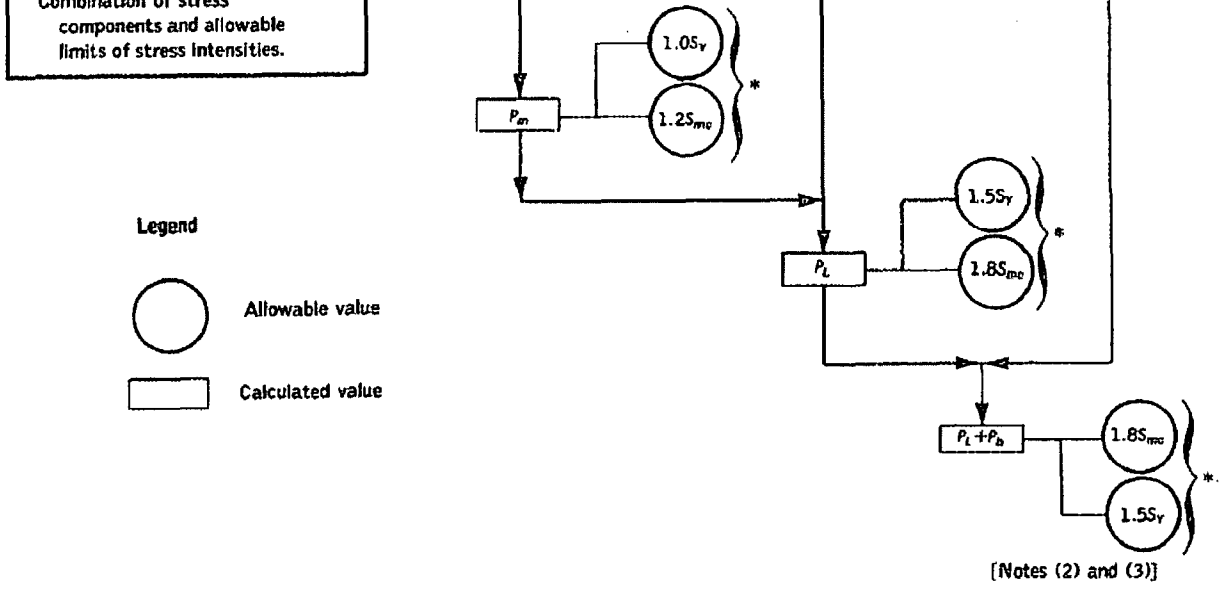

NOTES:
(1) The symbols P_m, P_L, and P_b do not represent single quantities, but sets of six quantities representing the six stress components σ_x, σ_y, σ_z, τ_{xy}, τ_{yz}, τ_{zx}.
(2) Values shown are for a solid rectangular section. See NE-3221.3(d) for other than a solid rectangular section.
(3) Values shown are applicable when $P_L \leq 0.67 S_y$. When $P_L > 0.67 S_y$, use the larger of the two limits,

$$[2.5 - 1.5 (P_L / S_y)] 1.2 S_{mc}$$

or

$$[2.5 - 1.5 (P_L / S_y)] S_y$$

*Use greater of values specified

FIG. NE-3221-3 STRESS CATEGORIES AND LIMITS OF STRESS INTENSITY FOR LEVEL C SERVICE LIMITS WHERE THE STRUCTURE IS INTEGRAL AND CONTINUOUS; AND FOR LEVEL D SERVICE LIMITS WHERE THE STRUCTURE IS NOT INTEGRAL AND CONTINUOUS, AND AT PARTIAL PENETRATION WELDS

Figure 7-3: Stress Intensity Limits for Level C

Stress Category		Primary	
	General Membrane	Local Membrane	Bending
Description (Table NE-3217-1)	Average primary stress across solid section. Excludes effects of discontinuities and concentrations.	Average stress across any solid section. Considers effects of discontinuities but not concentrations.	Component of primary stress proportional to distance from centroid of solid section. Excludes effects of discontinuities and concentrations.
Symbol (Note (1))	P_m	P_L	P_b
Combination of stress components and allowable limits of stress intensities.			

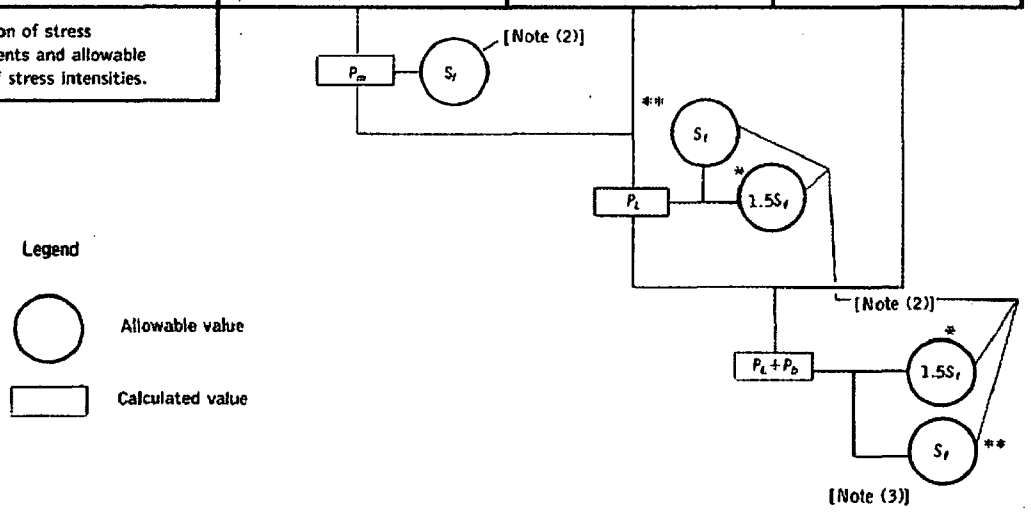

NOTES:
(1) The symbols P_m, P_L, and P_b do not represent single quantities, but sets of six quantities representing the six stress components σ_t, σ_l, σ_r, τ_{tl}, τ_{tr}, τ_{lr}.
(2) S_f is 85% of the general membrane allowable permitted in Appendix F. In the application of the rules of Appendix F, S_{m3}, if applicable, shall be as specified in Tables I-1.0.
(3) Values shown are for a solid rectangular section. See NE-3221.3(d) for other than a solid rectangular section.

* Elastic analysis
** Inelastic analysis

FIG. NE-3221-4 STRESS CATEGORIES AND LIMITS OF STRESS INTENSITY FOR LEVEL D SERVICE LIMITS WHERE THE STRUCTURE IS INTEGRAL AND CONTINUOUS

Figure 7-4: Stress Intensity for Level D

8.0 BUCKLING EVALUATION

This section contains the discussion of the buckling evaluation of the drywell steel containment. The buckling evaluation of elastic instability was performed for the drywell based on the rules outlined in Section III of the ASME Code for Class MC Components.

8.1 ASME Buckling Rules

The buckling and compressive allowables are given in NE-3222 of Reference 28.

The alternative to the requirements of the ASME Code Section III NE-3222 for determining allowable compressive stresses is ASME Code Case N-284-1 [24]. The buckling capacity of the shell is based on bifurcation analyses reduced by capacity reduction factors which account for:

1) The effect of imperfections and nonlinearity in geometry and boundary conditions.
2) The plasticity reduction factors which account for nonlinearity in material properties.

The basic compressive allowable stress values referred to by ASME Code Section III NE-3222.1 will correspond to a factor of safety of two in Code Case N-284-1. This factor is applied to the buckling stress values that are determined by classical analysis and reduced by appropriate capacity factors. The stability stress limits referred to by NE-3222.2 will correspond to the following factor of safety (FS):

(a) For Design Conditions and Level A and B Service Limits, FS = 2.0
(b) For Level C Service Limits, the allowable stress values are 120% of the values of (a); FS = 1.67.
(c) For Level D Service Limits, the allowable stress values are 150% of the values of (a); FS = 1.34.

The reduction in buckling capacity due to imperfections and nonlinearity in geometry and boundary conditions is provided through the use of capacity reduction factors, α_{ij}, where $i = \phi$,

θ, or ϕθ corresponding to the meridional direction or stress component, circumferential direction or stress component, and in-plane shear stress component, respectively, j = L, S, G corresponding to local buckling (buckling of shell plate between stiffeners or boundaries), stringer buckling (buckling between rings of shell plate and attached meridional stiffeners, and general instability (overall collapse), respectively.

8.2 Methodology

A theoretical buckling stress, σ_{ie}, is determined for the drywell by eigenvalue buckling finite element analysis for a given load case. For each eigenvalue, the analysis provides the buckling (or displacement) mode and a corresponding load factor, λ. This load factor identifies the theoretical buckling stress in that given load case that would cause buckling in the drywell, for the particular buckling mode. Therefore, if the stress in the buckling region is σ_c, the theoretical buckling stress is:

$$\sigma_{ie} = \lambda \sigma_c \tag{8-1}$$

Accounting for the imperfection and nonlinearity in geometry and boundary conditions, the allowable buckling stress, σ_{ca}, is given as:

$$\sigma_{ca} = \propto_{ij} \sigma_{ie} / FS = \alpha_{ij} \lambda \sigma_c / FS \tag{8-2}$$

where α_{ij} = capacity reduction factor to account for imperfection, where i refers to direction or stress component and j refers to buckling modes
FS = safety factor

The capacity reduction factor, α_{ij} in Equation (8-2), will be written as α for simplicity.

If the elastic buckling stress exceeds the elastic limit of the material, a plasticity reduction factor, η_i, can be used to account for non-linear material behavior. Equation (8-2) can be rewritten as:

$$\sigma_{ca} = \eta_i \alpha \ \lambda \sigma_c / FS \tag{8-3}$$

8.3 Capacity Reduction Factor

8.3.1 Spherical Shell

The capacity reduction factor α, is for either uniaxial compression or biaxial compressive stress in the spherical shell. If the buckling region is under compression in the axial direction and tension in the hoop direction, a modified capacity reduction factor, α_m, can be used. Equation (8-3) is modified to use a modified capacity factor to account for the tension in the hoop direction [23]:

$$\sigma_{ca} = \eta_i \alpha_m \lambda \sigma_c / FS \tag{8-4}$$

$$\text{where } \alpha_m = \alpha_{1L} + \alpha_p \tag{8-5}$$

$$\alpha_{1L} = \frac{\alpha_{2L}}{0.6} \tag{8-6}$$

α_{1L} = capacity reduction factor for a sphere under uniaxial compression [4]

α_{2L} = capacity reduction factor for a sphere under equal biaxial compression (8-7)

α_p = capacity reduction factor due to the effect of tensile stress in the orthogonal direction

$$= \frac{1.752}{3.24 + \frac{1}{\bar{p}}} \tag{8-8}$$

where $\bar{p} = \frac{\sigma_h}{E}\frac{R}{t}$ (8-9)

and R = shell radius
t = shell wall thickness
E = shell Young's modulus
σ_h = shell tensile hoop stress

8.3.2 Cylindrical Shell

For cylindrical shells under axial compression, the capacitor reduction factor can be calculated using Code Case 284-1 [24]. Per paragraph -1511 of Reference 24, the local buckling in the meridional direction can be calculated due to the effect of R/t and length as follows:

(a) Effect of R/t

$\alpha = 0.207$ for $R/t \geq 600$ (8-9a)

For $R/t < 600$, use smaller value of

$\alpha = 1.52 - 0.473 * \log_{10}(R/t)$ (8-9b)

$\alpha = 300\ \sigma_y / E - 0.033$ (8-9c)

(b) Effect of length

$\alpha = 0.627$ if $M < 1.5$ (8-10a)

$\alpha = 0.837 - 0.14M$ if $1.5 \le M < 1.73$ (8-10b)

$\alpha = 0.826/(M^{0.6})$ if $1.73 \le M < 10$ (8-10c)

$\alpha = 0.207$ if $M \ge 10$ (8-10d)

where

M = smaller value of $l_i/\sqrt{(Rt)}$ or $l_{si}/\sqrt{(Rt)}$

l_i = distance in meridional or circumferential direction between lines of support

l_{si} = one half of the sum of the distance l_i on either side of an intermediate size stiffener.

It is easily shown from Equation (8-3) that when there is no plasticity reduction factor (i.e. when the stress is below material yield strength or $\eta_i = 1$) and for the buckling stress σ_c is equal to the allowable buckling stress σ_{ca}, $\alpha\lambda$ is equal to the factor of safety. That is, the factor of safety, FS can be simply calculated by multiplying the capacity reduction factor α, to the load factor λ from the eigenvalue buckling analysis.

8.4 Plasticity Reduction Factor

Per Reference 24, when the product of the buckling stresses and the capacity reduction factor, i.e., $\alpha\lambda\sigma_c$, exceeds the proportional limit of the fabricated material, plasticity reduction factors, η_i, is used to account for the non-linear material properties.

Per References 24, the plasticity reduction factors, η_i, for either cylindrical or spherical shell under axial compression is given as:

$\eta_i = 1.0$ if $\Delta \le 0.55$ (8-11)

$\eta_i = \frac{0.45}{\Delta} + 0.18$ if $0.55 < \Delta \le 1.6$

$\eta_i = \frac{1.31}{1 + 1.15\Delta}$ if $1.6 < \Delta < 6.25$

$\eta_i = \frac{1}{\Delta}$ if $\Delta \ge 6.25$

where $\Delta = \alpha\lambda\sigma_c/\sigma_y$

8.5 Buckling Load Cases

Sections 6.0 and 7.0 discuss the stress evaluation of the drywell for different load conditions and load combinations. The buckling evaluation is impacted by cases where the stress condition is compressive. Thus, for the buckling evaluation, the number of load cases can be reduced significantly to those that produce compressive loads in the shell. Further, for purposes of this evaluation, since the primary area of concern is the sandbed region, the load cases of concern are those that produce compressive stresses in the sandbed region. It should be noted that the previous evaluations performed [1, 2] focused on the buckling capabilities in the sandbed region as it was generally concluded that the thinning in the sandbed region would potentially cause reduction of buckling capability in those regions only. However, the finite element modeling will also identify any buckling issues throughout the drywell shell for the load cases considered. Thus the impact on the buckling margin (general wall thinning at other regions) will also be part of the evaluation.

8.5.1 Limiting Cases

For the normal operating condition, the limiting condition is the refueling condition. During the refueling condition, the fuel pool is full of water which imposes a compressive load on the drywell shell.

For the emergency condition, the limiting condition is the post-accident condition. For this condition, the drywell is flooded (internally) with water.

For each of the evaluated load cases, the loads include the gravity loads and the compressive loads along the longitudinal axis of the drywell, and the external or hydrostatic pressure.

8.6 Analysis

The model used in the stress analysis is used in the buckling evaluation with one modification: Instead of using a seismic response spectrum, the seismic loads are simulated with a static seismic analysis using the g values from the response spectrum at the significant mode. This modification is necessary since a response spectrum analysis cannot be analyzed together with the buckling analysis.

A bifurcated (eigenvalue) buckling is performed for the two loading cases described in the previous section. The boundary conditions used in the buckling analyses are similar to the structural displacement used in stress analyses.

A total of 200 buckling modes were analyzed for both load cases.

The analyses were performed using ANSYS 11.0 [25].

8.7 Results

8.7.1 Capacity Reduction Factor

Using Equations 8-4, 8-10 and Figure 8-1, the capacity reduction factors under uniaxial compression for different components or regions of the drywell were calculated. The results are presented in Table 8-1. The identification of individual bays is shown in Figure 8-2.

In calculating the M factor in Equation 8-10 for the cylindrical shell or in Figure 8-1 for the spherical shell, the length l is taken as the distance between the horizontal stiffeners, concrete floor or knuckle. For the cylindrical shell, the longest distance is between the lower star truss stiffeners (elevation ~ 80') and the top of the knuckle (elevation ~ 72'). The distance is approximately 96 inches. For the upper spherical shell, the longest distance between supports is from the bottom of the knuckle (elevation ~62') to the top of upper beam seat (elevation ~ 49'). This distance is approximately 156 inches. For the middle and lower spherical shell, the longest

distance between supports is from the bottom of the upper beam seat (elevation ~ 44') to the concrete floor elevation (~ 11') for a distance of 396 inches.

It is shown that for the cylindrical shell, the capacity reduction factor is 0.330. For the spherical shell, the capacity reduction factors are 0.362, 0.207 and 0.244 for the upper, middle and lower portion of the spherical shell. In the sandbed regions, outside the locally thinned areas, the capacity reduction factors are 0.220, 0.245 and 0.230 for minimum, maximum and average. In the locally thinned areas, the minimum capacity reduction factor is 0.207.

8.7.2 Buckling Mode and Load Factor

A total of 200 eigenvalue buckling modes were computed for both the refueling case and the flooding case.

To identify the buckling mode for each region, the mode shape for each buckling mode is inspected for any visible sign of displacement. The visual inspection begins from the first mode to the last mode. The first identified mode is used as the buckling mode for that region. The load factor associated with the identified mode is used as the eigenvalue buckling load factor for the region.

The first identified buckling modes and the load factors are provided in Table 8-2 for the refueling case and the flooding case.

In addition, the displacements for all the buckling modes are post-processed to obtain the maximum displacement for each region and each mode. These maximum displacements are provided in Table 8-2 and Table 8-3, for the refueling case and the flooding case, respectively. The maximum displacements are used as a check to validate the visual identification of the buckling mode.

8.7.2.1 Refueling Case

A summary of the buckling mode and the corresponding load factor for all the regions is provided in Table 8-4. The lowest buckling mode for the refueling load case is in the cylindrical portion of the drywell. It is in the area of first quadrant, between the star truss and the knuckle region. It has the lowest load factor of 7.229.

In the spherical portion of the drywell, the lowest buckling mode occurs in the region between the upper beam seat and the knuckle region near the 90° azimuth. It has a load factor of 9.800.

The load factor for the buckling mode in the sandbed region is 11.584. This buckling mode is not obvious, but is confirmed by the next buckling mode in the sandbed region. This buckling load factor of 11.584 is used for all sandbed regions.

Among the three major components: cylindrical shell, spherical shell and sandbed, the cylindrical shell has the lowest load factor, even though the locally thinned areas are in the sandbed. This is because for the refueling load case, the loads are concentrated at the top of the cylindrical portion of the drywell, with the head removed. Thus, the closest and most likely buckling location would be at the junction between the cylindrical portion and the knuckle portion of the drywell.

8.7.2.2 Flooding Case

For the flooding case, the first 10 modes are associated with the vent header and downcomers. The load factor for the buckling mode in the sandbed is 7.162.

The buckling mode in the cylindrical portion of the drywell is very similar to those in the refueling case. It is mainly in the region between the knuckle and the star truss, in the first quadrant.

The first buckling mode for the spherical region is associated with the lower portion of the sphere, and the load factor is 7.344.

For the flooding case, there is no bifurcation failure in the upper and middle spherical shell in the first 200 eigenvalue buckling modes. For the buckling evaluations of these two regions, the load factor of 14.704 associated with buckling mode 200 is conservatively used.

8.8 Buckling Stress and Safety Factor

8.8.1 Refueling Case

The buckling stresses in the cylindrical portion of the drywell are shown in Figure 8-3. It is shown in the buckled region, the axial (meridional) stress (S_z) is all compressive with the maximum of 3.41 ksi at the penetration. The hoop stress (S_y) in the buckled region is also compressive. Per Reference 6, Article -1730, it is conservative to assume that there is no interaction between meridional and hoop compression.

To reduce the conservatism in this evaluation, the tensile hoop stress in the orthogonal direction was used in evaluating the safety factor. The presence of tensile hoop stress has the effect of increasing the capacity reduction factor [23], which results in the increase of the buckling safety factor.

The buckling stresses in the upper, middle, and lower spherical portions of the drywell are shown in Figure 8-4, Figure 8-5, and Figure 8-6, respectively. In the buckling region, the corresponding maximum compressive meridional stresses are 3.91 ksi, 4.78 ksi, and 4.52 ksi.

The buckling stresses in the sandbed region of the drywell are shown in Figure 8-7. The maximum compressive meridional stress for the entire sandbed region is 5.51 ksi. In the same region, the hoop stress is about 4.60 ksi tension.

The buckling stress plots for the Bay 1 through Bay 19 in the sandbed region are provided in Figure 8-8 through Figure 8-17, respectively. The maximum axial and hoop stresses for the individual sandbed bays are provided in Table 8-7.

With the above stresses, the appropriate capacity reduction factors (Section 8.7.1), the load factors (Section 8.7.2), and the safety factors for buckling are calculated using the equations in Section 8.2. The results are summarized in Table 8-5 for the cylinder, upper / middle / lower spherical regions, and the safety factors for individual bays of the sandbed region are provided in Table 8-7.

For the cylindrical portion of the drywell, the safety factor is 3.39. In the upper / middle / lower spherical shell regions, the safety factors are 4.27 / 3.60 / 3.60, respectively.

It should be noted that when calculating the capacity reduction factor for the cylinder, Miller's approach for the capacity reduction factor for a sphere was used [23]. This is based on the tests showing that internal pressure (i.e. tensile hoop stress) increases the axial buckling stress as long as the failure stress remains elastic. Table 8-7 presents the safety factors for individual bays in the sandbed region. The lowest safety factor is 3.54 for Bay 3.

The safety factors at the three regions of the drywell are larger than the ASME Code required safety factor of 2.00 for Level A/B service conditions.

8.8.2 Flooding Case

The plots of the buckling stresses for the flooding case are provided in Figure 8-18 through Figure 8-22, for the cylindrical region, upper / middle / lower spherical regions, and the sandbed region, respectively. Detailed buckling stress plots for the individual sandbed bays are provided in Figure 8-23 through Figure 8-32.

The results of the buckling safety factor evaluations are presented in Table 8-6 and Table 8-8. Table 8-6 provides the safety factor evaluation summary for the cylindrical region, upper /

middle / lower spherical regions. Table 8-8 presents the safety factors for individual bays in the sandbed region.

With reference to Table 8-6, the buckling safety factors for the cylindrical region and upper / middle / lower spherical regions are 3.46, 7.57, 4.76 and 2.22, respectively. The smallest buckling safety factor for an individual bay in the sandbed region is 2.02, for Bay 19, as shown in Table 8-8.

These safety factors are larger than the Code required safety factor of 1.67 for Level C service condition, and significantly exceed the required safety factor of 1.34 for Level D service condition.

8.9 Discussions and Conclusions

The effect of locally thinned areas in the sandbed region on the drywell buckling was evaluated. Per References 24 and 28, the required safety factor for buckling is 2.0 for Level A/B and 1.67 for Level C. The buckling evaluation was performed for two service loading conditions: refueling (Level A/B) and post-accident flooding (Level C). The eigenvalue (bifurcation) buckling approach was used. The evaluation examined the buckling safety factor for three main regions of the drywell, cylindrical portion, spherical portion and the sandbed region. The procedures follow the requirements of Code Case 284-1 [24] with guidelines from References 23 and 26 to account for the effect of tensile hoop stress in a spherical shell on the capacity reduction factor and the revised equations for the plasticity reduction factor.

The capacity reduction factor is 0.330, 0.362 / 0.207 / 0.244, and 0.207 in the cylindrical, upper / middle / lower spherical and sandbed regions of the drywell, respectively. The sandbed region's capacity reduction factor was conservatively based on the thinnest wall thickness among the locally thinned areas and the general area in any bay.

Table 8-9 summarizes the buckling safety factors for the different regions of the drywell.

For the refueling case, the minimum safety factor calculated is 3.39, which is associated with the cylindrical region. The minimum safety factor for the spherical region is 3.60. The minimum safety factor for the sandbed region is 3.54 in Bay 3. All these safety factors satisfy the Service Level A and B minimum required safety factor of 2.0.

For the post-accident flooding case, the minimum safety factor for the sandbed region is 2.02 in Bay 19. The minimum safety factor for the spherical and the cylindrical regions are 2.22 and 3.46, respectively. All these safety factors satisfy the licensed Service Level C and D minimum required safety factors of 1.67 and 1.34, respectively.

In conclusion, the eigenvalue buckling analyses show that the computed safety factors satisfy the ASME Code limits.

Table 8-1: Capacity Reduction Factor Under Uniaxial Compression

Region		R (in)	t (in)	l (in)	M	R/t	α/α_{1L}
Cylindrical		198	0.604	96	8.78	327.81	0.330
Spherical	Upper	420	0.676	156	9.26	---	0.362
	Middle	420	0.678	396	23.47	---	0.207
	Lower	420	1.160	396	17.94	---	0.244
Bay 1	Above 11'	420	0.826	396	21.26	---	0.220
	Below 11'	420	0.826	396	21.26	---	0.220
Bay 3	Above 11'	420	1.180	396	17.79	---	0.245
	Below 11'	420	0.950	396	19.82	---	0.229
Bay 5	Above 11'	420	1.185	396	17.75	---	0.245
	Below 11'	420	1.074	396	18.65	---	0.238
Bay 7	Above 11'	420	1.133	396	18.15	---	0.242
	Below 11'	420	1.034	396	19.00	---	0.235
Bay 9	Above 11'	420	1.074	396	18.65	---	0.238
	Below 11'	420	0.993	396	19.39	---	0.232
Bay 11	Above 11'	420	0.860	396	20.84	---	0.223
	Below 11'	420	0.860	396	20.84	---	0.223
Bay 13	Above 11'	420	0.907	396	20.29	---	0.226
	Below 11'	420	0.907	396	20.29	---	0.226
Bay 15	Above 11'	420	1.062	396	18.75	---	0.237
	Below 11'	420	0.935	396	19.98	---	0.228
Bay 17	Above 11'	420	0.863	396	20.80	---	0.223
	Below 11'	420	0.963	396	19.69	---	0.230
Bay 19	Above 11'	420	0.826	396	21.26	---	0.220
	Below 11'	420	0.826	396	21.26	---	0.220
Bay 1	Local (1)	420	0.696	396	23.16	---	0.209
Bay 13	Local (1)	420	0.658	396	23.82	---	0.207
Bay 15	Local (1)	420	0.711	396	22.92	---	0.210
Bay 17	Local (1)	420	0.663	396	23.73	---	0.207
	Local (1)	420	0.850	396	20.96	---	0.222
Bay 19	Local (1)	420	0.720	396	22.77	---	0.211

Note: (1) The local regions refer to the thinned areas within the individual bays.

Table 8-2: Refueling Case Load Factors and Maximum Displacements

Mode #	Load Factor	Cylinder	Sphere			Sandbed Region									
			Upper	Middle	Lower	Bay 1	Bay 3	Bay 5	Bay 7	Bay 9	Bay 11	Bay 13	Bay 15	Bay 17	Bay 19
1	7.229	1.00	0.00	0.00	0.00	0.00	0.00	0.00	0.00	0.00	0.00	0.00	0.00	0.00	0.00
2	7.459	1.02	0.00	0.00	0.00	0.00	0.00	0.00	0.00	0.00	0.00	0.00	0.00	0.00	0.00
3	7.460	1.02	0.00	0.00	0.00	0.00	0.00	0.00	0.00	0.00	0.00	0.00	0.00	0.00	0.00
4	7.465	1.01	0.00	0.00	0.00	0.00	0.00	0.00	0.00	0.00	0.00	0.00	0.00	0.00	0.00
5	7.943	1.04	0.00	0.00	0.00	0.00	0.00	0.00	0.00	0.00	0.00	0.00	0.00	0.00	0.00
6	7.990	1.07	0.00	0.00	0.00	0.00	0.00	0.00	0.00	0.00	0.00	0.00	0.00	0.00	0.00
7	8.078	1.03	0.00	0.00	0.00	0.00	0.00	0.00	0.00	0.00	0.00	0.00	0.00	0.00	0.00
8	8.096	1.06	0.00	0.00	0.00	0.00	0.00	0.00	0.00	0.00	0.00	0.00	0.00	0.00	0.00
9	8.677	1.31	0.00	0.00	0.00	0.00	0.00	0.00	0.00	0.00	0.00	0.00	0.00	0.00	0.00
10	8.827	1.35	0.00	0.00	0.00	0.00	0.00	0.00	0.00	0.00	0.00	0.00	0.00	0.00	0.00
11	9.230	1.01	0.01	0.00	0.00	0.00	0.00	0.00	0.00	0.00	0.00	0.00	0.00	0.00	0.00
12	9.292	1.04	0.00	0.00	0.00	0.00	0.00	0.00	0.00	0.00	0.00	0.00	0.00	0.00	0.00
13	9.590	1.22	0.01	0.00	0.00	0.00	0.00	0.00	0.00	0.00	0.00	0.00	0.00	0.00	0.00
14	9.736	1.09	0.01	0.00	0.00	0.00	0.00	0.00	0.00	0.00	0.00	0.00	0.00	0.00	0.00
15	9.800	0.03	1.39	0.01	0.00	0.00	0.00	0.00	0.00	0.00	0.00	0.00	0.00	0.00	0.00
16	10.005	0.03	1.34	0.02	0.00	0.00	0.00	0.00	0.00	0.00	0.00	0.00	0.00	0.00	0.00
17	10.096	0.06	1.39	0.01	0.00	0.00	0.00	0.00	0.00	0.00	0.00	0.00	0.00	0.00	0.00
18	10.272	0.05	1.34	0.03	0.00	0.00	0.00	0.00	0.00	0.00	0.00	0.00	0.00	0.00	0.00
19	10.285	1.29	0.02	0.00	0.00	0.00	0.00	0.00	0.00	0.00	0.00	0.00	0.00	0.00	0.00
20	10.343	1.15	0.01	0.00	0.00	0.00	0.00	0.00	0.00	0.00	0.00	0.00	0.00	0.00	0.00
21	10.372	1.20	0.02	0.00	0.00	0.00	0.00	0.00	0.00	0.00	0.00	0.00	0.00	0.00	0.00
22	10.388	0.13	1.39	0.02	0.00	0.00	0.00	0.00	0.00	0.00	0.00	0.00	0.00	0.00	0.00
23	10.399	1.28	0.02	0.00	0.00	0.00	0.00	0.00	0.00	0.00	0.00	0.00	0.00	0.00	0.00
24	10.543	0.04	1.39	0.05	0.00	0.00	0.00	0.00	0.00	0.00	0.00	0.00	0.00	0.00	0.00
25	10.652	0.00	0.02	1.30	0.01	0.00	0.00	0.00	0.00	0.00	0.00	0.00	0.00	0.00	0.00
26	10.729	0.08	1.39	0.03	0.00	0.00	0.00	0.00	0.00	0.00	0.00	0.00	0.00	0.00	0.00
27	10.839	0.00	0.05	1.32	0.03	0.00	0.00	0.00	0.00	0.00	0.00	0.00	0.00	0.00	0.00
28	10.862	0.07	1.39	0.06	0.00	0.00	0.00	0.00	0.00	0.00	0.00	0.00	0.00	0.00	0.00
29	10.923	1.04	0.01	0.00	0.00	0.00	0.00	0.00	0.00	0.00	0.00	0.00	0.00	0.00	0.00
30	10.962	1.04	0.00	0.00	0.00	0.00	0.00	0.00	0.00	0.00	0.00	0.00	0.00	0.00	0.00
31	11.079	0.04	1.42	0.04	0.00	0.00	0.00	0.00	0.00	0.00	0.00	0.00	0.00	0.00	0.00
32	11.150	0.00	0.01	1.30	0.35	0.00	0.00	0.00	0.00	0.00	0.00	0.00	0.00	0.00	0.00
33	11.181	0.04	1.37	0.06	0.01	0.00	0.00	0.00	0.00	0.00	0.00	0.00	0.00	0.00	0.00
34	11.186	0.00	0.04	1.28	0.28	0.00	0.00	0.00	0.00	0.00	0.00	0.00	0.00	0.00	0.00
35	11.378	1.07	0.01	0.00	0.00	0.00	0.00	0.00	0.00	0.00	0.00	0.00	0.00	0.00	0.00
36	11.382	0.01	0.07	1.24	0.03	0.00	0.00	0.00	0.00	0.00	0.00	0.00	0.00	0.00	0.00
37	11.383	1.06	0.01	0.00	0.00	0.00	0.00	0.00	0.00	0.00	0.00	0.00	0.00	0.00	0.00
38	11.450	0.00	0.03	1.04	0.28	0.00	0.00	0.00	0.00	0.00	0.00	0.00	0.00	0.00	0.00
39	11.469	0.03	1.39	0.06	0.01	0.00	0.00	0.00	0.00	0.00	0.00	0.00	0.00	0.00	0.00
40	11.474	0.00	0.02	1.05	0.35	0.00	0.00	0.00	0.00	0.00	0.00	0.00	0.00	0.00	0.00
41	11.528	0.00	0.03	1.08	0.09	0.00	0.00	0.00	0.00	0.00	0.00	0.00	0.00	0.00	0.00
42	11.535	0.00	0.04	1.12	0.13	0.00	0.00	0.00	0.00	0.00	0.00	0.00	0.00	0.00	0.00
43	11.553	0.03	1.44	0.36	0.01	0.01	0.00	0.00	0.00	0.00	0.00	0.00	0.00	0.00	0.01
44	11.583	0.01	0.27	1.11	0.11	0.00	0.00	0.00	0.00	0.00	0.00	0.00	0.00	0.00	0.00
45	11.584	0.05	1.43	0.78	0.08	0.01	0.00	0.00	0.00	0.00	0.00	0.00	0.00	0.00	0.01
46	11.658	0.00	0.20	1.26	0.15	0.00	0.00	0.00	0.00	0.00	0.00	0.00	0.00	0.00	0.00
47	11.682	1.02	0.01	0.00	0.00	0.00	0.00	0.00	0.00	0.00	0.00	0.00	0.00	0.00	0.00
48	11.698	0.00	0.11	1.31	0.16	0.00	0.00	0.00	0.00	0.00	0.00	0.00	0.00	0.00	0.00
49	11.716	0.05	1.59	0.32	0.06	0.00	0.00	0.00	0.00	0.00	0.00	0.00	0.00	0.00	0.00
50	11.722	1.08	0.01	0.00	0.00	0.00	0.00	0.00	0.00	0.00	0.00	0.00	0.00	0.00	0.00

Table 8-2: Refueling Case Load Factors and Maximum Displacements (continued)

Mode #	Load Factor	Cylinder	Sphere			Sandbed Region									
			Upper	Middle	Lower	Bay 1	Bay 3	Bay 5	Bay 7	Bay 9	Bay 11	Bay 13	Bay 15	Bay 17	Bay 19
51	11.724	0.01	0.06	1.04	0.39	0.00	0.00	0.00	0.00	0.00	0.00	0.00	0.00	0.00	0.00
52	11.787	0.00	0.04	1.30	0.44	0.00	0.00	0.00	0.00	0.00	0.00	0.00	0.00	0.00	0.00
53	11.797	0.00	0.06	1.05	0.28	0.00	0.00	0.00	0.00	0.00	0.00	0.00	0.00	0.00	0.00
54	11.798	0.00	0.06	1.32	0.37	0.00	0.00	0.00	0.00	0.00	0.00	0.00	0.00	0.00	0.00
55	11.887	1.05	0.01	0.00	0.00	0.00	0.00	0.00	0.00	0.00	0.00	0.00	0.00	0.00	0.00
56	11.903	0.04	1.29	0.36	0.05	0.07	0.01	0.00	0.00	0.00	0.00	0.00	0.00	0.01	0.06
57	11.917	0.01	0.22	1.16	0.32	0.01	0.00	0.00	0.00	0.00	0.00	0.00	0.00	0.00	0.01
58	11.932	0.01	0.13	0.01	0.29	1.26	0.10	0.01	0.00	0.00	0.00	0.01	0.01	0.11	1.00
59	11.935	0.07	1.36	0.19	0.18	0.80	0.06	0.00	0.00	0.00	0.00	0.00	0.01	0.07	0.63
60	11.987	0.04	1.36	0.20	0.02	0.02	0.00	0.00	0.00	0.00	0.00	0.00	0.00	0.00	0.01
61	11.993	0.00	0.09	1.09	0.25	0.01	0.00	0.00	0.00	0.00	0.00	0.00	0.00	0.00	0.01
62	12.050	0.00	0.04	1.14	0.14	0.00	0.00	0.00	0.00	0.00	0.00	0.00	0.00	0.00	0.00
63	12.070	0.01	0.20	1.13	0.25	0.01	0.00	0.00	0.00	0.00	0.00	0.00	0.00	0.00	0.00
64	12.074	0.01	0.34	1.03	0.18	0.00	0.00	0.00	0.00	0.00	0.00	0.00	0.00	0.00	0.00
65	12.080	0.07	1.34	0.54	0.12	0.00	0.00	0.00	0.00	0.00	0.00	0.00	0.00	0.00	0.00
66	12.110	0.06	1.31	0.25	0.04	0.01	0.00	0.00	0.00	0.00	0.00	0.00	0.00	0.00	0.00
67	12.167	0.00	0.05	1.05	0.33	0.00	0.00	0.00	0.00	0.00	0.00	0.00	0.00	0.00	0.00
68	12.176	0.01	0.15	1.11	0.40	0.00	0.00	0.00	0.00	0.00	0.00	0.00	0.00	0.00	0.00
69	12.184	0.00	0.03	1.05	0.26	0.00	0.00	0.00	0.00	0.00	0.00	0.00	0.00	0.00	0.00
70	12.196	0.01	0.25	1.30	0.22	0.00	0.00	0.00	0.00	0.00	0.00	0.00	0.00	0.00	0.00
71	12.236	0.28	1.29	0.30	0.03	0.00	0.00	0.00	0.00	0.00	0.00	0.00	0.00	0.00	0.00
72	12.242	1.21	0.05	0.03	0.01	0.00	0.00	0.00	0.00	0.00	0.00	0.00	0.00	0.00	0.00
73	12.244	0.17	0.21	1.11	0.25	0.00	0.00	0.00	0.00	0.00	0.00	0.00	0.00	0.00	0.00
74	12.315	0.02	0.19	1.27	0.19	0.00	0.00	0.00	0.00	0.00	0.00	0.00	0.00	0.00	0.00
75	12.324	0.10	1.36	0.51	0.05	0.00	0.00	0.00	0.00	0.00	0.00	0.00	0.00	0.00	0.00
76	12.347	0.01	0.15	1.02	0.23	0.00	0.00	0.00	0.00	0.00	0.00	0.00	0.00	0.00	0.00
77	12.388	0.06	0.80	1.03	0.27	0.00	0.00	0.00	0.00	0.00	0.00	0.00	0.00	0.00	0.00
78	12.392	0.13	1.43	0.70	0.23	0.00	0.00	0.00	0.00	0.00	0.00	0.00	0.00	0.00	0.00
79	12.418	1.08	0.03	0.19	0.08	0.00	0.00	0.00	0.00	0.00	0.00	0.00	0.00	0.00	0.00
80	12.419	0.84	0.17	1.06	0.45	0.01	0.00	0.00	0.00	0.00	0.00	0.00	0.00	0.01	0.01
81	12.435	0.06	0.26	1.03	0.44	0.00	0.00	0.00	0.00	0.00	0.00	0.00	0.00	0.00	0.00
82	12.439	0.32	1.34	0.25	0.06	0.00	0.00	0.00	0.00	0.00	0.00	0.00	0.00	0.01	0.01
83	12.443	1.05	0.07	0.02	0.00	0.00	0.00	0.00	0.00	0.00	0.00	0.00	0.00	0.00	0.00
84	12.461	0.02	0.30	0.89	0.26	0.00	0.00	0.00	0.00	0.00	0.00	0.00	0.00	0.00	0.00
85	12.494	1.01	0.02	0.01	0.00	0.00	0.00	0.00	0.00	0.00	0.00	0.00	0.00	0.00	0.00
86	12.500	0.13	1.27	0.86	0.14	0.00	0.00	0.00	0.00	0.00	0.00	0.00	0.00	0.01	0.02
87	12.516	0.01	0.03	0.04	0.26	0.30	0.02	0.00	0.00	0.00	0.00	0.01	0.02	0.73	1.27
88	12.517	0.04	0.61	1.04	0.38	0.09	0.00	0.00	0.00	0.00	0.00	0.00	0.01	0.21	0.37
89	12.528	0.03	0.58	1.13	0.49	0.00	0.00	0.00	0.00	0.00	0.00	0.00	0.00	0.01	0.02
90	12.541	0.02	0.31	1.15	0.47	0.00	0.00	0.00	0.00	0.00	0.00	0.00	0.00	0.01	0.01
91	12.578	0.01	0.22	1.15	0.22	0.00	0.00	0.00	0.00	0.00	0.00	0.00	0.00	0.00	0.01
92	12.594	0.15	0.37	1.13	0.27	0.00	0.00	0.00	0.00	0.00	0.00	0.00	0.00	0.00	0.00
93	12.596	1.00	0.01	0.03	0.01	0.00	0.00	0.00	0.00	0.00	0.00	0.00	0.00	0.00	0.00
94	12.607	0.01	0.12	1.13	0.43	0.00	0.00	0.00	0.00	0.00	0.00	0.00	0.00	0.00	0.00
95	12.645	0.08	1.37	0.74	0.22	0.00	0.00	0.00	0.00	0.00	0.00	0.00	0.00	0.00	0.00
96	12.721	0.07	1.30	0.56	0.08	0.00	0.00	0.00	0.00	0.00	0.00	0.00	0.00	0.01	0.01
97	12.769	0.01	0.08	1.06	0.50	0.00	0.00	0.00	0.00	0.00	0.00	0.00	0.00	0.00	0.00
98	12.779	1.04	0.03	0.03	0.01	0.00	0.00	0.00	0.00	0.00	0.00	0.00	0.00	0.00	0.00
99	12.780	0.06	0.09	1.06	0.25	0.00	0.00	0.00	0.00	0.00	0.00	0.00	0.00	0.00	0.00
100	12.802	0.12	0.10	1.05	0.30	0.00	0.00	0.00	0.00	0.00	0.00	0.00	0.00	0.00	0.00

Table 8-2: Refueling Case Load Factors and Maximum Displacements (continued)

Mode #	Load Factor	Cylinder	Sphere			Sandbed Region									
			Upper	Middle	Lower	Bay 1	Bay 3	Bay 5	Bay 7	Bay 9	Bay 11	Bay 13	Bay 15	Bay 17	Bay 19
101	12.803	1.07	0.01	0.08	0.02	0.00	0.00	0.00	0.00	0.00	0.00	0.00	0.00	0.00	0.00
102	12.809	0.02	0.25	1.13	0.52	0.00	0.00	0.00	0.00	0.00	0.00	0.00	0.00	0.00	0.00
103	12.839	1.14	0.63	0.44	0.06	0.00	0.00	0.00	0.00	0.00	0.00	0.00	0.00	0.00	0.00
104	12.840	1.06	1.52	1.07	0.15	0.01	0.00	0.00	0.00	0.00	0.00	0.00	0.00	0.00	0.01
105	12.865	1.07	0.44	0.56	0.25	0.00	0.00	0.00	0.00	0.00	0.00	0.00	0.00	0.00	0.00
106	12.866	1.07	0.33	0.44	0.20	0.00	0.00	0.00	0.00	0.00	0.00	0.00	0.00	0.00	0.00
107	12.881	0.04	0.33	1.11	0.15	0.00	0.00	0.00	0.00	0.00	0.00	0.00	0.00	0.00	0.00
108	12.882	0.11	1.44	1.04	0.33	0.00	0.00	0.00	0.00	0.00	0.00	0.00	0.00	0.00	0.00
109	12.908	0.02	0.60	1.04	0.28	0.00	0.00	0.00	0.00	0.00	0.00	0.00	0.00	0.00	0.00
110	12.928	0.04	1.38	0.61	0.20	0.01	0.00	0.00	0.00	0.00	0.00	0.00	0.00	0.00	0.01
111	12.937	0.02	0.49	1.07	0.38	0.00	0.00	0.00	0.00	0.00	0.00	0.00	0.00	0.00	0.00
112	12.966	0.07	1.37	0.86	0.25	0.12	0.06	0.00	0.00	0.00	0.00	0.00	0.00	0.03	0.11
113	12.969	0.01	0.27	1.15	0.40	0.02	0.01	0.00	0.00	0.00	0.00	0.00	0.00	0.00	0.02
114	12.974	0.02	0.32	1.05	0.33	0.00	0.00	0.00	0.00	0.00	0.00	0.00	0.00	0.00	0.00
115	12.976	0.01	0.02	0.01	0.50	1.31	0.63	0.02	0.01	0.00	0.01	0.01	0.01	0.26	1.12
116	13.022	0.01	0.54	1.07	0.42	0.01	0.00	0.00	0.00	0.00	0.00	0.00	0.00	0.00	0.00
117	13.027	0.02	0.51	1.10	0.45	0.00	0.00	0.00	0.00	0.00	0.00	0.00	0.00	0.00	0.00
118	13.032	0.02	0.58	1.01	0.37	0.00	0.00	0.00	0.00	0.00	0.00	0.00	0.00	0.00	0.00
119	13.042	0.06	1.45	1.06	0.41	0.00	0.00	0.00	0.00	0.00	0.00	0.00	0.00	0.00	0.00
120	13.070	1.03	0.01	0.00	0.00	0.00	0.00	0.00	0.00	0.00	0.00	0.00	0.00	0.00	0.00
121	13.086	0.01	0.37	1.10	0.49	0.00	0.00	0.00	0.00	0.00	0.00	0.00	0.00	0.00	0.00
122	13.110	0.33	1.35	0.85	0.32	0.02	0.01	0.00	0.00	0.00	0.00	0.00	0.00	0.00	0.02
123	13.111	0.03	0.00	0.01	0.42	1.26	0.67	0.01	0.00	0.00	0.00	0.00	0.00	0.18	0.86
124	13.113	1.04	0.03	0.02	0.01	0.02	0.01	0.00	0.00	0.00	0.00	0.00	0.00	0.00	0.01
125	13.185	0.01	0.30	1.08	0.28	0.00	0.00	0.00	0.00	0.00	0.00	0.00	0.00	0.00	0.00
126	13.193	0.01	0.43	0.93	0.29	0.00	0.00	0.00	0.00	0.00	0.00	0.00	0.00	0.00	0.00
127	13.225	0.02	0.46	1.13	0.44	0.00	0.00	0.00	0.00	0.00	0.00	0.00	0.00	0.00	0.00
128	13.249	0.01	0.23	1.08	0.27	0.00	0.00	0.00	0.00	0.00	0.00	0.00	0.00	0.00	0.00
129	13.276	0.01	0.23	1.28	0.39	0.00	0.00	0.00	0.00	0.00	0.00	0.00	0.00	0.00	0.00
130	13.288	0.01	0.28	1.01	0.28	0.00	0.00	0.00	0.00	0.00	0.00	0.00	0.00	0.00	0.00
131	13.297	0.04	1.35	0.57	0.09	0.00	0.00	0.00	0.00	0.00	0.00	0.00	0.00	0.00	0.00
132	13.332	0.05	0.77	1.13	0.45	0.00	0.00	0.00	0.00	0.00	0.00	0.00	0.00	0.00	0.00
133	13.341	0.01	0.25	1.07	0.25	0.00	0.00	0.00	0.00	0.00	0.00	0.00	0.00	0.00	0.00
134	13.365	1.06	0.01	0.01	0.00	0.00	0.00	0.00	0.00	0.00	0.00	0.00	0.00	0.00	0.00
135	13.374	0.05	0.52	1.02	0.33	0.00	0.00	0.00	0.00	0.00	0.00	0.00	0.00	0.00	0.00
136	13.381	0.03	0.27	1.07	0.32	0.00	0.00	0.00	0.00	0.00	0.00	0.00	0.00	0.00	0.00
137	13.401	0.03	0.23	1.19	0.32	0.00	0.00	0.00	0.00	0.00	0.00	0.00	0.00	0.00	0.00
138	13.411	1.12	0.27	0.43	0.11	0.00	0.00	0.00	0.00	0.00	0.00	0.00	0.00	0.00	0.00
139	13.413	1.12	0.36	0.55	0.14	0.00	0.00	0.00	0.00	0.00	0.00	0.00	0.00	0.00	0.00
140	13.431	0.14	1.23	0.80	0.09	0.01	0.00	0.00	0.00	0.00	0.00	0.00	0.00	0.02	0.02
141	13.441	0.01	0.29	1.30	0.30	0.00	0.00	0.00	0.00	0.00	0.00	0.00	0.00	0.00	0.00
142	13.463	0.13	1.29	0.65	0.06	0.00	0.00	0.00	0.00	0.00	0.00	0.00	0.00	0.00	0.01
143	13.474	0.00	0.01	0.01	0.58	0.18	0.08	0.00	0.00	0.00	0.01	0.01	0.05	0.96	1.31
144	13.489	0.04	1.24	0.72	0.08	0.00	0.00	0.00	0.00	0.00	0.00	0.00	0.00	0.02	0.03
145	13.499	0.02	0.58	1.03	0.17	0.00	0.00	0.00	0.00	0.00	0.00	0.00	0.00	0.01	0.01
146	13.547	0.03	0.43	1.11	0.57	0.00	0.00	0.00	0.00	0.00	0.00	0.00	0.00	0.01	0.01
147	13.564	0.06	1.32	0.88	0.06	0.00	0.00	0.00	0.00	0.00	0.00	0.00	0.00	0.00	0.01
148	13.597	0.01	0.49	1.13	0.33	0.00	0.00	0.00	0.00	0.00	0.00	0.00	0.00	0.00	0.00
149	13.603	0.02	0.58	1.15	0.38	0.00	0.00	0.00	0.00	0.00	0.00	0.00	0.00	0.00	0.00
150	13.641	0.03	1.28	0.86	0.30	0.00	0.00	0.00	0.00	0.00	0.00	0.00	0.00	0.00	0.00

Table 8-2: Refueling Case Load Factors and Maximum Displacements (concluded)

Mode #	Load Factor	Cylinder	Sphere			Sandbed Region									
			Upper	Middle	Lower	Bay 1	Bay 3	Bay 5	Bay 7	Bay 9	Bay 11	Bay 13	Bay 15	Bay 17	Bay 19
151	13.668	0.00	0.13	1.12	0.42	0.00	0.00	0.00	0.00	0.00	0.00	0.00	0.00	0.00	0.00
152	13.694	0.01	0.19	1.01	0.24	0.00	0.00	0.00	0.00	0.00	0.00	0.00	0.00	0.00	0.00
153	13.703	0.01	0.26	1.11	0.41	0.00	0.00	0.00	0.00	0.00	0.00	0.00	0.00	0.00	0.00
154	13.721	0.06	1.18	0.63	0.28	0.00	0.00	0.00	0.00	0.00	0.00	0.00	0.00	0.00	0.00
155	13.731	0.09	1.13	0.93	0.26	0.00	0.00	0.00	0.00	0.00	0.00	0.00	0.00	0.00	0.00
156	13.749	0.01	0.24	1.05	0.40	0.00	0.00	0.00	0.00	0.00	0.00	0.00	0.00	0.00	0.00
157	13.757	0.06	1.27	1.06	0.39	0.00	0.00	0.00	0.00	0.00	0.00	0.00	0.00	0.00	0.00
158	13.767	0.03	0.53	1.06	0.39	0.00	0.00	0.00	0.00	0.00	0.00	0.00	0.00	0.00	0.00
159	13.794	0.04	0.69	1.08	0.27	0.01	0.00	0.00	0.00	0.00	0.00	0.00	0.00	0.00	0.00
160	13.807	0.30	1.45	0.95	0.24	0.00	0.00	0.00	0.00	0.00	0.00	0.00	0.00	0.01	0.01
161	13.834	1.03	0.04	0.04	0.01	0.00	0.00	0.00	0.00	0.00	0.00	0.00	0.00	0.00	0.00
162	13.845	0.38	0.82	1.03	0.34	0.00	0.00	0.00	0.00	0.00	0.00	0.00	0.00	0.00	0.00
163	13.860	1.01	0.02	0.03	0.01	0.00	0.00	0.00	0.00	0.00	0.00	0.00	0.00	0.00	0.00
164	13.871	0.16	0.75	1.10	0.40	0.01	0.00	0.00	0.00	0.00	0.00	0.00	0.00	0.00	0.01
165	13.879	0.00	0.00	0.01	0.23	1.27	0.31	0.00	0.00	0.00	0.00	0.00	0.03	0.29	0.98
166	13.884	0.06	1.14	1.08	0.38	0.00	0.00	0.00	0.00	0.00	0.00	0.00	0.00	0.00	0.00
167	13.894	0.04	0.54	1.19	0.27	0.00	0.00	0.00	0.00	0.00	0.00	0.00	0.00	0.00	0.00
168	13.938	0.05	1.18	0.63	0.14	0.00	0.00	0.00	0.00	0.00	0.00	0.00	0.00	0.00	0.00
169	13.942	0.06	0.62	1.02	0.18	0.00	0.00	0.00	0.00	0.00	0.00	0.00	0.00	0.00	0.00
170	13.968	0.01	0.16	1.01	0.25	0.00	0.00	0.00	0.00	0.00	0.00	0.00	0.00	0.00	0.00
171	13.976	0.09	1.11	1.17	0.24	0.00	0.00	0.00	0.00	0.00	0.00	0.00	0.00	0.00	0.00
172	13.982	0.01	0.23	1.01	0.28	0.00	0.00	0.00	0.00	0.00	0.00	0.00	0.00	0.00	0.00
173	14.020	0.05	0.69	1.04	0.41	0.00	0.00	0.00	0.00	0.00	0.00	0.00	0.01	0.01	0.00
174	14.044	0.03	0.65	1.02	0.13	0.00	0.00	0.00	0.00	0.00	0.00	0.00	0.00	0.00	0.00
175	14.064	0.05	1.42	0.79	0.24	0.01	0.01	0.00	0.00	0.00	0.00	0.00	0.00	0.01	0.00
176	14.108	0.03	0.55	0.89	0.25	0.00	0.00	0.00	0.00	0.00	0.00	0.00	0.01	0.02	0.00
177	14.116	0.02	0.38	0.86	0.25	0.00	0.00	0.00	0.00	0.00	0.00	0.00	0.00	0.00	0.00
178	14.134	0.00	0.01	0.01	0.31	0.04	0.01	0.00	0.00	0.00	0.02	0.02	0.65	1.27	0.07
179	14.141	0.03	0.58	1.13	0.47	0.00	0.00	0.00	0.00	0.00	0.00	0.00	0.01	0.01	0.00
180	14.152	0.04	1.34	0.86	0.32	0.00	0.00	0.00	0.00	0.00	0.00	0.00	0.02	0.04	0.00
181	14.156	0.06	0.96	0.83	0.34	0.00	0.00	0.00	0.00	0.00	0.00	0.00	0.01	0.02	0.00
182	14.199	0.03	0.31	1.05	0.36	0.01	0.01	0.00	0.00	0.00	0.00	0.00	0.00	0.01	0.00
183	14.214	0.06	0.30	1.02	0.27	0.01	0.01	0.00	0.00	0.00	0.00	0.00	0.00	0.00	0.00
184	14.217	0.04	0.26	1.16	0.27	0.01	0.01	0.00	0.00	0.00	0.00	0.00	0.01	0.01	0.00
185	14.230	0.32	0.60	1.19	0.34	0.01	0.00	0.00	0.00	0.00	0.00	0.00	0.01	0.02	0.00
186	14.236	1.07	0.04	0.06	0.02	0.01	0.01	0.00	0.00	0.00	0.00	0.00	0.00	0.00	0.00
187	14.252	0.07	0.47	1.08	0.42	0.00	0.00	0.00	0.00	0.00	0.00	0.00	0.00	0.00	0.00
188	14.270	0.04	0.59	1.02	0.26	0.12	0.08	0.00	0.00	0.00	0.00	0.00	0.00	0.00	0.01
189	14.277	0.06	0.62	1.02	0.26	0.25	0.17	0.01	0.00	0.00	0.00	0.00	0.00	0.01	0.03
190	14.281	0.01	0.02	0.02	0.51	1.31	0.88	0.02	0.01	0.00	0.01	0.01	0.01	0.05	0.17
191	14.336	1.03	0.09	0.05	0.01	0.01	0.00	0.00	0.00	0.00	0.00	0.00	0.00	0.00	0.00
192	14.343	0.68	1.16	0.87	0.22	0.01	0.01	0.00	0.00	0.00	0.00	0.00	0.00	0.01	0.00
193	14.351	0.08	0.52	1.08	0.34	0.01	0.01	0.00	0.00	0.00	0.00	0.00	0.01	0.01	0.00
194	14.379	0.05	0.39	1.01	0.27	0.00	0.00	0.00	0.00	0.00	0.01	0.01	0.01	0.01	0.00
195	14.392	1.00	0.08	0.11	0.02	0.00	0.00	0.00	0.00	0.00	0.00	0.00	0.00	0.00	0.00
196	14.395	0.33	0.80	0.87	0.19	0.00	0.00	0.00	0.00	0.00	0.00	0.00	0.00	0.00	0.01
197	14.414	0.13	1.02	1.05	0.48	0.00	0.00	0.00	0.00	0.00	0.00	0.00	0.00	0.01	0.00
198	14.444	0.24	1.07	1.07	0.39	0.00	0.00	0.00	0.00	0.00	0.01	0.01	0.00	0.01	0.00
199	14.453	1.01	0.03	0.05	0.02	0.01	0.00	0.00	0.00	0.00	0.01	0.01	0.00	0.00	0.00
200	14.469	0.15	1.02	1.01	0.39	0.00	0.00	0.00	0.00	0.00	0.01	0.01	0.00	0.00	0.00

Table 8-3: Flooding Case Load Factors and Maximum Displacements

Mode #	Load Factor	Cylinder	Sphere			Sandbed Region									
			Upper	Middle	Lower	Bay 1	Bay 3	Bay 5	Bay 7	Bay 9	Bay 11	Bay 13	Bay 15	Bay 17	Bay 19
1	6.524	0.00	0.00	0.00	0.00	0.00	0.00	0.00	0.00	0.00	0.00	0.00	0.00	0.00	0.00
2	6.655	0.00	0.00	0.00	0.00	0.00	0.00	0.00	0.00	0.00	0.00	0.00	0.00	0.00	0.00
3	6.684	0.00	0.00	0.00	0.00	0.00	0.00	0.00	0.00	0.00	0.00	0.00	0.00	0.00	0.00
4	6.768	0.00	0.00	0.00	0.00	0.00	0.00	0.00	0.00	0.00	0.00	0.00	0.00	0.00	0.00
5	6.793	0.00	0.00	0.00	0.00	0.00	0.00	0.00	0.00	0.00	0.00	0.00	0.00	0.00	0.00
6	6.794	0.00	0.00	0.00	0.00	0.00	0.00	0.00	0.00	0.00	0.00	0.00	0.00	0.00	0.00
7	6.854	0.00	0.00	0.00	0.00	0.00	0.00	0.00	0.00	0.00	0.00	0.00	0.00	0.00	0.00
8	6.946	0.00	0.00	0.00	0.00	0.00	0.00	0.00	0.00	0.00	0.00	0.00	0.00	0.00	0.00
9	6.971	0.00	0.00	0.00	0.00	0.00	0.00	0.00	0.00	0.00	0.00	0.00	0.00	0.00	0.00
10	7.073	0.00	0.00	0.00	0.00	0.00	0.00	0.00	0.00	0.00	0.00	0.00	0.00	0.00	0.00
11	7.162	0.00	0.00	0.00	0.02	0.01	0.01	0.01	0.01	0.01	0.01	0.01	0.01	0.01	0.01
12	7.175	0.00	0.00	0.00	0.04	0.02	0.02	0.02	0.02	0.02	0.02	0.02	0.02	0.02	0.02
13	7.279	0.00	0.00	0.00	0.00	0.00	0.00	0.00	0.00	0.00	0.00	0.00	0.00	0.00	0.00
14	7.285	0.00	0.00	0.00	0.00	0.01	0.00	0.00	0.00	0.00	0.00	0.00	0.00	0.00	0.01
15	7.344	0.01	0.02	0.02	0.23	1.26	0.36	0.03	0.01	0.01	0.02	0.02	0.05	0.56	1.19
16	7.354	0.00	0.00	0.00	0.00	0.02	0.01	0.00	0.00	0.00	0.00	0.00	0.00	0.01	0.02
17	7.363	0.00	0.00	0.00	0.00	0.01	0.00	0.00	0.00	0.00	0.00	0.00	0.00	0.00	0.01
18	7.365	0.00	0.00	0.00	0.00	0.01	0.00	0.00	0.00	0.00	0.00	0.00	0.00	0.00	0.00
19	7.428	0.00	0.00	0.00	0.00	0.00	0.00	0.00	0.00	0.00	0.00	0.00	0.00	0.00	0.00
20	7.502	0.00	0.00	0.00	0.00	0.02	0.01	0.00	0.00	0.00	0.00	0.00	0.00	0.00	0.01
21	7.615	0.00	0.00	0.00	0.00	0.00	0.00	0.00	0.00	0.00	0.00	0.00	0.00	0.00	0.00
22	7.671	0.00	0.00	0.00	0.00	0.00	0.00	0.00	0.00	0.00	0.00	0.00	0.00	0.00	0.00
23	7.706	0.00	0.00	0.01	0.22	0.73	0.42	0.02	0.00	0.00	0.01	0.01	0.07	0.93	1.26
24	7.761	0.00	0.00	0.00	0.00	0.01	0.00	0.00	0.00	0.00	0.00	0.00	0.00	0.01	0.01
25	7.796	0.00	0.00	0.00	0.00	0.00	0.00	0.00	0.00	0.00	0.00	0.00	0.00	0.00	0.00
26	7.805	0.00	0.00	0.00	0.00	0.00	0.00	0.00	0.00	0.00	0.00	0.00	0.00	0.00	0.00
27	7.956	0.00	0.00	0.00	0.00	0.02	0.01	0.00	0.00	0.00	0.00	0.00	0.00	0.01	0.02
28	8.024	0.01	0.01	0.01	0.19	1.26	0.94	0.04	0.01	0.01	0.03	0.03	0.04	0.29	0.64
29	8.082	0.00	0.00	0.00	0.00	0.02	0.01	0.00	0.00	0.00	0.00	0.00	0.00	0.00	0.01
30	8.142	0.00	0.00	0.00	0.01	0.00	0.00	0.00	0.00	0.00	0.02	0.02	0.00	0.00	0.00
31	8.177	0.00	0.00	0.00	0.00	0.00	0.00	0.00	0.00	0.00	0.00	0.00	0.00	0.00	0.00
32	8.220	0.01	0.01	0.02	0.30	0.04	0.03	0.01	0.02	0.25	1.26	1.24	0.23	0.07	0.06
33	8.231	0.00	0.00	0.00	0.01	0.01	0.00	0.00	0.00	0.01	0.04	0.04	0.01	0.01	0.01
34	8.314	0.00	0.00	0.00	0.00	0.00	0.00	0.00	0.00	0.00	0.02	0.02	0.00	0.00	0.00
35	8.352	0.00	0.00	0.00	0.01	0.02	0.01	0.00	0.00	0.00	0.00	0.00	0.00	0.02	0.03
36	8.363	0.00	0.00	0.00	0.00	0.00	0.00	0.00	0.00	0.00	0.00	0.00	0.00	0.00	0.00
37	8.405	0.01	0.02	0.02	0.33	1.11	0.35	0.02	0.01	0.01	0.11	0.10	0.21	0.92	1.31
38	8.410	0.00	0.00	0.00	0.02	0.06	0.02	0.00	0.00	0.00	0.01	0.01	0.01	0.04	0.06
39	8.467	0.00	0.00	0.00	0.01	0.01	0.00	0.00	0.00	0.00	0.00	0.00	0.01	0.02	0.01
40	8.490	0.00	0.00	0.00	0.01	0.01	0.01	0.00	0.00	0.00	0.00	0.00	0.00	0.01	0.01
41	8.603	0.00	0.00	0.00	0.00	0.00	0.00	0.00	0.00	0.00	0.00	0.00	0.00	0.00	0.00
42	8.606	0.00	0.00	0.00	0.00	0.00	0.00	0.00	0.00	0.00	0.00	0.00	0.00	0.00	0.00
43	8.623	0.01	0.01	0.02	0.44	1.24	0.52	0.03	0.00	0.02	0.10	0.24	0.96	1.23	1.30
44	8.688	0.00	0.00	0.00	0.01	0.03	0.01	0.00	0.00	0.00	0.00	0.01	0.01	0.02	0.03
45	8.703	0.00	0.00	0.00	0.00	0.01	0.01	0.00	0.00	0.00	0.00	0.00	0.01	0.02	0.01
46	8.719	0.00	0.00	0.00	0.00	0.01	0.00	0.00	0.00	0.00	0.00	0.01	0.01	0.01	0.01
47	8.781	0.01	0.01	0.01	0.28	0.53	0.37	0.03	0.01	0.03	0.11	0.39	1.04	1.27	0.84
48	8.817	0.00	0.00	0.00	0.00	0.00	0.00	0.00	0.00	0.00	0.00	0.00	0.01	0.01	0.00
49	8.871	0.00	0.00	0.00	0.01	0.01	0.01	0.00	0.00	0.00	0.00	0.00	0.00	0.00	0.01
50	8.993	0.01	0.01	0.01	0.28	0.31	0.23	0.02	0.07	1.07	1.26	0.90	0.89	0.27	0.12

Table 8-3: Flooding Case Load Factors and Maximum Displacements (continued)

Mode #	Load Factor	Cylinder	Sphere			Sandbed Region									
			Upper	Middle	Lower	Bay 1	Bay 3	Bay 5	Bay 7	Bay 9	Bay 11	Bay 13	Bay 15	Bay 17	Bay 19
51	9.029	0.01	0.01	0.01	0.38	1.30	1.00	0.08	0.04	0.65	0.76	0.57	0.57	0.30	0.60
52	9.035	0.01	0.02	0.02	0.33	1.12	0.87	0.09	0.06	0.71	0.82	1.26	1.26	0.56	0.59
53	9.049	0.00	0.00	0.00	0.02	0.02	0.01	0.00	0.00	0.01	0.03	0.09	0.09	0.03	0.01
54	9.118	0.00	0.00	0.00	0.00	0.00	0.00	0.00	0.00	0.00	0.00	0.02	0.02	0.01	0.00
55	9.135	0.00	0.00	0.00	0.00	0.00	0.00	0.00	0.00	0.02	0.02	0.00	0.00	0.00	0.00
56	9.148	1.00	0.00	0.00	0.00	0.00	0.00	0.00	0.00	0.00	0.00	0.00	0.00	0.00	0.00
57	9.169	0.00	0.00	0.00	0.00	0.00	0.00	0.00	0.00	0.00	0.00	0.00	0.00	0.00	0.00
58	9.206	1.11	0.00	0.00	0.00	0.00	0.00	0.00	0.00	0.00	0.00	0.00	0.00	0.00	0.00
59	9.222	0.00	0.00	0.00	0.10	1.27	0.45	0.02	0.00	0.00	0.01	0.05	0.08	0.41	1.21
60	9.234	0.00	0.00	0.00	0.00	0.01	0.00	0.00	0.00	0.01	0.01	0.01	0.00	0.00	0.01
61	9.238	1.07	0.00	0.00	0.00	0.00	0.00	0.00	0.00	0.00	0.00	0.00	0.00	0.00	0.00
62	9.300	0.00	0.00	0.00	0.01	0.00	0.00	0.01	0.00	0.00	0.00	0.00	0.00	0.00	0.00
63	9.332	0.00	0.00	0.00	0.00	0.00	0.00	0.00	0.00	0.01	0.01	0.01	0.00	0.00	0.00
64	9.396	0.01	0.01	0.01	0.46	0.01	0.01	0.00	0.01	0.43	1.30	1.26	0.19	0.02	0.01
65	9.546	1.01	0.00	0.00	0.00	0.00	0.00	0.00	0.00	0.00	0.00	0.00	0.00	0.00	0.00
66	9.547	0.02	0.00	0.00	0.01	0.00	0.00	0.00	0.01	0.00	0.00	0.00	0.00	0.00	0.00
67	9.624	0.00	0.00	0.00	0.01	0.01	0.00	0.00	0.00	0.01	0.01	0.01	0.02	0.03	0.01
68	9.629	0.00	0.00	0.00	0.02	0.02	0.01	0.00	0.00	0.00	0.00	0.01	0.03	0.05	0.01
69	9.655	0.01	0.01	0.01	0.39	0.03	0.02	0.00	0.00	0.01	0.03	0.19	0.91	1.31	0.06
70	9.727	0.00	0.00	0.00	0.02	0.01	0.01	0.00	0.00	0.00	0.00	0.00	0.01	0.02	0.01
71	9.810	0.00	0.00	0.00	0.02	0.02	0.02	0.01	0.00	0.00	0.00	0.00	0.01	0.01	0.02
72	9.890	0.00	0.00	0.00	0.01	0.02	0.02	0.01	0.00	0.00	0.00	0.00	0.00	0.02	0.02
73	9.976	0.00	0.00	0.00	0.02	0.03	0.02	0.02	0.00	0.00	0.00	0.01	0.01	0.02	0.02
74	10.076	1.05	0.00	0.00	0.01	0.00	0.00	0.00	0.00	0.00	0.01	0.03	0.03	0.00	0.00
75	10.078	0.07	0.00	0.01	0.21	0.05	0.02	0.01	0.00	0.10	0.21	0.67	0.66	0.06	0.05
76	10.087	0.00	0.00	0.00	0.04	0.03	0.02	0.01	0.00	0.02	0.04	0.12	0.12	0.03	0.04
77	10.134	0.01	0.01	0.01	0.11	0.60	0.35	0.25	0.04	0.15	0.18	0.06	0.14	0.55	0.65
78	10.161	0.04	0.01	0.01	0.42	0.10	0.05	0.03	0.13	1.09	1.31	0.22	0.15	0.09	0.10
79	10.174	1.08	0.00	0.00	0.00	0.00	0.00	0.00	0.00	0.01	0.01	0.00	0.00	0.00	0.00
80	10.219	0.00	0.00	0.00	0.02	0.12	0.04	0.02	0.01	0.00	0.00	0.01	0.04	0.16	0.19
81	10.263	0.00	0.00	0.00	0.02	0.05	0.08	0.06	0.00	0.01	0.01	0.01	0.02	0.09	0.10
82	10.367	0.00	0.00	0.00	0.09	0.29	0.42	0.32	0.03	0.01	0.01	0.00	0.04	0.16	0.20
83	10.419	0.00	0.00	0.00	0.04	0.11	0.18	0.14	0.02	0.02	0.01	0.01	0.01	0.10	0.14
84	10.506	0.00	0.00	0.00	0.02	0.01	0.01	0.01	0.00	0.01	0.02	0.02	0.01	0.01	0.01
85	10.567	0.00	0.00	0.00	0.02	0.07	0.09	0.08	0.02	0.02	0.01	0.01	0.01	0.05	0.07
86	10.604	0.00	0.01	0.01	0.13	0.46	0.64	0.52	0.06	0.04	0.02	0.02	0.02	0.30	0.35
87	10.632	1.00	0.00	0.00	0.00	0.00	0.00	0.00	0.00	0.00	0.00	0.00	0.00	0.00	0.00
88	10.710	1.00	0.00	0.00	0.00	0.00	0.00	0.00	0.00	0.00	0.00	0.00	0.00	0.00	0.00
89	10.791	0.00	0.00	0.00	0.15	0.03	0.04	0.05	0.28	0.28	0.76	0.84	0.46	0.10	0.03
90	10.811	0.00	0.00	0.00	0.02	0.00	0.00	0.00	0.03	0.03	0.08	0.09	0.05	0.01	0.00
91	10.826	1.26	0.00	0.00	0.00	0.00	0.00	0.00	0.00	0.00	0.00	0.00	0.00	0.00	0.00
92	10.864	0.00	0.00	0.00	0.02	0.01	0.01	0.01	0.05	0.05	0.04	0.04	0.03	0.02	0.02
93	10.940	0.01	0.01	0.01	0.22	0.03	0.06	0.18	0.69	0.69	0.15	0.14	0.10	0.05	0.04
94	10.973	1.28	0.00	0.00	0.00	0.00	0.00	0.00	0.00	0.00	0.00	0.00	0.00	0.00	0.00
95	11.057	0.00	0.00	0.00	0.04	0.02	0.01	0.03	0.14	0.14	0.02	0.03	0.02	0.01	0.02
96	11.090	0.00	0.00	0.00	0.02	0.00	0.00	0.00	0.01	0.01	0.01	0.01	0.01	0.00	0.00
97	11.158	0.00	0.00	0.00	0.09	0.30	0.31	0.11	0.03	0.02	0.01	0.01	0.02	0.26	0.29
98	11.159	0.00	0.00	0.00	0.03	0.12	0.12	0.04	0.03	0.03	0.01	0.01	0.01	0.09	0.12
99	11.196	0.01	0.01	0.01	0.35	0.72	0.47	0.25	0.04	0.08	0.19	0.37	1.02	1.27	0.91
100	11.266	0.00	0.00	0.00	0.01	0.01	0.01	0.01	0.02	0.02	0.01	0.01	0.01	0.02	0.01

Table 8-3: Flooding Case Load Factors and Maximum Displacements (continued)

Mode #	Load Factor	Cylinder	Sphere			Sandbed Region									
			Upper	Middle	Lower	Bay 1	Bay 3	Bay 5	Bay 7	Bay 9	Bay 11	Bay 13	Bay 15	Bay 17	Bay 19
101	11.300	0.00	0.00	0.00	0.01	0.02	0.02	0.01	0.00	0.02	0.02	0.02	0.02	0.04	0.03
102	11.468	0.00	0.00	0.00	0.00	0.00	0.00	0.00	0.00	0.00	0.00	0.00	0.00	0.00	0.00
103	11.482	0.00	0.00	0.00	0.03	0.07	0.06	0.07	0.07	0.06	0.08	0.19	0.23	0.11	0.08
104	11.518	1.07	0.00	0.00	0.00	0.00	0.00	0.00	0.00	0.00	0.00	0.00	0.00	0.00	0.00
105	11.532	1.04	0.00	0.00	0.00	0.00	0.00	0.00	0.00	0.00	0.00	0.00	0.00	0.00	0.00
106	11.535	0.01	0.00	0.00	0.05	0.11	0.11	0.05	0.03	0.04	0.10	0.32	0.39	0.20	0.12
107	11.599	0.01	0.02	0.02	0.41	0.13	1.10	1.26	1.25	0.40	0.11	0.08	0.05	0.08	0.08
108	11.621	0.00	0.00	0.00	0.01	0.00	0.02	0.03	0.03	0.01	0.00	0.00	0.00	0.00	0.00
109	11.707	0.00	0.00	0.00	0.01	0.01	0.04	0.03	0.02	0.03	0.02	0.03	0.02	0.01	0.01
110	11.743	0.00	0.00	0.00	0.02	0.01	0.05	0.04	0.04	0.05	0.05	0.05	0.01	0.00	0.01
111	11.861	0.01	0.01	0.01	0.30	0.85	1.28	0.83	0.74	0.21	0.26	0.69	0.89	0.79	0.55
112	11.912	0.00	0.00	0.01	0.38	0.42	1.30	1.17	1.03	0.33	0.30	0.29	0.53	0.43	0.31
113	12.077	0.00	0.00	0.01	0.22	0.49	0.69	0.44	0.42	1.27	1.17	1.06	0.62	0.56	0.42
114	12.130	0.00	0.00	0.01	0.30	0.55	0.89	0.39	0.25	0.85	0.77	0.82	1.26	0.99	0.70
115	12.193	1.15	0.00	0.00	0.00	0.00	0.00	0.00	0.00	0.00	0.00	0.00	0.00	0.00	0.00
116	12.249	0.00	0.00	0.00	0.00	0.00	0.00	0.00	0.00	0.01	0.00	0.00	0.00	0.00	0.00
117	12.357	1.02	0.00	0.00	0.00	0.00	0.00	0.00	0.00	0.00	0.00	0.00	0.00	0.00	0.00
118	12.403	0.00	0.00	0.00	0.01	0.01	0.01	0.00	0.00	0.00	0.00	0.00	0.00	0.01	0.01
119	12.405	1.09	0.00	0.00	0.00	0.00	0.00	0.00	0.00	0.00	0.00	0.00	0.00	0.00	0.00
120	12.424	1.04	0.00	0.00	0.00	0.00	0.00	0.00	0.00	0.00	0.00	0.00	0.00	0.00	0.00
121	12.429	0.02	0.00	0.01	0.24	0.07	0.09	0.06	0.71	0.91	1.19	1.30	0.71	0.16	0.08
122	12.433	0.00	0.00	0.00	0.00	0.00	0.00	0.00	0.00	0.00	0.00	0.00	0.00	0.00	0.00
123	12.476	0.00	0.00	0.00	0.00	0.00	0.00	0.00	0.00	0.00	0.00	0.00	0.00	0.00	0.00
124	12.537	0.00	0.00	0.00	0.00	0.01	0.01	0.00	0.01	0.01	0.00	0.00	0.00	0.01	0.01
125	12.563	0.00	0.00	0.00	0.00	0.00	0.01	0.00	0.01	0.01	0.00	0.00	0.01	0.00	0.01
126	12.584	0.01	0.01	0.02	0.37	0.30	0.32	0.12	1.30	1.31	0.45	0.27	0.24	0.25	0.32
127	12.606	0.00	0.00	0.01	0.35	1.20	1.27	0.37	0.59	0.59	0.28	0.21	0.36	0.98	1.27
128	12.628	0.00	0.00	0.00	0.01	0.03	0.03	0.01	0.00	0.00	0.00	0.00	0.01	0.02	0.03
129	12.746	0.00	0.00	0.00	0.00	0.01	0.01	0.00	0.00	0.00	0.00	0.00	0.00	0.01	0.01
130	12.758	0.00	0.00	0.00	0.00	0.00	0.00	0.00	0.00	0.00	0.00	0.00	0.00	0.00	0.00
131	12.826	0.00	0.00	0.00	0.00	0.01	0.01	0.00	0.00	0.00	0.00	0.00	0.00	0.00	0.01
132	12.863	0.00	0.00	0.00	0.00	0.00	0.00	0.00	0.00	0.00	0.00	0.00	0.00	0.00	0.00
133	12.921	0.00	0.00	0.00	0.01	0.00	0.00	0.00	0.00	0.00	0.00	0.01	0.02	0.01	0.00
134	12.932	0.00	0.00	0.00	0.00	0.00	0.00	0.00	0.00	0.00	0.00	0.01	0.02	0.01	0.00
135	12.949	0.01	0.01	0.01	0.36	0.21	0.18	0.07	0.04	0.13	0.28	0.58	1.29	0.88	0.17
136	12.979	0.00	0.00	0.00	0.01	0.01	0.01	0.00	0.00	0.00	0.00	0.01	0.01	0.01	0.01
137	12.998	0.00	0.00	0.00	0.01	0.00	0.00	0.00	0.00	0.01	0.01	0.03	0.03	0.02	0.01
138	13.011	0.00	0.00	0.00	0.01	0.01	0.01	0.00	0.00	0.00	0.01	0.02	0.04	0.03	0.01
139	13.044	0.00	0.00	0.00	0.00	0.00	0.00	0.00	0.00	0.00	0.00	0.00	0.00	0.00	0.00
140	13.054	0.00	0.00	0.00	0.00	0.00	0.00	0.00	0.00	0.00	0.00	0.00	0.00	0.00	0.00
141	13.095	0.00	0.00	0.00	0.01	0.01	0.00	0.00	0.00	0.00	0.00	0.00	0.00	0.01	0.01
142	13.103	1.19	0.01	0.00	0.00	0.00	0.00	0.00	0.00	0.00	0.00	0.00	0.00	0.00	0.00
143	13.120	0.01	0.01	0.01	0.19	0.18	0.10	0.10	0.17	0.44	0.69	1.29	1.28	0.42	0.25
144	13.154	0.00	0.00	0.00	0.01	0.01	0.01	0.00	0.01	0.02	0.03	0.06	0.06	0.02	0.01
145	13.202	0.00	0.00	0.00	0.01	0.01	0.01	0.01	0.00	0.00	0.00	0.01	0.01	0.01	0.01
146	13.239	0.00	0.00	0.00	0.00	0.00	0.01	0.00	0.00	0.00	0.00	0.01	0.01	0.00	0.00
147	13.303	1.30	0.01	0.00	0.00	0.00	0.00	0.00	0.00	0.00	0.00	0.00	0.00	0.00	0.00
148	13.313	0.01	0.01	0.02	0.37	0.16	0.11	1.31	1.31	0.29	0.11	0.05	0.05	0.09	0.16
149	13.324	0.00	0.00	0.00	0.03	0.01	0.00	0.09	0.09	0.02	0.01	0.00	0.00	0.00	0.01
150	13.359	0.00	0.00	0.00	0.00	0.01	0.01	0.00	0.00	0.00	0.00	0.00	0.00	0.01	0.01

Table 8-3: Flooding Case Load Factors and Maximum Displacements (concluded)

Mode #	Load Factor	Cylinder	Sphere			Sandbed Region									
			Upper	Middle	Lower	Bay 1	Bay 3	Bay 5	Bay 7	Bay 9	Bay 11	Bay 13	Bay 15	Bay 17	Bay 19
151	13.377	0.00	0.00	0.00	0.00	0.00	0.00	0.00	0.00	0.00	0.00	0.00	0.00	0.00	0.00
152	13.435	0.00	0.00	0.00	0.02	0.08	0.04	0.02	0.02	0.00	0.01	0.01	0.03	0.05	0.08
153	13.444	0.00	0.00	0.01	0.09	0.42	0.21	0.09	0.09	0.02	0.03	0.07	0.15	0.24	0.43
154	13.517	0.00	0.00	0.00	0.00	0.00	0.00	0.01	0.01	0.00	0.00	0.00	0.00	0.00	0.00
155	13.542	0.00	0.00	0.00	0.01	0.01	0.00	0.00	0.00	0.00	0.00	0.00	0.00	0.00	0.01
156	13.564	0.00	0.00	0.00	0.01	0.01	0.00	0.00	0.00	0.00	0.00	0.01	0.01	0.00	0.01
157	13.618	1.05	0.00	0.00	0.00	0.00	0.00	0.00	0.00	0.00	0.00	0.00	0.00	0.00	0.00
158	13.620	0.00	0.00	0.00	0.01	0.02	0.01	0.01	0.00	0.00	0.00	0.00	0.00	0.01	0.02
159	13.663	1.09	0.01	0.00	0.00	0.00	0.00	0.00	0.00	0.00	0.00	0.00	0.00	0.00	0.00
160	13.681	0.00	0.00	0.00	0.01	0.01	0.01	0.01	0.01	0.01	0.00	0.00	0.00	0.01	0.01
161	13.715	0.00	0.00	0.00	0.00	0.01	0.00	0.00	0.00	0.00	0.00	0.00	0.00	0.00	0.00
162	13.730	0.00	0.00	0.00	0.01	0.00	0.00	0.00	0.00	0.00	0.00	0.00	0.00	0.00	0.00
163	13.740	0.00	0.00	0.00	0.00	0.01	0.01	0.00	0.00	0.00	0.00	0.00	0.00	0.00	0.01
164	13.764	0.00	0.00	0.00	0.00	0.00	0.00	0.01	0.01	0.00	0.00	0.00	0.00	0.00	0.00
165	13.784	0.00	0.00	0.00	0.01	0.01	0.00	0.00	0.01	0.03	0.02	0.01	0.00	0.00	0.01
166	13.809	0.00	0.00	0.01	0.23	1.20	0.80	0.35	0.12	0.38	0.27	0.11	0.20	0.86	1.27
167	13.834	0.00	0.01	0.01	0.39	0.22	0.14	0.16	0.39	1.29	0.92	0.23	0.12	0.15	0.23
168	13.846	0.00	0.00	0.00	0.03	0.03	0.02	0.01	0.03	0.09	0.06	0.02	0.02	0.02	0.03
169	13.865	0.00	0.00	0.00	0.00	0.01	0.01	0.00	0.00	0.00	0.00	0.00	0.00	0.01	0.01
170	13.871	0.00	0.00	0.00	0.00	0.00	0.00	0.00	0.00	0.00	0.00	0.00	0.00	0.00	0.00
171	13.882	0.00	0.00	0.00	0.00	0.00	0.00	0.00	0.00	0.00	0.00	0.00	0.00	0.00	0.00
172	13.924	0.00	0.00	0.00	0.01	0.01	0.00	0.00	0.01	0.01	0.01	0.01	0.01	0.01	0.01
173	14.008	0.00	0.00	0.00	0.01	0.01	0.00	0.00	0.00	0.01	0.01	0.00	0.00	0.00	0.00
174	14.029	0.00	0.00	0.00	0.01	0.01	0.00	0.01	0.00	0.00	0.00	0.00	0.00	0.00	0.01
175	14.068	0.00	0.00	0.00	0.00	0.00	0.00	0.00	0.00	0.00	0.00	0.00	0.00	0.00	0.00
176	14.074	0.00	0.00	0.00	0.00	0.00	0.00	0.00	0.00	0.00	0.00	0.00	0.00	0.00	0.00
177	14.153	0.00	0.00	0.00	0.00	0.00	0.00	0.00	0.00	0.00	0.00	0.00	0.00	0.00	0.00
178	14.218	0.00	0.00	0.00	0.01	0.02	0.04	0.03	0.01	0.00	0.00	0.00	0.00	0.01	0.01
179	14.232	0.00	0.00	0.00	0.01	0.03	0.05	0.04	0.01	0.00	0.00	0.00	0.01	0.02	0.03
180	14.240	0.00	0.00	0.01	0.18	0.60	1.02	0.76	0.12	0.02	0.04	0.05	0.13	0.33	0.53
181	14.258	0.00	0.00	0.00	0.00	0.00	0.00	0.01	0.01	0.01	0.00	0.00	0.01	0.01	0.00
182	14.266	0.00	0.00	0.00	0.00	0.00	0.01	0.01	0.00	0.00	0.00	0.00	0.00	0.00	0.00
183	14.314	0.00	0.00	0.00	0.00	0.01	0.01	0.01	0.01	0.01	0.00	0.00	0.00	0.00	0.01
184	14.321	0.00	0.00	0.00	0.00	0.00	0.00	0.00	0.00	0.00	0.00	0.00	0.00	0.00	0.00
185	14.343	0.00	0.00	0.00	0.01	0.01	0.02	0.01	0.00	0.00	0.00	0.00	0.00	0.00	0.01
186	14.375	0.00	0.00	0.00	0.00	0.00	0.00	0.00	0.00	0.00	0.00	0.00	0.00	0.00	0.00
187	14.417	0.00	0.00	0.00	0.00	0.00	0.00	0.00	0.01	0.01	0.01	0.00	0.00	0.00	0.00
188	14.419	0.01	0.00	0.00	0.01	0.01	0.01	0.03	0.05	0.05	0.02	0.02	0.01	0.01	0.01
189	14.429	1.06	0.01	0.00	0.00	0.00	0.00	0.00	0.00	0.00	0.00	0.00	0.00	0.00	0.00
190	14.449	0.00	0.00	0.00	0.01	0.01	0.01	0.02	0.04	0.04	0.01	0.01	0.01	0.00	0.00
191	14.471	1.03	0.00	0.00	0.00	0.00	0.00	0.00	0.00	0.00	0.00	0.00	0.00	0.00	0.00
192	14.502	0.01	0.02	0.02	0.70	1.26	0.42	0.30	0.55	0.53	0.34	0.28	0.17	0.34	1.25
193	14.515	0.00	0.00	0.00	0.12	0.21	0.08	0.06	0.12	0.12	0.05	0.03	0.02	0.06	0.21
194	14.529	0.00	0.00	0.00	0.05	0.09	0.04	0.09	0.21	0.20	0.12	0.09	0.05	0.03	0.09
195	14.537	0.00	0.00	0.00	0.02	0.04	0.02	0.06	0.13	0.13	0.08	0.06	0.04	0.01	0.04
196	14.577	0.00	0.00	0.00	0.01	0.00	0.00	0.01	0.02	0.02	0.02	0.02	0.01	0.00	0.00
197	14.581	0.00	0.00	0.00	0.00	0.00	0.00	0.00	0.00	0.00	0.00	0.00	0.00	0.00	0.00
198	14.624	0.00	0.00	0.00	0.00	0.00	0.00	0.00	0.00	0.00	0.01	0.01	0.00	0.00	0.00
199	14.694	0.00	0.00	0.00	0.00	0.00	0.00	0.00	0.01	0.01	0.00	0.00	0.00	0.00	0.00
200	14.704	0.00	0.00	0.00	0.00	0.00	0.00	0.00	0.01	0.01	0.01	0.01	0.00	0.00	0.00

Table 8-4: Buckling Load Factor

Region		Refueling Case		Flooding Case	
		Buckling Mode	Load Factor	Buckling Mode	Load Factor
Cylindrical		1	7.229	56	9.148
Spherical	Upper	15	9.800	200 (1)	14.704
	Middle	25	10.652	200 (1)	14.704
	Lower	32	11.150	15	7.344
Bay 1		45	11.584	11	7.162
Bay 3		45	11.584	11	7.162
Bay 5		45	11.584	11	7.162
Bay 7		45	11.584	11	7.162
Bay 9		45	11.584	11	7.162
Bay 11		45	11.584	11	7.162
Bay 13		45	11.584	11	7.162
Bay 15		45	11.584	11	7.162
Bay 17		45	11.584	11	7.162
Bay 19		45	11.584	11	7.162

Note: (1) With reference to Table 8-3, no significant mode (up to 200) is identified for these regions. Conservatively, the load factor for mode 200 is used.

Table 8-5: Refueling Buckling Evaluation (except Sandbed Region)

Region	Cylindrical	Spherical		
		Upper	Middle	Lower
R, Shell Radius (in)	198	420	420	420
t, Wall Thickness (in)	0.604	0.676	0.678	1.160
σ_y, Yield Strength (ksi)	36.3	36.3	36.3	36.3
E, Young's Modulus (ksi)	29,000	29,000	29,000	29,000
λ, Load Factor [1]	7.229	9.800	10.652	11.150
α/α_{1L}, Capacity Reduction Factor	0.330	0.362	0.207	0.244
σ_1, Meridional Compressive Stress (ksi)	3.41	3.91	4.78	4.52
σ_2, Hoop Tension Stress (ksi)	9.41	2.29	4.61	4.22
Pbar	0.106	0.049	0.098	0.053
α_p, Capacity Reduction Factor (due to tensile effect)	0.139	0.074	0.131	0.079
α_m, Modified Capacity Reduction Factor	0.469	0.436	0.338	0.323
Δ , Parameter (= $\alpha m \lambda \sigma_1 / \sigma_y$)	0.318	0.460	0.474	0.448
η, Plasticity Reduction Factor	1.000	1.000	1.000	1.000
σ_{ic}, Theoretical Buckling Stress (ksi)	11.55	16.71	17.20	16.27
SF, Safety Factor	3.39	4.27	3.60	3.60

Notes: (1) The load factor is taken from Table 8-4.

Table 8-6: Flooding Buckling Evaluation (except Sandbed Region)

Region	Cylindrical	Spherical		
		Upper	Middle	Lower
R, Shell Radius (in)	198	420	420	420
t, Wall Thickness (in)	0.604	0.676	0.678	1.160
σ_y, Yield Strength (ksi)	36.3	36.3	36.3	36.3
E, Young's Modulus (ksi)	29,000	29,000	29,000	29,000
λ, Load Factor (1)	9.148	14.704	14.704	7.344
α/α_{1L}, Capacity Reduction Factor	0.330	0.362	0.207	0.244
σ_1, Meridional Compressive Stress (ksi)	2.61	2.65	4.73	10.48
σ_2, Hoop Tension Stress (ksi)	2.65	6.66	16.15	22.59
Pbar	0.030	0.143	0.345	0.282
α_p, Capacity Reduction Factor (due to tensile effect)	0.048	0.171	0.285	0.258
α_m, Modified Capacity Reduction Factor	0.378	0.533	0.492	0.502
Δ , Parameter (= $\alpha m \lambda \sigma_1 / \sigma_y$)	0.249	0.572	0.943	1.065
η, Plasticity Reduction Factor	1.000	0.967	0.657	0.603
σ_{ic}, Theoretical Buckling Stress (ksi)	9.02	20.07	22.50	23.29

Notes: (1) The load factor is taken from Table 8-4.

Table 8-7: Refueling Buckling Evaluation, Sandbed Region

	Bay 1[(1)]	Bay 3	Bay 5	Bay 7	Bay 9	Bay 11	Bay 13[(1)]	Bay 15[(1)]	Bay 17[(1)]	Bay 19[(1)]
R, Shell Radius (in)	420	420	420	420	420	420	420	420	420	420
t, Wall Thickness (in)	0.696	0.950	1.074	1.034	0.993	0.860	0.658	0.711	0.663	0.720
σ_y, Yield Strength (ksi)	36.3	36.3	36.3	36.3	36.3	36.3	36.3	36.3	36.3	36.3
E, Young's Modulus (ksi)	29,000	29,000	29,000	29,000	29,000	29,000	29,000	29,000	29,000	29,000
λ, Load Factor[(2)]	11.584	11.584	11.584	11.584	11.584	11.584	11.584	11.584	11.584	11.584
α/α_{1L}, Capacity Reduction Factor	0.209	0.229	0.238	0.235	0.232	0.223	0.207	0.210	0.207	0.211
σ_1, Meridional Compressive Stress (ksi)	5.03	4.74	4.38	4.37	4.13	4.42	4.72	4.76	5.51	5.24
σ_2, Hoop Tension Stress (ksi)	3.82	3.33	3.38	3.45	3.44	3.93	3.96	3.81	4.60	4.02
Pbar	0.079	0.051	0.046	0.048	0.050	0.066	0.087	0.078	0.100	0.081
α_p, Capacity Reduction Factor (due to tensile effect)	0.111	0.076	0.070	0.073	0.076	0.095	0.119	0.109	0.133	0.112
α_m, Modified Capacity Reduction Factor	0.320	0.305	0.308	0.308	0.308	0.318	0.326	0.319	0.340	0.323
Δ , Parameter (= $\alpha m \lambda \sigma_1 / \sigma_y$)	0.513	0.462	0.430	0.430	0.405	0.449	0.491	0.484	0.598	0.541
η, Plasticity Reduction Factor	1.000	1.000	1.000	1.000	1.000	1.000	1.000	1.000	0.933	1.000
σ_{ic}, Theoretical Buckling Stress (ksi)	18.63	16.77	15.61	15.60	14.72	16.31	17.83	17.57	20.24	19.62
SF, Safety Factor	3.70	3.54	3.56	3.57	3.56	3.69	3.78	3.69	3.67	3.74

Notes: (1) The thickness for these bays corresponds to the localized thinned area.
(2) The load factor is taken from Table 8-1.

Table 8-8: Flooding Buckling Evaluation, Sandbed Region

	Bay 1[(1)]	Bay 3	Bay 5	Bay 7	Bay 9	Bay 11	Bay 13[(1)]	Bay 15[(1)]	Bay 17[(1)]	Bay 19[(1)]
R, Shell Radius (in)	420	420	420	420	420	420	420	420	420	420
t, Wall Thickness (in)	0.696	0.950	1.074	1.034	0.993	0.860	0.658	0.711	0.663	0.720
σ_y, Yield Strength (ksi)	36.3	36.3	36.3	36.3	36.3	36.3	36.3	36.3	36.3	36.3
E, Young's Modulus (ksi)	29,000	29,000	29,000	29,000	29,000	29,000	29,000	29,000	29,000	29,000
λ, Load Factor[(2)]	7.162	7.162	7.162	7.162	7.162	7.162	7.162	7.162	7.162	7.162
α/α_{1L}, Capacity Reduction Factor	0.209	0.229	0.238	0.235	0.232	0.223	0.207	0.210	0.207	0.211
σ_1, Meridional Compressive Stress (ksi)	11.78	9.45	9.95	10.04	10.20	11.18	11.33	10.13	11.43	12.23
σ_2, Hoop Tension Stress (ksi)	23.26	19.15	17.54	18.09	18.81	21.38	20.85	21.09	25.50	21.94
Pbar	0.484	0.292	0.237	0.253	0.274	0.360	0.459	0.430	0.557	0.441
α_p, Capacity Reduction Factor (due to tensile effect)	0.330	0.263	0.235	0.244	0.254	0.291	0.323	0.315	0.348	0.318
α_m, Modified Capacity Reduction Factor	0.539	0.492	0.473	0.479	0.486	0.514	0.530	0.525	0.555	0.529
Δ , Parameter (= $\alpha m \lambda \sigma_1 / \sigma_y$)	1.253	0.917	0.928	0.948	0.979	1.134	1.185	1.049	1.251	1.277
η, Plasticity Reduction Factor	0.539	0.671	0.665	0.654	0.640	0.577	0.560	0.609	0.540	0.532
σ_{ic}, Theoretical Buckling Stress (ksi)	24.52	22.33	22.40	22.53	22.73	23.75	24.08	23.19	24.51	24.68
SF, Safety Factor	2.08	2.36	2.25	2.24	2.23	2.12	2.13	2.29	2.14	2.02

Notes: (1) The thickness for these bays corresponds to the localized thinned area.
(2) The load factor is taken from Table 8-1.

Table 8-9: Summary of Buckling Safety Factors

(a) Refueling Case

Region		Safety Factor	Level A/B Allowable
Cylindrical		3.39	2.00
Spherical	Upper	4.27	2.00
	Middle	3.60	2.00
	Lower	3.60	2.00
Sandbed [1]		3.54	2.00

(1) The buckling safety factor is associated with Bay 3.

(b) Flooding Case

Region		Safety Factor	Level C Allowable
Cylindrical		3.46	1.67
Spherical	Upper	7.57	1.67
	Middle	4.76	1.67
	Lower	2.22	1.67
Sandbed [1]		2.02	1.67

(1) The buckling safety factor is associated with Bay 19.

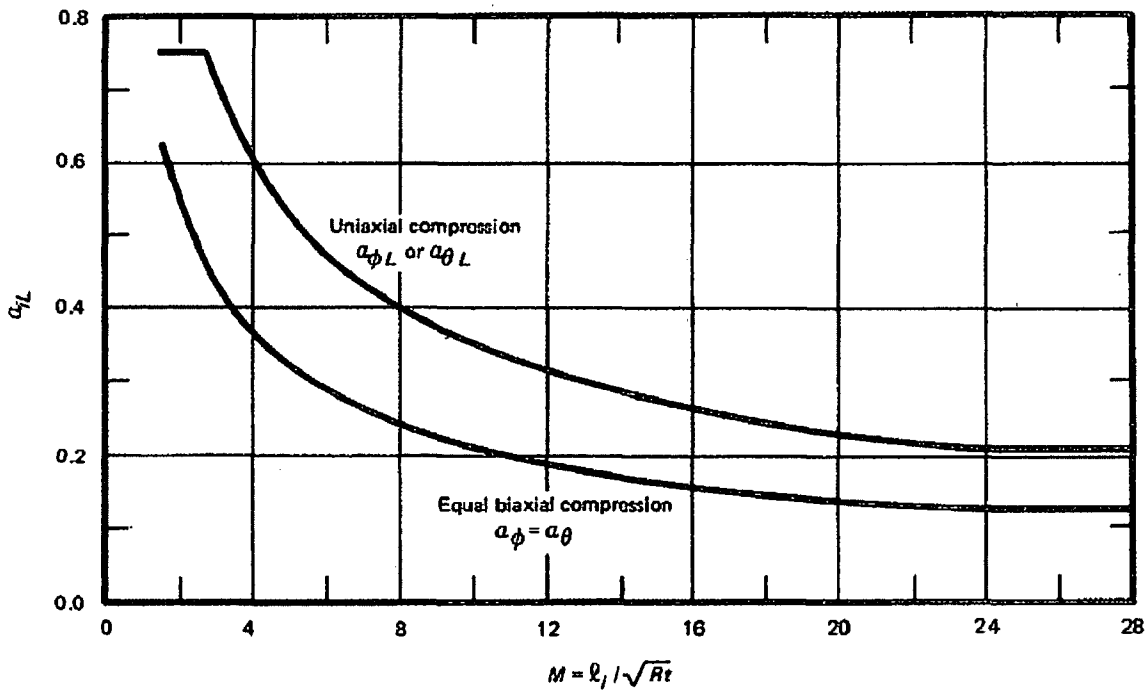

Figure 8-1: Capacity Reduction Factors for Local Buckling of Stiffened and Unstiffened Spherical Shells [24]

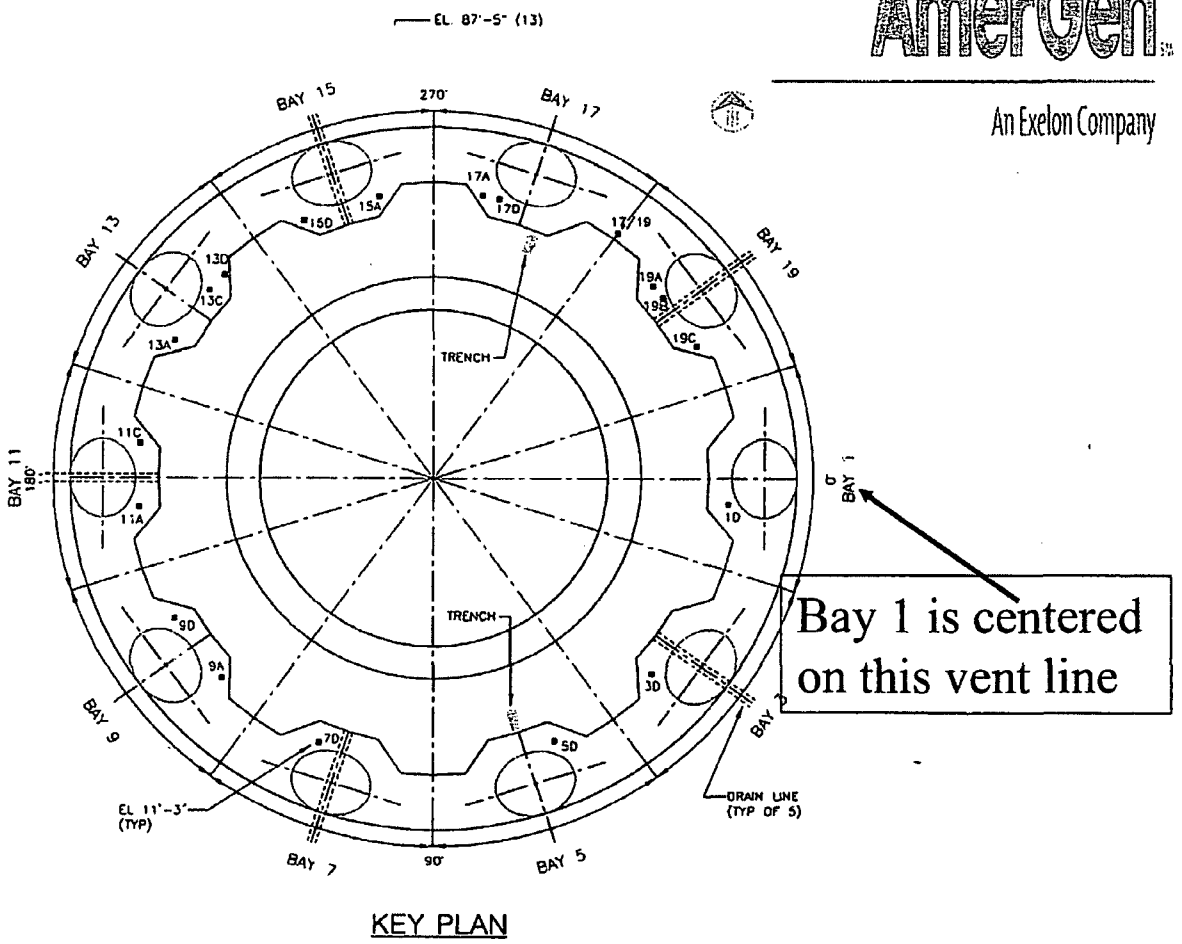

Figure 8-2: Identification of Bay Numbers in the Sandbed Region

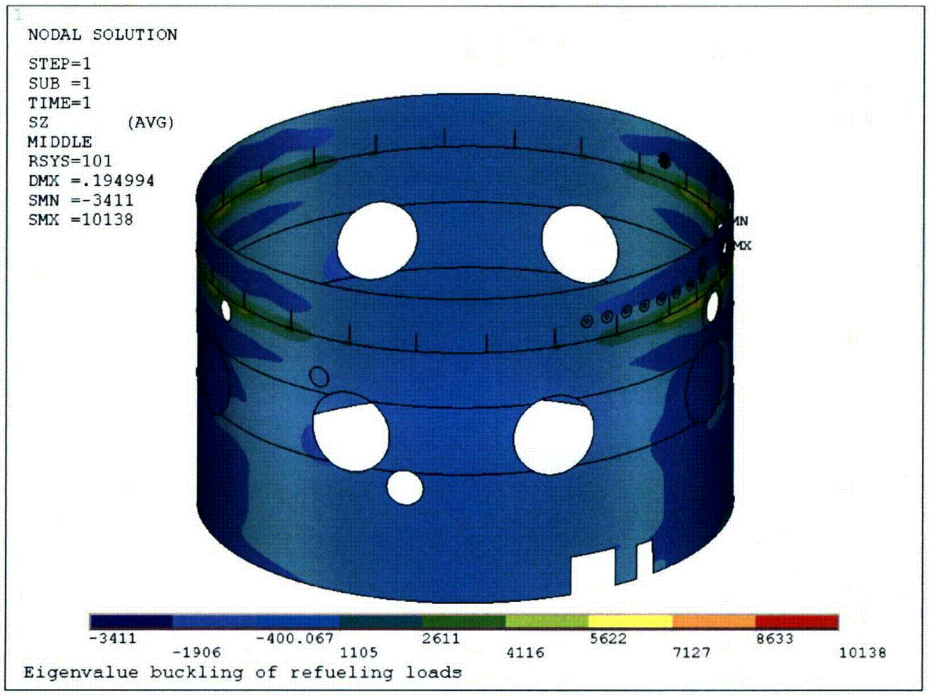

(a) Axial Stress

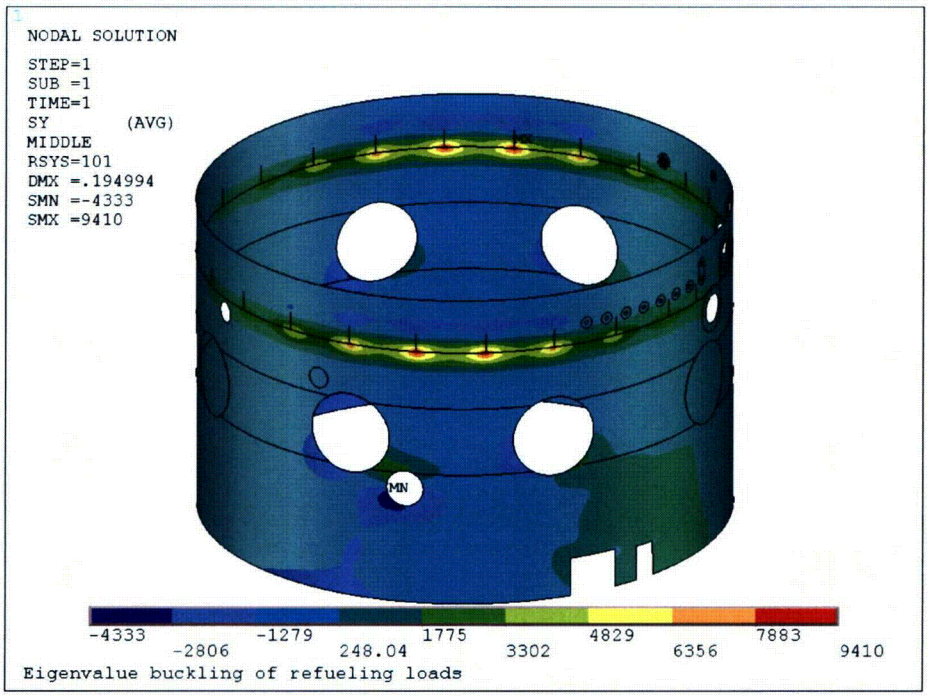

(b) Hoop Stress

Figure 8-3: Refueling Buckling Stress, Cylindrical Region

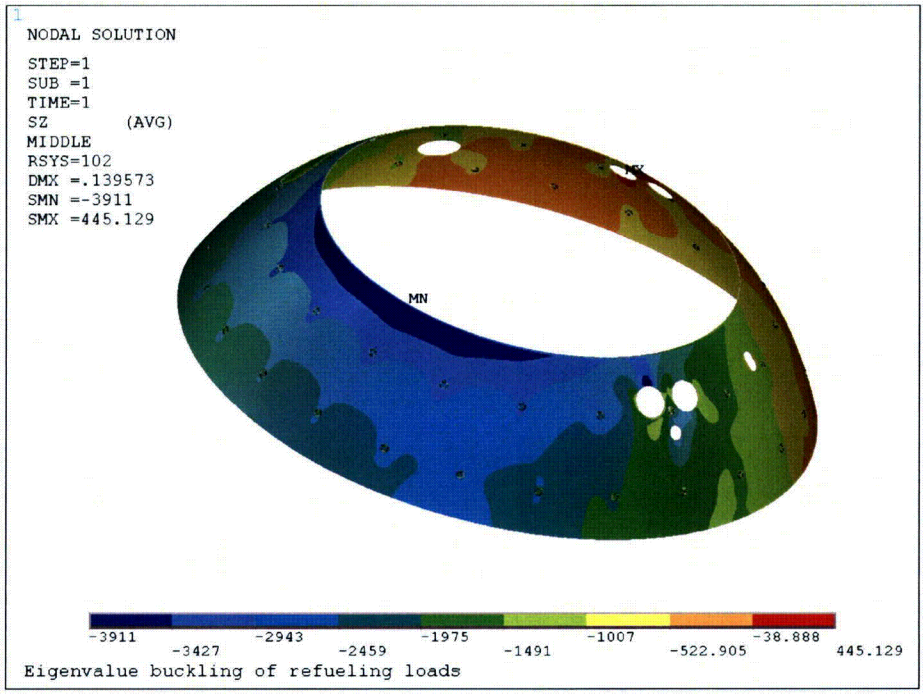

(a) Meridional Stress

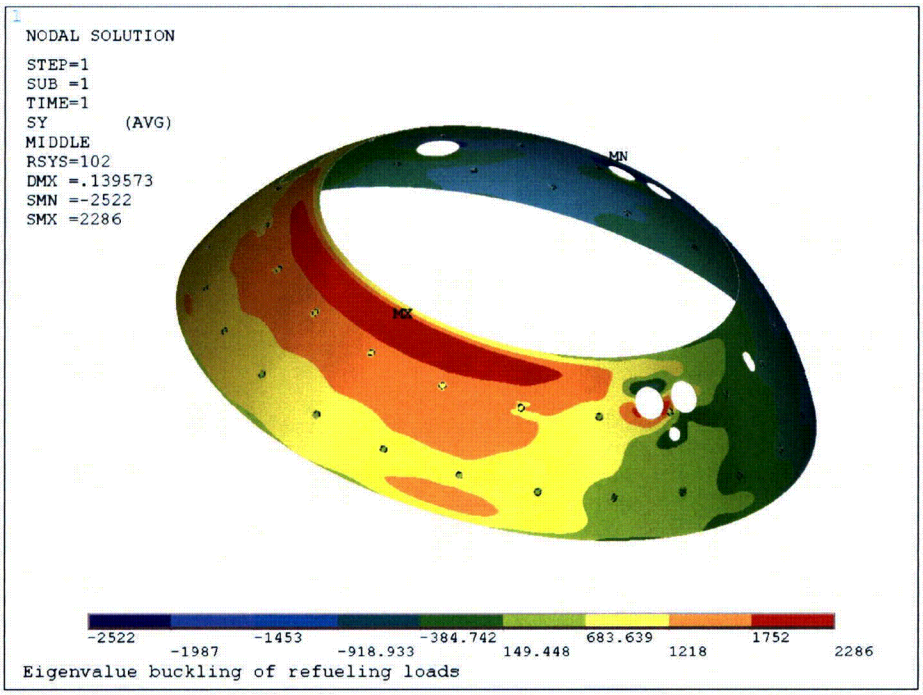

Hoop Stress

Figure 8-4: Refueling Buckling Stress, Upper Spherical Region

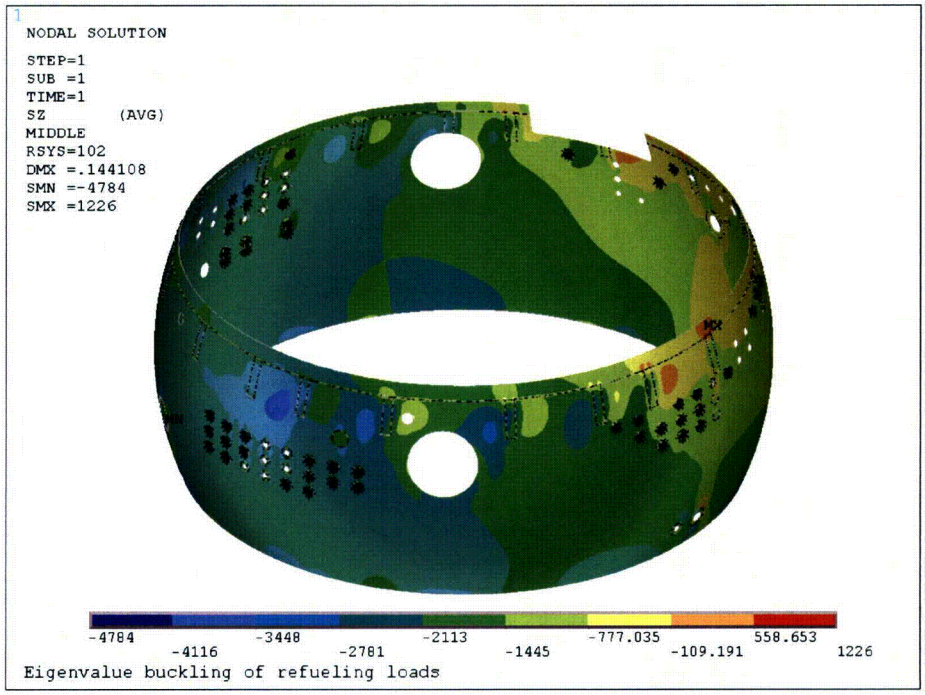

(a) Meridional Stress

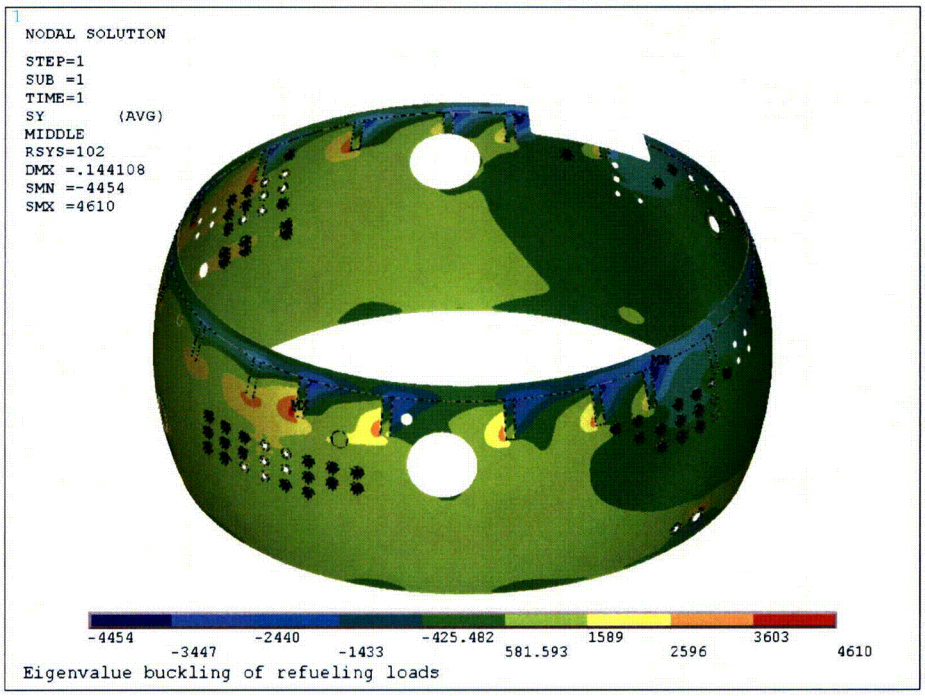

(b) Hoop Stress

Figure 8-5: Refueling Buckling Stress, Middle Spherical Region

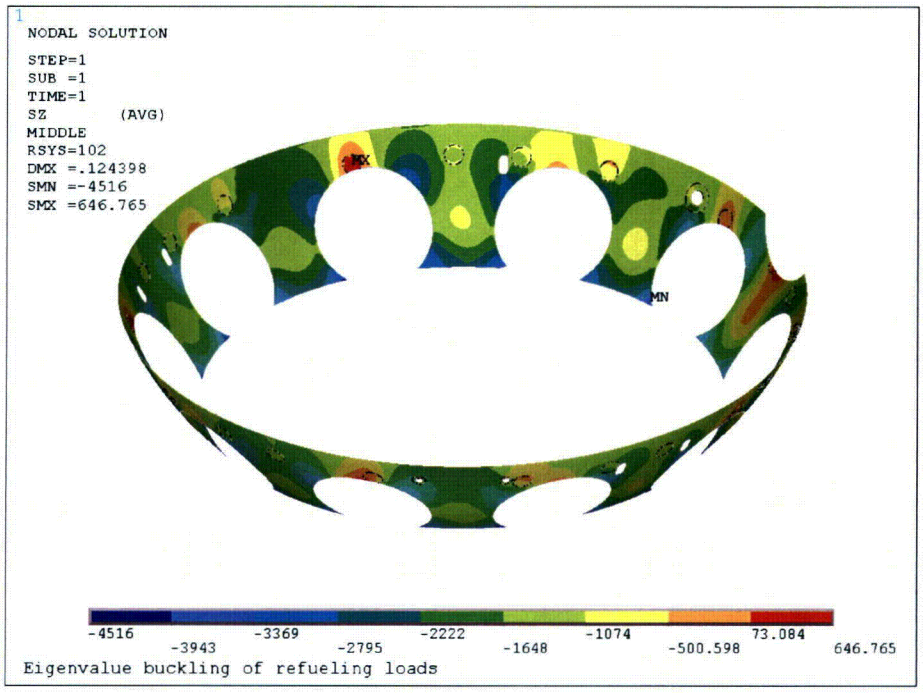

(a)Meridional Stress

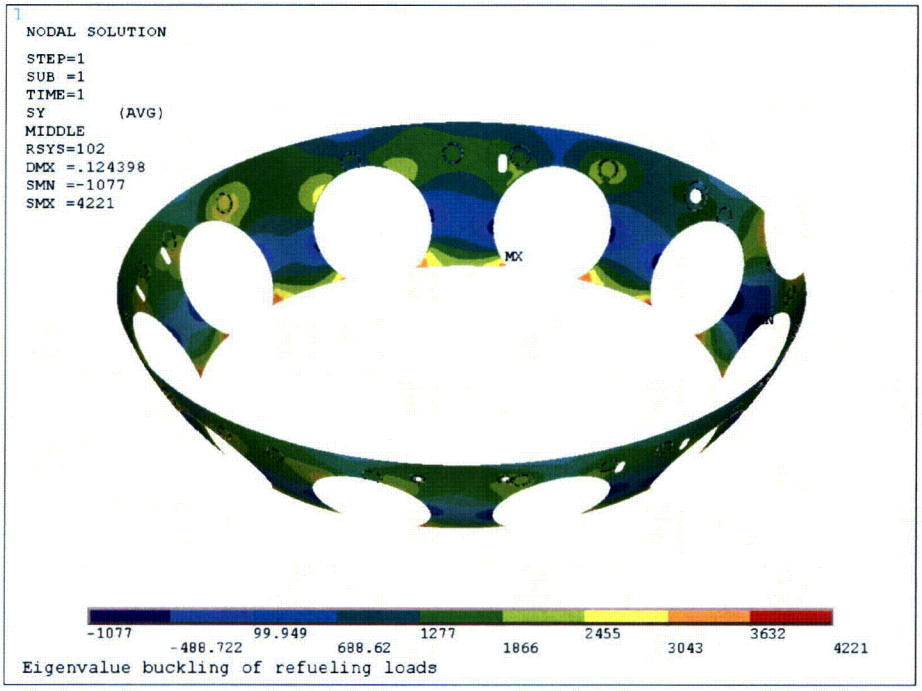

(b) Hoop Stress

Figure 8-6: Refueling Buckling Stress, Lower Spherical Region

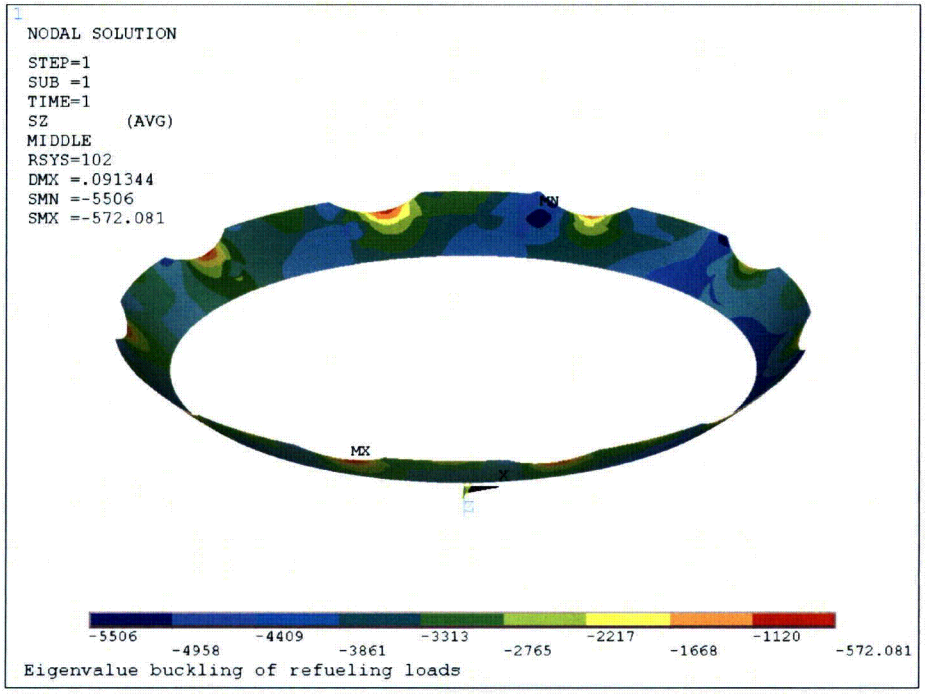

(a) Meridional

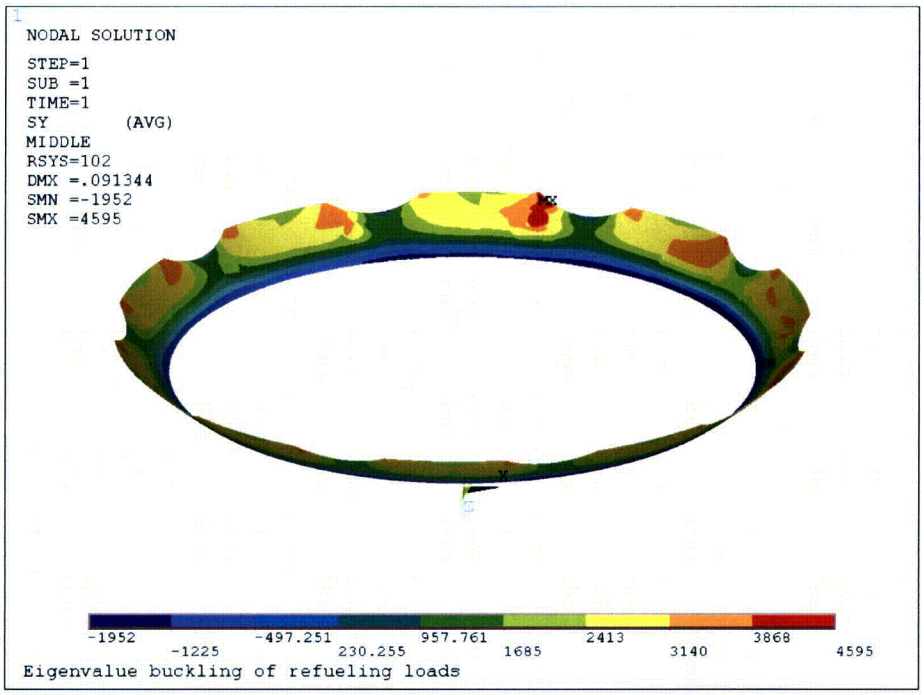

Hoop Stress

Figure 8-7: Refueling Buckling Stress, Sandbed Region

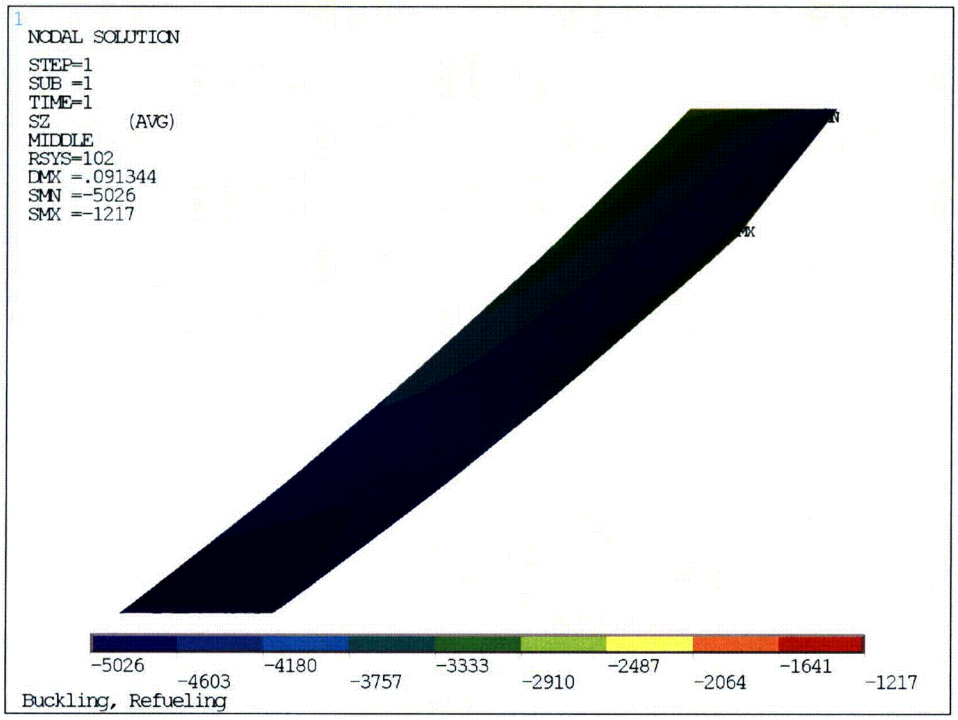

(a) Meridional Stress

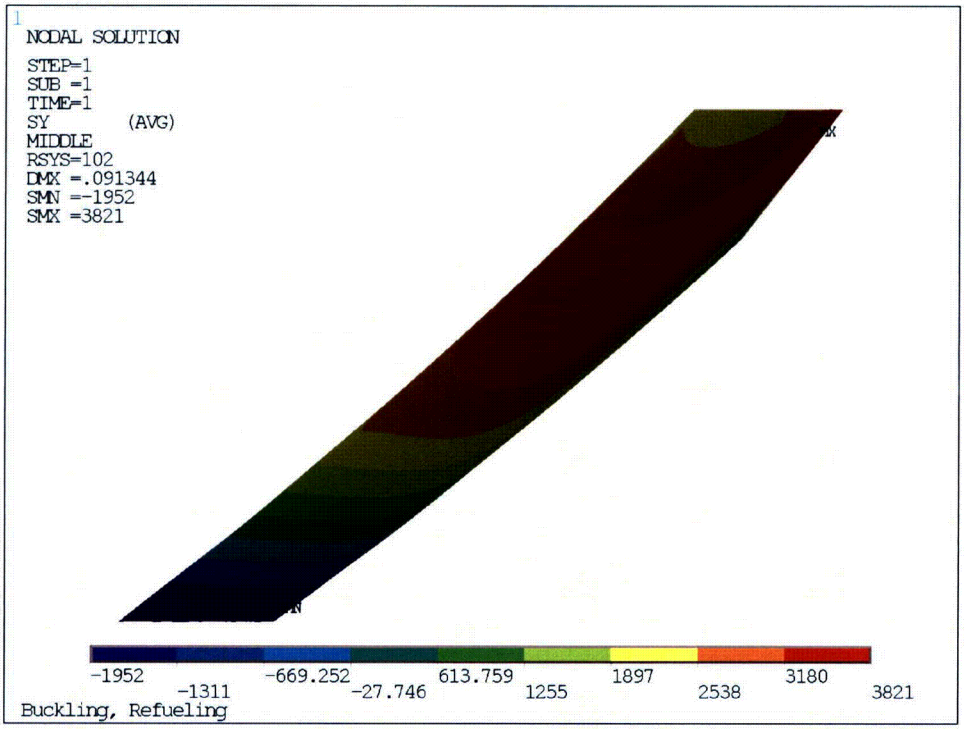

(b) Hoop Stress

Figure 8-8: Refueling Buckling Stress, Bay 1 Sandbed Region

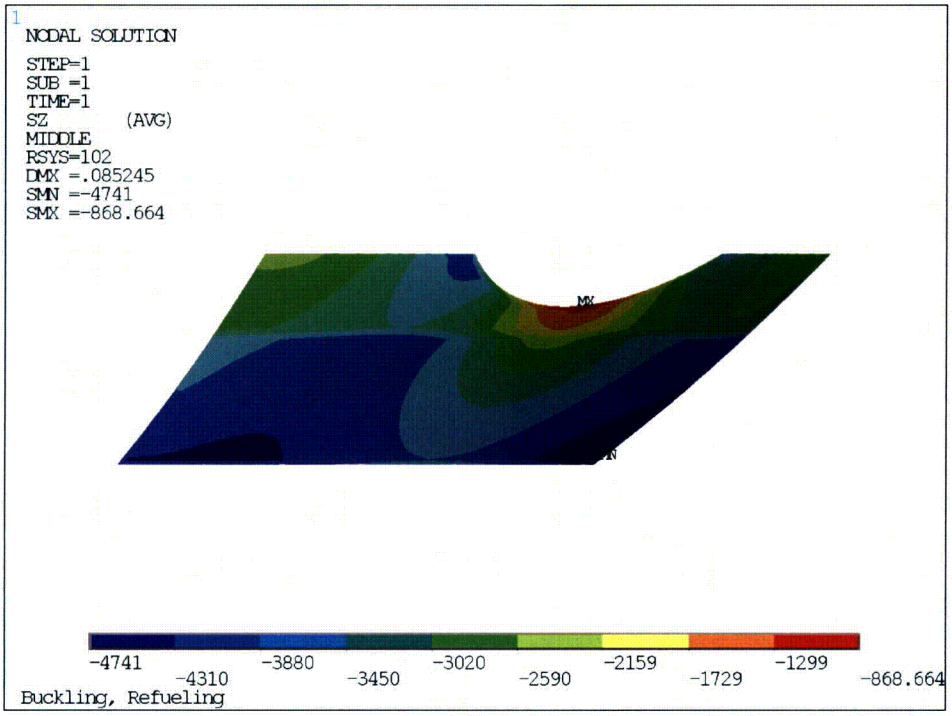

(a) Meridional Stress

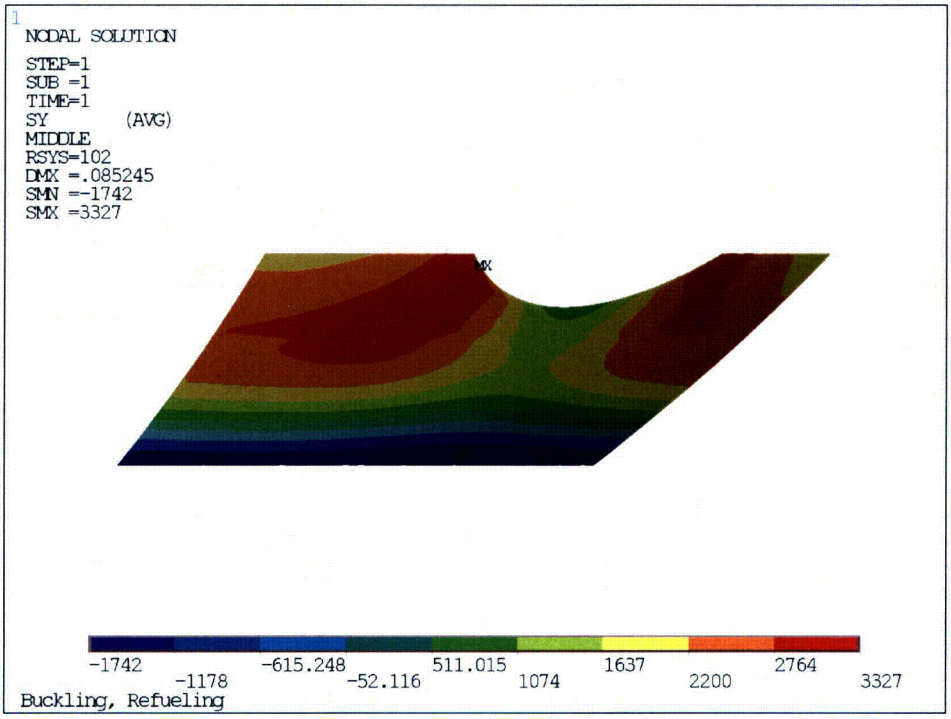

(b) Hoop Stress

Figure 8-9: Refueling Buckling Stress, Bay 3 Sandbed Region

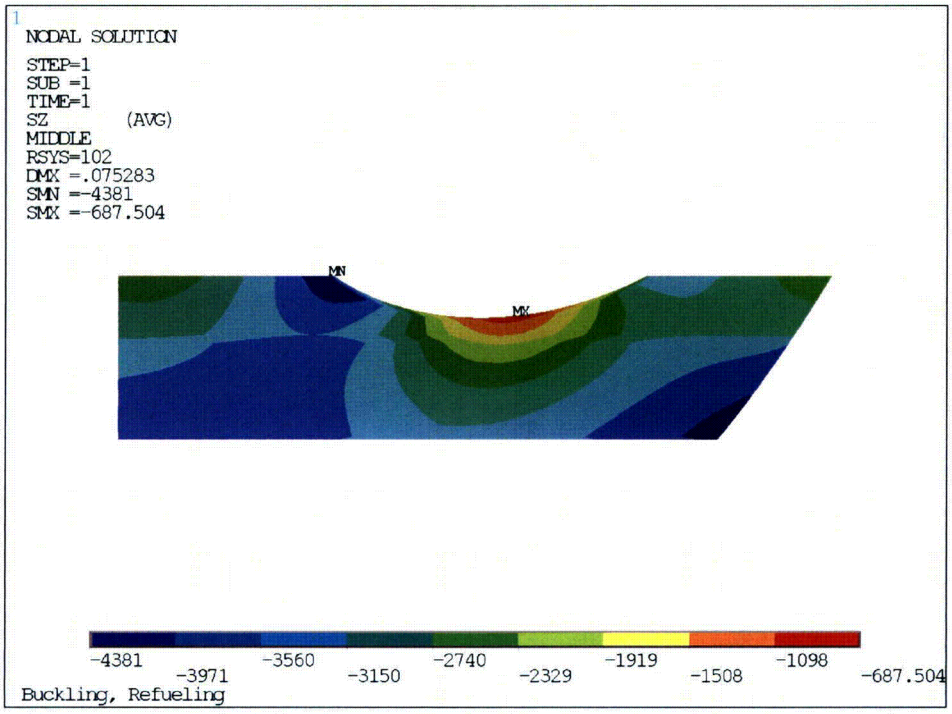

(a) Meridional Stress

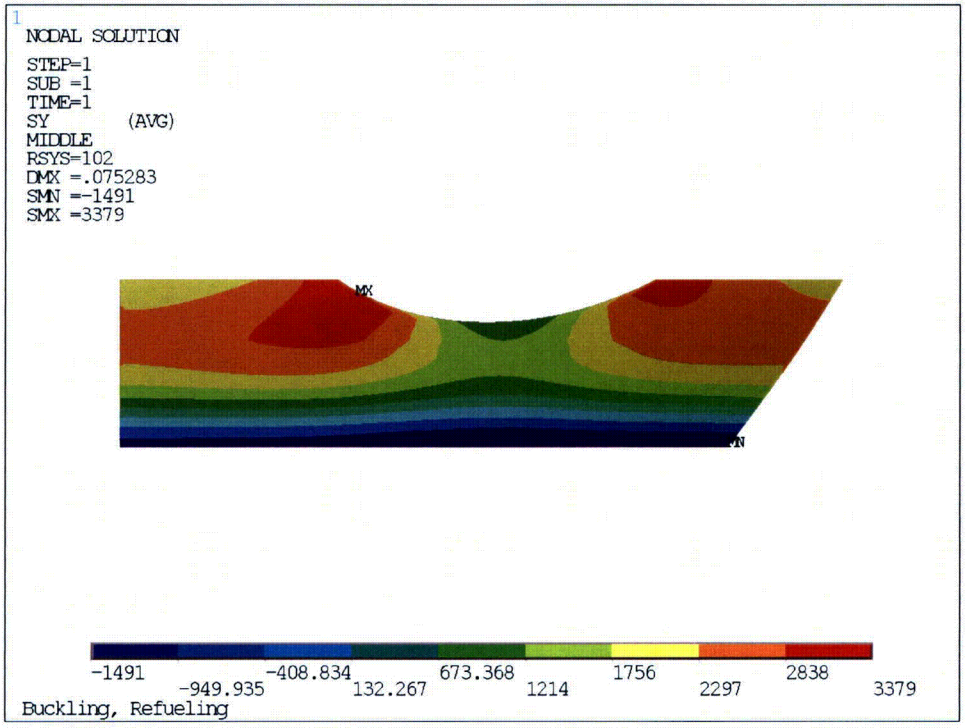

(b) Hoop Stress

Figure 8-10: Refueling Buckling Stress, Bay 5 Sandbed Region

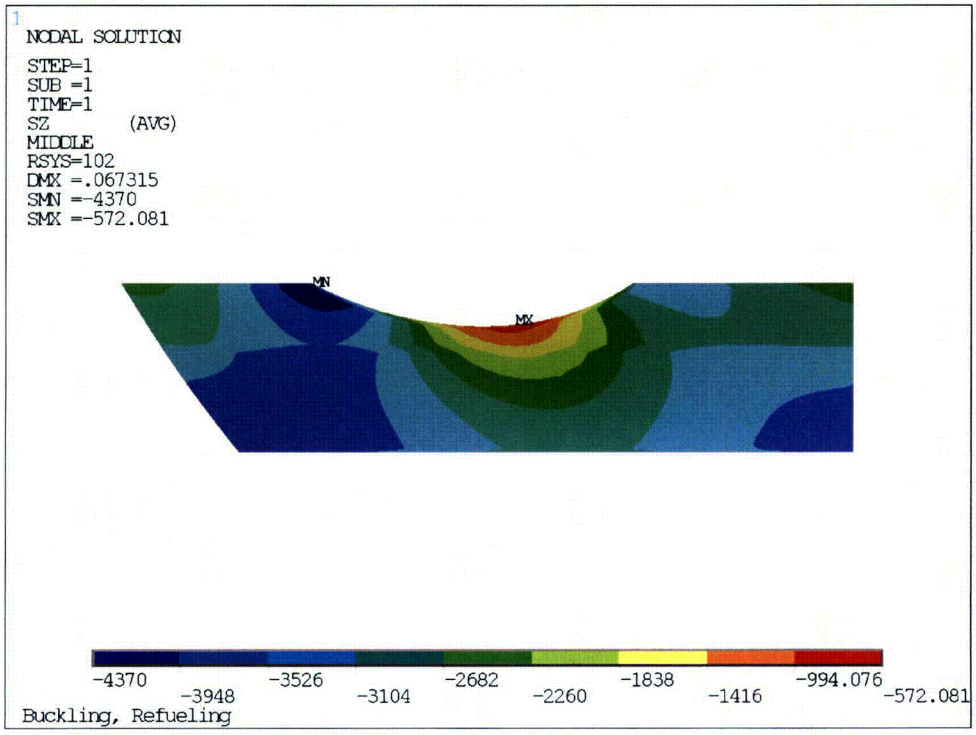

(a) Meridional Stress

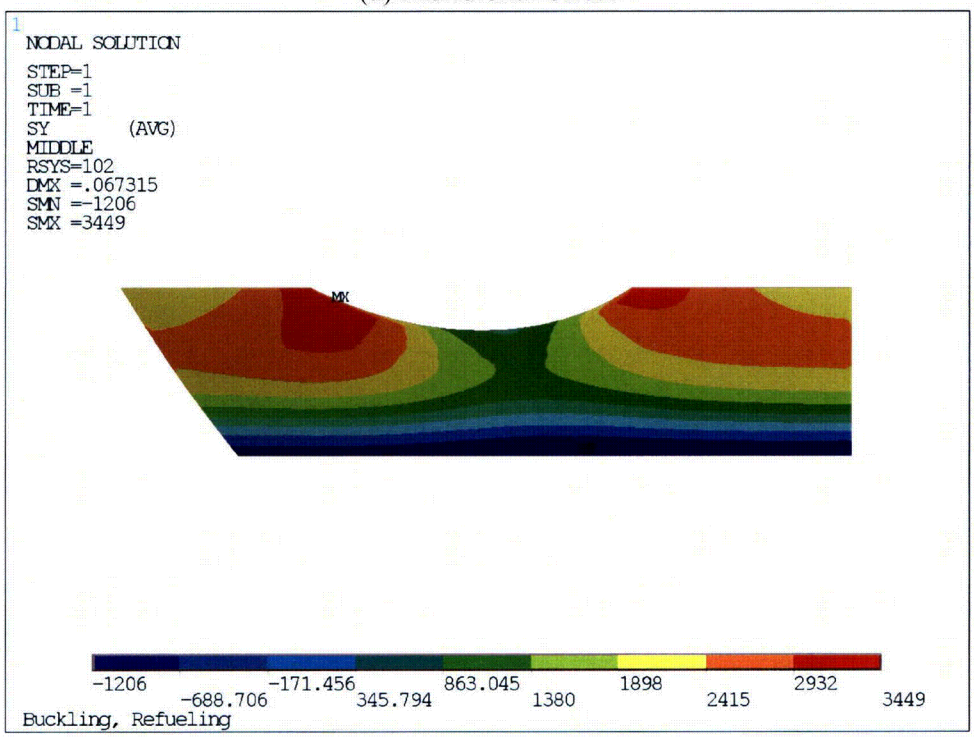

(b) Hoop Stress

Figure 8-11: Refueling Buckling Stress, Bay 7 Sandbed Region

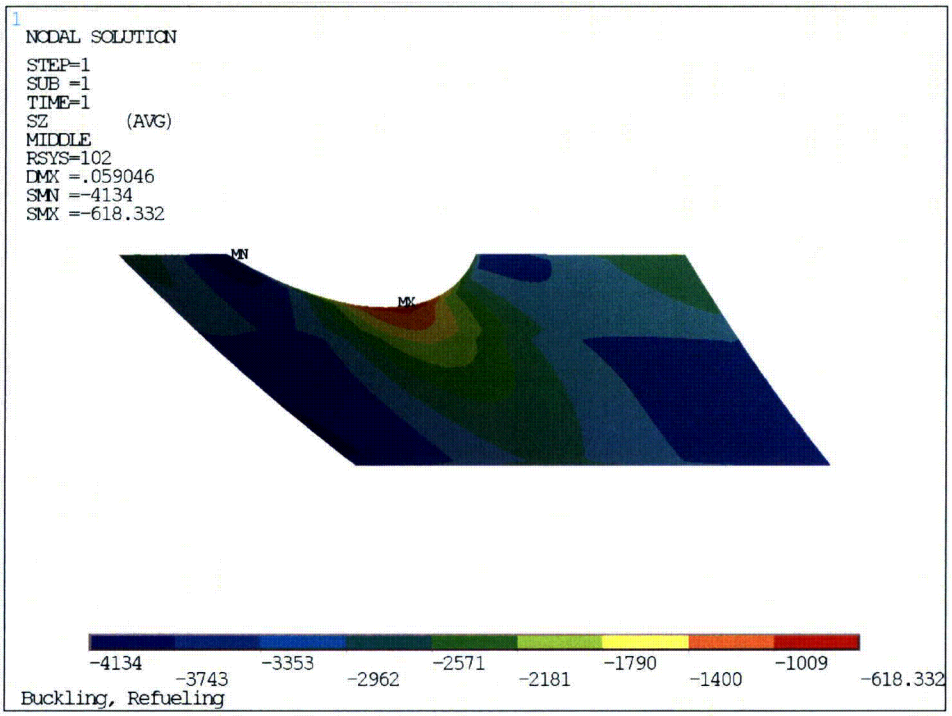

(a) Meridional Stress

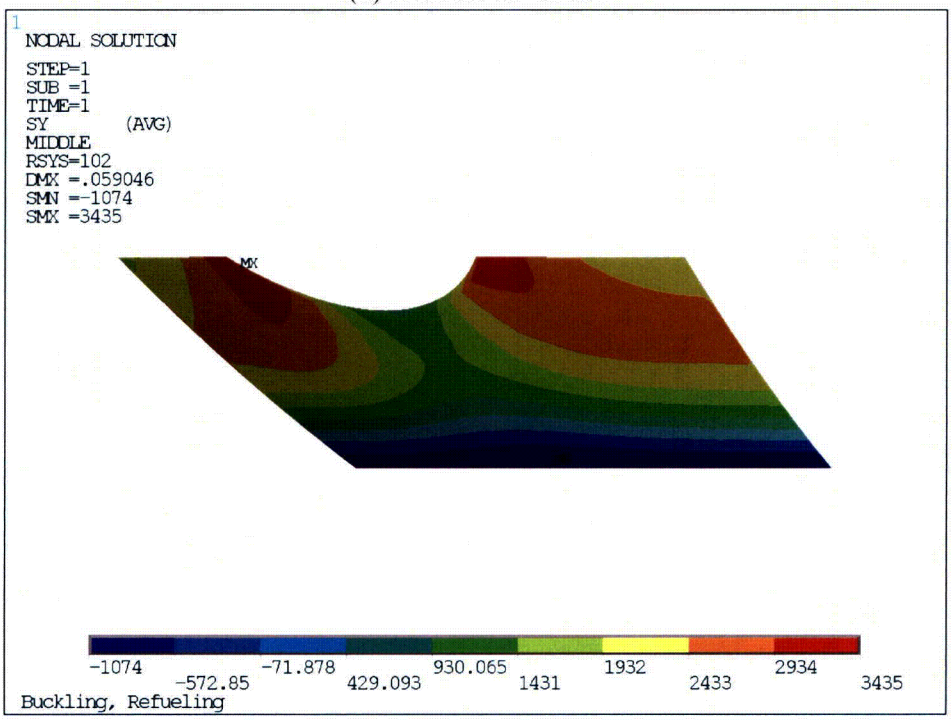

(b) Hoop Stress

Figure 8-12: Refueling Buckling Stress, Bay 9 Sandbed Region

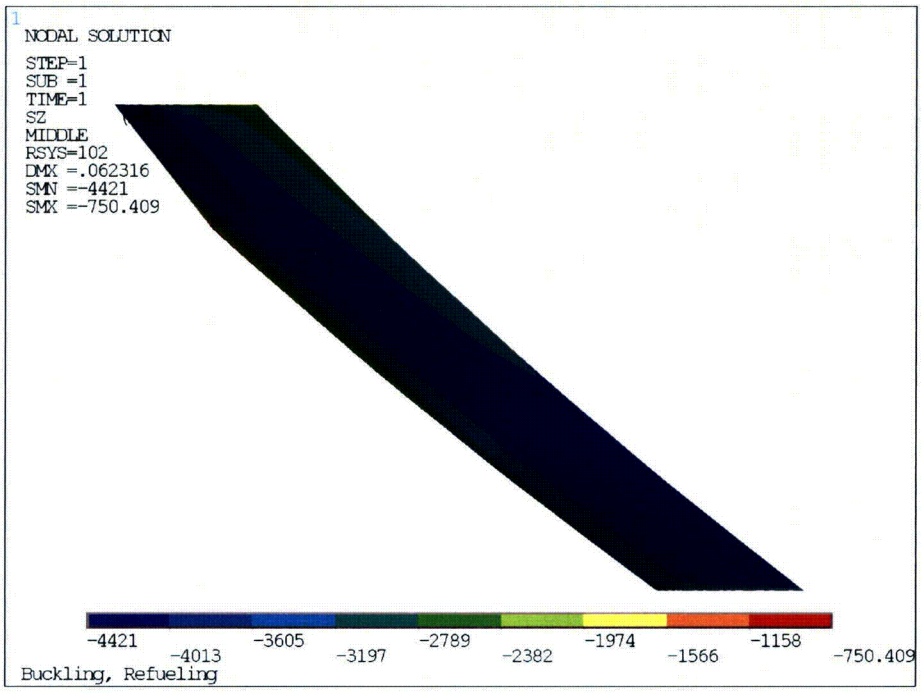

(a) Meridional Stress

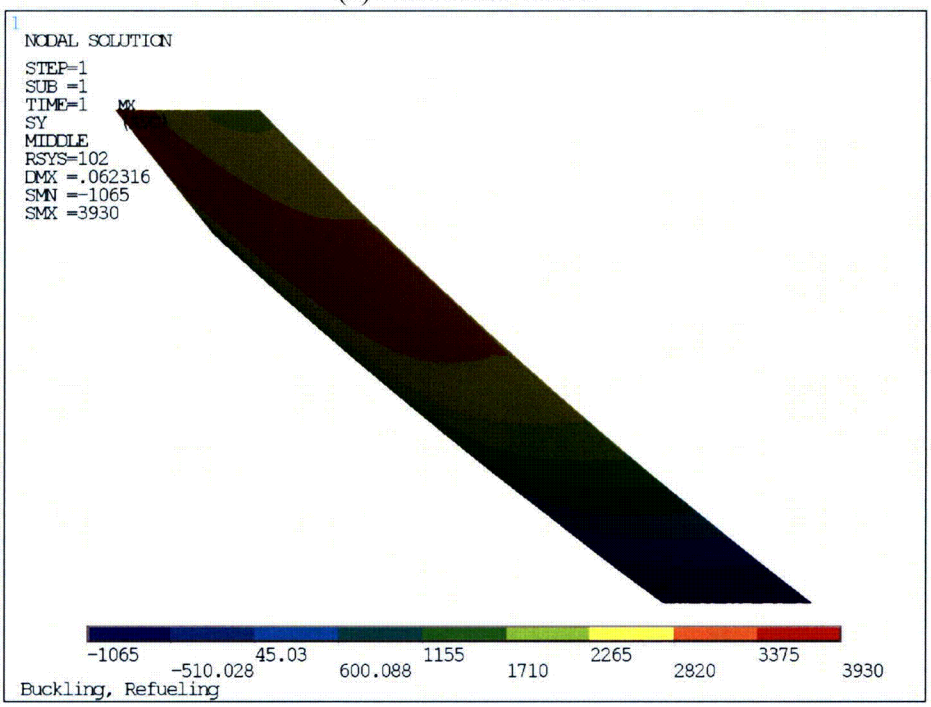

(b) Hoop Stress

Figure 8-13: Refueling Buckling Stress, Bay 11 Sandbed Region

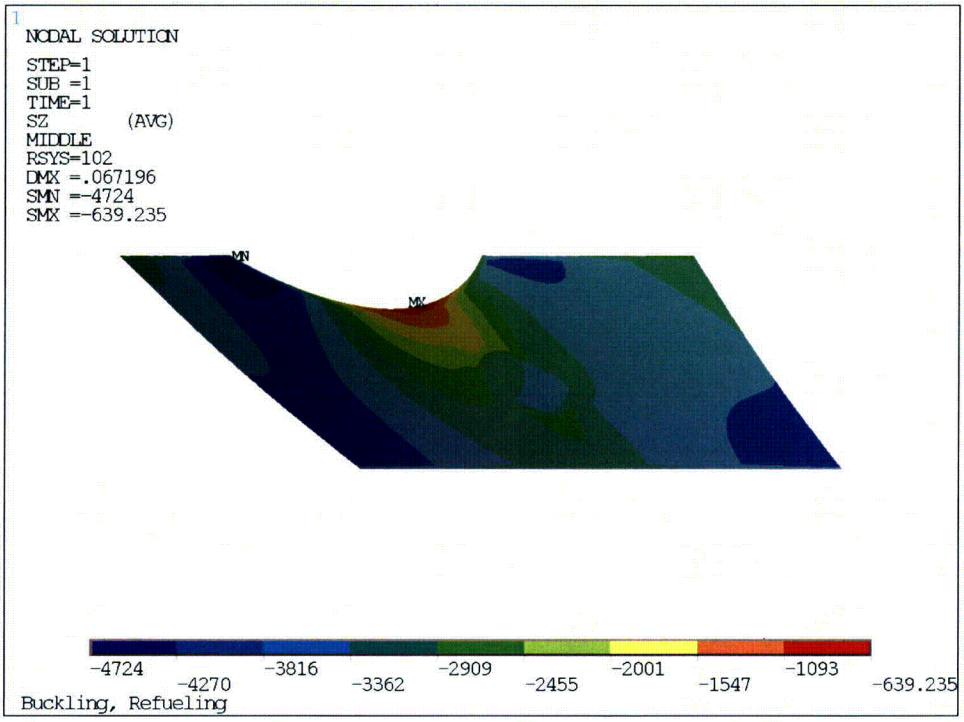

(a) Meridional Stress

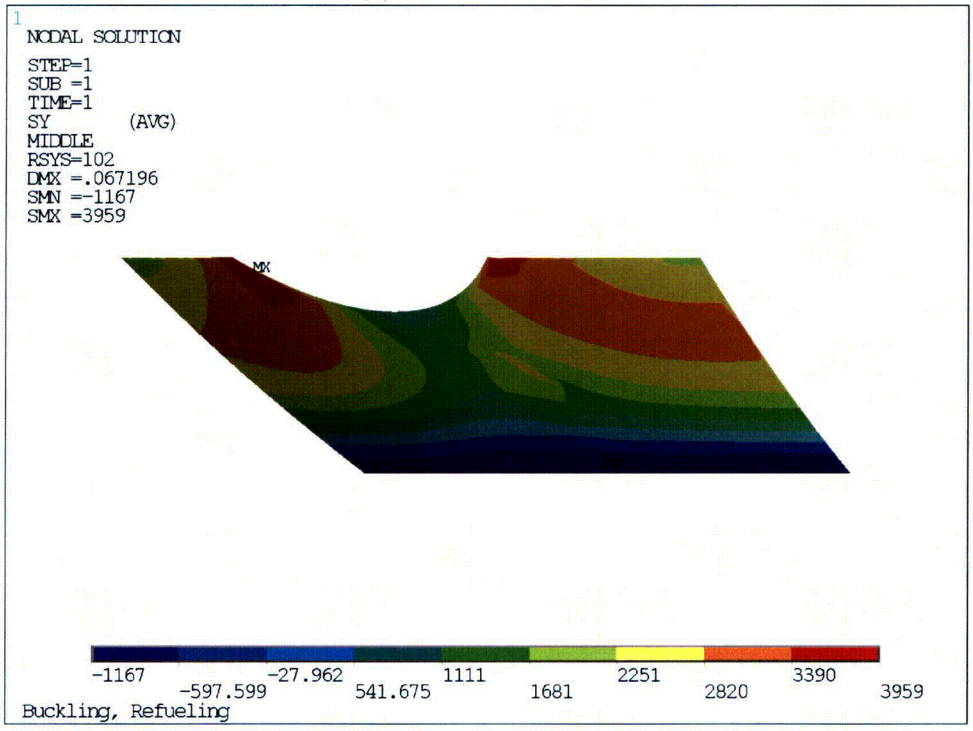

(b) Hoop Stress

Figure 8-14: Refueling Buckling Stress, Bay 13 Sandbed Region

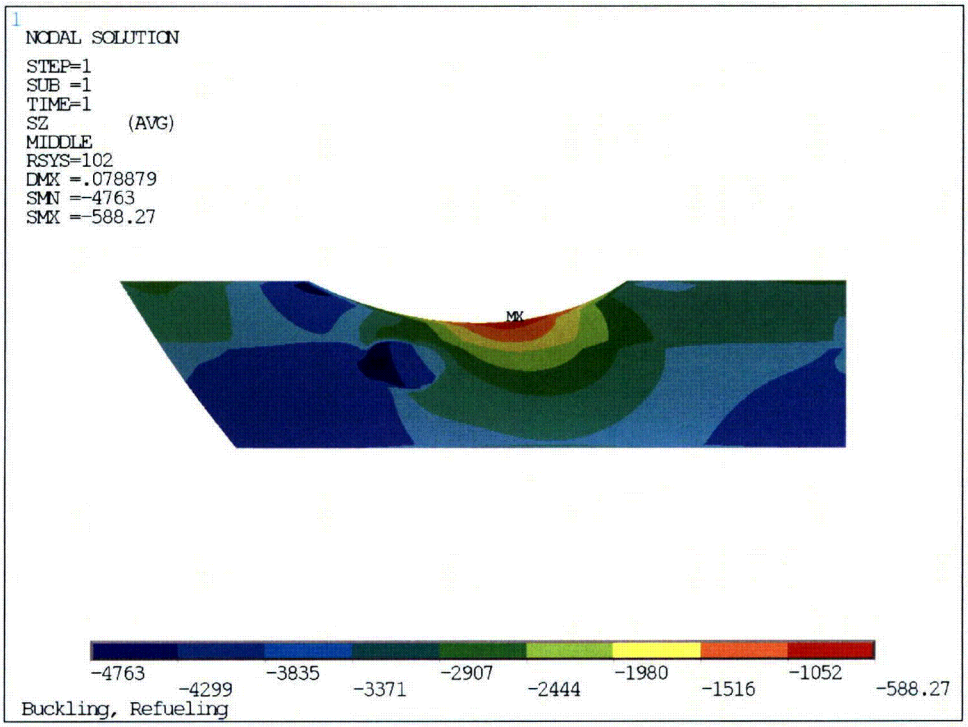

(a) Meridional Stress

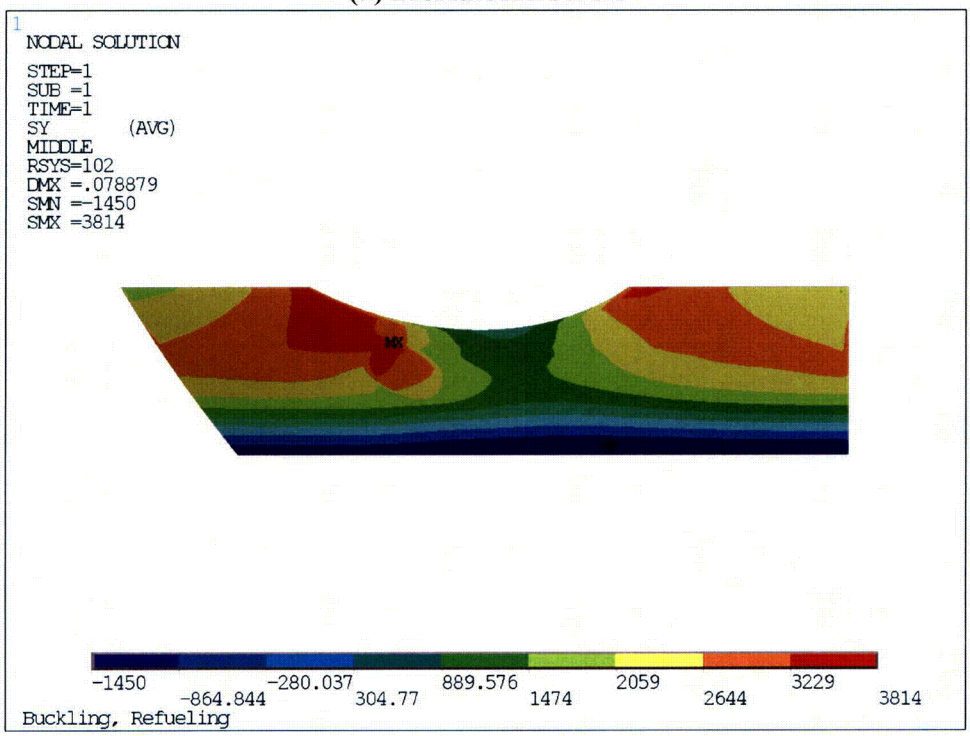

(b) Hoop Stress

Figure 8-15: Refueling Buckling Stress, Bay 15 Sandbed Region

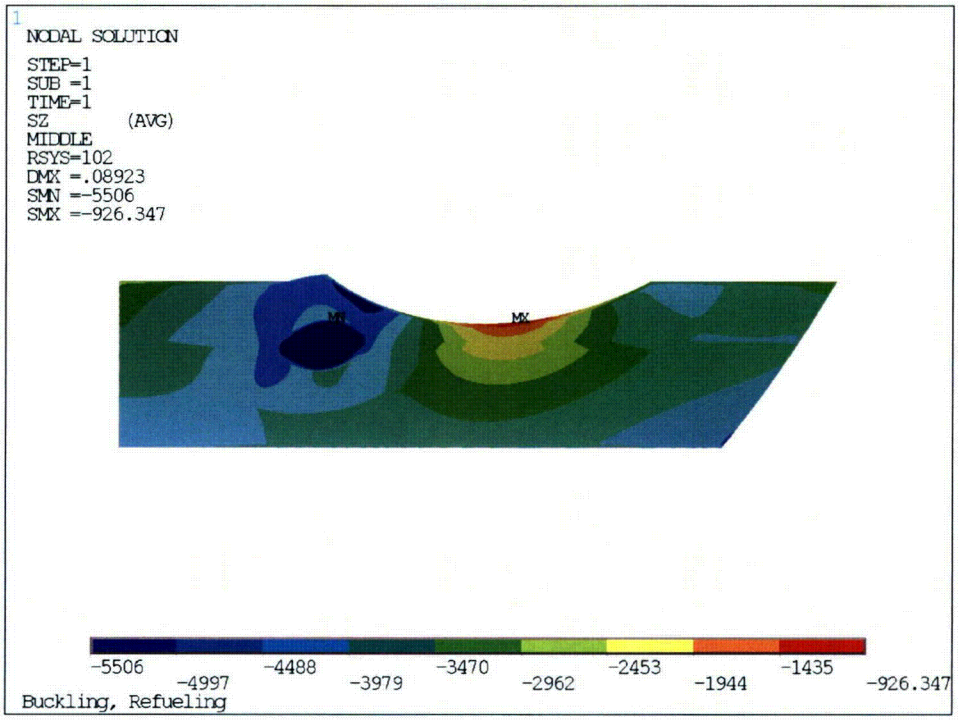

(a) Meridional Stress

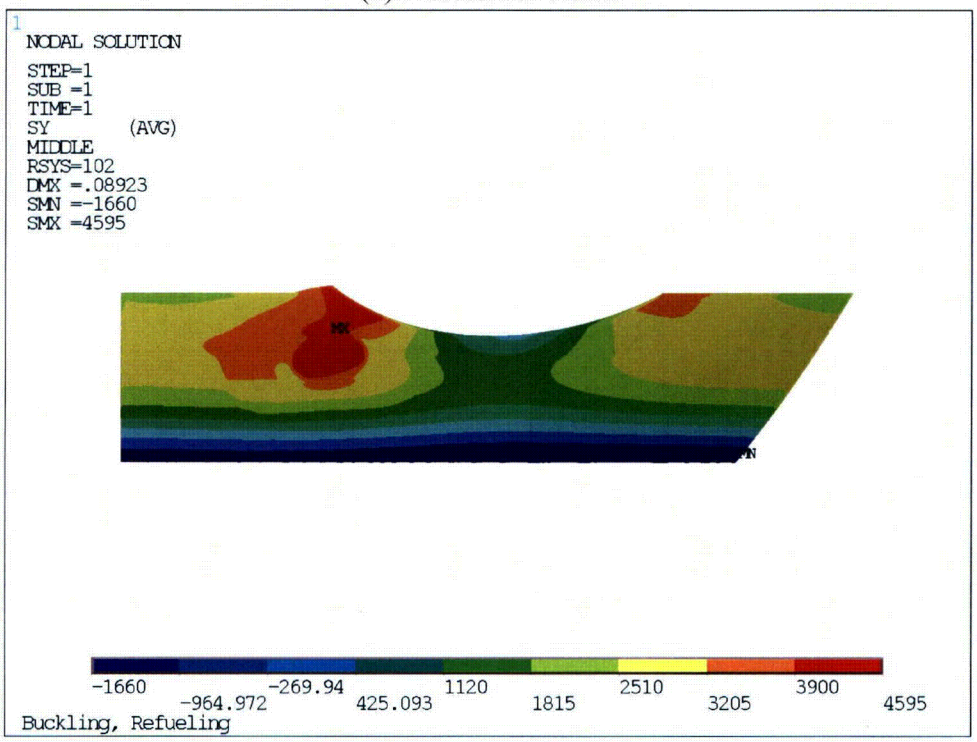

(b) Hoop Stress

Figure 8-16: Refueling Buckling Stress, Bay 17 Sandbed Region

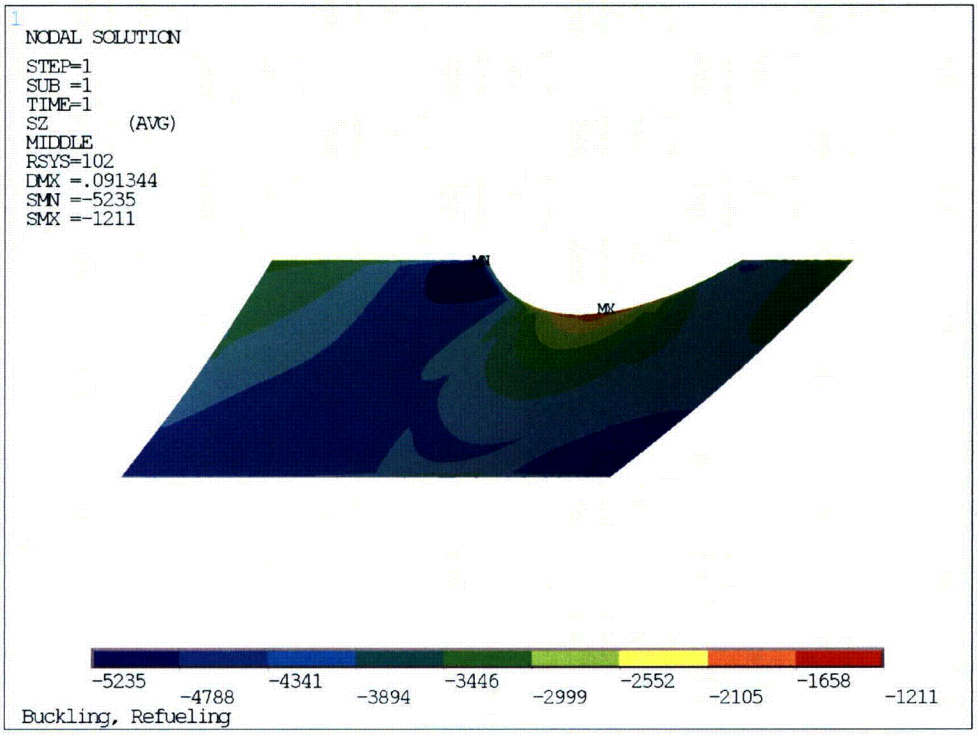

(a) Meridional Stress

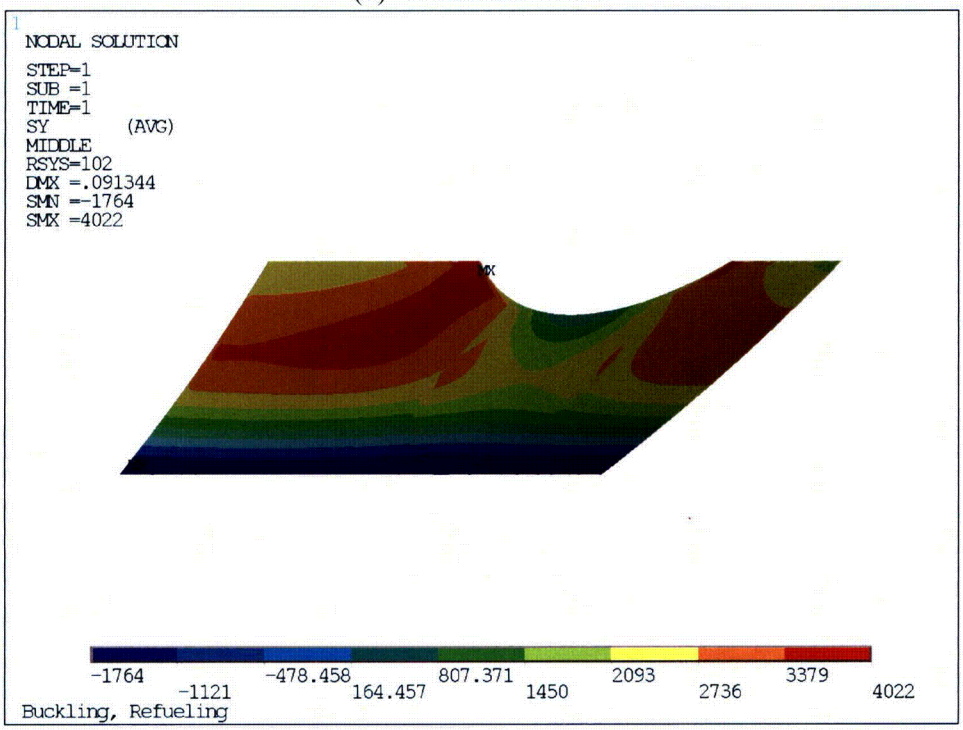

(b) Hoop Stress

Figure 8-17 Refueling Buckling Stress, Bay 19 Sandbed Region

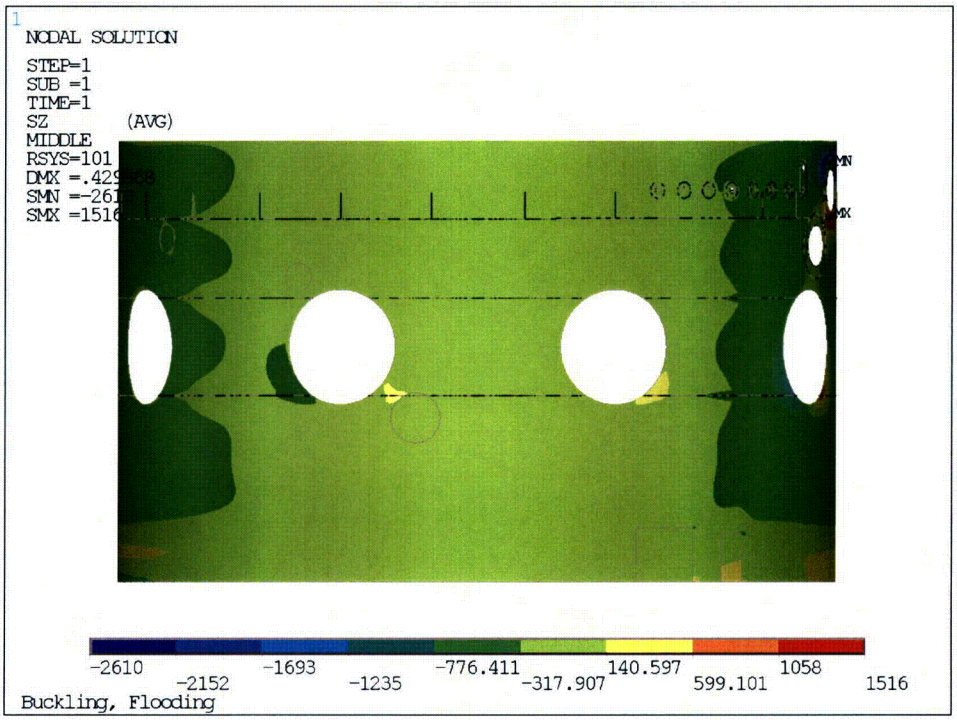

(a) Meridional Stress

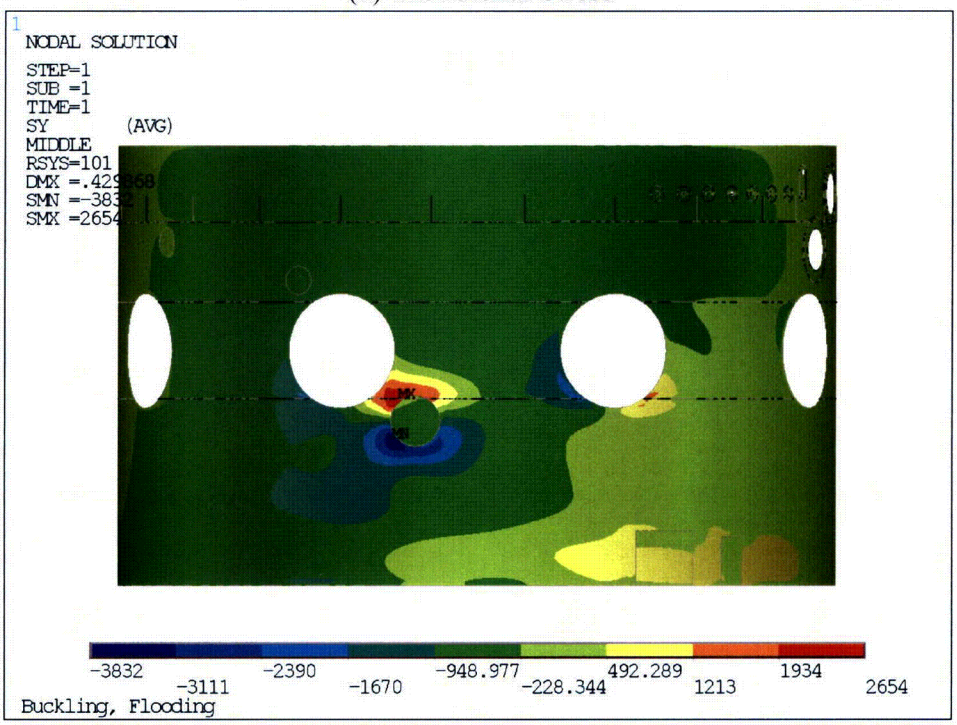

(b) Hoop Stress

Figure 8-18: Flooding Buckling Stress, Cylindrical Region

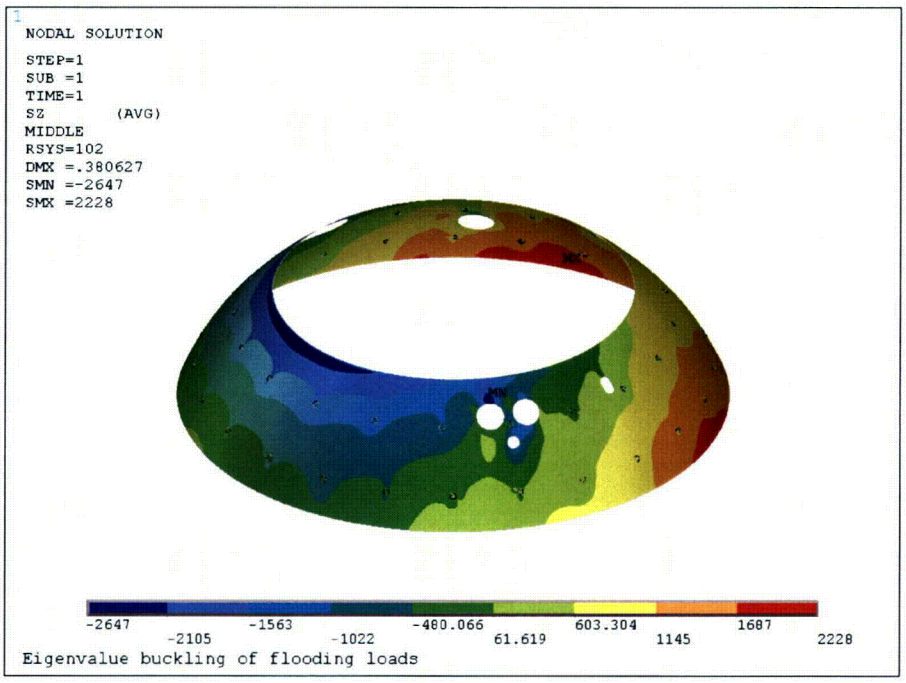

(b) Meridional Stress

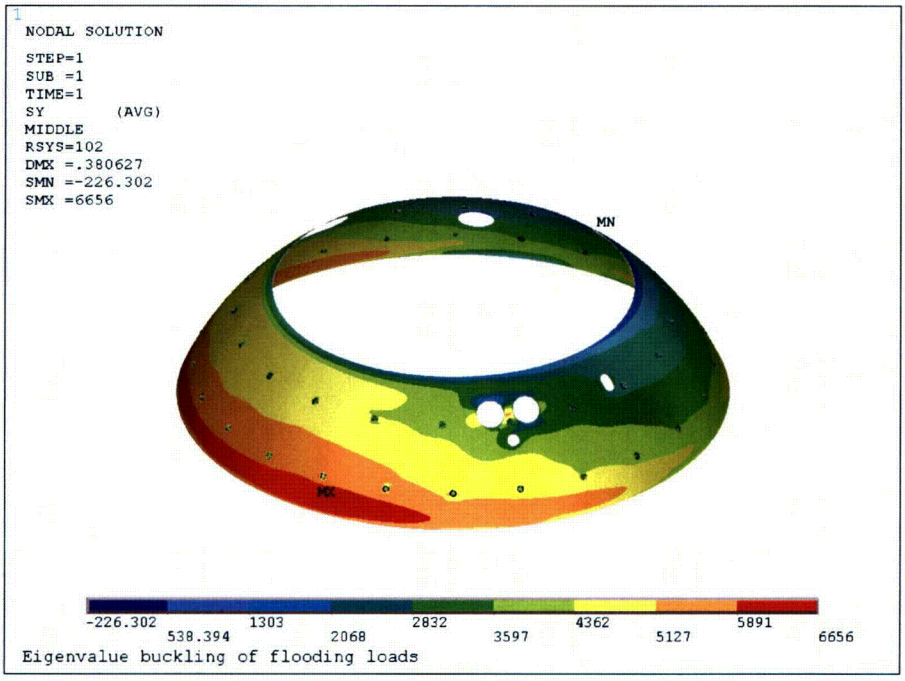

(b) Hoop Stress

Figure 8-19: Flooding Buckling Stress, Upper Spherical Region

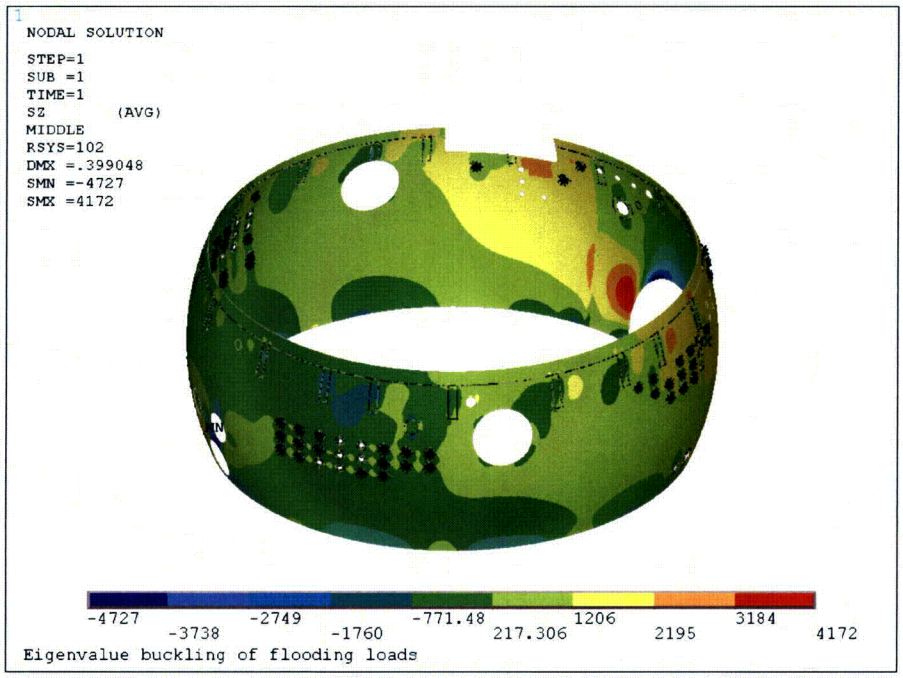

(c) Meridional Stress

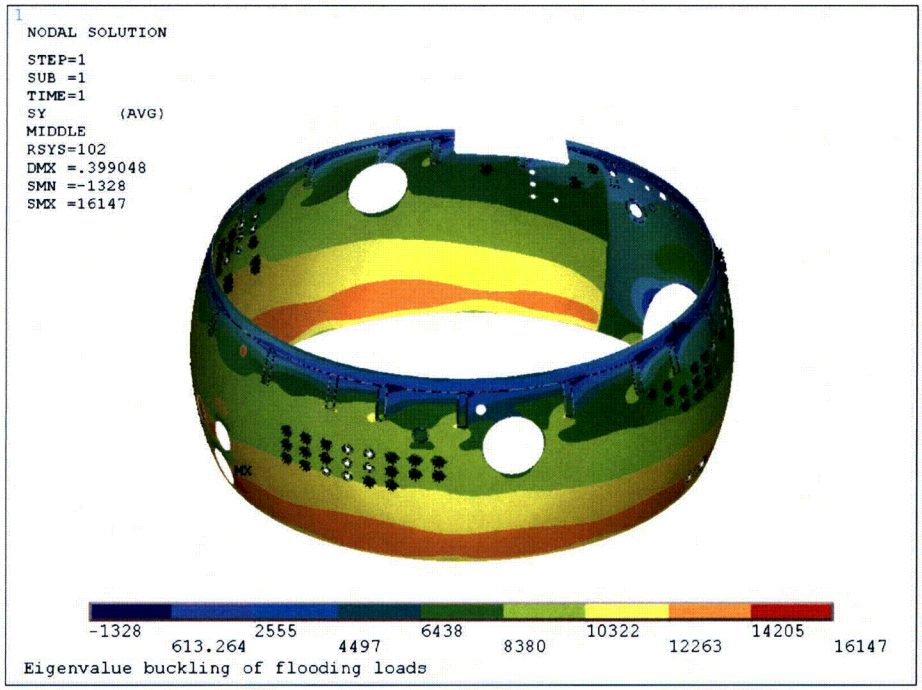

(b) Hoop Stress

Figure 8-20: Flooding Buckling Stress, Middle Spherical Region

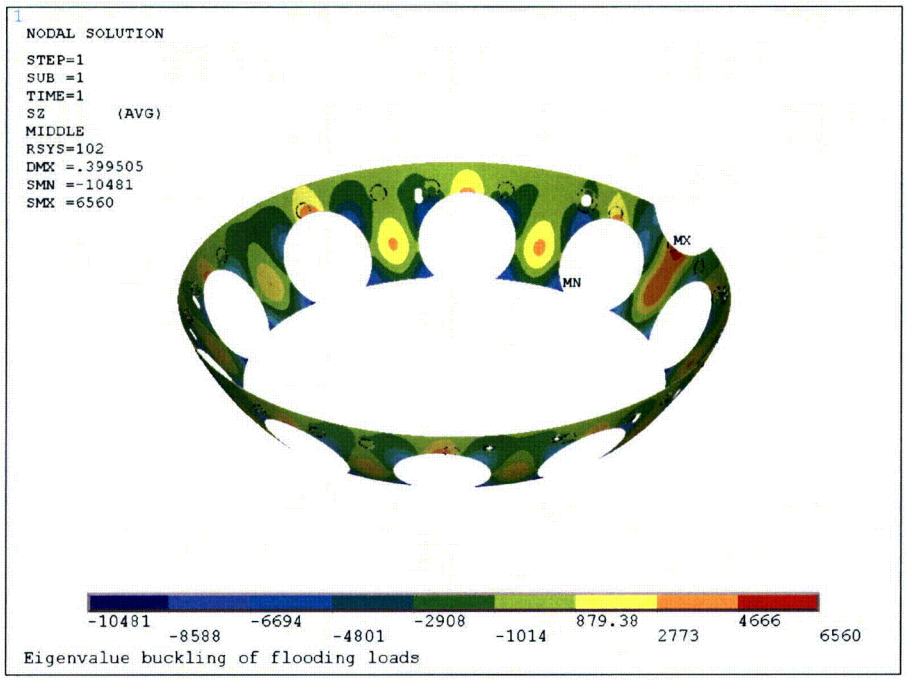

(d) Meridional Stress

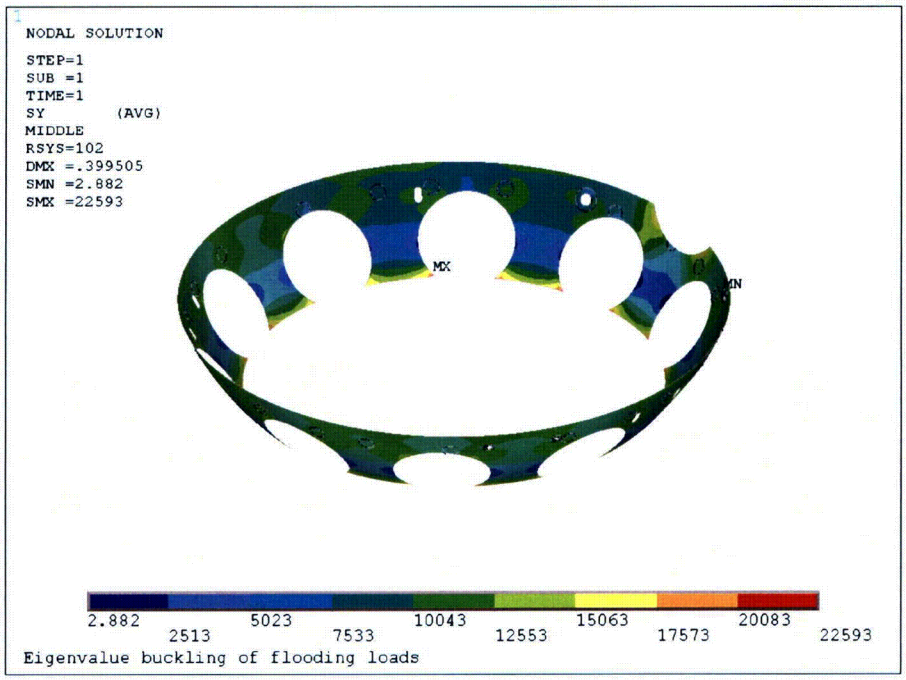

(b) Hoop Stress

Figure 8-21: Flooding Buckling Stress, Lower Spherical Region

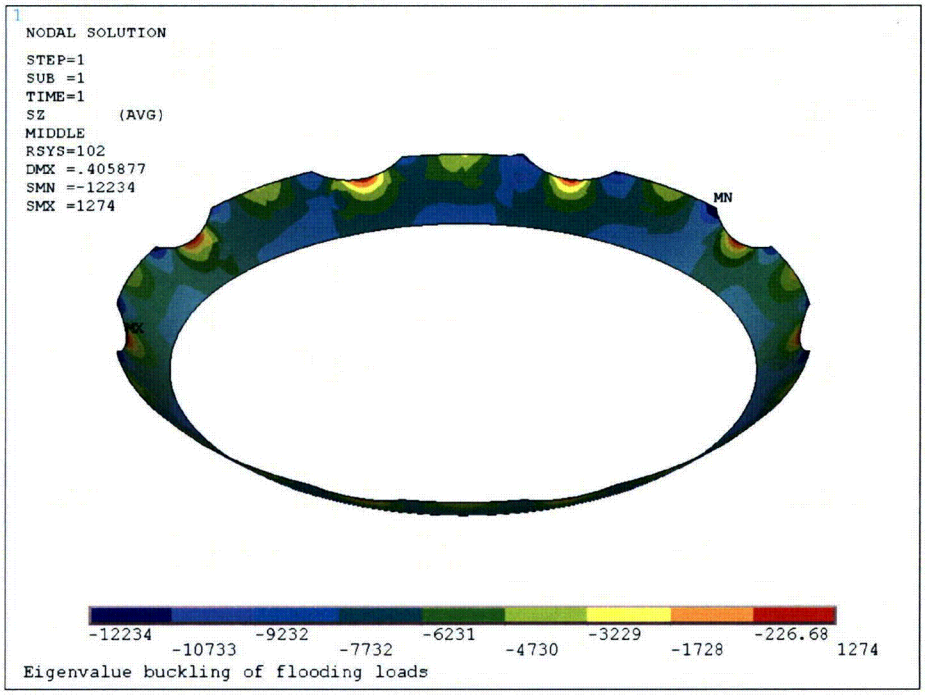

(a) Meridional Stress

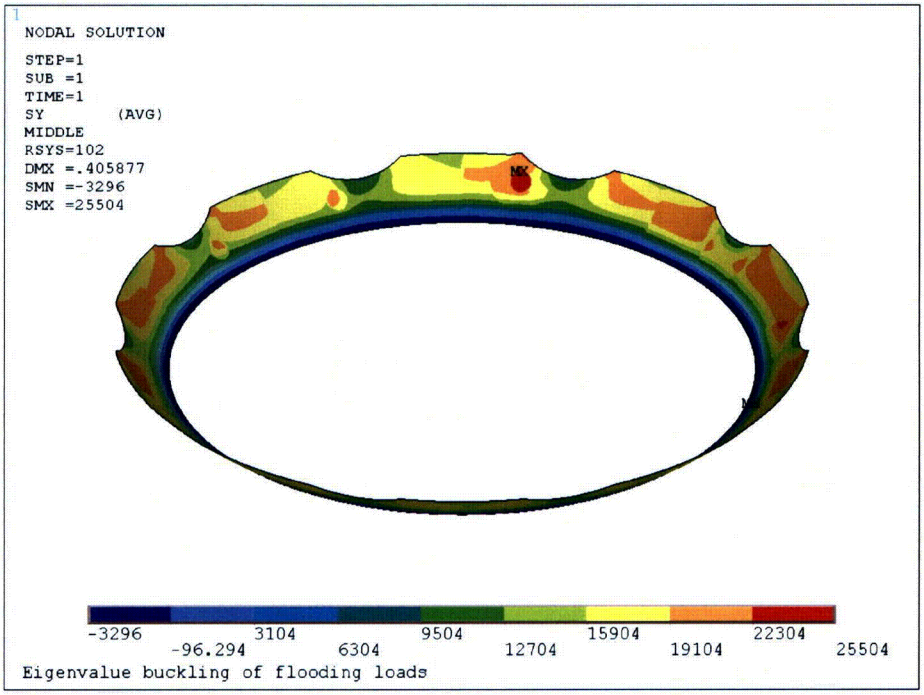

(b) Hoop Stress

Figure 8-22: Flooding Buckling Stress, Sandbed Region

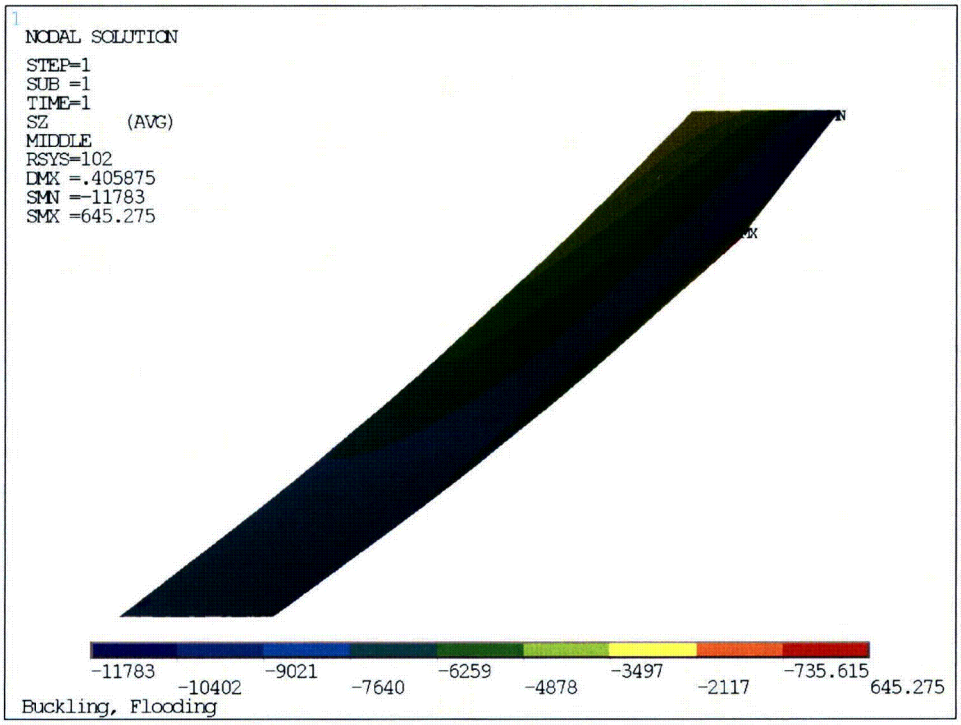

(a) Meridional Stress

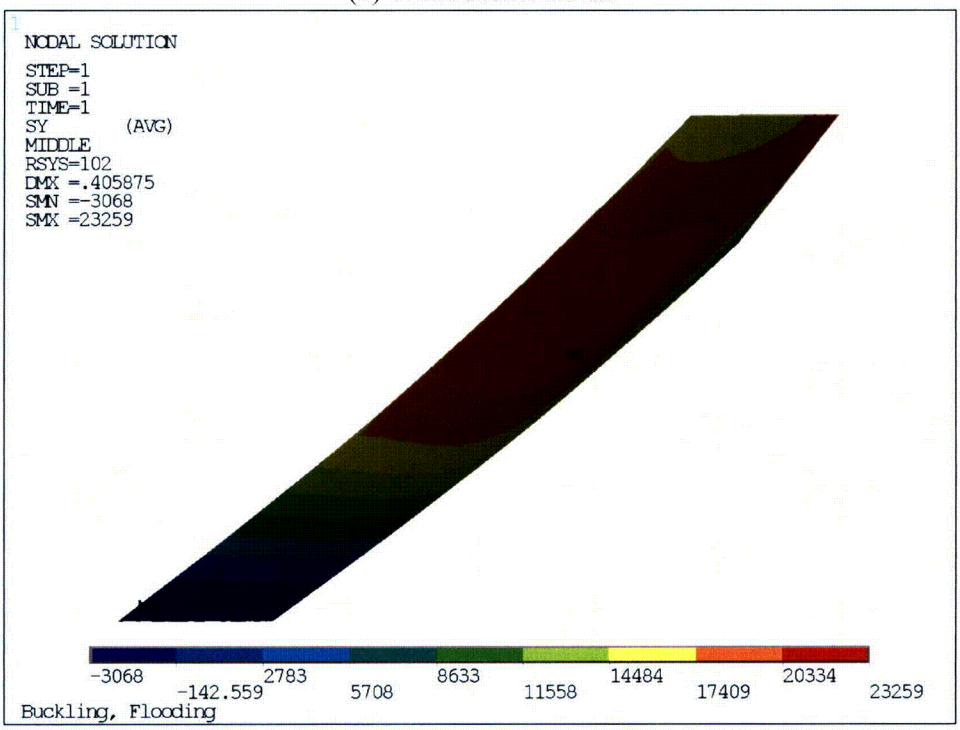

(b) Hoop Stress

Figure 8-23: Flooding Buckling Stress, Sandbed Bay 1

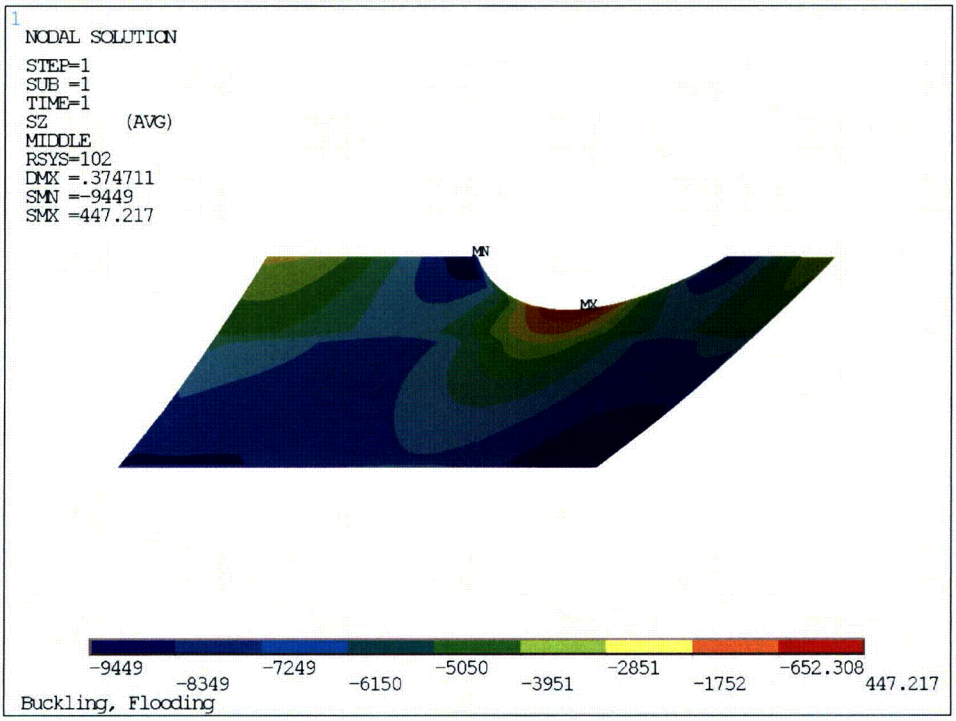

(a) Meridional Stress

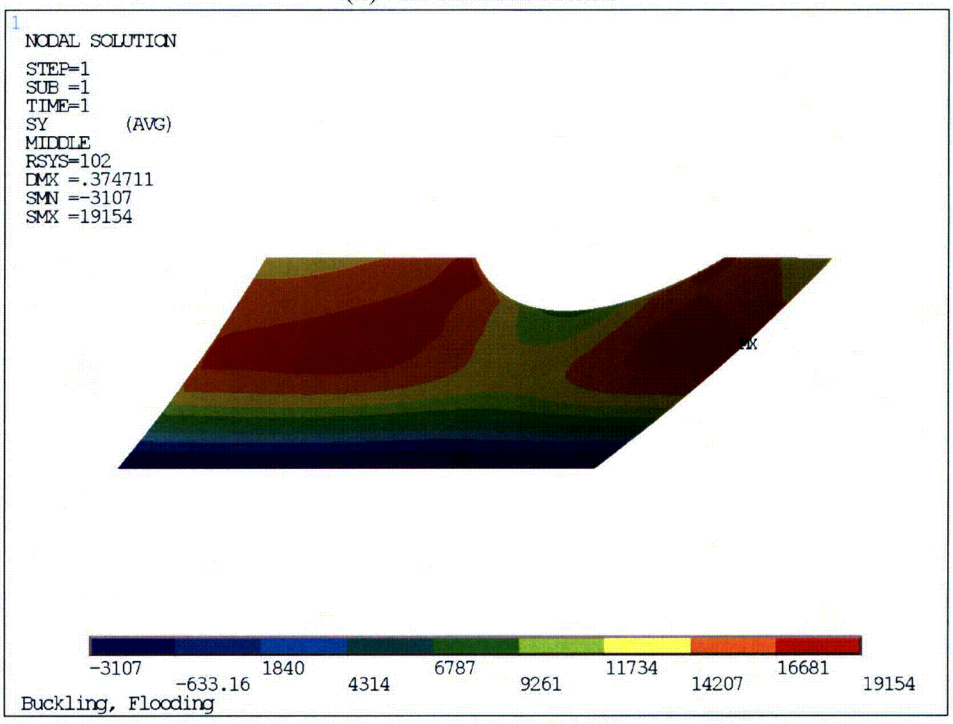

(b) Hoop Stress

Figure 8-24: Flooding Buckling Stress, Sandbed Bay 3

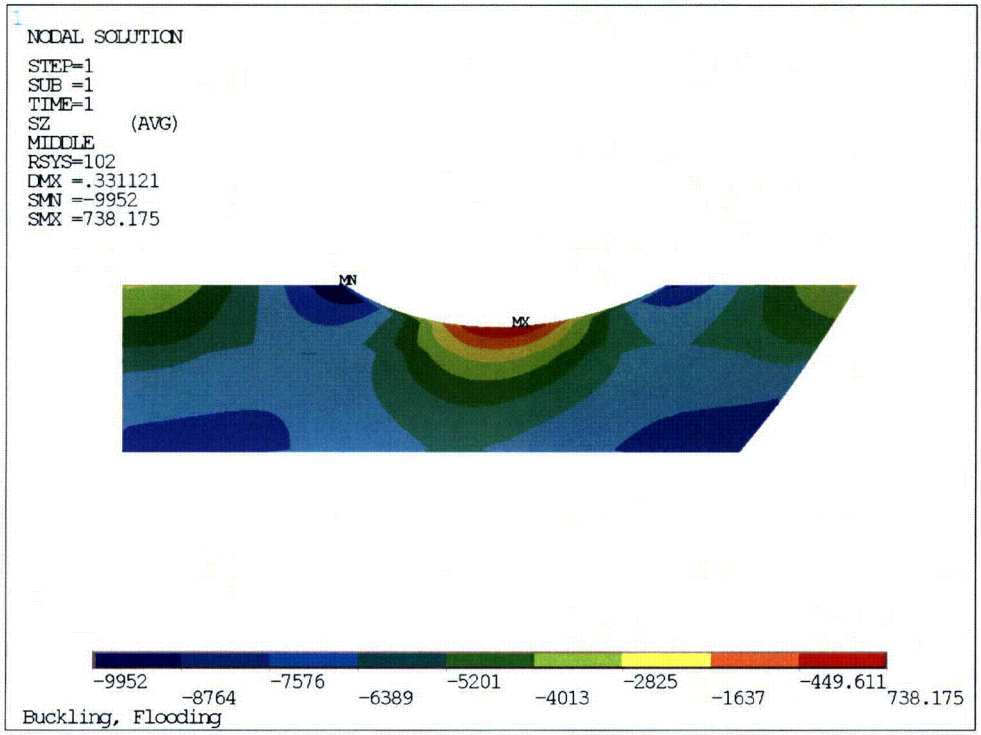

(a) Meridional Stress

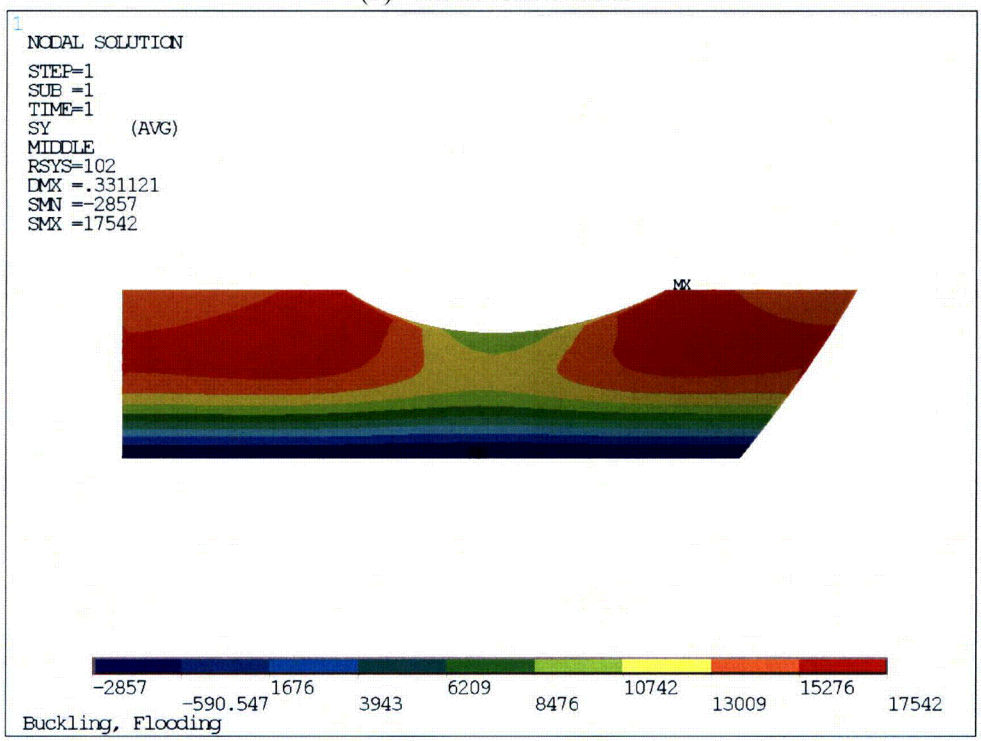

(b) Hoop Stress

Figure 8-25: Flooding Buckling Stress, Sandbed Bay 5

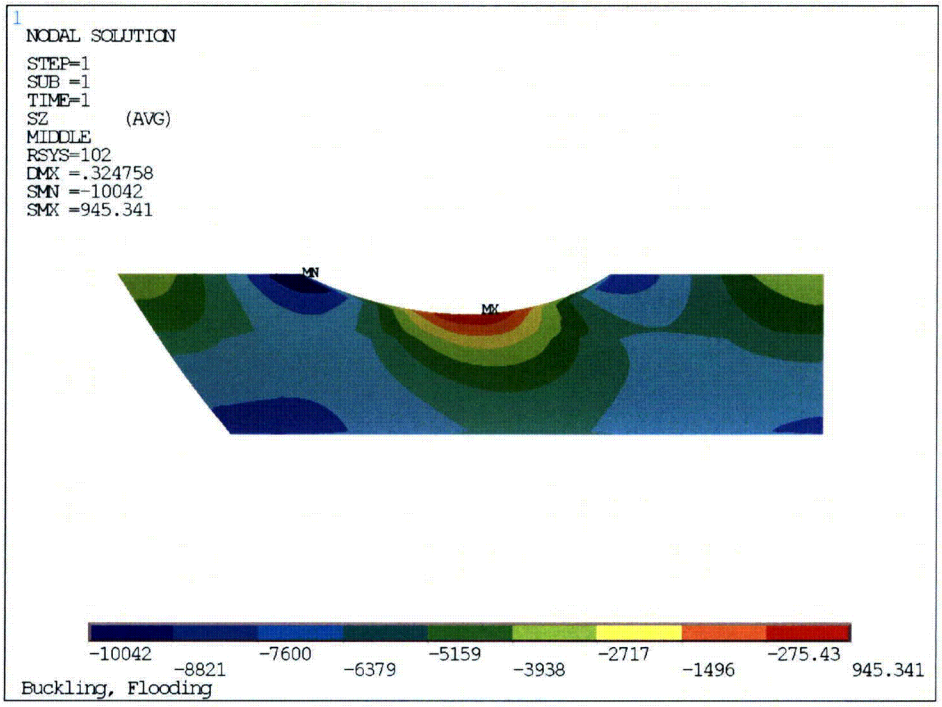

(a) Meridional Stress

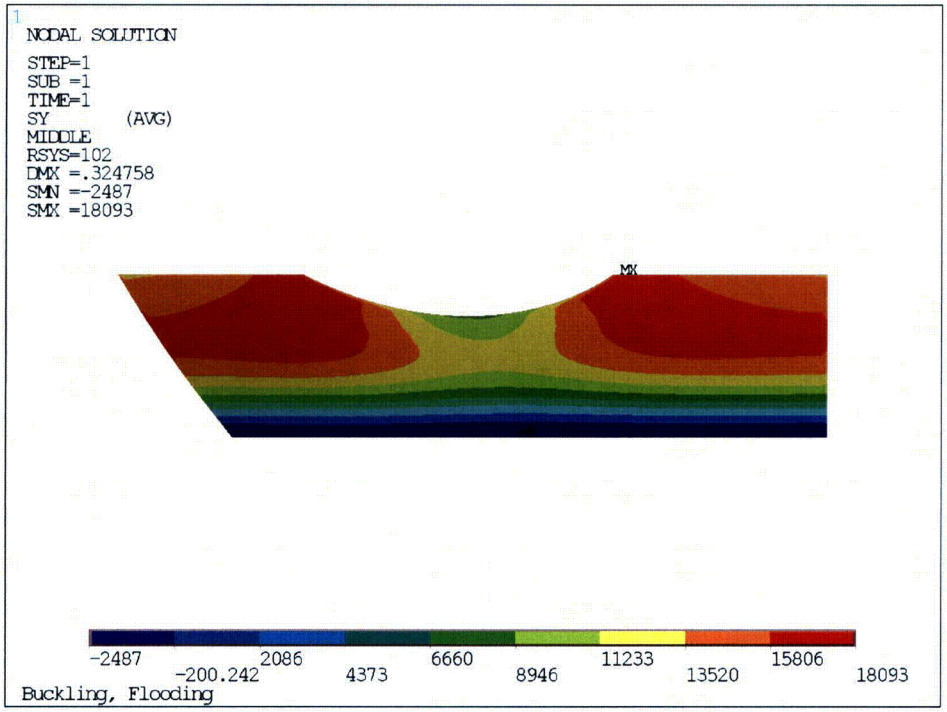

(b) Hoop Stress

Figure 8-26: Flooding Buckling Stress, Sandbed Bay 7

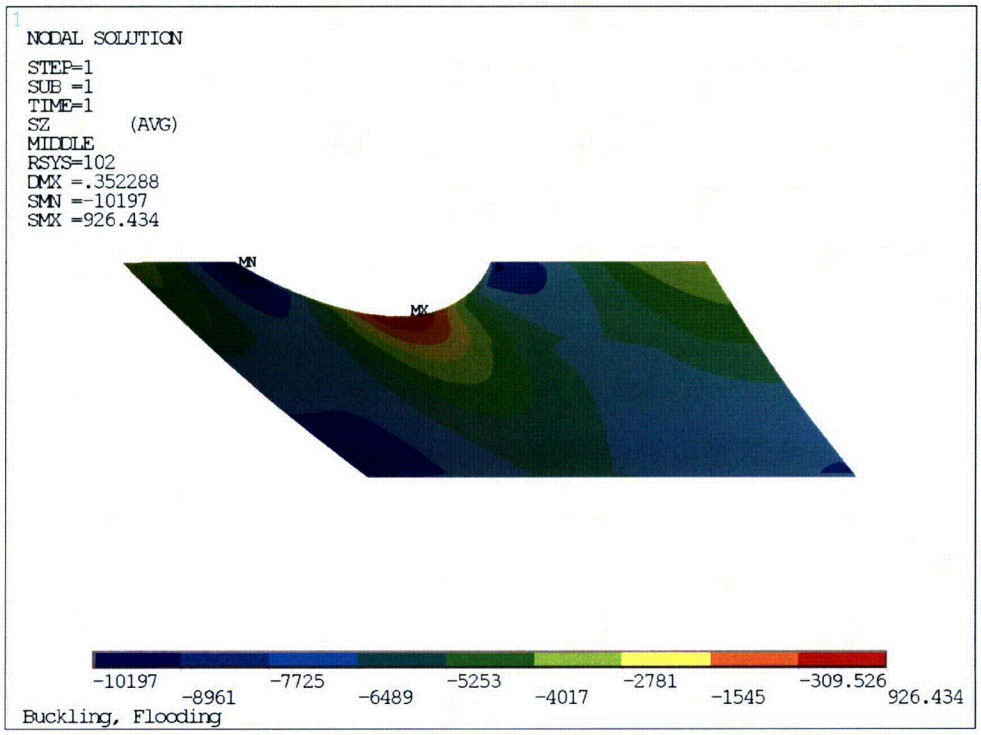

(a) Meridional Stress

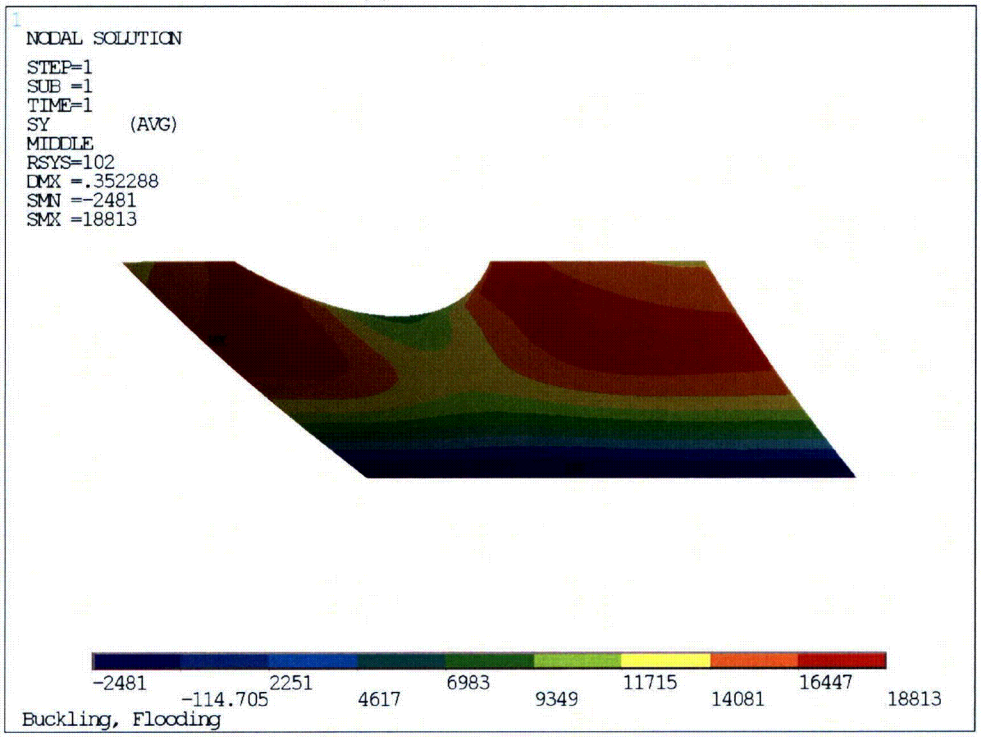

(b) Hoop Stress

Figure 8-27: Flooding Buckling Stress, Sandbed Bay 9

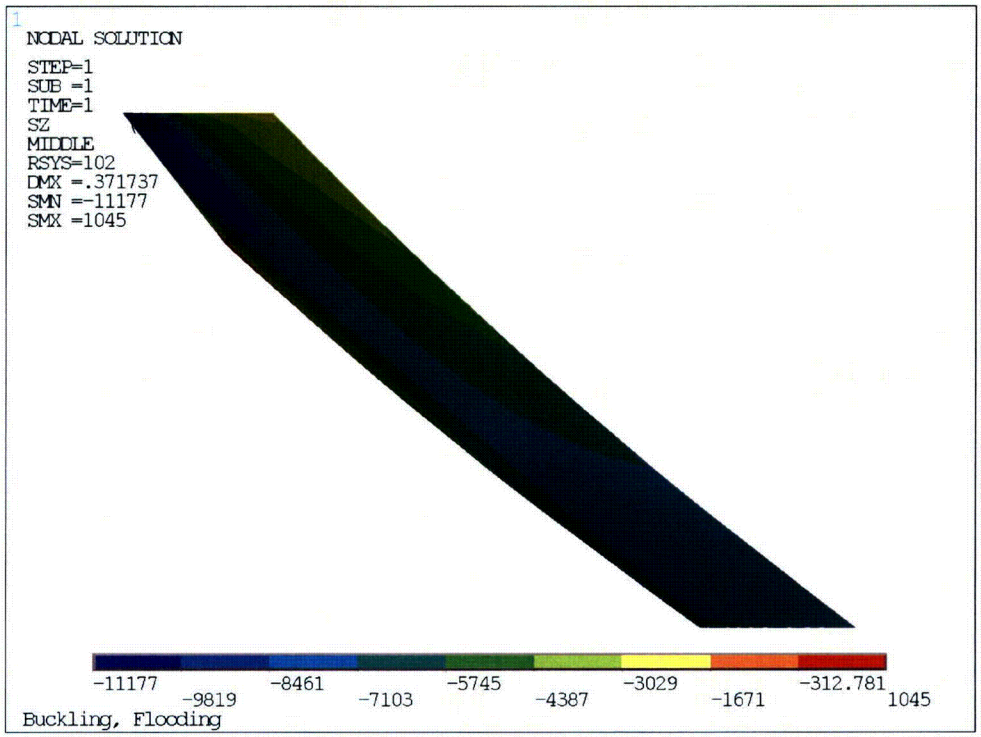

(a) Meridional Stress

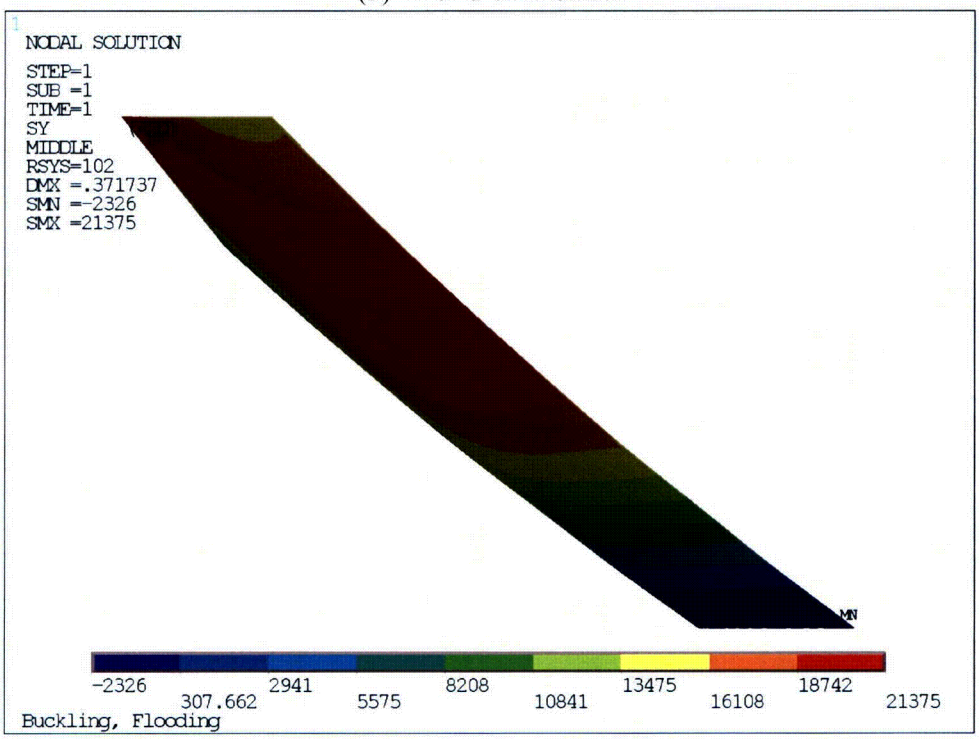

(b) Hoop Stress

Figure 8-28: Flooding Buckling Stress, Sandbed Bay 11

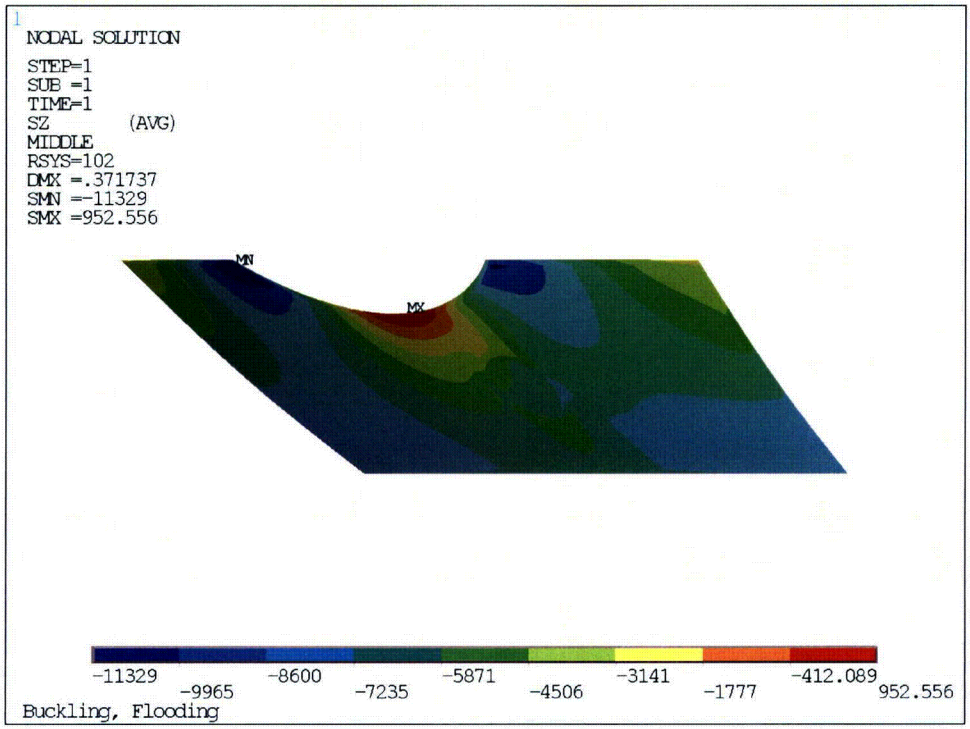

(a) Meridional Stress

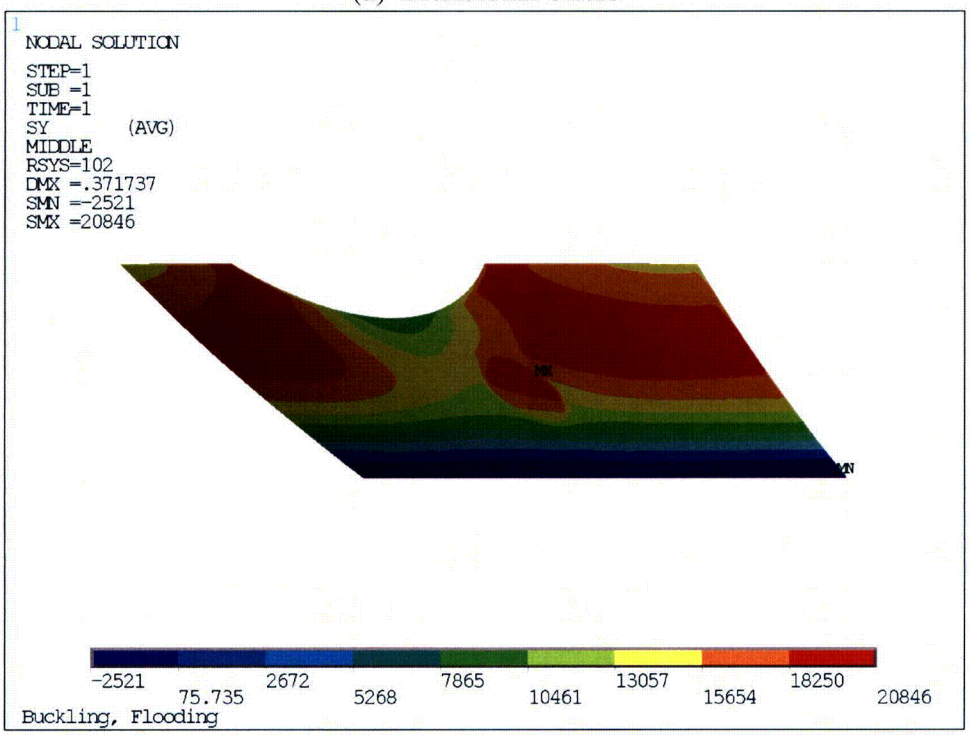

(b) Hoop Stress

Figure 8-29: Flooding Buckling Stress, Sandbed Bay 13

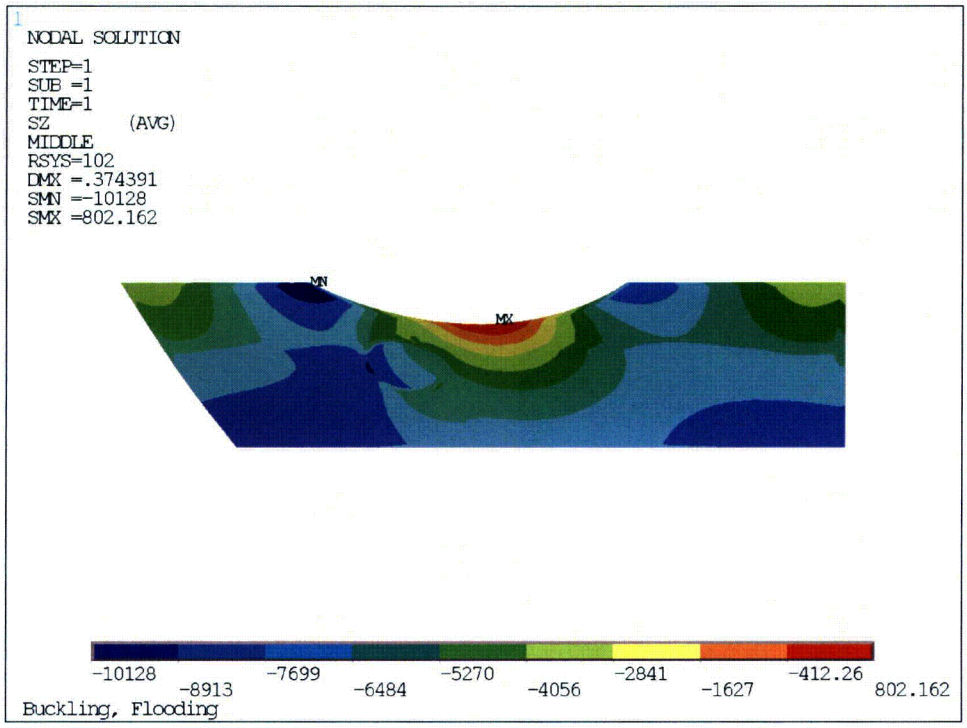

(a) Meridional Stress

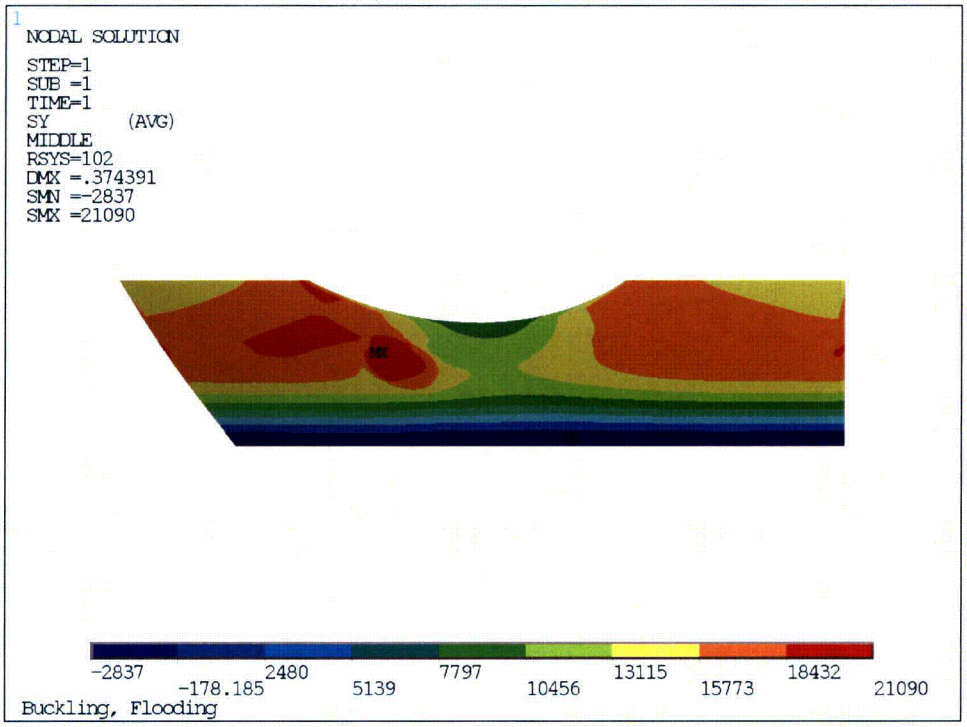

(b) Hoop Stress

Figure 8-30: Flooding Buckling Stress, Sandbed Bay 15

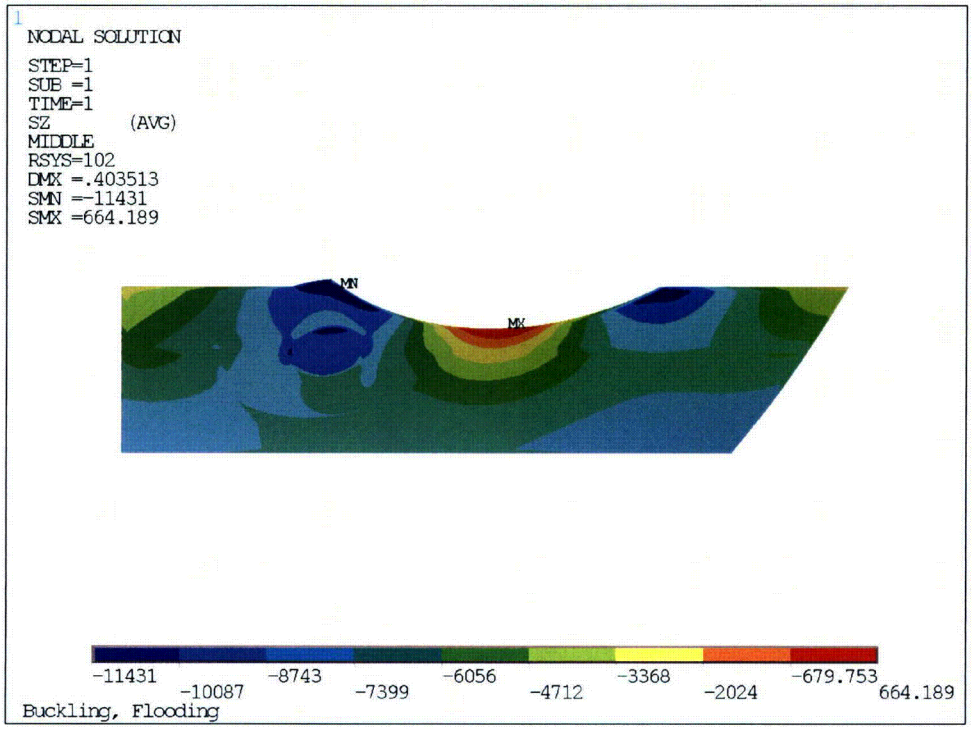

(a) Meridional Stress

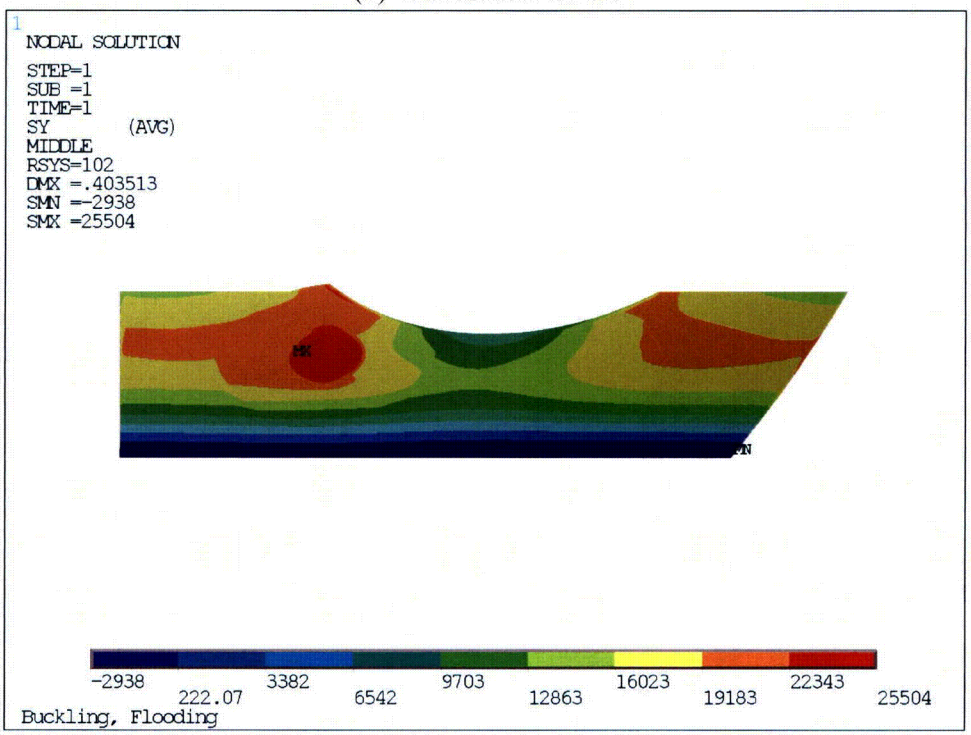

(b) Hoop Stress

Figure 8-31: Flooding Buckling Stress, Sandbed Bay 17

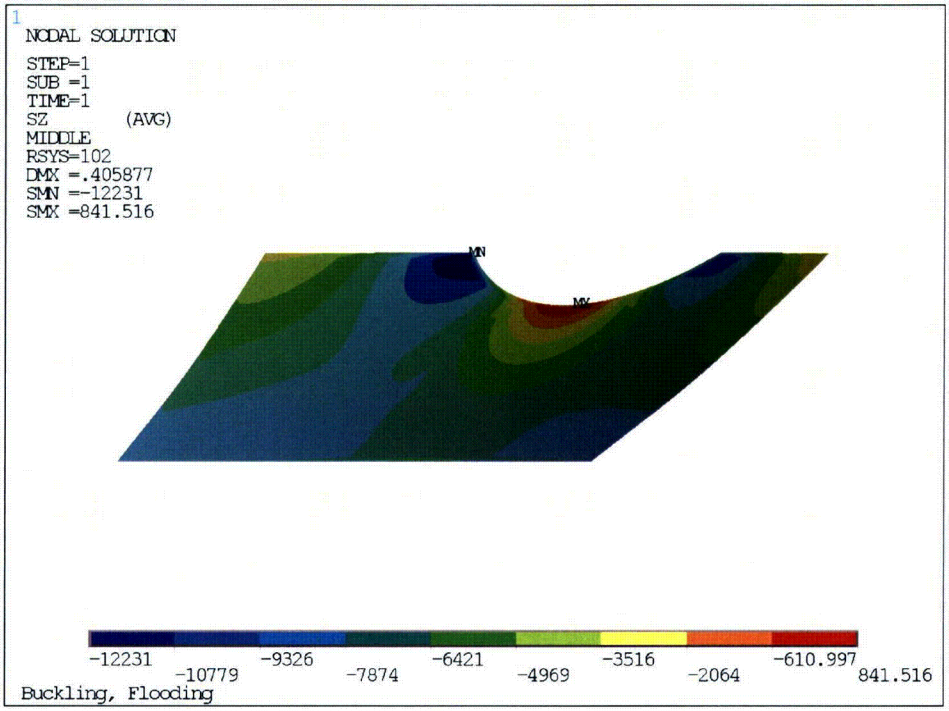

(a) Meridional Stress

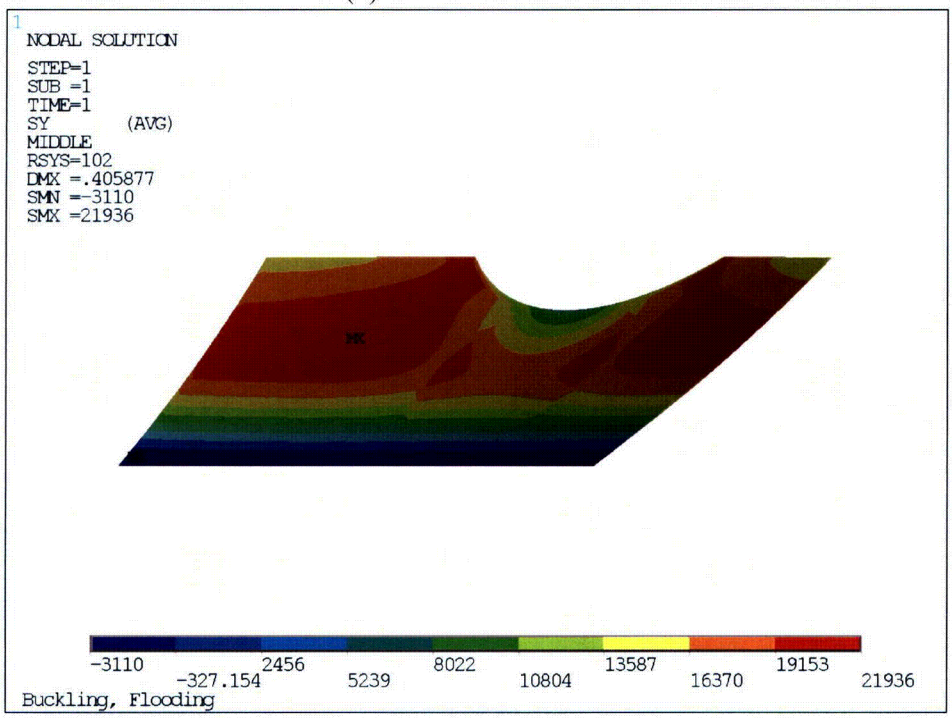

(b) Hoop Stress

Figure 8-32: Flooding Buckling Stress, Sandbed Bay 19

9.0 PENETRATION EVALUATION

There are 208 penetrations in the drywell. These are summarized in Tables 5-3 and 5-4. The sizes of these penetrations vary from 36" to 1" in diameter except the vent openings (X-49) and Equipment Hatch (X-1). The penetrations details are shown in Reference 3. The majority of the penetrations, 161 out of 208, are 8" or less in diameter. There are 20 penetrations with a 24" diameter.

There are nineteen penetrations that are in the suppression chamber. Also there are two manhole openings, X-64 and X-52.

The penetration material is A-333 Grade O, as shown in Table 5-3, except some of the penetrations with A-201 B and two penetrations (X13 & X14) have stainless steel (A312, Type 304). The reinforcing plate material is A-212 B.

9.1 Design of Penetrations

It is stated in Reference 5 that:

> 'Burns & Roe reviewed and approved all nozzle and penetrations designs prior to release for fabrication. This included materials, specifications, fabrications procedures, and quality control requirements as well as design calculations. The designs fulfill the requirements of the ASME Boiler and Pressure Vessel Code, Section III for Class B vessels for all modes of plant operation, including any design accident conditions.'

There are four types of penetration design as described in Reference 5. These are identified as Type 1, Type 2, Type 3 and Electrical Penetrations. These four types of penetrations are described verbatim from Reference 5 as follows:

Type 1 Penetrations

Type 1 pipe penetrations are those which must accommodate thermal movement and experience relatively high thermal stress. These are the high temperature lines such as the steam and feedwater system lines. These pipes are capable of exerting a reaction force due to line thermal expansion or containment movement which cannot be restrained by the containment shell and are therefore provided with a bellows expansion seal. Where necessary, these lines are anchored outside the containment to limit the movement of the line relative to the containment. This design assures integrity of the penetration during plant operation.

The penetration nozzle passes through the concrete and is welded to the primary containment vessel. The process line which passes through the nozzle is free to move axially, with the bellows expansion joint accommodating the movement. A guard pipe immediately surrounds the processes line and is designated to protect the bellows and maintain the penetration seal should the process line fail within the penetration. A seal arrangement is also provided which will permit periodic leakage testing of these penetrations.

Type 2 Penetrations

Type 2 pipe penetrations are those in which the piping or ventilation duct penetrations are welded directly to the nozzle. Bellows and guard pipes are not necessary in this design, since the thermal stresses are small and are accounted for in the design limits. Typical of this type of penetration are the shutdown cooling piping and standby liquid control piping.

Type 3 Penetrations

Type 3 pipe penetrations are those pipe lines which penetrate the containment, where the reactive forces can be restrained directly by the containment shell and are provided with full strength attachment welds between the pipe and the containment shell. These penetrations are designed for long-term integrity without use of a bellows seal. Typical of this type of penetration are the containment spray supply piping and the core spray supply piping.

Electrical Penetrations

The electrical penetrations include electrical power, signal, and instrument leads. Although two types of electrical penetrations are shown, they are basically of the same design. Electrical penetrations require a special design to achieve minimum leakage because of the problem imposed by creepage of electrical insulation. The penetration nozzle is welded to the primary containment vessel, and the ends are field welded in place during installation. A bonding resin is utilized in the seals where the cable merges. This arrangement provides a leak-tight configuration which is leak tested after installation, and provides a means for periodic leak testing thereafter.

It should be noted that one noticeable difference between Types 1, 2 and 3 is that Type 3 penetration has an integral insert plate while Types 1 and 2 have a reinforcing plate welded on to the drywell.

9.2 Code Requirements for Openings and Reinforcements

9.2.1 Section VIII, 1962 Edition

The rules governing the requirements of openings and reinforcements are in Paragraph UG-36 of Reference 7. In summary, it is stated in Paragraph UG-36 (b) that:

'Properly reinforced openings in cylindrical and spherical shells are not limited as to size and shall comply with the provisions which follow, and with the additional provisions of Par. UA-7.'

In addition, it is stated in Paragraph UG-36 (c) that:

'(2) All openings shall be reinforced to satisfy the requirements of Par. UG-37, except as given in (3) below.

(3) Single openings in vessels not subject to rapid fluctuations in pressure do not required reinforcement other than that inherent in the construction under the following conditions:

(a) Welded or brazed attachment not larger than:
3 in. pipe size – in vessel shells or heads 3/8 in. or less
2 in. pipe size – in vessel shells or heads over 3/8 in.
(b) Threaded, studded, or expanded connections in which the hole cut in the shell or head is not greater than 2 in. pipe size.'

The rules of reinforcement required for openings in shell and formed heads are given in Par. UG-37, Reference 7.

The pressurization of the drywell due to operating condition should not be classified as rapid pressurization except in the design basis accident where the pressure increases during the postulated accident from about 5 psig to above 30 psig in more than 20 seconds, (Reference 5 Figures I-2 and I-3, Pages I-5 and I-6) due to a line break in a loss of coolant accident.

9.2.2 Section VIII, 1989 Edition

The rules governing the requirements of openings and reinforcements are in Article D-5 of Reference 6. It is stated in Part AD, AD-510 that:

'(a) A single opening has a diameter not exceeding $0.2\sqrt{(R_m t)}$, or if there are two or more openings within any circle of diameter $2.5\sqrt{(R_m t)}$, then the sum of the diameters of such unreinforced openings shall not exceed $0.25\sqrt{(R_m t)}$.
(b) No two unreinforced openings shall have their centers closer to each other, measured on the inside of the vessel wall, than 1.5 times the sum of their diameters.
(c) No unreinforced opening shall have its center closer than $2.5\sqrt{(R_m t)}$ to the edge of a locally stressed area in the shell, where R_m is the mean radius and t is the nominal thickness of the vessel shell or head at the location of the opening(s); locally stressed area means any area in the shell where the primary local membrane stress exceeds 1.1 S_m, but

excluding those areas where such primary local membrane stress is due to an unreinforced opening.'

In addition, the required reinforcement for openings in shells and formed head has to be satisfied as stated in Part AD, AD-540 of Reference 15.

The maximum penetration sizes that do not require reinforcement area are summarized using criteria from different ASME Code Editions. Any penetration less than 2" does not require reinforcement independent of editions of Code. Using ASME Section VIII, '89 Edition, the penetration size can be as large as 3" before reinforcement is needed. It should also be noted that only pressure loading is required for the opening and reinforcement evaluation.

9.2.3 Section III, 1989 Edition

The rules governing the requirements of openings and reinforcements are in NE-3330 of Reference 28 which states that stress analysis is not required for pressure loading if the rules of NE-3330 are met. The major requirement in NE-3330 is the 'Reinforcement Requirements for Openings in Shells and Formed Heads' stated in NE-3332.

It is also stated in NE-3332.1 that:

'...single circular openings need not be provided with reinforcement if the openings have diameters equal to or less than 2 ½ in.'

9.3 Code Compliance

Reference 29 raises a concern that 'the design of Penetration did not meet ASME Section III, 1980 requirements'.

The objective of Reference 29 was:

'1. Determine what does not meet ASME Section III, 1980- Review Previous Material.
2. Determine Significance
3. Develop Alternatives.'

The results of Reference 29 (summarized):

'Penetrations listed on Table 1 (Ref. 29) and noted as not complying with ASME III, 1980 are indicated by 16 mark numbers.

The welding details did not precisely conform. However full penetration weld were always provided between vessel shell and nozzle and area replacement always met ASME III, 1980.

Nevertheless, approximate analyses were preformed for internal pressure which indicated ASME III NE-3331 was satisfied obviating the need for conformance to rules of NE-3330.

In short, the non-compliances with rules of NE-3330, ASME III, 1980 are minor in nature. However, the analyses indicate compliance in accordance with NE-3331(a), ASME III, 1980.

Note: External loads on piping penetrations has been addressed by GPUN Memo 5320-90-151 (July 26/90) as required by NE-3311.'

9.4 Area of Reinforcement Requirements

In the current evaluation, the rules of ASME Code Section III, NE-3330 are used. The openings and reinforcement for metal containment are specified in NE-3330. Specifically, the required

area of reinforcement is defined in NE-3332.2. The boundaries of the area reinforcement are defined in NE-3334.

9.5 Area of Reinforcement Calculation

The area reinforcement calculation is facilitated using a spreadsheet that calculates the required area and the limits of boundaries for reinforcement defined under the rules of different editions of ASME Pressure Vessel and Boiler Code.

The drywell wall thicknesses are based on the minimum measured general thickness as described in Reference 4. Nominal wall thicknesses of the penetrations and reinforcing/insert plates were used. In addition for conservatism, the fillet welds between the penetration and insert plates and between the insert plates and drywell shell are not included in the area reinforcement evaluation.

9.6 Area of Reinforcement Calculation Results

The results of the area reinforcement calculation are summarized in Table 9-1. It is shown that the metal area requirements are satisfied for all penetrations. In addition, there are significant margins between the available metal areas and the required metal areas.

There are some openings that are in close proximity to each other such that they may have to be evaluated as multiple openings according to NE-3335.1. To be classified as multiple openings, the openings have to be spaced within two times their average diameters. It was determined that all penetrations identified as possible multiple openings have the distances between the penetration centers larger than the requirements in NE-3335.1.

Subarticle NE-3335.1 (1) states:

> 'When the distances between the centers of the openings is greater than 1 1/3 times their average diameter, the area of reinforcement between them shall be not less than 50% of the total required for these openings.'

9.7 Code Reconciliation

The original code of record for Oyster Creek is ASME Boiler and Pressure Vessel Code, Section VIII, 1962 Edition [7]. The current penetration evaluation is based on ASME Boiler and Pressure Vessel Code, Section III, Subsection MC, 1989 Edition [28].

The requirements in Reference 7 for openings and reinforcement are stated in Paragraphs UG-36 to UG-46. The requirements in Reference 28 for openings and reinforcement are stated in Subarticle NE-3330. Penetrations not requiring reinforcement are summarized in Table 9-2. Section III and Section VIII use similar equations to specify the maximum penetration size that would require no reinforcement.

$A = dt_r$ Section VIII, '62 Edition (9-1)

$A = dt_r F$ Section III, Subsection MC, '89 Edition (9-2)

Even though the equation (9-2) has an additional correction F, the Section III, '89 Edition Code recommends a value of F = 1.00 be used. Therefore, Section VIII. '62 Edition and Section III, '89 Edition both require the same area of reinforcement.

The limit of reinforcement measured along the vessel wall is very similar in both Codes (Par. UG-40 (b), Section VIII vs Subparagraph NE-3334.1 (a), Section III). There is an additional requirement in Section III (2/3 of required reinforcement within a specific distance, Subparagraph NE-3334.1 (b)) that is not in Section VIII.

The limit of reinforcement measured normal to the vessel wall for Section VIII, '62 Edition is specified in Par. UG-40 (c) which is very similar to requirements specified in Section III, '89 Edition, Subparagraph NE-3334.2 (c). Section III also provides more specific requirements based on the penetration configuration.

Metal available for reinforcement is specified in Par. UG-40 (d), Section VIII, '62 Edition. In Section III, '89 Edition, it is specified in Paragraph NE-3335. The areas available include metal

in vessel and penetration wall above the required thickness, metal in welds and metal in reinforcing plates, all within the area limits. One additional requirement is in Section III (NE-3335 (d)) that the mean coefficient of thermal expansion of metal to be included as reinforcement shall be within 15% of the value of the vessel wall material. Since the reinforcing plate material is the same as the drywell material (A212-B), there is no difference in the mean coefficient of thermal expansion.

9.8 Discussions and Conclusions

An area reinforcement evaluation was performed for the Oyster Creek Drywell according to the rules specified in ASME Boiler and Pressure Vessel Code, Section III, Subsection MC, Subarticle NE-3330. In this evaluation, the 'minimum measured general thickness' on the drywell (i.e. cylindrical, knuckle and spherical plates) was used. Nominal thickness was used on the penetrations and reinforcing plates. No allowance for future corrosion was considered.

The results of the evaluation show that the area reinforcement requirement is satisfied for all penetrations. It also shows that the requirements for multiple openings are met. In addition, a reconciliation on the requirements was performed between Section VIII, '62 Edition and Section III, '89 Edition. There are no differences in the required reinforcing area (Section III has more requirements in the limits of area reinforcements which had no effect on this evaluation).

Table 9-1: Area Reinforcement Calculation Results

Penetration Identification					Area Reinforcement (in^2)	
OC Marking	**CBI Marking**	**Elevation**	**Azimuth**	**Size (in)**	**Required**	**Available**
X-38	27-X38	72'-11" & 73'-9"	209° to 215°	3	1.68	5.42
X-39	27-X39	72'-11' & 73'-9"	55°-30' & 61°-30'	3	1.68	5.42
X-40	12-N3-1, 12-N3-2 & 12-N3-9	42'-0", 44'-0" & 46'- 0"	20°, 25°, 210°, 215°, & 300°	3	2.08	7.12
X-41	13-N3-6 & 13-N3-7	19'-9" & 20'-6"	47°, 61°, 191°, 205°, & 277°	3	2.08	9.69
X-42	26-X42-43	61'-9"	58°-30'	3	1.78	4.60
X-43	26-X42-43	62'-4"	58°-30'	3	1.78	4.60
X-44	17-N3-13 & 17-N3-12A	91'-0"	25° & 335°	3	1.96	5.94
X-46	28-X46	86'-0"	120°	3	1.96	4.50
	17-N3-12A	86'-0"	330°	3	1.96	6.27
X-47	12-N3-5	47'-0"	320°, 325° & 330°	3	2.08	7.12
	28-X47	47'-0"	335°	3	2.08	5.19
X-50	24-X50	47'-0" & 48'-6"	284° to 306°	3	1.78	4.58
X-59	17-N3-13A	90'-0"	25°	3	1.96	6.26
X-60	17-N3-12A	90'-0"	30° to 60°	3	1.96	6.87
X-73	39-X73	72'-6" & 73'-6"	45° & 225°	3	1.68	5.42
X-6	28-X6	87'-9"	150°	6	3.12	8.25
X-23	12-N6-5	43'-0"	330°	6	3.61	8.40
X-24	12-N6-4	47"-0"	15°, 234° & 315°	6	3.61	8.40
	28-X24	47'-0"	101° & 162°	6	3.31	6.98
X-25 to X-27	12-N6-2	44'-0"	30°, 35°, 40°, 45°, 55° & 60°	6	3.61	8.40
X-45	14-N6-6, 7, 9 14-N6-6A, 7A, 9A	35'-10.25" & 36'-11.75"	219°-19', 225°-05', 235°-03', 219°-19', 225°-05' & 235°-03"	6	3.61	12.96
X-45	24-X45	36'-5"	213°-8'	6	3.37	19.10
X-61	12-N6-3	42'	55°	6	3.31	6.97
X-62	14-N6-10	90'-0"	315°	6	3.35	6.42

Table 9-1: Area Reinforcement Calculation Results (cont'd)

Penetration Identification					Area Reinforcement (in^2)	
OC Marking	**CBI Marking**	**Elevation**	**Azimuth**	**Size (in)**	**Required**	**Available**
X-38	27-X38	72'-11" & 73'-9"	209° to 215°	3	1.68	5.42
X-39	27-X39	72'-11' & 73'-9"	55°-30' & 61°-30'	3	1.68	5.42
X-40	12-N3-1, 12-N3-2 & 12-N3-9	42'-0", 44'-0" & 46'- 0"	20°, 25°, 210°, 215°, & 300°	3	2.08	7.12
X-41	13-N3-6 & 13-N3-7	19'-9" & 20'-6"	47°, 61°, 191°, 205°, & 277°	3	2.08	9.69
X-42	26-X42-43	61'-9"	58°-30'	3	1.78	4.60
X-43	26-X42-43	62'-4"	58°-30'	3	1.78	4.60
X-44	17-N3-13 & 17-N3-12A	91'-0"	25° & 335°	3	1.96	5.94
X-46	28-X46	86'-0"	120°	3	1.96	4.50
	17-N3-12A	86'-0"	330°	3	1.96	6.27
X-47	12-N3-5	47'-0"	320°, 325° & 330°	3	2.08	7.12
	28-X47	47'-0"	335°	3	2.08	5.19
X-50	24-X50	47'-0" & 48'-6"	284° to 306°	3	1.78	4.58
X-59	17-N3-13A	90'-0"	25°	3	1.96	6.26
X-60	17-N3-12A	90'-0"	30° to 60°	3	1.96	6.87
X-73	39-X73	72'-6" & 73'-6"	45° & 225°	3	1.68	5.42
X-6	28-X6	87'-9"	150°	6	3.12	8.25
X-23	12-N6-5	43'-0"	330°	6	3.61	8.40
X-24	12-N6-4	47"-0"	15°, 234° & 315°	6	3.61	8.40
	28-X24	47'-0"	101° & 162°	6	3.31	6.98
X-25 to X-27	12-N6-2	44'-0"	30°, 35°, 40°, 45°, 55° & 60°	6	3.61	8.40
X-45	14-N6-6, 7, 9 14-N6-6A, 7A, 9A	35'-10.25" & 36'-11.75"	219°-19', 225°-05', 235°-03', 219°-19', 225°-05' & 235°-03"	6	3.61	12.96
X-45	24-X45	36'-5"	213°-8'	6	3.37	19.10
X-61	12-N6-3	42'	55°	6	3.31	6.97
X-62	14-N6-10	90'-0"	315°	6	3.35	6.42

Table 9-2: Penetration Size Not Requiring Area Reinforcement

Code		Penetration Size	Note
VIII, '62 Edition	Par. UG-36(c)(3)(a)	3"	Vessel shells or heads 3/8 in or less
		2"	Vessel shells or heads over 3/8 in.
VIII, '89 Edition	Part AD, AD-510	2 ¼"	Cylindrical Shell
		2 ½"	Upper Spherical Shell
		3"	Lower Spherical Shell
III, '89 Edition	NE-3332.1	2 ½"	

10.0 SUMMARY AND CONCLUSIONS

The evaluations contained in this summary report document the basis of acceptability of the Oyster Creek Steel Drywell Containment with the observed wall thinning in the sandbed region based on wall thickness measurements obtained during the October 2006 refueling outage, as confirmed by measurements obtained during the October 2008 refueling outage. In comparison to previous analyses, this evaluation more accurately quantifies the margin of the drywell with respect to buckling and ASME Code Stress Allowables.

The evaluation used a detailed three-dimensional finite element model that was refined to model the non-symmetric conditions. The level of detail in this model is significantly greater than earlier models.

This evaluation clearly demonstrates that, even with the conservative assumptions that remain in the analysis as identified in this report, the Oyster Creek drywell shell meets ASME Code Allowable Stresses for all conditions analyzed and has factors of safety that are well above those in the current license basis analysis.

Conservative approaches and assumptions have been included in the evaluations contained in this report. Notable conservatisms include the following:

- Seismic Response Spectra
  The drywell is supported at two locations; at 10'-3" base, and at 82'-9" star truss location. The seismic spectra at 82'-9" start truss support location are significantly higher than the spectra at 10'-3" base. The bounding seismic response spectra are used as the seismic input for the drywell. This introduces significant conservatism in the seismic response of the structure.

- Post Accident Flooding Case Contributing Water Mass
  100% of the water is included as added mass in the drywell in the seismic analysis. In a seismic event, substantial portion of the water will be acting on the bioshield wall, which

has been conservatively neglected. The assumption that the entire seismic energy of the water is absorbed by the drywell is conservative.

- Welded Steel Structure Damping Ratio

  The original NRC Regulatory Guide 1.92 (issued in October 1973) recommends that the damping ratio to be used in Operating Basis Earthquake for welded steel structure is 2%. Revision 1 of Regulatory Guide 1.92 (issued in March 2007) recommends a 3% damping value for welded structures. The use of an increased damping value will reduce the component stresses in the refueling case, in which the Operating Basis Earthquake is included as one of the load cases.

- Service Level C Limits versus Service Level D Limits

  The Post Accident Flooding Case is evaluated using the Service Level C Limits, which are significantly lower than the Service Level D Limits. Post Accident Flooding condition is a highly unlikely event, and is generally categorized as a Service Level D event. Using the Service Level D Limits would have yielded additional margins on the analysis results for the Post Accident Flooding Load Case.

- Support Provided by Star Truss / Bioshield Wall

  There are a total of 8 Star Trusses connecting the drywell to the bioshield wall at 82'-9" elevation. The structural support provided by the Star Truss / Bioshield Wall has been conservatively neglected from the analyses. The structural support will take on some load, which is a conservatism in the analyses, especially the buckling analysis.

- Sizes of Locally Thinned Areas

  The sizes of the locally thinned areas in the sandbed region have been conservatively mapped. An extended circular boundary has been drawn to enclose the postulated locally thinned areas. This generally results in a larger, thinner area being modeled in the analysis producing conservative analysis results in the sandbed region.

11.0 REFERENCES

1. CB&I Report, 'Structural Design of the Pressure Suppression Containment Vessels,' Chicago Bridge & Iron Co. Contract #9-0971, , SI File OC-15Q-207.
2. General Electric Report, 'An ASME Section VIII Evaluation of Oyster Creek Drywell for Without Sand Case, Part 1, Stress Analysis,' DRF #00664, Index No. 9-3, Rev. 0, February 1991, SI File OC-15Q-210.
3. Chicago Bridge & Iron Company Drawings, Jersey Central Power & Light Co., Oyster Creek, NJ, File No. OC-15Q-201 and 202

   Drawing No. 9-0971

   a. Sh. No. 2, Rev. 10
   b. Sh. No. 2A, Rev. 4
   c. Sh. No. 3, Rev. 2
   d. Sh. No. 4, Rev. 1
   e. Sh. No. 7, Rev. 5
   f. Sh. No. 14, Rev. 3
   g. Sh. No. 17, Rev. 4
   h. Sh. No. 19, Rev. 2
   i. Sh. No. 27, Rev. 1
   j. Sh. No. 28, Rev. 2
   k. Sh. No. 29, Rev. 7
   l. Sh. No. 30, Rev. 5
   m. Sh. No. 31, Rev. 5
   n. Sh. No. 32, Rev. 2
   o. Sh. No. 33, Rev. 4
   p. Sh. No. 36, Rev. 4
   q. Sh. No. 39, Rev. 1
   r. Sh. No. 42, Rev. 1
   s. Sh. No. 146, Rev. 1
   t. Sh. No. 40, Rev. 1
   u. Sh. No. 61, Rev. 6
   v. Sh. No. 38, Rev. 1
   w. Sh. No. 35, Rev. 4
   x. Sh. No. 34, Rev. 4
   y. Sh. No 12 – 38
   z. Sh. No. 6, Rev. 3
   aa. Sh. No. 21, Rev. 2
   ab. Sh. No. 1, Rev.2
   ac. No. 146, Rev.1 1

   Drawing No: 4086-4, Rev. 4

4. Exelon Document Tech Eval 330592-27-27, "Representative Drywell Thickness," SI File No. OC-15Q-234.
5. Ralph Parsons Report, "Oyster Creek Nuclear Power Plant Unit No. 1, Primary Containment Design Report," Ralph M. Parsons Co for General Electric Co.
6. ASME, Boiler and Pressure Vessel Code, Section III, Appendices, 1989 Edition.
7. ASME, Boiler and Pressure Vessel Code, Section VIII, 1962 Edition, with applicable addenda.
8. ASTM International, Annual Book of ASTM Standards, Section One, Volume 01.04, West Conshohocken, PA, 2004.
9. ASTM International, Annual Book of ASTM Standards, Section One, Volume 01.04, West Conshohocken, PA, 1967.
10. ASTM Designation: A212-64, "Standard Specification for High Tensile Strength Carbon-Silicon Steel Plates for Boilers and Other Pressure Vessels," 1964, SI File OC-15Q-236.
11. ER-AA-335-018, Rev. 3, "ASME IWE (Class MC) Containment Visual Examination Record," SI File No. OC-15Q-230.
12. ANSYS Mechanical, Revision 8.1, (with Service Pack 1) ANSYS Inc., June 2004
13. Oyster Creek Nuclear Generating Station, FSAR , Rev. 13, Chapter 6, April 2003, SI File OC-15Q-205.
14. Oyster Creek Nuclear Generating Station, FSAR, Update 7, Chapter 3, December 1992, SI File OC-15Q-205..
15. ASME Boiler and Pressure Vessel Code, Section VIII, 1989 Edition
16. EQE International Report, 'Design Basis Seismic Response Analysis for the Oyster Creek Nuclear Generating Station Reactor, Intake, and Turbine Buildings, Volumes I, II and III,' Report No. 50069-R-001, September 1995, SI File OC-15Q-202.
17. Oyster Creek Nuclear Generating Station, FSAR, Update 14, Chapter 3.7, October 2005, SI File OC-15Q-205.
18. Calculation, 'Soil-Structure-Interaction Re-Analysis of the OCNGS Drywell for the Flooded Condition,' ABS Consulting Calculation No. 1817851-C-001, Rev. 1, 4/7/008, SI File OC-15Q-239.

19. Regulatory Guide 1.61, 'Damping Values for Seismic Design of Nuclear Power Plant,' U. S. Nuclear Regulatory Commission, October 1973.
20. EQE Calculation No. 200494-C-001, "OCNGS Reactor Building and Turbine Building Displacements," Revision 0, SI File OC-15Q-213.
21. Teledyne Report, "Justification for use of Section III, Subsection NE, Guidance in Evaluation of the Oyster Creek Drywell," Technical References TR-7377-1. November 1990, SI File OC-15Q-219.
22. ASTM International, Annual Book of ASTM Standards, Section one, Volume 01.04, West Conshohocken, OA, 1995.
23. Miller Report, "Applicability of ASME Code Case N-284-1 to Buckling Analysis of Drywell Shell," June 15, 2006, SI File OC-15Q-222
24. ASME Boiler and Pressure Vessel Code, Section III, Case N-284-1, "Metal Containment Shell Buckling Design Method, Class MC, Section III, Division 1," March 1995.
25. ANSYS, Release 11.0, ANSYS, Inc., June 2007.
26. Miller, "Research Related to Buckling of Nuclear Components," 7th International Conference on Structural Mechanics in Reactor Technology, Chicago, Ill.
27. Burns and Roe Drawing 4114, 'Reactor Building Containment Vessel Penetrations, Rev. 6, SI File OC-15Q-232.
28. ASME, Boiler and Pressure Vessel Code, Section III, Division 1, Subsection NE, Class MC Components, 1989 Edition, with Winter 1991 addenda.
29. GPU Nuclear Document, "O.C. Drywell Penetration Reinforcement," No. C-1302-187-5320-007, Rev. 1, SI File OC-15Q-217.
30. Baumeister, T., Avallone, E. and Baumeister, T., "Marks' Standard Handbook for Mechanical Engineers," Eight Edition, McGraw-Hill, 1978.
31. Regulatory Guide 1.61, "Damping Values for Seismic Design of Nuclear Power Plants," Rev. 1, Office of Nuclear Regulatory Research, U. S. Nuclear Regulatory Commission, March 2007.
32. Crane, ALOYCO valve catalog, Corrosion Resistant Valves, Cullman, AL, SI File OC-15Q-237.

33. Drawing, "Drywell and Suppression System, Flow Diagram," Drawing No. GE 237E726, Sheet 1, Rev. 74, April, 2006, SI File No. OC-15Q-231.
34. Drawing, "Reactor Building Containment Vessel Penetrations," Drawing No. 4114-6, Rev. 6, June 1996, SI File OC-15Q-232.
35. Beyer, W., "CRC, Standard Mathematical Tables," 26th Edition, CRC Press, Boca Raton, Florida, 1982.
36. Regulatory Guide 1.92, "Combining Modal Response and Spatial Components in Seismic Response Analysis," Revision 2, Office of Nuclear Regulatory Research, U. S. Nuclear Regulatory Commission, July 2006.
37. U.S. Nuclear Regulatory Commission, 'SEP Evaluation of Effect of Pipe Break on Structures, Systems and Components Inside Containment, Topic III-5.A for the Oyster Creek Nuclear Power Plant,' Docket No. 50-219.
38. SI Report, "Oyster Creek Drywell Sandbed Region Wall Thinning Sensitivity Analysis," Report No. 0006004.402, Revision 0, September 2008.
39. USA Standard Code for Pressure Piping, USAS B31.1.0, "Power Piping," 1983 Edition with 1984 Addenda, American Society of Mechanical Engineers.
40. Exelon Document Technical Evaluation 334592-27-33, SI File No. OC-15Q-239.
41. Oyster Creek Nuclear Generating Station Final Safety Analysis Report, Update 7, Section 3.8, December 1992, SI File No. OC-15Q-205.
42. Galambos, T.V., "Guide to Stability Design Criteria for Metal Structures," 4th Edition, John Wiley & Sons.
43. Oyster Creek Nuclear Generating Station, FSAR, Update 9, Chapter 3, December 1992, SI File OC-15Q-205.

Enclosure 2

Sensitivity Analysis for Three-Dimensional Structural Analysis